# Spatio-temporal Variability of Atmospheric Ozone over Indian Subcontinent and its Relation to Meteorological Parameters

*Thesis submitted to*

**COCHIN UNIVERSITY OF SCIENCE AND TECHNOLOGY**

*In partial fulfilment for the award of degree of*

## DOCTOR OF PHILOSOPHY

IN

## ATMOSPHERIC SCIENCE

**By**

## Anila Alex



**DEPARTMENT OF ATMOSPHERIC SCIENCES**
**COCHIN UNIVERSITY OF SCIENCE AND TECHNOLOGY**
**COCHIN 682 016, INDIA**

**August  2013**

Dedicated to

**My Father and Mother**

# CERTIFICATE

Certified that the thesis entitled *Spatio-temporal Variability of Atmospheric Ozone over Indian Subcontinent and its Relation to Meteorological Parameters* is an authentic record of the research work carried out by **Ms. Anila Alex** under my supervision and guidance in the Department of Atmospheric Sciences, Cochin University of Science and Technology, in partial fulfilment of the requirements for the Ph.D. degree of Cochin University of Science and Technology. I also certify that no part of the work has been submitted to any University or Institution for the award of any Degree or Diploma.

Cochin-682016
August, 2013

Prof. K. Mohankumar
Supervising Guide

# DECLARATION

I hereby declare that this thesis entitled *Spatio-temporal Variability of Atmospheric Ozone over Indian Subcontinent and its Relation to Meteorological Parameters* is an authentic record of the research work carried out by me and no part of this work has been submitted to any University or Institution for the award of any Degree or Diploma.

Cochin-682016                                                                                                          Anila Alex

August, 2013

## *Acknowledgements*

I would like to express my deepest gratitude to my supervising guide Dr. K.Mohankumar. He introduced me to this topic and his constant support and guidance helped me to complete this thesis. I remember the many occasions he motivated and supported me when I was totally out of confidence. This thesis would not have become a reality without his patience in guiding me and enthusiasm in correcting the thesis. Words are inadequate to express my thanks for him.

I hereby express my sincere thanks to Dr. C. A.Babu, Head, Department of Atmospheric Sciences for his readiness to help all the time and for the provision of all the necessary facilities during the entire tenure of my research work. I also wish to express my sincere thanks to Dr. K.R. Santosh, Mr.B.Chakrapani and Dr.V. Madhu for their support. I also thank my teachers Dr.H.S. Ram Mohan and Dr.C.K.Rajan for their suggestions. My special thanks to Dr. Venu.G.Nair for all his suggestions and support throughout my research work.

I take this opportunity to thank all those people who was at the CAPG lab with me during my P.hD. I remember my former collegues Dr.Abish, Ms. Smitha A, Ms. Asha. and Dr. Resmi as well as Mr. Vijayakumar and Mr. Johnson. Their presence made a very pleasant and enjoyable atmosphere for me to do research.  I also thank for all the suggestions and support by them. I also thank Mr. Krishnamohan, Mr. Jayakrishnan , Mr. Sivaprasad and Dr. Nithin for their support.  I also remember the care and help by Ms.Shinu, Mr.Shinto and Mr.Sudeep during the last stage of my work.

 I would like to express my heartfelt thanks to the office staff of Department of Atmospheric Science not only for carrying out all job related formalities but also for providing a very cordial atmosphere. I would also like to express special thanks to Mr. Yesodharan and Dr. Sreedevi M.G. for the care and support they gave me especially during the last stage of my work.

I am thankful to CSIR for providing me the fellowship for research. I also acknowledge the help from KNMI, Netherlands and NASA GSFC for providing me with necessary data through their websites and for the clarification to all my doubts regarding data.

# CONTENTS

## 2. Data and Methodology

## 3. Seasonal Variability of Total Ozone over India and Adjoining Regions

*Contents*

# PREFACE

Ozone present in the atmosphere not only absorbs the biologically harmful ultraviolet radiation but also is an important ingredient of the climate system. The radiative absorption properties of ozone make it a determining factor in the structure of the atmosphere. Ozone in the troposphere has many negative impacts on humans and other living beings. Another significant aspect is the absorption of outgoing infrared radiation by ozone thus acting as a greenhouse gas. The variability of ozone in the atmosphere involves many interconnections with the incoming and outgoing radiation, temperature circulation etc. Hence ozone forms an important part of chemistry-climate as well as radiative transfer models. This aspect also makes the quantification of ozone more important. The discovery of Antarctic ozone hole and the role of anthropogenic activities in causing it made it possible to plan and implement necessary preventive measures. Continuous monitoring of ozone is also necessary to identify the effect of these preventive steps.

The reactions involving the formation and destruction of ozone are influenced significantly by the temperature fluctuations of the atmosphere. On the other hand the variations in ozone can change the temperature structure of the atmosphere. Indian subcontinent is a region having large weather and climate variability which is evident from the large interannual variability of monsoon system over the region. Nearly half of Indian region comprises the tropical region. Most of ozone is formed in the tropical region and transported to higher latitudes. The formation and transport of ozone can be influenced by changes in solar radiation and various atmospheric circulation features. Besides industrial activities and vehicular traffic is more due to its large population. This may give rise to an increase in the production of tropospheric ozone which is greenhouse gas. Hence it becomes necessary to monitor the atmospheric ozone over this region. This study probes into the spatial distribution and temporal evolution of ozone over Indian subcontinent and discusses the contributing atmospheric parameters.

Ultraviolet radiation reaching the surface of the earth is strongly influenced by the ozone present in the entire depth of the atmosphere. Estimating the total column ozone is important to understand the amount of radiation getting into the earth's surface. Studying the seasonal distribution of ozone over a region can help to identify the effect of

circulation and seasonal cycle of solar radiation on ozone. The amount of ozone over a region also depends on the latitude of that region. The latitudinal dependence of ozone concentartion is examined in the thesis. The ultraviolet radiation reaching the earth's surface influenced by other factors like clouds and aerosols. Hence it is necessary to have an awareness of the sensitivity of atmospheric ozone on UV radiation. The day-today fluctuations of ozone and its dependence on UV radiation are also analysed in the thesis.

Influence of factors like variations in solar activity, atmospheric circulation patterns, Quasi Biennial Oscillation and El Nino Southern Oscillation on the concentration of atmospheric ozone is very complex. Analysing the contribution from these natural factors is important to understand the future evolution of ozone in the atmosphere and to have an insight into the effectiveness of the ozone depleting substance limiting measures undertaken by mankind. All of these phenomena occur on different timescales. Recognising the effect of each of these atmospheric phenomena requires the application of appropriate statistical tools.  An attempt is made in this study to identify the underlying patterns of ozone variation using principal component analysis.

Ozone variations in the upper stratosphere are mainly influenced by the ultraviolet radition from the sun whereas the main governing factor of ozone concentrations in the lower stratosphere is atmospheric transport. The effect of solar radiation and different atmospheric phenomena on ozone at various levels can vary from time to time Study of vertical distribution of ozone requires datasets with good spatial and temporal resolution. The study examines the possibility of a gridded dataset from satellite swath data to investigate the ozone variations over Indian subcontinent. Association of ozone with various meteorological parameters were also examined. The influence of transport on ozone becomes more prominent in the lower stratospheric region. The Upper troposphere lower stratosphere region is the interface between troposphere and stratosphere that plays an important role in the Stratosphere- troposphere exchange of trace gases. Ozone from the stratosphere can get into the troposphere through this region. Also ozone depleting substances like CFCs can get into the stratosphere from troposphere through this interface. Ozone can also act as a tracer of atmospheric motions. The variation of ozone at the Upper troposphere and lower stratosphere is also done in this study. The thesis consists of  seven chapters.

Chapter 1 gives an overview of the formation, destruction and distribution of ozone over the globe. The natural formation and destruction of ozone is described. Also the various chemical cycles leading to the formation and destruction of ozone in the atmospheric system are outlined. Some aspects of ozone climate interactions are also summarised. The structure of atmosphere and its circulation in the troposphere and stratosphere that plays an important role in the transport of ozone are also detailed in the chapter. Various reanalysis datasets used for the study and the methods of analysis are given in chapter 2. Total ozone data from Multisensor reanalysis which is used for the climatological study of ozone in this thesis is also explained. Details about Ozone Monitoring Instrument on board Aura satellite and the data provided by the instrument are given. Principal component and harmonic analysis were also described in detail. The in situ total ozone and vertical profile measurements of ozone over Indian region are also explained.

The seasonal spatial distribution of total ozone over Indian regions is examined in chapter 3. The distribution of ozone at various latitude zones over India is also analysed. The trend of ozone during different seasons along with annual trends is examined. Daily variation of total ozone over two stations was examined using total ozone data record from the stations. Sensitivity of erythemal ultraviolet radiation to total ozone over a tropical and subtropical station was quantified by computing the radiation amplification factor. Major modes of variability in total ozone were studied in chapter 4. To nature of the resultant modes were analysed by comparing with various indices of the corresponding Oscillations. Harmonic analysis of total ozone data was performed without filtering seasonal variations. Chapter 5 is an effort to explore the vertical distribution of ozone over Indian region using satellite data.

The stratosphere troposphere exchange and the distribution of upper troposphere lower stratosphere (UTLS) ozone for the tropical and subtropical station were compared in chapter 6. The tropopause height over the two stations were analysed and the ozone concentrations are found to follow the variations in tropopause height. Possible causes for this is checked using various parameters like potential vorticity, divergence, vertical velocity etc as well as with tropopause height variations. Variations in the height of the ozonopause (taken as the height of ozone minimum) and cold point tropopause were analysed to look for any possible concurrence in the fluctuations of the two. A summary of the thesis are presented in chapter 7. Future scope of research is also pointed out in the chapter. References are given in alphabetical order in the end.

# List of Tables

# List of figures

# Introduction

## 1.1.  An overview of atmospheric ozone

The air in the earth's atmosphere with its unique physical properties and chemical composition is optimal for the existence of all living beings including man. Major constituents of air are Nitrogen, Oxygen and small amount of Argon which together account for about 99.9 percent of air. Component gases of air exist in constant proportion because of the strong mixing by turbulent diffusion below a height of about 100 km. Apart from the major constituents the air also constitutes certain trace elements which are present by less than 0.1 percent altogether on an average. The trace gas constituents show variable concentrations.  Ozone is one among these trace gas elements.

Ozone exists with a concentration of only a few molecules per million molecules in the atmosphere. Ozone has a pungent odour that allows ozone to be detected even in very low amounts. Ozone will rapidly react with many chemical compounds and is explosive in concentrated amounts. It is an unstable blue gaseous allotrope of oxygen consisting of three oxygen atoms. Ozone molecule is not linear, but has an interatomic distance of about 1.278 A between any two pair of oxygen atoms and with an angle of 116°49' between them. It was discovered around 1840, by C.F. Schönbein. It is a strong oxidant. Ozone absorbs radiation in the ultraviolet and infrared wavelengths. Ultraviolet and visible radiation from the sun forms the major source of energy to the atmosphere. This incoming energy is balanced by the emission of infrared radiation from the surface of the earth and atmosphere. As an absorber of wavelengths in both the infrared and ultraviolet wavelengths ozone has a crucial role in earth's energy budget.

 Heating associated with absorption of solar ultraviolet (UV) radiation by ozone defines the vertical structure of the atmosphere and the existence of the stratosphere.   The

modification of UV radiation reaching the earth's surface by stratospheric ozone can bring changes in the chemical composition of the troposphere. Nearly 90% of ozone is present in the stratosphere. Remaining 10% resides in the troposphere. The most important part played by stratospheric ozone is the absorption of harmful ultraviolet radiation. Hence ozone in the stratosphere is considered as good ozone. Tropospheric ozone is considered as a pollutant since breathing ozone in higher doses (a few molecules per million molecules of air) can cause negative impact in human body. It is also an important component of urban smog pollution.

## 1.2.    Radiative forcing by ozone

Stratospheric ozone absorbs solar radiation in the Hartley (200-290 nm) and Huggins (290-340 nm) bands in the ultraviolet region and partly in the visible wavelengths through absorption of the Chappius (500-700 nm) band. The shorter wavelengths of the Hartley bands were absorbed above 45 km while the absorption of Chappius band is dominant below 30 km. The absorption of Infrared radiation by ozone occurs mainly in the 9.6 μm region. Radiative forcing has been used as a common tool to compare ozone changes with other components affecting the radiative balance (Isaksen and Harris, 2003) The increase in tropospheric ozone has led to a positive radiative forcing, with a larger contribution from the thermal infrared radiative forcing component than the solar forcing. Most of the global studies of the radiative effect of the increase in tropospheric ozone are based on models and there are significant differences in the estimate for same column ozone change.

Reductions in lower stratospheric ozone imply a positive shortwave and a negative longwave radiative forcing (Ramaswamy, 1992; Kiehl et al., 1999 and Myhre et al., 2001). While tropospheric ozone increases lead to a positive radiative forcing in both the shortwave and longwave spectral regions (Isaksen, 2005). But the vertical profile is of crucial importance as the solar and thermal infrared radiative forcing has different signs for ozone reduction in the stratosphere (Wang and Sze, 1980; Lacis et al., 1990; Hansen et al., 1997). Estimates of radiative forcing for future ozone changes show a large spread due to the large uncertainty in emission scenarios for future emission of ozone precursors. The concentration of ozone in the troposphere has increased significantly

since pre industrial times (Oltmans et al., 1998) due to human activities, and its global increase is estimated to give the third largest radiative forcing (RF).

The main causes for the increase in tropospheric ozone is the emissions of ozone precursors such as nitrogen oxides, carbon monoxide, methane and non methane hydrocarbons (Bernsten et al., 1997; Bernsten et al., 2000, Wong et al., 2004). Furthermore, there are large regional variations in RF due to the large regional differences in ozone perturbations. The largest regional radiative forcings are observed in the polluted regional areas in the northern hemisphere (IPCC, 2001). The possible future increases in ozone concentrations could give important contributions to climate forcing, on a regional scale, as well as global scale. Fig 1.1. illustrates the radiative forcing produced by various green house gases. It can be seen that stratospheric ozone causes a slight negative radiative forcing. But the positive radiative forcing exerted by ozone is more and third in its contribution to the net radiative forcing.
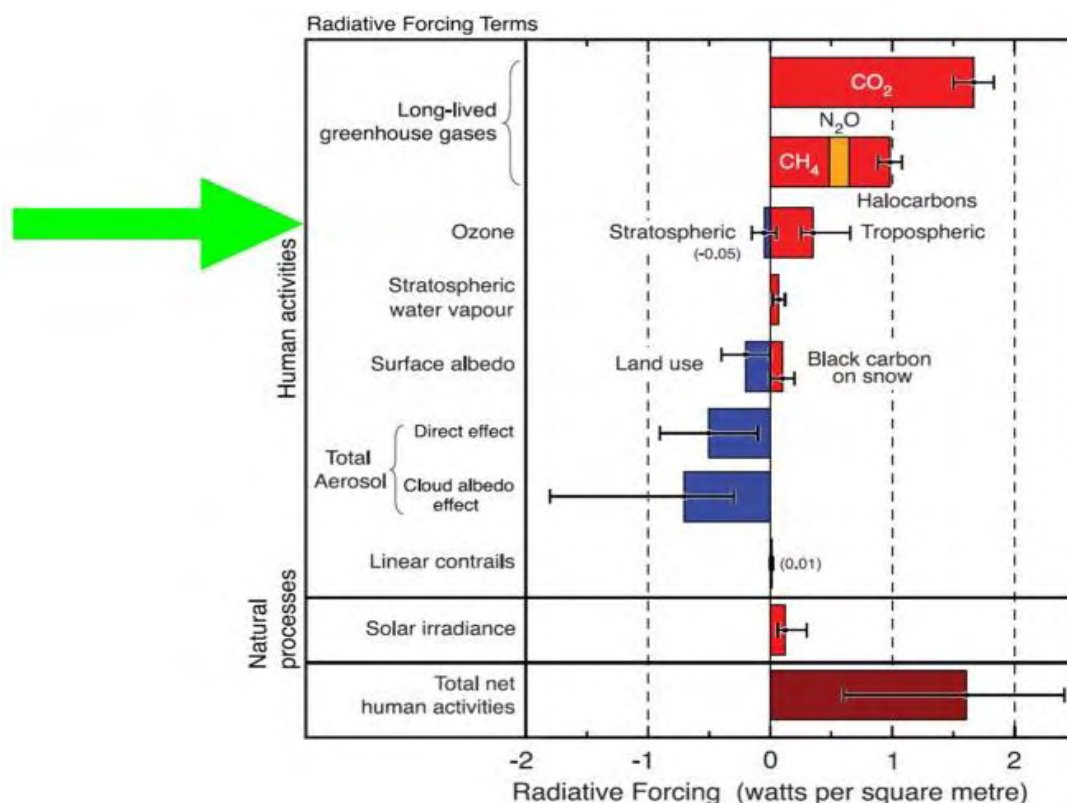


Fig.1.1. Radiative forcing of climate from 1750 and 2005 (Adopted from, IPCC AR4, 2007)

## 1.3.   Ultraviolet radiation

Ultraviolet radiation is the region of the electromagnetic spectrum where photons are sufficiently energetic to change energy states within atoms and molecules, sometimes even breaking them apart (Mohankumar, 2008). It can be divided into three on the basis of wavelength as UV-a, UV-b, UV-c. UV-a radiation has wavelength from 320-400nm, UV-b, 280-320 nm and UV-c, 200-280 nm. UV-c radiation which has the shortest wavelengths is absorbed in the upper atmosphere. A portion of UV-b reaches the surface of the earth after absorption by ozone. UV wavelengths range from 1 to 400 nm. These rays are energetic enough to break the bonds of DNA and causing damage to cells. these damaged leading to dangerous forms of skin cancer.  Increased UV radiation can also cause cataracts.

UV-b radiation can affect the growth of higher plants and mosses. Fungi and bacteria are also more sensitive to damge by UV radiation. Increased UV-b radiation can also damage aquatic ecosystems. It can also affect the reproduction and development of phytoplankton, zooplankton, fish eggs and larvae. These changes can bring about changes in biomass productivity and thus would result in reduced sink capacity of atmospheric carbon dioxide. Ultraviolet radiation can also change certain toxic chemicals from their chemical forms into biologically available forms. They reach humans by bioaccumulation of these chemicals in aquatic food chain.

## 1.4.   Basics of ozone formation and destruction

### 1.4.1.  Chapman mechanism

The basic mechanism for atmospheric ozone formation and destruction from oxygen species was proposed by Sydney Chapman in 1930. Main reactions which constitute the Chapman mechanism are as follows.

Solar ultraviolet radiation of wavelength less than 242 nm slowly dissociates molecular oxygen.

$$O_2 + h\nu \rightarrow 2O \qquad\qquad ... (1.1)$$

The oxygen atom (O) reacts rapidly with $O_2$ in the presence of a third molecule, denoted as M (usually $O_2$ or $N_2$) to form ozone,

$$O + O_2 + M \rightarrow O_3 + M \qquad\qquad ... (1.2)$$
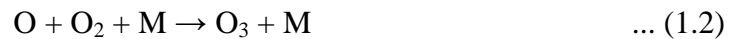
The $O_3$ molecule formed in above reaction strongly absorbs radiation in the wavelength below 320 nm to decompose back to O and $O_2$.

$$O_3 + h\nu \rightarrow O + O_2 \qquad\qquad ... (1.3)$$

Additionally, $O_3$ can react with atomic oxygen to convert back to $O_2$ molecules.

$$O + O_3 \rightarrow 2O_2 \qquad\qquad ... (1.4)$$

Reactions (1.1) and (1.2) i.e. the photolysis of oxygen molecules and dissociation of ozone by reaction with an oxygen atom, are slow reactions. But the conversion oxygen a to ozone and back (depicted by) reactions (1.2) and (1.3) occurs at a very fast rate. The thermal energy generated from these reactions is mainly responsible for the heating of the stratosphere. Highest rates of ozone production in the atmosphere can be found at around 30 km in the tropical stratosphere (Grewe, 2006) Fig.1.2. gives the schematic representation of the Chapman reactions.

### 1.4.2. Ozone loss by homogenous reactions

Observed ozone concentrations in the atmosphere cannot be explained completely by Chapman reactions. Estimated total ozone values from Chapman mechanism are too high in tropics and too low at higher latitudes. Other mechanisms in controlling ozone amount are the stratospheric circulation and ozone destruction by catalytic reactions involving atomic chlorine and bromine (Molina and Rowland, 1974), hydroxyl radical and nitric oxide (Crutzen, 1970). All of these radicals have natural and anthropogenic sources.
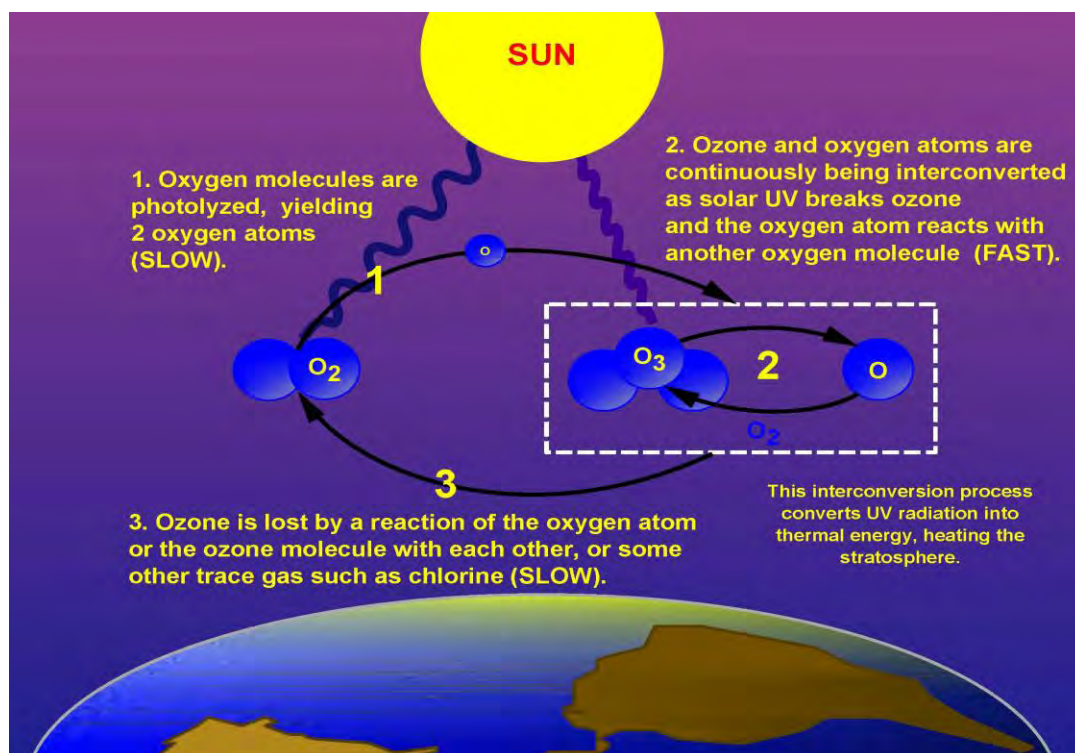
Fig.1.2. Schematic of Ozone formation and destruction by Chapman mechanism.

The reactions can be represented in general form as

$$X + O_2 \rightarrow XO + O_2 \qquad \qquad ...(1.5)$$

$$O + XO \rightarrow O_2 + X \qquad \qquad ...(1.6)$$

Where, X and XO are chain carriers involving HOx, NOx, ClOx and BrOx families and X=OH, NO, Cl, Br.

The reaction catalysed by NO causing destruction of ozone is most efficient at heights around 35-40 km (Crutzen, 1970). Ozone destruction by reaction with hydrogen radicals, occurs effectively near the tropopause (Brasseur and Solomon, 1986). Most important is the reaction of ozone with the chlorine radicals that lead to the formation of Antarctic ozone hole. Most of OH and NO in the stratosphere is of natural origin, but human activity has dramatically increased chlorine and bromine. They are found in certain stable

compounds, especially chlorofluorocarbons (CFCs), which may find their way to the stratosphere. There has been considerable increase in CFCs starting from 1960s due to their larger usage as refrigerants, aerosol propellants and foam blowing agents. Reactions between various families of compounds also can give rise to certain reservoir species like chlorine nitrate ($ClONO_2$) which are relatively nonreactive. The formation of the reservoir species makes less chlorine available for the formation of more reactive and hence ozone destroying forms of chlorine.

### 1.4.3. Heterogenous Chemistry and Antarctic ozone hole

Significant depletion of stratospheric ozone in spring over Antarctic was reported by British Antarctic Survey team in 1985 (Farman et al., 1985). These findings were later confirmed by satellite data. Enormous decreases in high latitude ozone during spring have become a regular phenomenon, and is widely known as *Antarctic ozone hole*. Maximum ozone depletion occurs at the heights at which the polar stratospheric clouds (PSCs) were formed. Hence it was realized that the PSCs which are the special clouds formed during polar winter play larger role in ozone loss through heterogenous chemistry. Polar stratosphere is very cold during winter and early spring, especially in southern hemisphere, polar stratospheric temperature can reach as low as 185 K. Low temperatures make the polar night jet isolated from the surrounding for quite long time. In such a dynamical situation even very little amount of water vapor gets condensed to form the polar stratospheric clouds (PSCs). A natural layer of aerosols (mainly sulphates) in polar lower stratosphere generally provides the required cloud condensation nuclei. In Southern Hemisphere (SH), polar stratospheric temperatures are extremely low, PSCs form in early winter and persist till late winter (Peter, 1997).

PSCs act as platforms for ozone destruction by a series of chemical reactions that involves the formation of active chlorine that can destroy ozone. In Arctic stratosphere, due to unstable polar vortex denitrification and dehydration are not regular phenomenon.

In first step, PSCs absorbs gaseous HCl efficiently followed by heterogeneous reaction,

$$HCl(s) + ClONO_2 \rightarrow Cl_2 + HNO_3 \qquad\qquad ... (1.7)$$
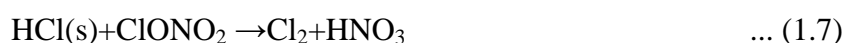
where (s) denotes the species on the surface of ice.

This reaction occurs when temperatures drop below 200 K. Gaseous $Cl_2$ released from PSCs in above reaction rapidly photolyses to produce free chlorine atoms, while $HNO_3$ remains trapped in the ice. Such a trapping of $HNO_3$ further facilitates catalytic ozone loss by removing NOx from the system which might otherwise react with ClO to form $ClONO_2$,

$$Cl_2 + h\nu \rightarrow 2Cl \qquad \qquad ... (1.8)$$

$$2[Cl + O_3 \rightarrow ClO + O_2] \qquad \qquad ... (1.9)$$

Efficiency of ozone loss by above reaction critically depends on cold temperatures and sunlight. Absence of either of them leads to termination of ozone destruction mechanism. Cold temperatures are needed to form PSCs to provide surfaces for heterogenous reactions. The reservoir species such as $ClONO_2$ and $H_2O_2$ reacts heterogeneously with PSCs on which HCl have been absorbed to form HCl, HOCl or $ClNO_2$. Sunlight is required to photolyse gaseous $Cl_2$, HCl and $ClONO_2$. Such conditions are available in polar stratosphere during early spring, which causes such large ozone losses and hence the formation of the ozone hole.

## 1.5. Montreal Protocol

Montreal protocol was the first international agreement to restrain the emissions of chlorofluorocarbons (CFCs) that cause damage to the ozone layer. Several subsequent amendments (London 1990, Copenhagen 1992), were also performed to respond to the increased urgency to protect the ozone layer. The Montreal Protocol has emerged to be one of the most successful international environmental treaties, and by now the production and use of CFCs has almost ended. Ozone levels have started recovering in accordance with the slowdown of stratospheric halogen emissions, due to the global phase-out of many ODS from the successful implementation of the Montreal Protocol and its amendments (WMO, 2006, 2010). Tropospheric total chlorine concentrations

(mostly CFCs) reached its highest value in early 1994 and will continue to diminish over the coming decades.

## 1.6. Ozone distribution in the atmosphere

### 1.6.1. Zonal distribution of atmospheric ozone

The actual distribution of ozone is not simply a balance between production and loss. Winds can transport ozone away from the production region, altering the basic distribution of ozone, and the impact of ozone on the surface UV. The total column amount of ozone generally increases from the tropics to higher latitudes in both hemispheres. Generally column amounts are greater in the northern hemisphere high latitudes compared to southern hemisphere high latitudes. The highest amounts of column ozone over the Arctic occur in the northern spring (March-April), but in Antarctic, the lowest amounts of column ozone occur in the southern spring (September-October).
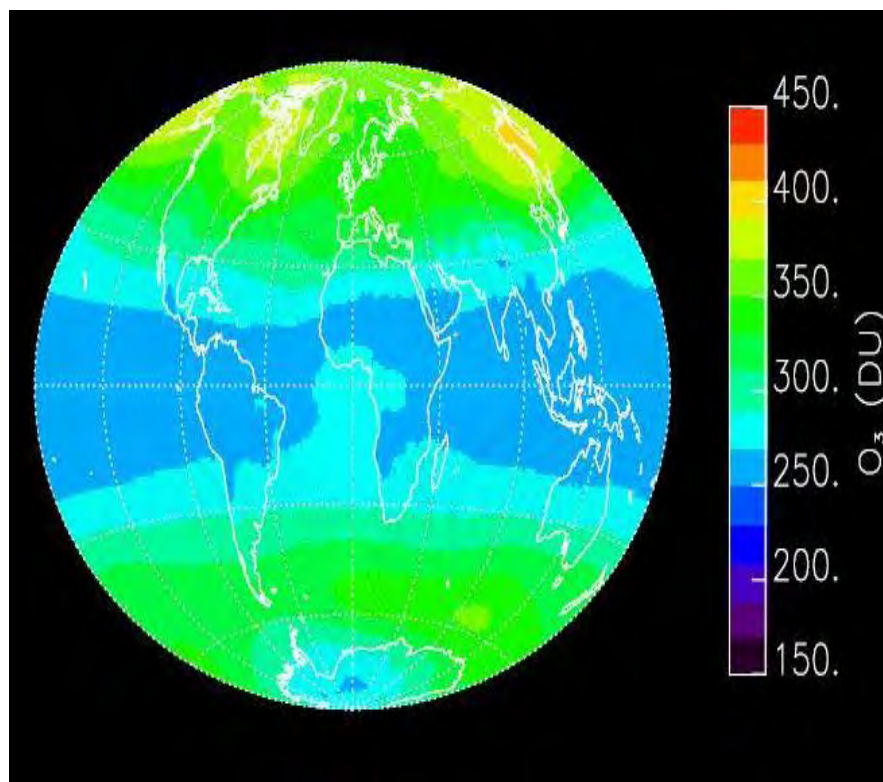


Fig.1.3. Global distribution of atmospheric ozone (Source: Stratospheric ozone. An Electronic textbook)

Highest values of column amount ozone anywhere in the world are found over the Arctic region during the northern spring period of March and April. The amounts then decrease during the progress of the northern summer. Meanwhile, the lowest amounts of column ozone are found over the Antarctic in the southern spring period of September and October, due to ozone hole phenomena. Global distribution and mean annual cycle of ozone can be seen in Figures 1.3 and 1.4 respectively.
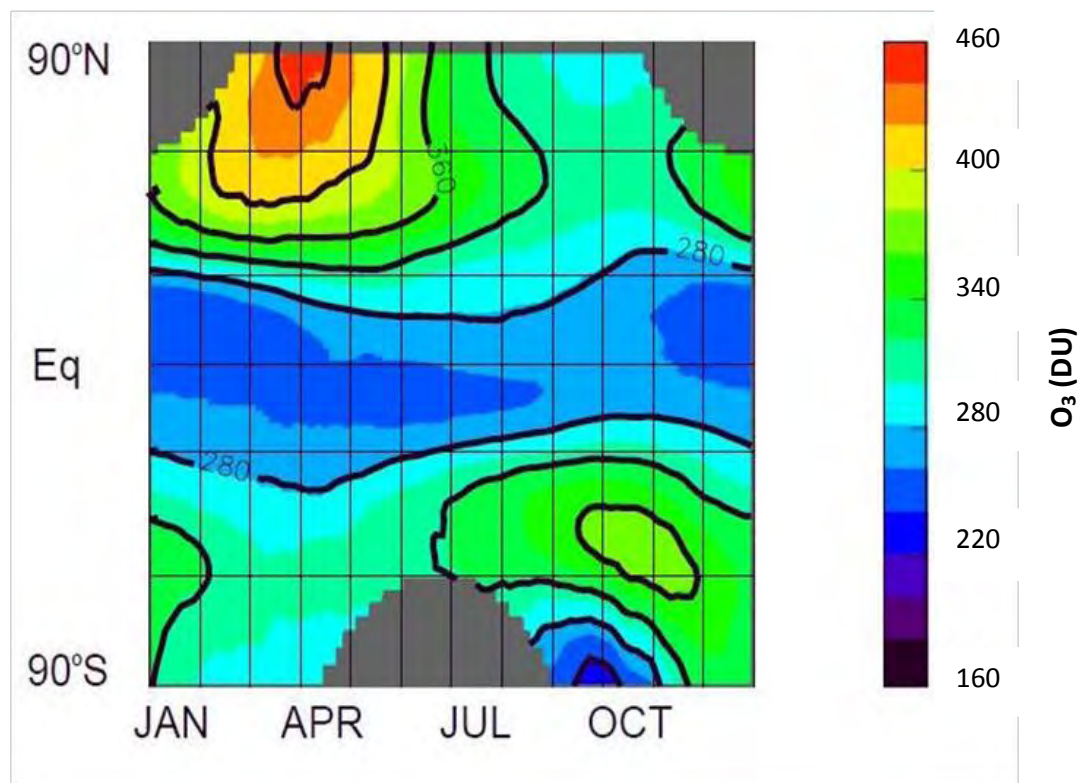


Fig.1.4. Mean annual cycle of atmospheric ozone (Source: Stratospheric ozone. An Electronic textbook)

### 1.6.2. Vertical Distribution of ozone

Ozone over a given location depends on creation destruction and transport. Production of ozone occurs chiefly in the stratosphere where there is sufficient ultraviolet (UV) light from the sun is available. Consequently most of ozone molecules are found in the stratosphere. Near the surface of earth, less ultraviolet (UV) light penetrates to break apart the regular oxygen molecules that are required for the creation of ozone, which at a given spot depends on the amount of ozone already in a column above the spot. Thus, it

is obvious that ozone formation in the stratosphere reduces the formation of ozone lower down in the troposphere. This makes the ozone concentration small at low altitudes. The atmosphere thins rapidly with height. The amount of oxygen for ozone creation decreases at higher altitudes. Thus, less ozone is able to form even though the UV light is available. The result of these two contrasting effects i.e. less UV light with decreasing height and less oxygen with increasing height produce the observed ozone profiles. Ozone amounts peak between 20 and 40 kilometres with a steady decrease above and below the peak. Ozone can be vanishingly small near the surface and as high as 10 ppmv in the stratosphere. Characteristic vertical profile of ozone is given in Fig.1.5.
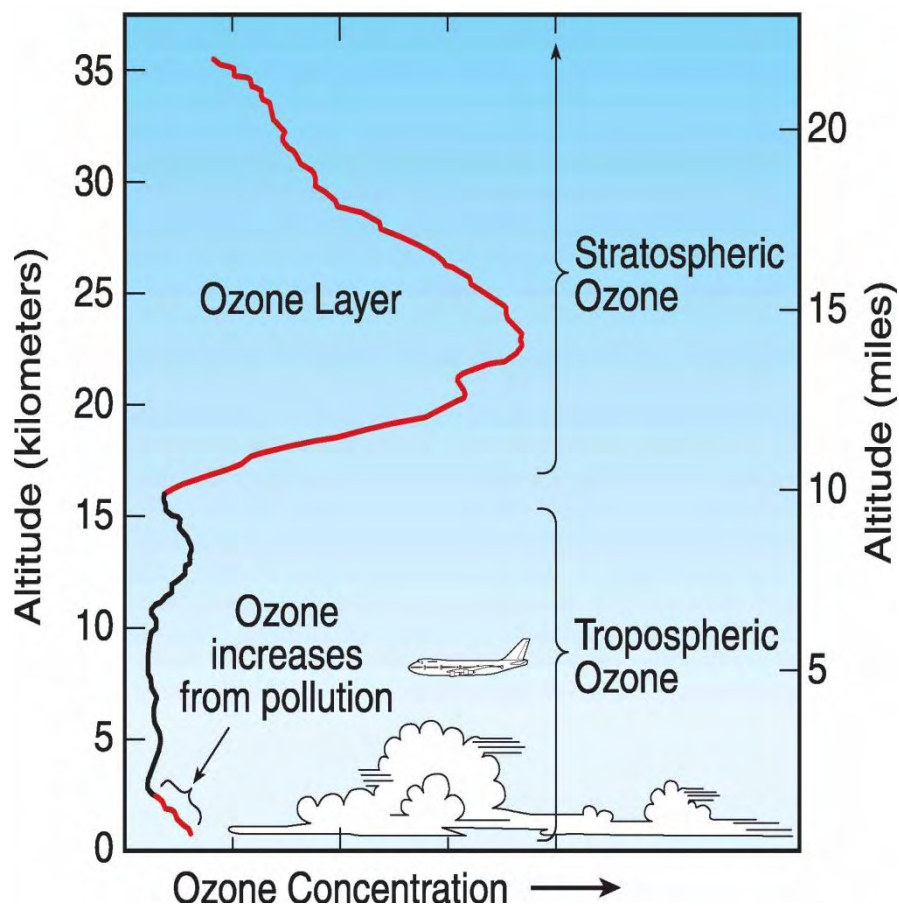


Fig. 1.5. Vertical distribution of ozone in the tropics, middle latitudes and high latitudes. (Source: WMO Scientific Assessment of Ozone Depletion)

## 1.7.    Structure and Circulation of the Stratosphere

The temperature of the stratosphere increases with height. Thus warmer air overlays colder air. If an air parcel is to be displaced to a higher altitude, it would be colder than its surroundings. Due to its higher density, the parcel would sink back to its original location. Eventhough it would overshoot slightly because of its momentum, it would drop to a location where it would be warmer than its surroundings. Thus the stratosphere is stably stratified.

The stratosphere itself can be divided into four distinct regions (Stratospheric Ozone: an Electronic Textbook). They are

(a) **The tropics:** which stretch from about 20°N to 20°S. This is the photochemical source region of ozone production due to the sufficient availability of high energetic ultraviolet radiation.

(b) **The middle latitudes:** characterised by the turbulent mixing of airmasses from tropics and poles.

(c) **The polar vortex:** In the stratosphere during winter, a band of strong winds referred to as a jet stream sets up along the zone of greatest temperature change along the polar night terminator, the line that divides sunlight from the long polar night. This is called polar night jet. The region poleward of the polar night jet which is isolated from the rest of the stratosphere is called polar vortex.

(d) **The lowermost stratosphere:** which is special region that contains a mixture of both tropospheric and stratospheric air. The general circulation in the stratosphere for equinox and solstice conditions.

During solstice conditions, the horizontal temperature and pressure distinction between the warm summer hemisphere and the cold winter hemisphere result in pole-to-pole gradients. Winds then blow towards west in the summer hemisphere and eastwards in the winter hemisphere. At the time of equinoxes the equatorial area is warmer compared to the poles, As result of the pressure gradient from the equator to poles and the Coriolis force, westerlies occur in both the hemispheres.
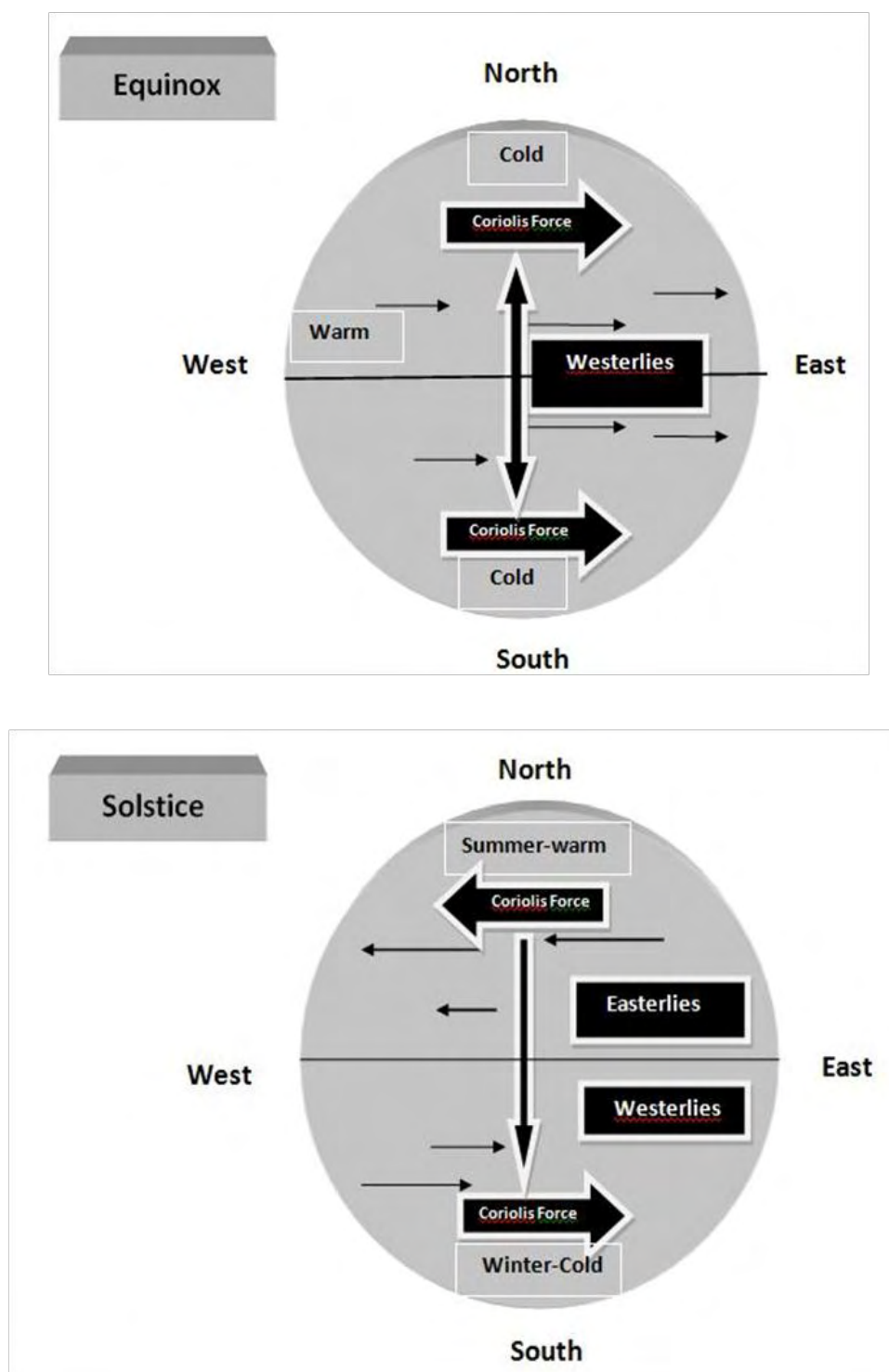
Fig.1.6. Circulation in the stratosphere for equinox and solstice (NH summer) conditions. Coriolis force deflects air flow to the right (west) in the NH and to the left (east) in the SH.

## 1.8.    Brewer Dobson circulation

The Brewer Dobson Circulation (BDC) is a slow, meridional overturning circulation in hemispheric-scale that occurs in the stratosphere (Brewer, 1949, Dobson, 1956). This circulation establishes itself during the winter season with air moving upward in the tropics which subsequently moves poleward and downward in the extratropics. The circulation explains the observed distribution of stratospheric trace gases, like ozone and water vapour.
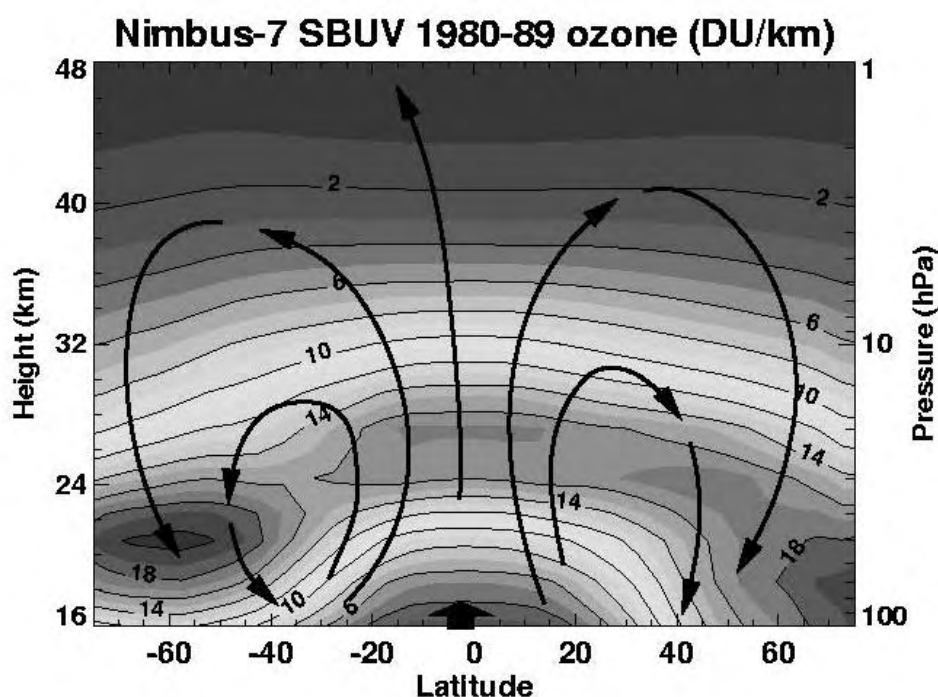


Fig.1.7. Time-altitude representation of global distribution of ozone. The arrows represent the Brewer-Dobson Circulation. (Source: Stratospheric Ozone. An Electronic textbook )

The air uplifted through tropopause is very low in ozone and high in CFCs. The circulation transports the uplifted mass poleward, on the order of 20-30 meters per day and nearly 90% of the mass move towards middle latitudes.  Ozone is being created during the slow uplift of air, by the interaction of solar UV radiation and molecular oxygen. The slow lifting circulation allows enough time for ozone to build-up irrespective of the slow rate of ozone production reactions. Most of the CFCs passing the tropical tropopause get transported to higher latitudes even though intense ultraviolet

radiation can break them apart. This is because a few molecules can reach the higher levels to react with the strong UV radiation. The time needed to reduce the CFC-levels to 63% is about 120 years.

This poleward and downward circulation branch of Brewer-Dobson circulation tends to enhance ozone concentrations in the lower stratosphere of the middle and higher latitudes. This circulation is caused by planetary waves that exist due to a combination of meridional temperature gradients and the rotation of the planet. These waves extends for thousands of kilometres in the horizontal and a few possess a horizontal extent of thousands of kilometers and a few kilometers in the vertical. Large scale topographical structures like mountains and land sea contrast, together with the meridional temperature gradients and Coriolis deflection, generates standing planetary waves that remain stationary or move slowly westward. They propagate vertically into the stratosphere. The general circulation is zonal in nature and the circulation from these waves cause a meridional rift inside the flow. Hence this circulation is known as meridional circulation (Newman et al., 2001; Plumb, 2002). When these waves reach the stratosphere, they deposit easterly momentum, thus slowing the westerly wintertime stratospheric jet stream. This is known as wave breaking.

Due to the deposition of the momentum the stratosphere get suddenly warmed. It produces the phenomenon of the stratospheric sudden warming. This result is a situation that is thermodynamically imbalanced. Wintertime radiational cooling in the polar stratosphere quickly begins. This cooling of air is accompanied by sinking motions, since colder air is denser and it sinks. It is this sinking motion that establishes the meridional overturning from equator to pole in the winter hemisphere. That is, the sinking air in the polar region must be balanced by a poleward flow of air into this region. For the conservation of mass, this air must come from the tropics. The Brewer-Dobson circulation cell is thus established as tropical air moving poleward to replace the sinking air at the poles is itself replaced by rising air in the tropics. The net chemical production is high in winter hemisphere (Chipperfield and Jones, 1999), with the long life of ozone molecules at higher latitudes combined with new ozone being produced photochemically by upwelling in the tropics. (Fusco and Salby 1999). The Brewer Dobson circulation thus acts as a photochemical engine that increases the overall ozone concentration.

 The average time of residence of air is about 5 years (Waugh and Hall, 2002). Hence it takes more than 50 years to process the ozone depleting substances that are present in the troposphere which is transported upward to the stratosphere. The rate at which the BDC pumps the tropospheric air into stratosphere is important since it determines the exposure of these substances to extreme ultraviolet radiation that destroys and removes them (Holton 1995). An increase of greenhouse gases can strengthen the BDC and speed up the recovery of ozone (Butchart and Scaife, 2001; Butchart et al., 2006; Li et al., 2007; Garcia and Randel, 2008). Model studies such as Austin et al. (2006) suggest that the rate of increase of tropical mass upwelling varies from decade to decade.

## 1.9.    Other factors affecting ozone concentration

### 1.9.1.   The Quasi-Biennial Oscillation

Quasi-biennial oscillation (QBO) is one of the large scale effect that causes the year-to-year variability in the total ozone distribution (Naujokat, 1986; Gray and Pyle, 1989; Reid, 1994).  The QBO is the reversal in direction of the zonal winds in the tropical stratosphere, which, at altitudes of 15 km to 30 km occurs on a time scale of 26 to 28 months, hence the name quasi-biennial. It is caused due to the internal dynamics of tropical waves.  The easterly winds are generally stronger than the westerly winds, persist longer at upper levels (approximately 30 km altitude), and have maximum wind speeds centered over the equator near 26 km. Westerly wind regimes descend faster in time and persist longer at lower levels than easterly wind regimes. Below 15 km, there is little evidence of the QBO. Near the equator, the oscillation is fairly symmetric, while in the subtropics, the oscillation combines with the annually (seasonally) varying westerlies of the winter hemisphere.

Photochemical balance of the stratosphere is affected by the temperature changes associated with QBO which can change reaction rates and thus changing the ozone amount. The phenomenon also causes direct modification of the Brewer-Dobson circulation.  When QBO is in its easterly phase, the polar vortex is less secluded and hence, warmer. A positive temperature gradient from pole to equator (cold to warm) causeses increasing westerly winds with height, while a negative temperature gradient from pole to equator (warm to cold) generates decreasing westerly or increasing easterly

winds with height. This physical relationship shows that the transition zone between westerly and easterly winds will be a warm temperature region. These temperatures can alter ozone in two ways. First, in the tropical upper stratosphere, temperatures modulate photochemical reaction rates, such that warm temperatures are linked with lower ozone and colder temperatures are coupled with higher ozone levels.

Second, temperatures can directly influence the circulation by amending the heating and cooling rates. The QBO descending easterly phase keeps colder temperatures between the overlying easterlies and underlying westerlies. When the QBO is in its westerly phase, the polar vortex is more stable, more isolated and as a result , colder. The latter situation is more conducive for the formation of PSC and therefore cold give rise to a higher degree of ozone depletion inside the vortex (Lait et al., 1989).  Earlier vortex breakup is possible if the middle stratospheric winds are in the opposite direction to the circulation around the vortex, i.e. when the QBO is in its easterly phase. The result is that the infrared cooling to space will be smaller than normal in the QBO cold region.

Because the heating from solar UV is roughly constant, the weakened cooling to space means that the total heating in the tropics is somewhat higher. This greater heating in the tropics results in a acceleration of the normal Brewer-Dobson lifting in the tropics. On the other hand, the QBO descending westerly phase maintains warmer temperatures between the overlying westerlies and underlying easterlies This result in great infrared cooling of the space than normal in the QBO warm region. Again, because the heating from solar UV is nearly constant, the greater cooling to space means that the total heating in the tropics is somewhat smaller. This lesser heating in the tropics results in a slowing up of the normal Brewer-Dobson lifting in the tropics (Baldwin *et al.,* 2001). These downward and upward motions associated with the QBO at the equator are balanced by upward and downward motion in the subtropics, respectively. This circulation cell which is connected by poleward or equatorward motions, is called the QBO-induced meridional circulation.

The subtropical branch of the QBO-induced circulation cell is positioned roughly between 15°N and 15°S. The QBO-induced circulation has an effect on trace gas constituents in the tropical stratosphere. QBO signals in ozone, methane, hydrogen fluorine and nitrous oxide have been reported from long term satellite observations.

Ozone is primarily under dynamical control below 30 km in the tropical regions, and thus is affected by the QBO-induced circulation that exists atop the Brewer-Dobson circulation. But for the region above 30 km, ozone becomes increasingly under photochemical control, and thus responds to the QBO-induced temperature anomalies rather than transport effects.

The descending westerlies of the QBO are coupled with a vertical circulation pattern that produces downward motion in the tropics and upward motion in the subtropics, thus weakening the normal Brewer-Dobson circulation in the tropics. Because the upward motion of air is slowed down and because the vertical gradient of ozone mixing ratio is positive in the lower stratosphere (i.e. increasing ozone with altitude), ozone production can continue for longer periods. The result is a positive column ozone anomaly in the tropics and a negative anomaly in the subtropics. In the descending easterly phase of the QBO when the Brewer-Dobson circulation in the tropics is enhanced, ozone production has less time to occur, and the column ozone anomalies are inverted, resulting in a negative ozone anomaly in the tropics and a positive ozone anomaly in the subtropics.

QBO signals are observed in dynamical variables and constituents fields, such as column ozone and water vapor, in the stratosphere. Estimates of the magnitude of the midlatitude total ozone QBO range from 5-20 DU. The QBO depends on atmospheric waves. The three principal types of waves are gravity waves, mixed Rossby-gravity waves, and Kelvin waves. Dissipation of vertically propagating equatorial waves is the source of momentum responsible for causing the wind QBO (Lindzen and Holton, 1968; Holton and Lindzen, 1972). These waves, results from unsteady latent heating inside tropical convection and they transfer energy into the middle atmosphere, driving the zonal mean winds.

## 1.9.2. Solar cycle

The solar radiation changes on short as well as long time scales. Changes in solar UV irradiance influence atmospheric ozone burden through radiative and chemical interaction with climate. The small changes in UV radiation can alter ozone production rate and hence dynamical structure of the atmosphere through radiative heating. There is also observational evidence of increase in ozone in tropics during solar maxima (Hood et al., 1997, Randel and Wu, 2007). Modelling studies with general circulation models

show consistent dynamical response with enhanced solar radiation and associated ozone changes. This response can be amplified through QBO, changes in Hadley cell circulation and movement of Ferrel cell (planetary waves are generated in this region) towards the polar region.

The variation in solar irradience can also have an effect on the stratospheric circulation because of changes in the radiative heating of the stratosphere as a result of the solar influence on ozone production (Hood, 2003). There is in fact a small positive correlation, with a 1-2% variation in total ozone, in phase with the solar cycle (Staehelin et al., 2001). There is also a 27 day cycle in solar irradiance, which results from the rotation period of the sun. The effect of this can be seen in upper stratospheric ozone values, which exibit a peak to trough difference of 4 - 6%.

### 1.9.3. El Nino Southern Oscillation

El Nino is a shifting of the warmest sea surface temperatures from the western Pacific to the eastern and central Pacific. This occurs with a frequency of nearly 3-5 years. The change in surface pressure associated with El Nino is known as the Southern Oscillation. The Southern Oscillation involves the shifting of the low pressure zone which is typically present over the western Pacific and Indian Ocean, to the eastern Pacific. The shifting location of convective cells brought about by ENSO results in a change in the tropical circulation. Effects of the ENSO are also felt in the extra tropics. The change in circulation patterns associated with ENSO can bring about changes in ozone amounts also.

The effect of the ENSO phenomenon on total ozone was has been the subject of many studies (Bojkov 1987; Shiotani 1992; Randel and Cobb 1994; Kayano 1997; Thompson and Hudson, 1999). An El Nino event can result in a weaker than normal polar vortex, and a strengthened meriodinal transport, which would have increased transport of ozone to the extratropics. The corresponding increase in decent over the polar areas would have warmed the polar stratosphere and lead to high Arctic total ozone in late winter. Hasebe (1993) deduced that the variations in tropopause height due to ENSO related convection anomalies can bring changes in ozone concentrations.

### 1.9.4. Changes in greenhouse gases

Significant increases in well-mixed greenhouse gases (GHGs) is estimated in recent decades (IPCC, 2001). Anthropogenic emissions are still increasing and there is no sign of a future decline of their atmospheric concentrations. These emissions are normally believed to lead to global warming in the troposphere and cooling in the stratosphere and may accelerate the rate of climate change. Increases in GHGs also have a dual effect. It leads to global warming and global warming increases GHGs emission through natural processes. The average global surface temperature is expected to rise by 0.6- 2.5°C in the next century, with considerable regional variation. Evaporation will increase as the climate warms, which will increase average global precipitation. Soil moisture is likely to decline in many regions and intense rainstorms are likely to become more frequent. The changes in temperature caused by GHG increases can affect the ozone concentrations by influencing the reaction rates of ozone formation and destruction.

### 1.9.5. Volcanic eruptions and aerosols

After large volcanic eruptions, sulphur containing gases, such as $H_2S$ and $SO_2$, fine particles of magma and ash are injected in to the stratosphere. They get converted to $H_2SO_4$. This takes up water and forms aerosol droplets. Heterogenous reactions on the surface of aerosols lead to the destruction of ozone. The increased aerosol loading can also influence the dynamics of the stratosphere due to the absorption of heat by aerosols. Thus they can influence vertical and meridional circulation. The enhanced meriodional circulation increases the ozone concentrations in the extratropical lower stratosphere (Chandra and Stolarski, 1991).

The residence time of volcanic aerosols in the stratosphere is around 12-18 months (Staehelin et al., 2001), after which time ozone values should have largely recovered. The increased heterogeneous chemical.ozone losses are not beleived to be large in the tropics, however they become more important at higher latitudes in winter and spring when temperatures are lower and solar zenith angles are higher. Because of the increase in surface area avaliable for heterogeneuous halogen activation reactions, volcanic eruptions should cause more ozone loss when the abundance of halogens in the stratosphere is higher.

### 1.9.6. North Atlantic Oscillation and Arctic Oscillation

The North Atlantic Oscillation (NAO) is a regional climate pattern. It is the large scale fluctuation in atmospheric pressure between the subtropical high pressure system located near the Azores in the Atlantic Ocean and the sub polar low pressure system near Iceland. Arctic Oscillation (AO) is considered as the global extension of NAO. In this circulation pattern the atmospheric pressure over the polar regions varies out-of-phase with that over middle latitudes (about $45^{\circ}$N) on time scales ranging from weeks to decades. These two atmospheric modes play an important role in controlling the ozone amounts of midlatitudes. The surface pressure steers surface winds and winter storms from west to east across the north Atlantic affecting climate from England to Western Europe as far eastward as central Siberia and eastern Mediterranean and southward to west Africa. When the NAO is in its positive phase, tropopause pressure is higher at high latitudes and lower at low latitudes. Since total ozone is related to tropopause pressure, this results in higher ozone values at higher latitudes and lower total ozone values at lower latitudes.

The mixing of ozone poor vortex air into the mid latitudes may also have a considerable impact on ozone trends in the northern mid-latitudes. This mixing depends upon the amount of ozone destruction within the vortex, and upon the rate at which the ozone depleted air is transported into the mid-latitudes. Dilution is expected to affect ozone values at lower latitudes up until about November of the same year, but it is not expected that any signal will be carried over into the next year. However, if there is an increasing amount of dilution every year, it can contribute to a long term seasonal ozone trend.

## 1.10. Interaction of ozone with weather and climate

Long term decrease in stratospheric ozone concentration has been reported in a number of studies (WMO, 2006, 2010). But the coupling between stratospheric ozone and climate (or associated forcing) is quite complex and contains variety of direct and indirect effects and feedback mechanisms. Although ozone abundance is very small (just a few parts per million), it is a strong greenhouse gas and hence plays an important role in determining radiative (and dynamical) structure of the atmosphere. Some of the important mechanisms of ozone-climate interaction are shown in Figure. 1.9
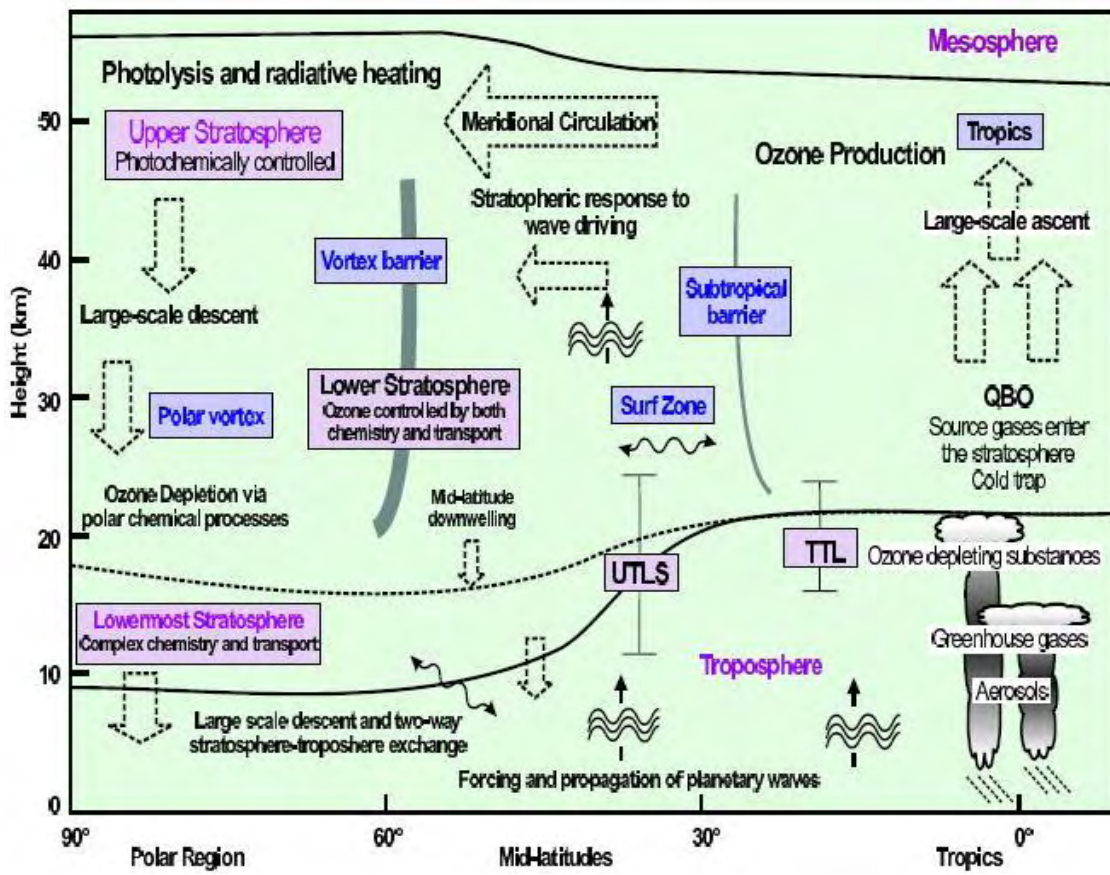
Fig. 1. 8. Schematic diagram of the different regions and some of the important processes in the troposphere and stratosphere. Broad arrows indicates direction of BD circulation and wavy arrows denote transport along isentropic surfaces. The average position of the tropopause is denoted by the lower thick-black line, the average position of the stratopause by the upper thick-black line, and the 380-K isentropic surface by the thick-black dotdashed line. (Source: Eyring et al., 2005)

Some of these mechanisms contribute significantly to ozone variability while some of them have quite minor influence on ozone. In order to understand future evolution of ozone layer, it is necessary to have a good understanding of their influences. Interactions between ozone and climate change can be mediated through changes in chemistry, dynamics and radiation of the atmosphere.
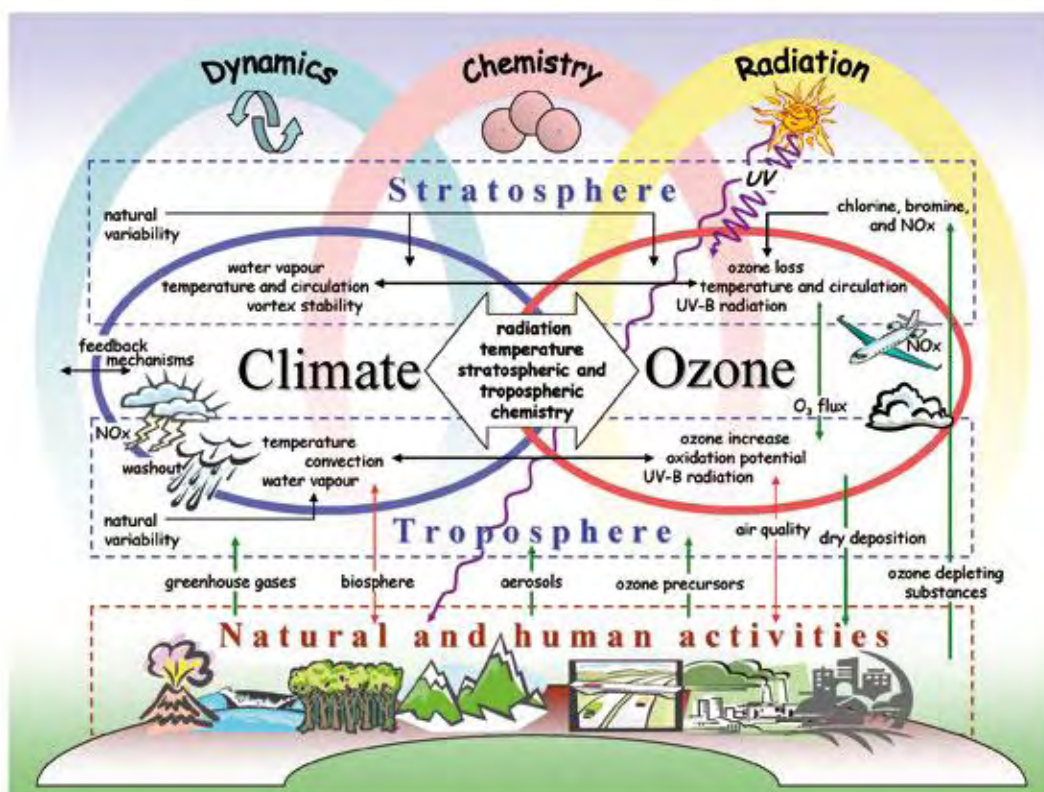
Fig.1.9. Different pathways of ozone-climate interactions (Source: EC Air pollution research report no.81, 2003)

## 1.10.1. Daily variations of ozone in response to weather patterns

Total ozone undergoes strong day-to-day variations associated with synoptical processes and these variations can be comparable with the annual cycle magnitude. Dobson et al. (1930), based on total ozone observations from several European sites, found that on average high total ozone values coincide with cyclones and low values with anticyclones. The weather-ozone relationship results from redistribution of ozone in the lower stratosphere by horizontal and vertical advection (e. g. Reed, 1950). The passage of a wave crest (anticyclone) causes ascending motions in the upper troposphere and lifting of the tropopause as well as adiabatical cooling. Since the concentration of ozone is low below the tropopause and rapidly increasing above such ascending motion results in convergence of ozone-poor air below the tropopause and divergence of ozone-rich air above, leading to net decrease in total ozone column. The passage of a wave trough

(cyclone) has the opposite effect and total ozone increases .The same mechanism explains the fact that total ozone correlates well with temperature and geopotential in the UTLS region.

Meridional advection also plays an important role in the ozone-weather relationship. Ozone amount increases northward in the NH (with the exception of the summer polar region) thus southward advection associated with troughs brings air with higher ozone concentration while northward advection in ridges brings air with lower ozone concentration. The maximum negative correlation between total ozone and geopotential are found in the region which coincides with the strongest northward ozone gradient (Stanford et al., 1995). Hence both vertical and meridional advection works in the same direction producing growth of total ozone in troughs and reduction in ridges.

## 1.11. Stratospheric cooling and ozone

The lower stratosphere is observed to be decreasing in the recent decades (WMO, 2010) and ozone change is thought to be the main contributing factor to this decrease (Ramaswamy et al. 2006; Eyring et al. 2006). The temperature decrease is found at higher altitudes but is also marked at lower latitudes. Myhre et al., (2001) found that the longwave component of ozone absorption is more dependent on altitude changes than the solar component. Changes in stratospheric temperature have a two way effect. Ozone loss reactions in the stratosphere are determined by the concentration of chlorine, bromine, nitrogen and hydrogen oxides, and the reactions rates are highly responsive to the temperatures.

A reduction in stratospheric temperatures leads to an increase in heterogenous chemical ozone loss and this decrease further augments stratospheric cooling. In addition, variations in temperatures ultimately affect climate by altering stratospheric (and tropospheric) dynamical processes. As shown by Ramaswamy et al. (2001), global and annually averaged stratospheric temperatures have diminished during the past three decades. Radiosonde and satellite data denote statistically significant cooling trend in middle stratosphere after 1980s compared to prior period. It has been suggested that the effects of ozone and $CO_2$ are responsible for the observed stratospheric cooling

(Ramaswamy et al., 2001) and such change may further intensify the strength and duration of the polar vortex and subsequently augment the ozone depletion (Langematz et al., 2003).

## 1.12. Other relevant concepts

### 1.12.1. The Upper Troposphere and Lower Stratosphere

The Upper Troposphere/Lower Stratosphere (UTLS) region is crucial for troposphere-stratosphere coupling as well as for chemistry-climate coupling (e.g. Shepherd, 2007). During its transport across this interface airmass encounters different atmospheric characteristics in atmospheric parameters  Thus the passage through  across this region causes the transition in the properties of the air from stratospheric to tropospheric regime and vice versa. The tropopause can be considrered as the 380 K isentropic (line of constant potential temperature) surface. Moving from the equator to poles, a considerable part of the stratosphere comes under the 380K isentrope. This region is called the lowermost stratosphere. The region from the top of convective outflow to the lower stratosphere is called the upper troposphere/lower stratosphere and it is very important in the stratosphere troposphere exchange of ozone and other trace gases and they display strong gradients across the tropopause (Pan et al., 2004). Changes in the temperature of the tropopause influence the radiative forcing by green house gases in the UTLS region (Forster and Shine, 1997), thus affecting the climate (Solomon, 2010).

Tropopause altitude shows temporal as well as spatial variation. The temporal variation of tropopause in times scales such as from sub-daily to solar cycle.  Since these troughs and ridges propagate, the tropopause height exhibits frequent fluctuations at a particular location during midlatitude winters (Mohanakumar, 2008). Severe thunderstorms in the intertropical convergence zone (ITCZ) and over midlatitude continents in summer continuously push the tropopause upwards and as such deepen the troposphere. A pushing up of tropopause by 1 km reduces the tropopause temperature by about 10 K. Thus in areas and also in times when the tropopause is exceptionally high, the tropopause temperature becomes very low, sometimes below 190 K.

The highest tropopause is seen over south Asia during the summer monsoon season,where the tropopause occasionally peaks around 18 km. On the other hand, cold conditions lead to lower tropopause, evidently due to weak convection (Mohanakumar, 2008). There are various tropical tropopause definitions which has some advantages and disadvantages. These definitions are based on the thermal properties of the tropical atmosphere. It is at the tropopause where the transition from decreasing temperature with altitude to increasing temperature with altitude occurs. The tropopause separates the troposphere from the stratosphere. The position of the tropopause varies with latitude. The equatorial tropopause is situated at around altitude 18 km and it slopes down to higher latitudes reaching about 8km at the pole. This corresponds to the 380 K isentropic surface. The tropopause altitude also varies from troughs to ridges, with low tropopause altitude in cold troughs and high in warm ridges.

## 1.12.2. Stratosphere-troposphere coupling

Waves from the troposphere are key driver of stratospheric (and mesospheric) dynamics. The extra-tropical tropospheric waves drive the meridional BD circulation. Equatorial tropospheric waves generate the dominant mode of variability in the equatorial stratosphere, the quasi-biennial oscillation In turn, the QBO affects, among other things, the middle atmospheric large-scale circulation and the timing of the breakdown of the wintertime stratospheric polar vortex (Baldwin et al., 2001). Wave interactions between the troposphere and the stratosphere are also at play in the dominant modes of inter-annual variability at the poles. In fact, stratospheric dynamics are expected to also play an important role in determining tropospheric weather and climate. Firstly through non-local inversion or changes in the potential vorticity (PV) distribution that changes refractive index in lower stratosphere, which guides the upward propagation of planetary waves. Any change in the PV distribution in the lower stratosphere will inevitably give rise to changes in wind and temperature in the troposphere (e.g. stronger downwelling in polar region or tropopause folds at mid-latitude).

The second mechanism is via Rossby wave propagation. The propagation of Rossby waves out of the troposphere might be sensitive through the variation in the refractive properties of the lower stratospheric, or there might be downward reflection of Rossby waves from higher in the stratosphere. Along with the dynamical coupling, chemical

properties of these two layers can be influenced by stratosphere-troposphere exchange or STE (Holton et al. 1995). STE significantly influences tropospheric ozone which is considered one of the most critical gaseous pollutants, as it affects the tropospheric oxidation capacity and has adverse effects on human health, on vegetation and on soil microbes and also is a powerful greenhouse gas.

The troposphere contains about 10% of the ozone in the atmosphere, 90% being located in the stratosphere. Major part of the tropospheric ozone has stratospheric origin as consequence of the stratospheric intrusions associated with tropopause folding in cyclogenesis processes. Increase in tropospheric ozone is reported at many places that can modify radiative, chemical and dynamical properties of the troposphere. Another important aspect of STE is that it regulates the lifetime ofchemically important species such as $H_2O$ or CFCs in the stratosphere which in turn can have significant influences on the future evolution of ozone layer.

## 1.13. General principles of ozone measurement

### 1.13.1. *In situ* methods

In situ measurements of ozone involve the direct sampling of ozone from a given mass of air. The sample of air is directly brought into the instrument and analysed for the relative amount of ozone concentrations. The direct measurement of ozone is done using ozonesonde. Detailed description of these instruments is given in next chapter.

### 1.13.2. Remote sensing techniques

Remote sensing technique employs the indirect measurement of the changes in atmospheric radiation caused by the presence of the parameter. For measuring atmospheric the alteration the radiation travelling through the atmosphere caused by atmospheric ozone is observed. Ground based remote sensing of ozone can be done using Dobson/ Brewer Spectrophotometers. Details of these instruments are provided in next chapter. Ozone measurements from satellites can be used to measure atmospheric ozone in a very large scale and over regions where the installation of ground based instruments are not possible. Remote sensing techniques can be passive or active. Passive

remote techniques make use of the natural sources of radiation whereas active remote sensing employs of artificial sources of radiation for measuring an atmospheric parameter.

Major remote sensing techniques for satellite platforms are based on different viewing geometries. The four techniques for remote sensing which are passive in nature are (1) the backscatter ultraviolet (BUV) technique, (2) the occultation technique, (3) the limb emission technique, and (4) the limb scattering technique.

**Backscatter ultraviolet (BUV) technique**: Measurements are made of solar ultraviolet (UV) light entering the atmosphere (referred to as the irradiance) at a particular wavelength and of the solar UV that is either reflected from the surface or scattered back from the atmosphere. For determining total ozone, two pairs of measurements are made. One measurement is made at a wavelength that is strongly absorbed by ozone and the other measurement of incoming UV irradiance and backscattered UV radiance is made at a wavelength that is weakly absorbed by ozone. The differences in the pair measurements at the two wavelengths are used to infer how much ozone is present in the atmosphere. Total column ozone is the amount is estimated by measuring backscattered radiances at wavelengths between 312 nm and 340 nm.

The ratios of radiance to irradiance measurements at these wavelengths provide estimates of the column ozone amount. For measuring vertical profiles of ozone BUV profiling technique is used. Ultraviolet absorption increases with decreasing wavelength, such that radiation with shorter wavelengths is largely absorbed at higher altitudes whereas longer UV wavelength can penetrate more into the atmosphere to be absorbed by the ozone present there. Hence backscattered radiation at specific UV wavelengths can only be scattered from above a particular height and this helps in the vertical measurement of ozone. A big advantage of the BUV technique is that by looking directly down at the atmosphere below in a viewing geometry called nadir viewing, the satellite is able to get a good horizontal resolution. Examples of instruments using BUV technique are Total Ozone Mapping Spectrometer (TOMS), Solar Backscatter Ultraviolet Instrument (SBUV) and Global Ozone Monitoring Instrument (GOME).

**Occultation Technique** – This technique is used for the measuring the vertical profiles. The instruments measure radiation directly though the limb of the atmosphere. By measuring the amount of absorption of radiation through the atmosphere at different wavelengths (e.g. UV, visible, infrared), occultation instruments can infer the vertical profiles of a number of trace constituents, including ozone. (a) Advantage: improved vertical resolution -- (b) Disadvantage: limited spatial coverage -- SAGE I, II, and III -- The Stratospheric Aerosol and Gas Experiment II (SAGE II). HALOE -- The Halogen Occultation Experiment (HALOE).

**Limb Emission**: Instruments based upon the limb emission technique infer ozone amounts from measurements of longwave radiation (infrared or microwave) thermally emitted in the atmosphere along the line of sight of the instrument. By taking a number of measurements above a given location, the limb emission sensors are able to create a vertical profile of trace gas concentrations. The resulting vertical resolution is quite good, usually on the order of 3 kilometers. Examples of limb emission instruments are Limb Infrared Monitor of the Stratosphere (LIMS), Cryogenic Limb Array Etalon Spectrometer (CLAES) and Tropospheric Emission Spectrometer (TES) instruments will employ low power consuming mechanical coolers for their detectors and measure even more atmospheric constituents because of advanced technology.

**Limb Scattering**: It employs aspects of the other three techniques. The viewing geometry is similar to that of both limb emission and occultation, which provides good vertical resolution. It also measures scattered solar radiation in a manner similar to the BUV measurement, but the light source is in earth's limb. This technique works best with ozone, however other trace gases like water vapor, nitrogen dioxide, and sulphur dioxide are also measurable. The measurements are made in the UV, visible, and near infrared. Scanning Imaging Absorption SpectroMeter for Atmospheric CHartographY (SCIAMACHY).
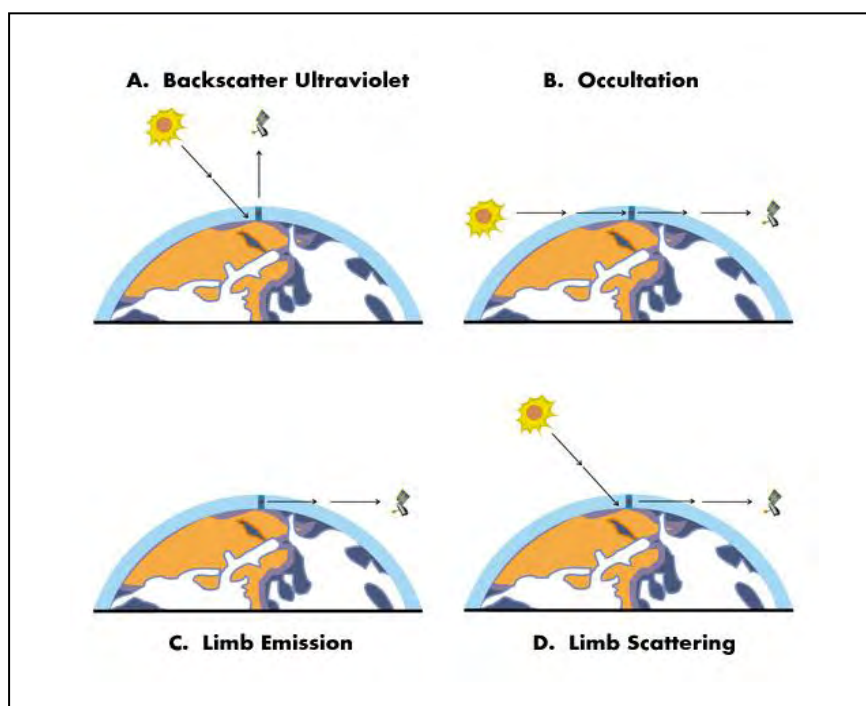
Fig. 1.10. Various viewing geometries for satellite measurements of ozone (Source: Stratospheric
        Ozone: An Electronic Textbook)

## 1.14.  Objectives of the thesis

The quantity of atmospheric ozone over a region is mainly a function of season and latitude.  Apart from the changes due to variations in solar radiation circulation features and atmospheric oscillations can make changes in ozone amounts. The work aims to study the seasonal and spatial variability of ozone over Indian region. Continuous monitoring of the temporal evolution of ozone is necessary to know about the variations caused by changing climate. The trends in ozone concentrations over the region and the trend for different seasons is analysed as a part of this work. The most important factor that can be influenced by ozone variations in the atmosphere is the ultraviolet radiation at the surface. The changes in biologically harmful radiation due to ozone changes were analysed by the computing the Radiation amplification factor over two Indian stations.

A major portion of ozone variability is expected to be explained by natural cycles or oscillations, with varying time periods in the atmosphere. The effects from all these cycles are combined in a complicated manner to contribute to a major portion ozone changes. The study intends to isolate the spatial and temporal effects of these natural

cycles by applying analysis methods like principal component analysis and harmonic analysis to the ozone dataset. Another purpose of the thesis is to explore the ozone concentrations at the various layers of the atmosphere. The identification and proper treatment of suitable datasets has to be performed. The temporal and spatial variation of ozone over Indian region has been studied in the thesis by selecting and gridding the satellite data into sufficient resolution.

One of the major aims of the study is to understand the nature of ozone variations in the UTLS region over India. The study of the meteorological parameters at the UTLS region is also intended in order to understand their influence on ozone amount variations. The distinct nature of the troposphere and stratosphere can be studied better by analysing the nature of the boundary that separate the two regions. The ozone concentrations between the two regions display sharp gradients due to their difference in their dynamics. The study also aims to study the ozone gradients near the tropopause region and its temporal variation along with the thermal tropopauses and upper tropospheric ozone minimum.

## 1.15. Relevance of the thesis

One of the major aims of the thesis is to understand the present state of atmospheric ozone over India and surrounding regions. A study of ozone over India can serve as good representation of ozone changes in tropics and subtropics. Besides the region is affected by monsoon circulation and hence the effect of synoptic scale effects of circulation over ozone can be recognised more clearly by studying ozone in this region. Nearly half of the study region lies in the tropics where there is high amount of solar radiation throughout the years. In order to prepare for the changes in ultraviolet radiation resulting from ozone changes it is essential to have a good knowledge of atmospheric ozone over this region.

Ozone amounts over the region can be influenced by the circulation features associated with monsoon. The variation in the tropical and subtropical region to look for monsoon induced changes near the tropopause is also examined. Knowing about the changes of ozone concentrations at various vertical layers is essential to understand the causative factors for the changes in total column ozone. One of the major factors that inhibit the correct estimation of atmospheric ozone is the lack of datasets with sufficient temporal

and spatial resolution. An attempt is made to restructure an existing satellite dataset into regular gridded values and to visualize the resultant ozone variations.

Another motive of the study is to understand the seasonal exchange of ozone from the stratosphere to troposphere. This is important to quantify the amount of tropospheric ozone over Indian region. Industrial and vehicular pollution can produce an increase in tropospheric ozone. Identifying the amount of ozone intruded from the stratosphere helps to estimate the ozone production due to human activities. This can help to plan the control measures for tropospheric ozone production. In the present day context of climate change it is very important to have knowledge of the long term trend in ozone over specific regions. This can be used to identify the impact of regional weather and climate variations on ozone amounts .This is also helpful to look for the rate of recovery of ozone from pre industrial values and to have a sustainable planning that helps in the recovery of ozone.

# Chapter 2

---

# Data and Methodology

---

Datasets of sufficient temporal extent and global coverage with good resolution is essential to understand the three dimensional structure and evolution of atmospheric ozone. Information about the vertical variation of ozone is imperative to understand the influence of dynamics and chemistry on ozone. Long term data records with timescales of decades are needed to unravel the intricate relation between long term trend and human or natural factors. Satellite data is good source to study the variability of atmospheric dynamics and composition. Different satellites have different global coverages and different resolutions. Measurement of atmospheric ozone by satellites started in 1979. Also the data record of by the satellites span less than 30 years because of the age of the satellites. But almost all the satellites cannot provide a data record more than 30 years due to the sort life time of satellites in the space. As the total column ozone measurements are concerned, the same sensor (TOMS) was put on three different satellites after the breakdown of each from 1979 to 2005. Still there exists a gap of 1-2 years between the Meteor and Nimbus-3 were launched.

*In situ* datasets can give reliable information about an atmospheric parameter. The *in situ* data for total column ozone is provided by Brewer and Dobson spectrophotometer. For obtaining the vertical structure of ozone ozonesonde data can be used.

## 2.1. Units of ozone measurement.

Total column ozone measurements given by Multi sensor reanalysis used in the thesis are given in Dobson Units. Ozone Monitoring Instrument (OMI) ozone profile data is given in partial column ozone i.e. the total amount of ozone between two adjacent layers is also given in Dobson units. Dobson unit (DU) is a measurement of the total amount of ozone in a column extending vertically from earth's surface to the top of the atmosphere. This

measurement of ozone is directly gives indication about the amount of UV light reaching the surface. If all the ozone molecules present in a column of the atmosphere were brought to surface and stacked at 0°C and 1013.25 hPa pressure, Dobson unit gives a measure of the thickness of the stacks.

$$1 \text{ DU} = 10^{-3} \text{m}$$

One Dobson unit can contain about $2.7 \times 10^{16}$ molecules/cm$^2$.

Ozone profile data from ozone sonde given in partial pressures which have units of millipascal was multiplied by 10 and then divided by the pressure of the corresponding layer to convert it to ozone volume mixing ratio in parts per million volume (ppmv).

$$\text{Ozone }_{ppmv} = (\text{Ozone }_{mPa} \text{ X } 10) / \text{Pressure (hPa)}$$

## 2.2. Reanalysis Data sets

Reanalysis data has been used in the study wherever temporal and spatial regularity of data is required. Sources of reanalysis data used in the study are European Centre for Medium Range Weather Forecasting (ECMWF) and National Centre for Environmental Prediction. Reanalysis data provide a multivariate, spatially complete, and coherent record of the global atmospheric circulation (Dee et.al., 2011). They are consistent with laws of physics as well as observations.

### 2.2.1 ECMWF-Interim reanalysis

European Center for Medium-Range Forecasts (ECMWF) Interim Re-Analysis (ERA-Interim) is the latest and most updated reanalysis data set produced at ECMWF (http://www. ecmwf.int, Dee et al., 2011). This reanalysis offers global coverage high spatial resolution than the ERA -40 and extends from 1989 to the present. It is designed as an intermediate to a future dataset that will act as the continuation of ECMWF-40. ERA Interim uses ECMWF Integrated Forecast System (IFS) approach in which background (first-guess) values are compared with observed values at the observation time rather than the analysis time, and the differences are applied at analysis time. The main components of

the forecast model include atmosphere, land surface and ocean waves. The purpose of the ERA-Interim is to address certain data assimilation problems in ERA-40 including stratospheric circulation. It gives a higher horizontal resolution of approximately 79 km compared to ERA-40. The vertical resolution is same as ERA-40 with 60 layers with the top of the atmosphere at 0.1 hPa. The time step for the model is 30 minutes.

Vertical ozone profile from ERA interim is used in the thesis on the occasions when temporally continuous data for more than 30 years is required to study the climatological variation. Data from any of the previous and existing satellites are not continuous due to the comparatively short lifetime of satellites. Satellites covering the entire pressure levels from 1000 to 1 hPa and above are providing data for less than 10 years. Station data from various stations over India are not regular in space and time. Hence ERA interim data for 1989 to 2012 at the 37 pressure level for ozone and meteorological parameters are used in this study. Thus ozone profile data from ECMWF served as a good tool to study the correlation between ozone and meteorological parameters. Observations are combined with prior information from a forecast model every 12 hours to estimate the evolution of various atmospheric parameters. It involves computing variational analysis for the upper atmospheric fields like ozone, temperature etc and separate analysis of surface and near surface parameters. These are used to initialize a short range forecast model which provides prior estimates needed for the next forecast cycle.

Ozone is used as a prognostic variable in ERA interim 4D-Var assimilation i.e. the ozone generated estimates are independent of other state variables. Any aspect of the model initial state can be modified later within the analysis window to fit with ozone observations. But to obtain accurate information of dynamics from this, high quality ozone data is needed. Assimilation of ozone profile to ERA-Interim caused produces unrealistic results for temperature and wind. This can be due to the conflict between observations from different sources. Hence the analysis scheme of ERA-Interim is modified in a manner to prevent the direct influence of ozone on dynamical fields. Ozone is represented in the model by means of a continuity equation relaxing to photochemical equilibrium for the local value of the ozone mixing ratio, the temperature and overhead column ozone. Heterogenous ozone destruction is parametrized as a function of equivalent chlorine content. Ozone climatology used in the radiation scheme distributes the ozone mixing ratio as a function of pressure, latitude and month following Fortuin and Langematz (1994). The

number of observations assimilated into the ERA-40 syastem has increased from $10^6$ to $10^7$ in the last two decades. This involves the integration of many satellite-borne sensors. Fig.2.1. represents the timeline of ozone measurements used in ERA Interim.

An improvement to the ERA-40 ozone, correcting the errors due to stratospheric irradiance assimilation has also been done in ERA-Interim. Ozonesonde data from WOUDC (World Ozone and Ultraviolet Data Centre) is not incorporated in ERA-Interim analysis. Dragani (2010a) and Dee (2011) carried out comparative study between ERA-Interim ozone and WOUDC data. Their results show that ERA-Interim show better agreement with ozonesonde data at most levels compared to ERA-40. ECMWF-Interim dataset has been used for comparing the satellite ozone data and for studying the relation of ozone with meteorological parameters in the theis.

### 2.2.2. NCEP reanalysis

The NCEP/NCAR reanalysis (Kalnay et al.,1996) gives various meteorological data for the period of 1948-present. The global spectral model used in this reanalysis is T62 with a resolution of 209 km. The model has 28 vertical levels. Tropopause pressure from National Centre for Environmental Prediction (NCEP) were used in the thesis for studying concurrent variations with ozone near tropopause. NCEP uses the thermal definition of tropopause heights from World Meteorological Organisation to compute tropopause pressures. It is computed as the lowest level at which the lapse rate decreases to 2 K/km or less, provided that the average lapse rate between this level and all higher levels within 2 km does not exceed 2K/km.

### 2.2.3. MultiSensor Reanalysis of total ozone (MSR)

Multisensor reanalysis total ozone has been used to study the total ozone variability over India and to study the major dynamical modes of variability of total ozone over India. This section outlines some of the details about the construction of the dataset done by R. J. van der et al. (2010). This dataset has been constructed from all the available column ozone data from polar orbiting satellites in the near ultraviolet Huggins bands. Total column ozone measurements from the retrieval of fourteen satellites (listed in table 2.1. below)

have been used in the dataset. These datasets covering long period are important in monitoring ozone and UV radiation (Mäder et al., 2007, Lindfors et al., 2009).
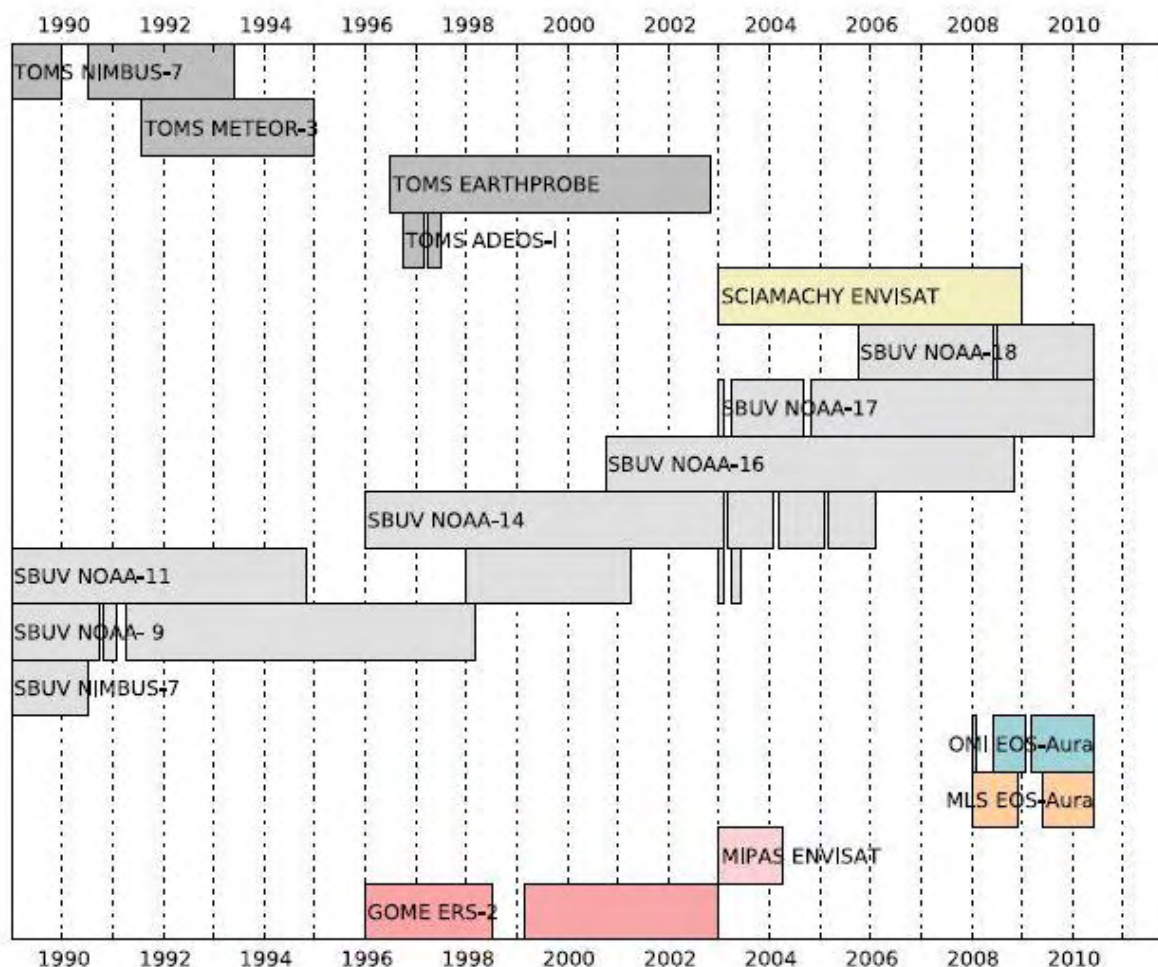


Fig.2.1. Datasets used for the construction of ECMWF-Interim ozone dataset. (Source: Dee et al., 2011)

Measurements used are originating from different instruments and different retrieval algorithms. Also various sensors suffer from problems like radiation damage. The data usually shows offsets in overlapping time periods and some show difference from ground observations. Hence the derivation of this reanalysis data involves bias correction based on independent ozonesonde observations and a new dataset is created. These datasets are corrected for parameters like solar zenith angle, viewing angle, trend and ozone effective temperature which are critical parameters for errors in the retrievals. The corrected datasets are subjected to 30 year data assimilation run using a sub optimal implementation of the

Kalman filter technique. This technique requires unbiased input data with a known Gaussian error distribution. It is based on chemical transport model driven by ECMWF meteorological fields. This model involves detailed stratospheric circulation and parameterisations of ozone hole and gas phase chemistry. The dataset is available on a grid of $1 \times 1.5°$ with for the time period 1978-2008.

Table.2.1. Component datasets of Multisensor reanalysis of total ozone

| Instrument | Time Period | Algorithm | Agency |
|---|---|---|---|
| TOMS Nimbus 7: | 1978-1993 | TOMS v.8 | NASA |
| TOMS EarthProbe: | 1996-2002 | TOMS v.8 | NASA |
| SBUV 7, 9a, 9d, 11, 16: | 1978-2004 | SBUV v.8 | NOAA |
| GOME : | 1995-2008 | GDP v.4 | ESA/DLR |
| GOME | 1995-2008 | TOGOMI v1.2 | KNMI |
| SCIAMACHY | 2002-2008 | SGP v.3 | ESA/DLR |
| OMI | 2004-2008 | TOMS v.3 | NASA |
| OMI | 2004-2008 | DOAS v.3 | KNMI |
| GOME-2 | 2007-2008 | GDP v.4.2 | EUMETSAT/DLR |
| Brewer(3,4),Dobson, Filter | 1978-2008 | - | WOUDC: |

Retrievals from the fourteen satellite instruments that altogether give data more than 30 years were collected first. Ground based measurements of ozone provide the longest data record available for the validation of satellite data. The collection of this data is available from World Ozone and Ultraviolet Data Centre. From this a WOUDC Station Instrument (WSI) list is defined. Daily average total ozone measurements from this list for 1979-2008 are extracted. Only direct sun measurements were used because of their superior quality compared to zenith sky measurements. Data with suspected fluctuations and anomalies were rejected by comparing with satellite datasets. In the next step an overpass dataset for each satellite product for each WSI listed station was created. Total ozone values derived from the measurements of scattered sunlight in polar orbit has been used. Overpass value

for an orbit is the satellite observation that has the centre of its footprint closest to the ground station. This distance depends on the satellite ground pixel size and varies from 50-200 km. The local date and time is defined as the satellite UTC plus correction based on the longitude of the station. Thus satellite data corresponding to the data reported from the ground station is obtained. Auxiliary data like solar zenith angle and viewing zenith angle, cloud properties and distance from the centre of the footprint to the ground station were also obtained. One value is selected from about fifteen overpass values per day. This value can be the one with the smallest reported observation error or one closest to the ground station.

Satellite and ground based data may contain seasonally dependent errors. The amplitude and phase differs from one satellite product to another. Thus some of the satellite products can have seasonal offsets between them. Also the seasonal offsets between satellite and ground stations could depend on latitude, solar zenith angle and effective ozone temperature. A dataset of effective ozone temperature is constructed in the next stage. The effective ozone temperature is defined as the integral over altitude of the ozone profile-weighted temperature. This is calculated from ECMWF 6 hourly temperature profiles and Fortuin and Kelder ozone climatology (Fortuin and Kelder, 1998). In order to reduce the systematic offsets between the satellites a reference dataset is chosen and the systematic effects in other datasets are reduced to bring them in line with the reference dataset. The direct sun measurements from the ground stations are used as the reference datasets because these are present for the full 30-year period.

For applying corrections to the data, a number of predictors were selected from the auxiliary information and the effective ozone temperature is also a predictor. The ozone differences (ground based minus satellite observations) are fitted as a function of these predictors using a simple multi-dimensional least squares fitting system. A level-2 MSR dataset has been created based on the corrections obtained. The dataset contains time, location, satellite product index and ozone. The corrected satellite dataset is combined with chemical dynamical and meteorological conditions of the atmosphere by means of data assimilation. A quality screening is implemented to reject unrealistic ozone observations. The data assimilation model is driven by 6-hourly meteorological fields such as wind, surface pressure and temperature of the medium range meteorological analysis of the

ECMWF. Comparison with observations show that the bias of MSR is less than 1% with an RMS standard deviation of 2% as compared to the corrected satellite observations used (Van der et al., 2010).

## 2.3. Ozone datasets

Ozonesonde data is very useful for studying the transport history of air parcels in the tropical tropopause layer. Profiles of ozone and temperature were obtained from World Ozone and Ultraviolet Data Centre (WOUDC) were obtained from the website www.woudc.org. WOUDC is coordinating the archival of ozone and ultraviolet radiation data. Long term measurements of total ozone, profile ozone and ultraviolet radiation is necessary to predict the future evolution of trace gases and to represent these variations in climate models appropriately. Total ozone measurements were done worldwide mainly using Dobson, Brewer and Filter ozonometers.

### 2.3.1. Dobson Spectrophotometer

The longest records of continuous reliable measurements are available from stations equipped with Dobson spectrometers (Dobson, 1930). The Dobson spectrophotometer which is a ground-based instrument was designed by Gordon Dobson in the 1920's. They measure the ozone amount in a column of the atmosphere by measuring the amount of solar radiation reaching the surface of the earth in the ultraviolet region of electromagnetic spectrum. The measuring principle of Dobson Spectrophotometer is based on the fact that the absorption coefficient of ozone in the near ultraviolet Huggins' band is a rapidly changing function of the wavelength. The ultraviolet radiation is measured at 2 to 6 different wavelengths from 305 to 345 nm. The presence of clouds and aerosols can also affect the amount of shortwave radiation reaching the ground; a region of the spectrum where ozone does not absorb is also measured simultaneously. Taking the ratio cancels the effect of clouds and aerosols and its value is directly proportional to the amount of ozone in the path of the UV light through the atmosphere.

The light entering the spectrophotometer is split into two beams (absorbing and non absorbing) that fall alternately on a photomultiplier tube. The more intense beam is

reduced in intensity by passing it through a piece of glass of varying thickness. The the glass wedge is adjusted until both beams have the same brightness. When the photomultiplier tube detects the beams are the same intensity, the position of the glass wedge is noted and the amount of ozone is then derived from lookup tables. Basic construction of a Dobson spectrophotometer is given in Figure. 2.2.
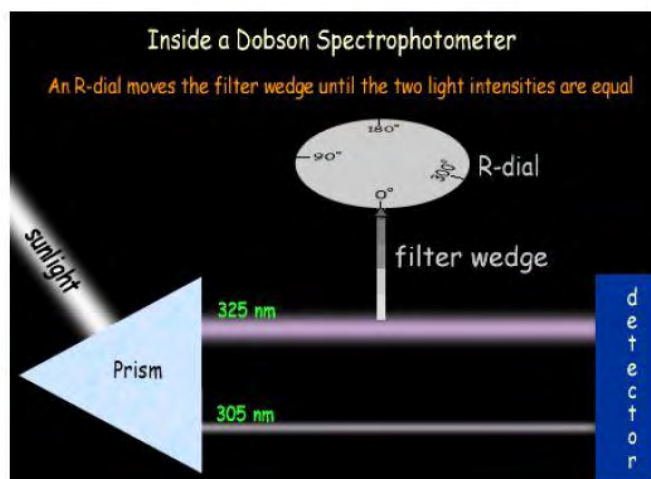


Fig.2.2. Schematic representation of Dobson Spectrophotometer

## 2.3.2. Brewer Spectrophotometer

This spectrophotometer measures ozone based on the same technique and with the same uncertainity as the Dobson instrument. The Brewer spectrophotometer is completely automated and can be programmed to make measurements at any given time during the day. The instrument measures ultraviolet light at five wavelengths (306, 310, 313, 317, 320 nm). The total column ozone amount is calculated by using a more complicated form of equation used for the Dobson instrument that includes terms for sulphur dioxide. The absolute accuracy for a total ozone measurement made by a well calibrated Brewer instrument is estimated to be +/- 2.0%.

### 2.3.3. Ozone sonde

An ozonesonde is an instrument to measure the vertical profile of ozone. The instrument is carried on a weather balloon platform and performs measurements of ozone profile during the balloon flight. The standard technique for measuring the vertical distribution of ozone is electrochemical concentration cell ozone sondes. The electrodes in the cell are made of platinum and they are connected by an iron bridge. The electrochemical cell uses potassium iodide (KI) solution in both the electrodes (Figure. 2.3). The cathode consists of 3 ml of dilute KI solution and anode consists of 1.5 ml of saturated KI solution. Air containing ozone is immediately forced into the cathode cell solution by means of a Teflon piston pump. Iodine is produced as a result of reaction of potassium iodide with iodine. One ozone molecule causes the production of two ions. The chemical reaction is given below

$$2KI + O_3 + H_2O \rightarrow 2KOH + I_2 + O_2$$
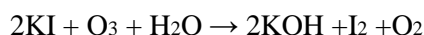
When the iodide changes to iodine, the two cells are no longer in electrical equilibrium. Current flows through the cell via external circuit, reducing iodine back to iodide. As the amount of ozone in the air increases, the faster the iodide is changed to iodine and the more electrons flow between the cells (current). The amount of current that flows between the chambers is measured and sent to the ground receiving station.The cell current is theoretically directly proportional to the amount of ozone

Ozone partial pressure is the computed using the equation.

$$P_{ozone} = C.\,i.\,T_p.\,t \qquad\qquad ...2.1$$

Where, $P_{ozone}$ = ozone partial pressure (in nanobars);

    C= constant

    i = current

    $T_P$ = pump temperature

    t = amount of time to force 100 milliliters of air through the system.
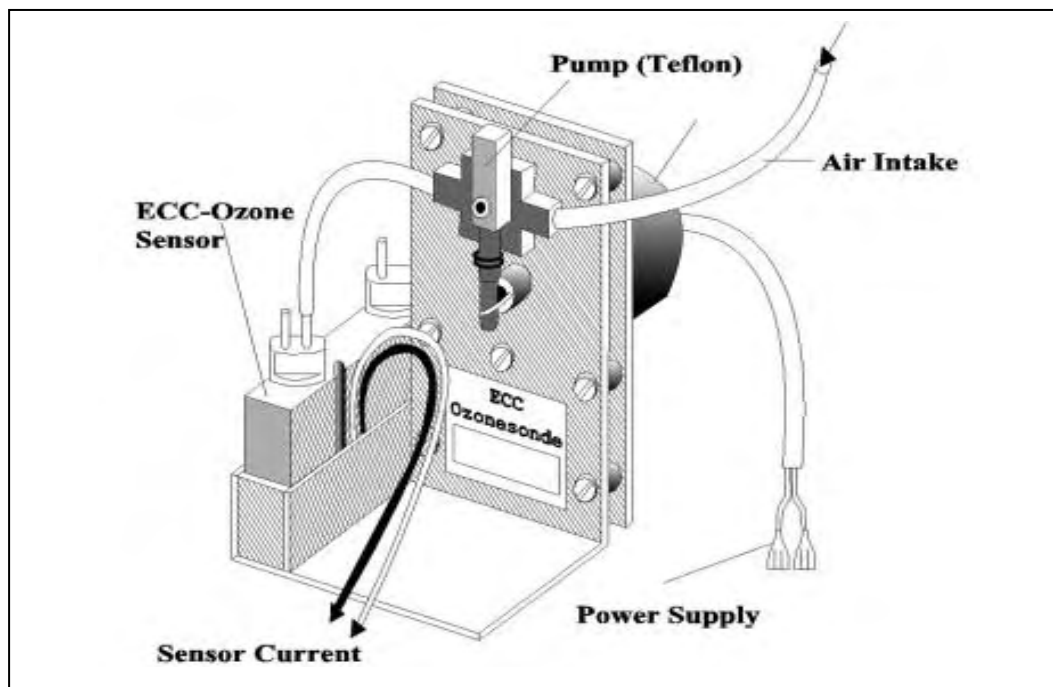
Fig.2.3. Ozonesonde instrument

## 2.4. Ozone measurements in India

The first ozone observations in India were made at Kodaikanal in 1928-1929 as part of Dobson's worldwide total ozone measurements. Detailed history of ozone measurements in India were given by Alexander and Chatterjee (1980). India Meteorological Department .acquired the first Dobson Spectrophotometer in 1940. Initial measurements were made at Pune . Daily observations  were made at Delhi from 1945 to 1947 and at Pune and Kodaikanal during 1948-1949. Meanwhile a network of six stations were established at Srinagar, New Delhi, Varanasi, Calcutta, Ahmedabad and Kodaikanal. All these stations were equipped with Dobson Spectrophotometer. Ramanathan and Dave (1957) developed a method for numerical evaluation of Umkehr data. The operation and maintenance of total ozone stations was taken over by India Meteorological Department from Physical Research Laboratory, Ahmedabad in 1963.
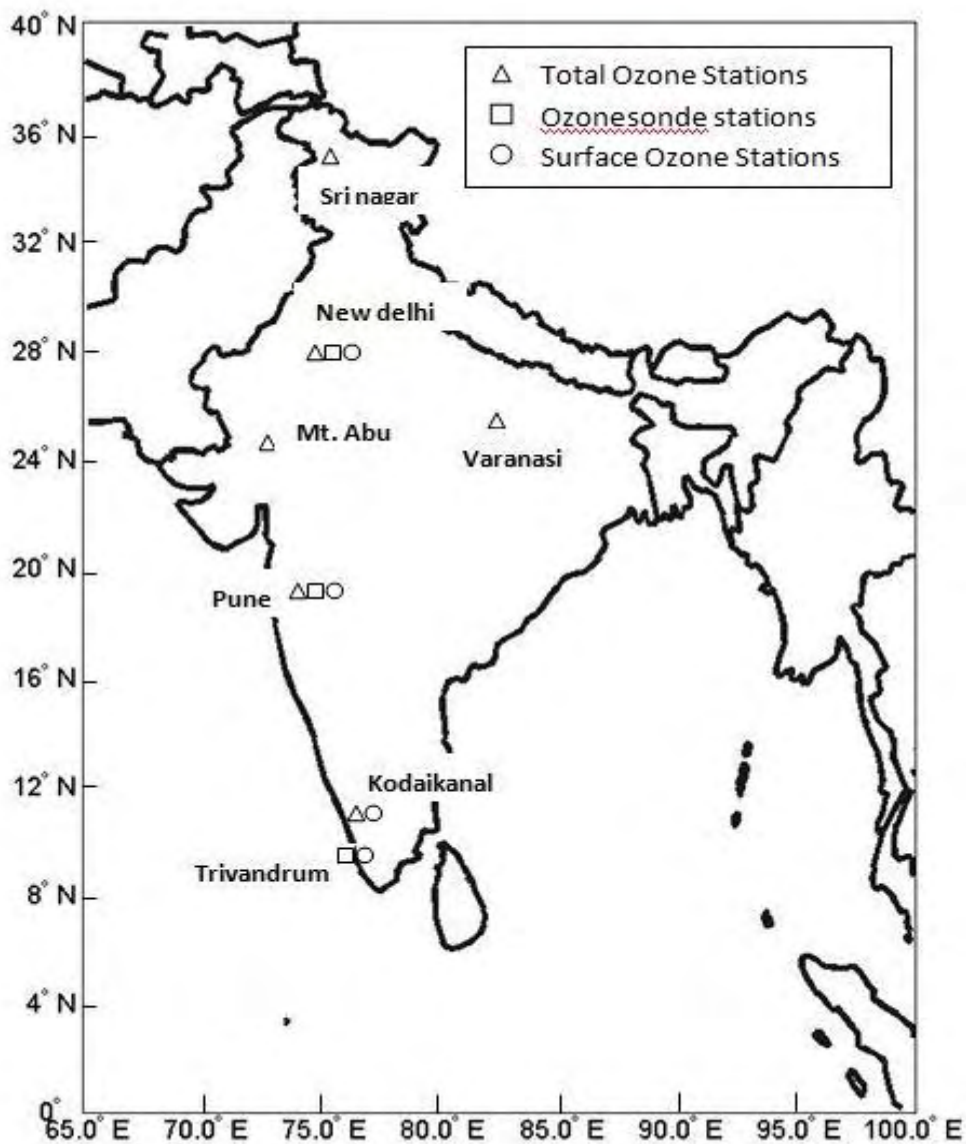
Fig.2.4. Area of study (0°N-40°N, 60°E-100°E) and the ozone measuring stations and available measurements at each station

Dobson instrument at Ahmedabad was shifted to Mt.Abu and those in Calcutta was shifted to Pune in 1973. Surface ozone measurements started at four stations in India in 1971 using the bubbler ozone sensor. This sensor is based on the chemical reaction of potassium iodide solution. Observation of the vertical distribution of ozone are being made at Trivandrum, Pune and New Delhi once very fortnight. Ozone measurements from India can be obtained from the archive of World Ozone and Ultraviolet Data Centre (WOUDC).

## 2.5. Satellite data

### 2.5.1. Ozone Monitoring Instrument

Ozone Monitoring Instrument onboard NASA Aura satellite provides the continuation of the TOMS record of total ozone and other parameters related to ozone chemistry and climate. Aura satellite orbit the earth in a 705 km sun synchronous polar orbit with a 98° inclination and an equatorial crossing time of 13;45±15 minute UTC. The OMI instrument is a contribution of the Netherlands's Agency for Aerospace Programs (NIVR) in collaboration with the Finnish Meteorological Institute (FMI) to the EOS Aura mission Schoeberl et al. (2006). OMI is an ultraviolet/visible (UV/VIS) nadir solar backscatter spectrometer, which provides nearly global coverage in one day with a spatial resolution of 13 km × 24 km. This instrument maps atmospheric ozone with a spatial resolution never achieved before. It also maps global distribution and trends in UV-b radiation. Measurements of key air quality components such as $NO_2 SO_2$, BrO, OClO, and aerosol characteristics are also provided by the instrument.
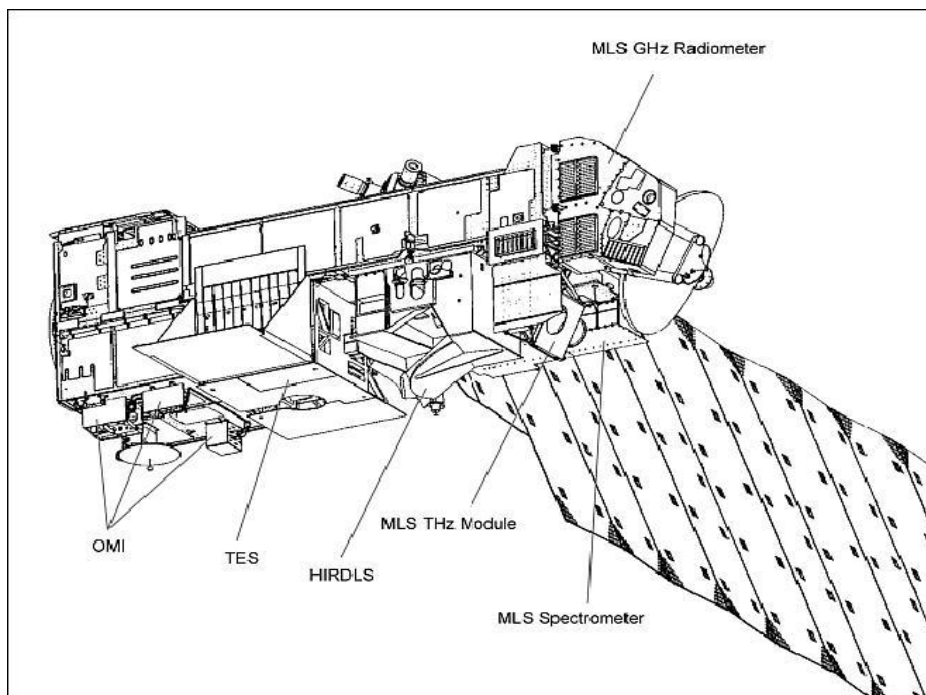


Fig.2.5. Aura satellite with its different sensors including OMI

The sensor employs hyperspectral imaging in a push-broom mode to observe solar backscatter radiation in the visible and ultraviolet. OMI views the earth in 740 wavelength bands along the satellite track with a swath large enough to provide global coverage in 14 orbits (1 day). The nominal 13 x 24 km spatial resolution can be zoomed to 13 x 13 km. OMI swath width is approximately 2600 km. OMI measures the complete spectrum in the UV visible wavelength range with a very high spatial resolution and daily global coverage using a two dimensional detector. The small pixel size of the instrument enables it to retrieve tropospheric information by viewing in between the clouds.
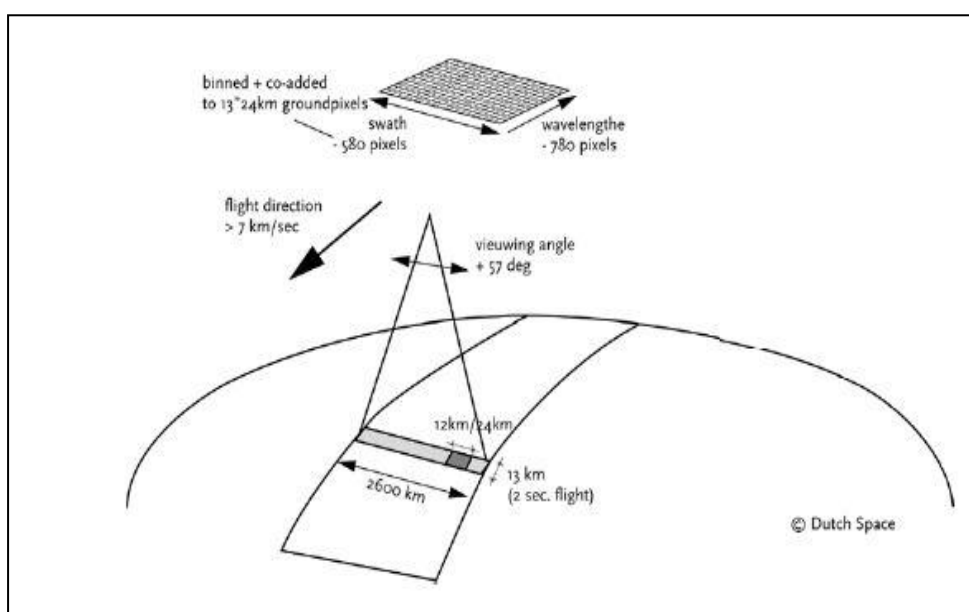


Fig. 2.6. OMI measurement principle

The telescope of OMI is nadir viewing with a large field of view of 114, which makes possible the larger swath width of 2600 km. One dimension of the 2-D CCD detectors covers the spectrum while the other covers the viewing direction. Thus the 2-D CCD detector enables to measure the spectral and spatial information at the same time. Main observation mode of OMI is the global measurement mode. It has two additional measurement modes called Spatial zoom–in measurement mode and Spectral zoom-in measurement mode. In a regular OMI earth radiance measurement five measurements with an exposure of 0.4 s are co-added resulting in a pixel size in the flight direction independent of the operation mode. The ground pixel size at nadir position in global mode

is 13 x 24 km  for UV-2 and VIS channels and 13 x 48 km for UV channel. For Spectral and Spatial zoom in modes the ground pixel size is reduced to 13 x 12 km for the UV-2 and VIS and 13 x 24 km for the UV-1.
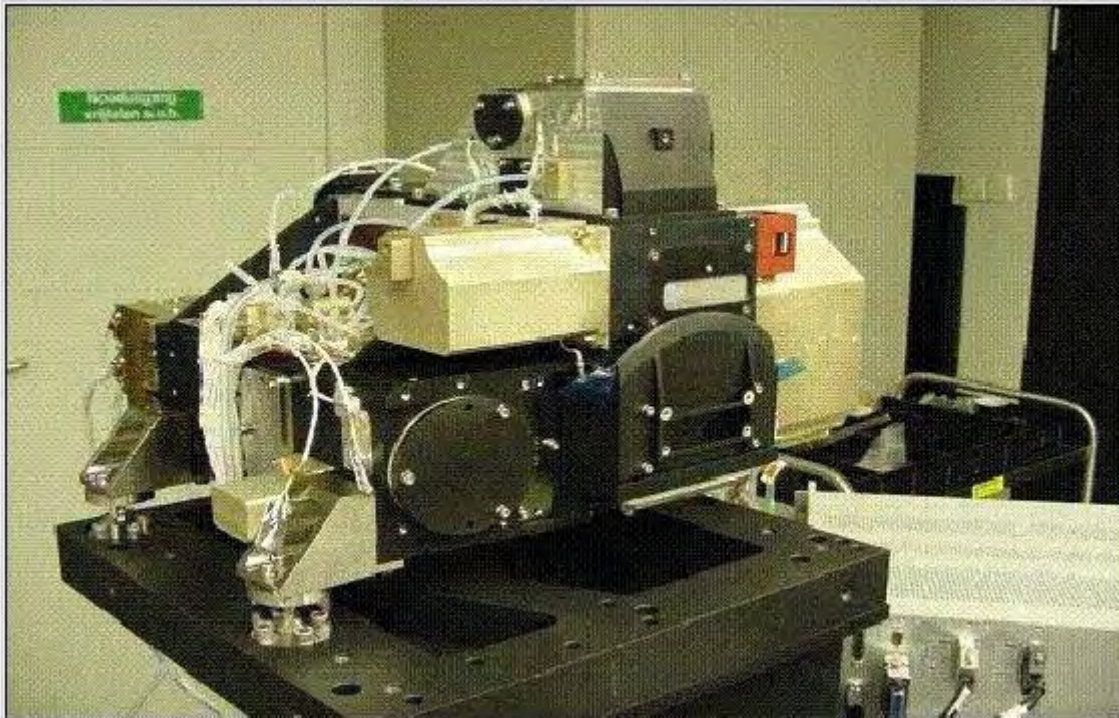


Fig.2.7. Ozone Monitoring Instrument

 Size of the pixels increases slowly in the swath direction from 13 x 24 km   to about 13 x 150 km for the global mode in the most outer swath angle. This effect is illustrated in Figure.  Due to this effect measurements within 500 km from the centre of the track are used for gridding in this study. Details about the instrument specifications of OMI can be obtained from Levelt et al. (2006). The retrieval technique used by OMI for ozone profiles is the optimal estimation method. The amount of ozone in each atmospheric layer is adjusted such that the difference between the modelled and measured radiance is minimal. Also a side constraint is applied such that the measured radiance does not differ much from the climatological average. Measurements are taken from UV1 channel (270-308.5 nm) and the first part of the UV2 channel (311.5-330 nm).  The algorithm uses the LABOS radiative transfer model which includes approximate treatment for rotational Raman scattering, pseudo spherical correction for direct sunlight etc. Algorithm performs forward calculations in the wavelength range 367-332 nm   with an error less than 0.2% in

reflectance. Ozone climatology from McPeters and Labow is used as *a-priori* profiles with the use of a different climatology for ozone hole conditions (OMI-ATBD (2002)).
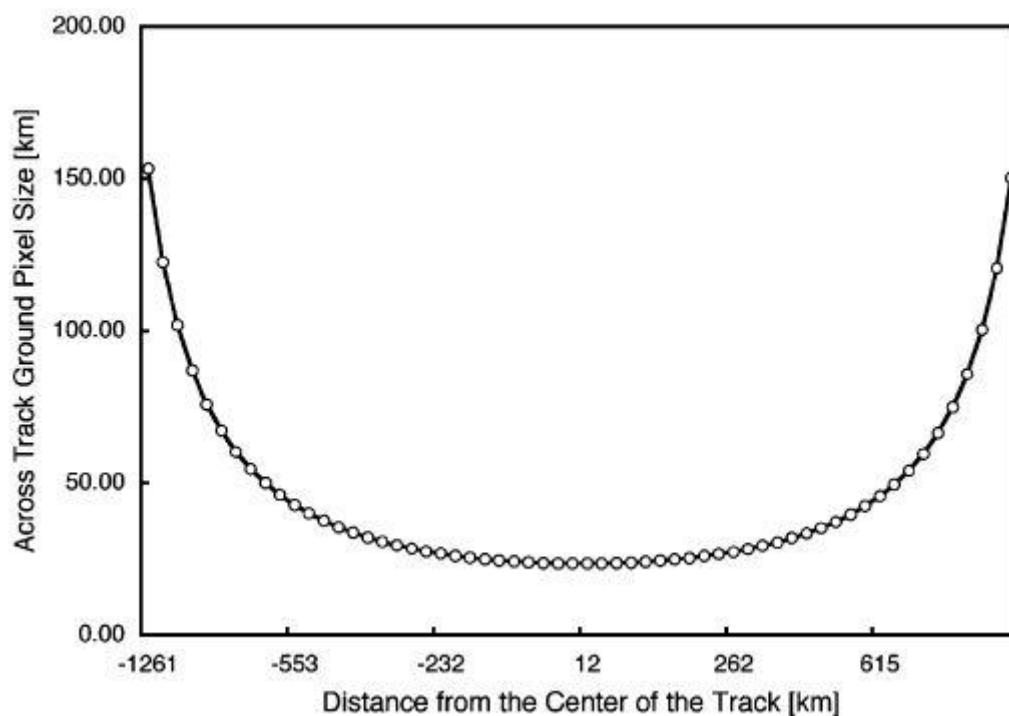


Fig.2.8. Variation of OMI ground pixel size with the distance from the centre of the track for OMI instrument

This present doctoral thesis makes use of the ozone profile measurements over Indian region to study the vertical distribution of ozone over India. Data in the HDF-EOS format is obtained from the website mirador.gsfc.nas.gov. Each data file consists of measurements of the sunlit part of a single orbit from north to south. The file also contains information about a-priori ozone profile, error covariance matrix and averaging kernel. The ozone profile listed in the output file is in DU per layer. The layers are listed in table 5.1. of the thesis.

### 2.5.2. Solar Radiation and Climate Experiment (SORCE) Data

Solar spectral irradiance from SORCE mission has been used in the thesis to study the variation of ultraviolet wavelengths from 2004 to 2012. The SORCE mission aims to study the Total Solar Irradiance (TSI) and Spectral Solar Irradiance (SSI) and the energy

variations in those wavelengths that affect the earth's climate. The spacecraft was launched in January 2003 in to a 645 km orbit with 40° inclination. It is equipped with four instruments that provide state-of-the-art measurements of incoming x-ray, ultraviolet, visible, near infrared and total solar radiation. SORCE carries four instruments including Spectral Irradiance Monitor (SIM), Solar Stellar Irradiance Comparison Experiment (SOLSTICE), Total Irradiance Monitor (TIM), and the XUV Photometer System (XPS).
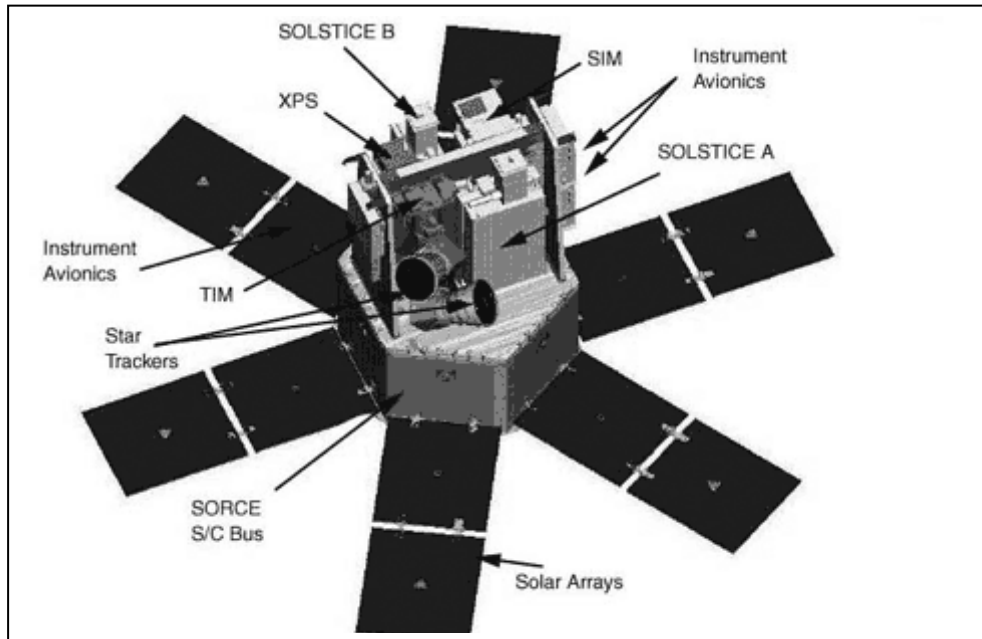


Fig.2.9. The SORCE satellite with its sensors

The energy of the sun striking the outermost atmosphere is estimated to be 1368 Watts per metre squared (W/m$^2$). This is called total solar irradiance. TSI depends only on the total energy per second produced by the sun (its absolute luminosity) and the distance from the sun to the earth. The total energy from the sun can be split into different wavelengths. The spectral measurements identify the sun's light by characterising sun's energy and emissions in the form of wavelengths. SORCE provides the measurements of the solar spectral irradiance from 1nm to 2000 nm, accounting for 95% of the spectral contribution to TSI. Only one percent of the TSI, mostly in the form of UV radiation, is absorbed by the upper atmosphere, mainly by stratospheric ozone. About 20 to 25% of the TSI and a majority of the near infrared radiation is absorbed in the lower atmosphere (troposphere), mainly by water vapour, trace gases, clouds, and darker aerosols. The remaining 45 to 50%

of predominately visible light penetrates the atmosphere and is taken in by the land and the oceans.

Incoming ultraviolet irradiances are given by the Spectral Irradiance Monitor (SIM) and SOlar Stellar Irradiance Comparison Experiment (SOLSTICE). The SIM instrument covers the wavelength range from 300 to 2400 nm with an additional channel to cover the 200-300nm ultraviolet spectral region. SIM is a single optical element Fèry prism spectrometer. Only one optical element is needed to focus and disperse the light on to a series of detectors in the spectrometer's focal plane. In this focal plane, four photodiode detectors and an electrical substitution radiometer (ESR) are used to detect solar radiation. SIM contains two completely independent and identical (mirror-image) spectrometers to provide redundancy and self-calibration capability. SORCE SOLSTICE makes daily solar ultraviolet (115-320 nm) irradiance measurements and compares them to the irradiance from an ensemble of 18 stable early-type stars.

Data for spectral irradiance is extracted from the website http://lasp.colorado.edu/sorce/data/ssi_data.htm. The data is given separately for each instrument that measure in a particular region of solar spectrum. Also a combined solar spectral irradiance file is provided which contains irradiances for wavelengths from 0.1-40 nm and 115-2400 nm. Daily values of irradiances for 200, 240, 280, 340, 360 and 380 nm were extracted and averaged to get monthly values used in this study.

## 2.5.3. Tropospheric Emission Monitoring Service (TEMIS) UV Index

Erythemal ultraviolet index values obtained from TEMIS were used in this thesis to study the concurrent variations of the incoming UV irradiance and ozone. The UV index is an estimation of the UV levels that affects the human skin. The TEMIS project aims to provide high quality data on ozone UV and other trace gases. The TEMIS UV index is based on the GOME satellite data computed using the total ozone product, the earth-sun distance, and a climatological database of the earth surface altitudes. The clear-sky UV index is the effective UV irradiance reaching the earth's surface and 1 unit is equal to 25 mW/m$^2$. It is obtained from CIE action spectrum for the susceptibility of Caucasian skin to sunburn.

Data for UV index is given for local noon when the sun is highest in the sky and for clear sky conditions. It is derived by integrating UV irradiance at the ground weighted by CIE spectral action function. The UV index can be regarded as a function of total column ozone and solar zenith angles at local solar noon. Column ozone amount is determined from satellite observations in combination with assimilation of the meteorological effects like wind, pressure, temperature. The solar zenith angle depends on the latitude and the day of the year.

## 2.6. Methods used

### 2.6.1. Principal component analysis (PCA)

Principle component analysis is a statistical analytical tool that is used to explore and organize data. Studies in Atmospheric Science require analysis of spatiotemporal data which is multidimensional. Hence principal component analysis in is used in Atmospheric Science for finding meaningful and recurring patterns inside these datasets which can be caused by various phenomena. This method takes a large number of correlated variables inside the dataset and organises in to a group of uncorrelated variables. These uncorrelated variables can be called principal components (PCs) of the dataset under consideration. These PCs retain maximal amount of variation and thus makes it easier to operate the data and make predictions. The principal components are represented in the order they represent variance – the first representing the largest proportion variance, second most of the rest of variance etc. Thus PCA is a powerful tool to highlight the similarities and differences in a dataset.

One of the major assumptions made in PCA is that the components derived from the analysis are a linear combination of the dataset. There are several variants of the method that explores the possibility of nonlinear combinations. Another assumption is that large variances represent important structures. But sometimes structures with large variances may contain large amount of noise and hence may not be important. PCA is independent of the method in which data is recorded and it does not require any adjustment of parameters used. The method does not specify any probability distribution for the observations and hence does not have statistical nature in that viewpoint. Another disadvantage is that PCA can only eliminate second order dependencies while higher order

dependencies can occur. This study makes use of the PCA in identifying the patterns in Total ozone over Indian subcontinent. The method used and the output are discussed in chapter 4

### 2.6.2. Harmonic analysis

Harmonic analysis represents the variations in a time series as having occurred from adding together of a series of sine and cosine functions. These trigonometric functions are chosen to have frequencies exhibiting integer multiples of the fundamental frequency determined by the sample size of the data series. The cosine and sine functions extend through indefinitely large negative and positive angles. The same wave pattern repeats every $2\pi$ radians or 360°. Both functions oscillate around their average value of zero, and attain maximum values of +1 and minimum values of −1.
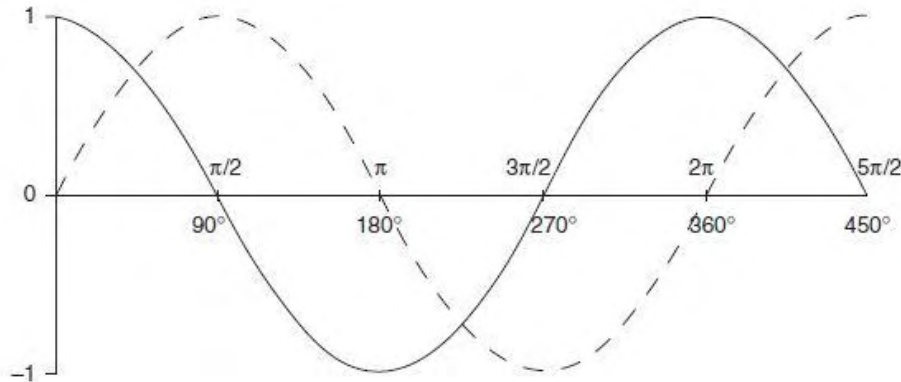


Fig.2.10. Portions of the cosine (solid) and sine (dashed) functions on the interval 0° to 450° or, equivalently, 0 to 5π/2 radians. Each executes a full cycle every 360° or 2 radians. (Source: Wilks, 2006)

The length of the data record, n is regarded as constituting a full cycle, or the fundamental period. Since the full cycle corresponds to 360° or $2\pi$ radians in angular measure, the time of the data record can be rescaled to angular dimensions using

$$\left(\frac{360\,°}{\text{cycle}}\right)\left(\frac{t\text{ time units}}{n\text{ time units}\big/\text{cycle}}\right)=\frac{t}{n}360°=2\pi\frac{t}{n} \qquad \ldots 2.2$$

The equation denotes the angle that subtends proportionally the same part of the distance between 0 and $2\pi$, as the point t is located in time between 0 and n.

The fundamental frequency is expressed as $2\pi/n$. This frequency expresses the fraction of the full cycle that is executed during a single time unit. In order to adjust the sine or cosine function the mean value of the data series is added to the sine or cosine function. The vertical stretching or shrinking of the dataset is accomplished by multiplying the function with a constant known as amplitude C. Thus the data series y can be expressed as

$$y = \bar{y} + C_1\cos\left(\frac{2\pi t}{n}\right) \qquad \ldots 2.3$$

The function is represented in the figure 2.11. Shifting of a harmonic function in the lateral direction is necessary to match the ridges and troughs of the data series.
The cosine function can be shifted to the right by the angle φ results in a new function that is maximised at φ and the data series can be represented as

$$y = \bar{y} + C_1\cos\left(\frac{2\pi t}{n} - \varphi\right) \qquad \ldots 2.4$$
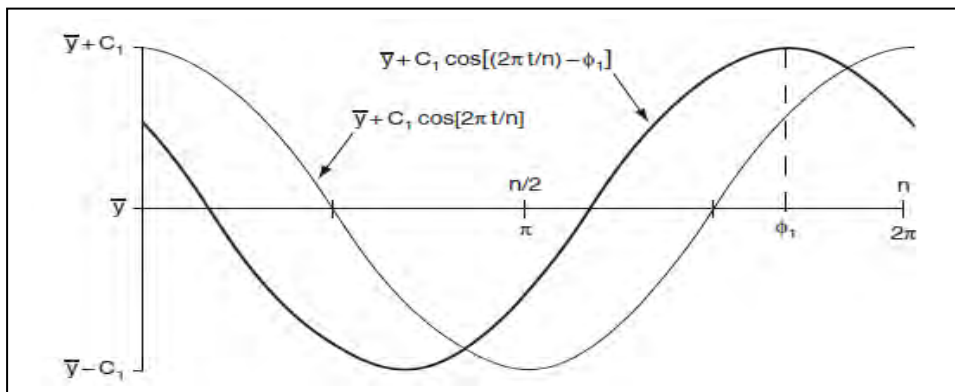


Fig.2.11. Representation of the data series by cosine function (thick black line) and shifting of the cosine function towards right by an angle φ (thin black line)

The angle φ is called phase angle or phase shift. A similar equation can be written for sine function also. Harmonic analysis of total ozone data is carried out in chapter 2 of the thesis using Fast Fourier Transform (FFT). The details are given in the same chapter.

# Seasonal Variability of Total Ozone over India and Adjoining Regions

## 3.1.  Introduction

Atmospheric ozone is one of the highly variable trace gas constituents of the atmosphere.  The concentration of ozone can vary in short to long term scales which can profoundly influence the vertical thermal structure of the atmosphere (Langematz et al., 2003). Deviation in ozone concentration can change the radiative properties of the atmosphere inflicting a negative radiative forcing due to absorption of shortwave radiation and a positive radiative forcing in the troposphere due to absorption of longwave radiation (Forster and Tourpali, 2001). The change in ozone amount over a region can be due to natural and anthropogenic factors. Human activities can influence the ozone amounts in the atmosphere through the emission of certain harmful substances that can destroy the ozone layer and also by the release of certain chemicals that can cause the production of ozone in the troposphere. Another indirect effect of mankind upon atmospheric ozone is the release of greenhouse gases causing climate change. This modifies the atmospheric circulation, temperature and the radiative interactions (both in shortwave and longwave spectrum) in the atmosphere which in turn can cause changes in the production and transport of ozone. The concentration of ozone over a region can vary mainly due to the changes in stratospheric ozone or to a small extent by deviations in tropospheric ozone.

 Stratospheric ozone is known to fluctuate in response to natural factors such as Quasi Biennial Oscillation, El Nino Southern Oscillation (ENSO), variations in transport associated with Brewer Dobson circulation and variability in annular modes. Changes

in stratospheric ozone distribution can impact the radiative balance of the atmosphere, with a feedback on the upper troposphere lower stratosphere region and climate, and on surface UV levels, it is important to understand not only its zonal mean temporal evolution but also its spatial distribution and variability (Canziani et.al, 2008). The detection and attribution of the trends in ozone depend on both long term changes and on the seasonal variability of ozone. A central problem is attributing these changes to causes such as dynamical variability, long term climate change, decreasing ozone depleting substances or the changing phase of the solar cycle (WMO Scientific Assessment of Ozone Depletion, 2010).

One of the main reason studying the variability of ozone layer is to check whether the control measures taken by mankind to prevent ozone depletion is effective in purpose. It is important to quantify the extent of ozone variability to isolate the effect of anthropogenic factors from the natural factors that cause ozone variability. A number of studies have attempted to explore the spatial and temporal distribution of total column ozone around India and surrounding regions. Sahoo *et.al.,* (2005) studied the variability of total column ozone over Indian subcontinent and found that the rate of decline is more over the northern parts of the region. Patil and Revadekar (2008) examined the total ozone column over Indian region for two different periods from 1979-1993 and 1997-2005 and found that the trends in extreme total ozone events are decreasing over the northern parts of India during winter. Pal (2010) found that the total column ozone over India shows an overall decreasing tendency. Kalapureddy et al. (2008) studied the total ozone variability over oceanic region around India and found that the total ozone content is around 298 DU with fluctuations around 10 DU.

The main causes of ozone variability in the upper stratosphere are photochemical production and destruction. But when it comes to lower stratosphere dynamical processes are the main causes of changes in ozone concentration since the lifetime of ozone in the stratosphere is larger than the timescale of transport. The variations in tropospheric ozone is due human activities like combustion of fossil fuels, biomass burning etc which can produce chemicals like nitrogen oxides and volatile organic carbon which in turn generates tropospheric ozone. Ozone can act as a tracer of circulation and can be influenced by the passage of weather systems and with the

seasonal variation of the circulation as well. Ozone plays an important role in modulating the solar radiation reaching the earth's atmosphere. There exist complex inter relations between solar activity, quasi biennial oscillation and other phenomena that can give the resultant ozone variation over a region.

Estimating the variability is also essential to understand the credibility of the ground based and satellite measurements in determining the ozone over various heights. Studying the ozone concentration over a region can help in understanding the radiative forcing that can be caused by ozone as well as the coupling with ozone and climate and hence understanding the coupling or feedbacks between ozone and climate. Destructive effects of solar UV-B radiation on humans and other biospheric species demands retrospective studies of UV climatologies, which focus on the factors affecting the ground-level UV irradiance (Eerme et al.,2002). Future of the Ozone layer remains uncertain i.e. whether it will return to similar or lower or higher values prior to ozone depletion period. It can be predicted only by analysing the trend in various regions of the globe (UNEP, 2006). The objective of this study is to understand the seasonal and spatial variation of total column ozone over Indian region and to understand the sensitivity of ultraviolet radiation to ozone concentrations over this area.

## 3.2. Data and Methodology

Multisensor reanalysis monthly data for total column ozone from Royal Netherlands Meteorological Institute was used for the study. It is a globally consistent dataset which is developed by integrating the different types of ozone observations and applying data assimilation. Data from 1979-2008 with a resolution of 1° Latitude×1.5°Longitude is used for this study. The data for Indian region (0°N-40° N, 60°E-100°E) was extracted and averaged for each month from 1979-2008 and climatological maps were constructed for each month to study the variations of total ozone along a year. Time series of monthly mean total ozone for 60-100°E longitudinal area for the latitudinal regions 0 to 20°N and 20 to 40°N was plotted from 1979-2008. Trends in total ozone were constructed using the least squares method, for the annual averaged total ozone values as well as the four seasons -summer, spring, autumn and winter. Zonally

averaged values of ozone for each of the 1 degree latitude bands were also computed for each month to study the variation of ozone with latitude.

The annual coefficients of relative variation and Total ozone percent variability (Akinyemi, 2007) were computed. The entire latitude extent of Indian region was divided into eight latitude zones- 0°N-5°N, 5°N-10°N, 10°N-15°N, 15°N-20°N, 20°N-25°N, 25°N-30°N, 30°N-35°N, 35°N-40°N. The annual coefficient of relative variation for each 5° latitude bands from 0 to 40°N and 60 to 100°E was calculated as follows

$$CRV = \frac{100 \; X \; Standard \; Deviation}{Mean} \qquad \ldots (3.1)$$

$$Annual \; CRV = \frac{100 \; X \; Annual \; Standard \; Deviation}{Annual \; Mean} \qquad \ldots (3.2)$$

Total ozone percent variability at each zone for each month is obtained by the equation

$$A \, (i) = \frac{R \, (i) \; X \; 100}{Q \, (i)} \qquad \ldots (3.3)$$

Where i=Months of the year

A(i)= Percent of total ozone concentration for the month i

R(i)=Range of ozone concentration among all the years studied

Q(i)= Average ozone concentration

Data for Local Noon erythemal ultraviolet radiation (UVER) for the years 1999 and 2000 was taken from Total Ozone Mapping Spectrometer website. The Radiation Amplification Factor (RAF) for erythemal UV radiation was computed for all the months of using the equation.

$$RAF = \frac{-\left(\frac{\Delta E_{uv}}{E_{uv}}\right)}{\left(\frac{\Delta O_3}{O_3}\right)} \qquad \ldots (3.4)$$

Where $E_{uv}$ is and $\Delta E_{uv}$ the solar irradiance at surface during clear sky conditions and the change in the same respectively. Similarly $O_3$ and $\Delta O_3$ are the total ozone concentration and the change in it respectively. The effect of ozone depletion on erythemal ultraviolet radiation is frequently expressed by means of the erythemal UV Radiation Amplification Factor (RAF) (Madronich, 1993). It is defined as the percentage increase in UVER that would result from a 1% decrease in the column amount atmospheric ozone (McKenzie, 1991)., RAF has become a widely used standard index (Bodhaine et al., 1997; Madronich et al., 1998; Dubrovsky, 2000; Zerefos, 2002). RAF was also computed using in situ data for total ozone from New Delhi and Pune during local solar noon and clear sky surface UV irradiance from TEMIS . This calculation is done using power law relationship.

$$RAF = \ln\left(\frac{E^*}{E}\right)\Big/\ln\left(\frac{O}{O^*}\right) \qquad\qquad \dots (3.5)$$

Where E and E* represent the UV irradiance for two instances and O and O* represent corresponding column ozone amounts.

## 3.3. Results and Discussion

### 3.3.1. Climatology of Ozone over Indian region

Figure 3.1 gives the climatological mean of total ozone from 1979-2008 from January to December. It is obvious from the figure that the ozone distribution over the region is zonally symmetric with the highest values in the subtropical region and lowest values in the tropical region. This is due to the photochemical production of ozone in the tropics and its transport to higher latitudes by atmospheric circulation. The region from 0°N to 25°N shows the comparatively low ozone concentrations over the entire region with an average value of about 250 DU. This low ozone region is more evident from late autumn to early spring (November to March). Ozone concentrations over this area increases slightly from April. This increase remains till the end of the monsoon season. Another notable feature is the development of a low ozone area over Tibet (28°N and 88°E) during the advent of the monsoon season (June). This area can be seen as an area of relatively higher ozone concentration during previous months (April and May).
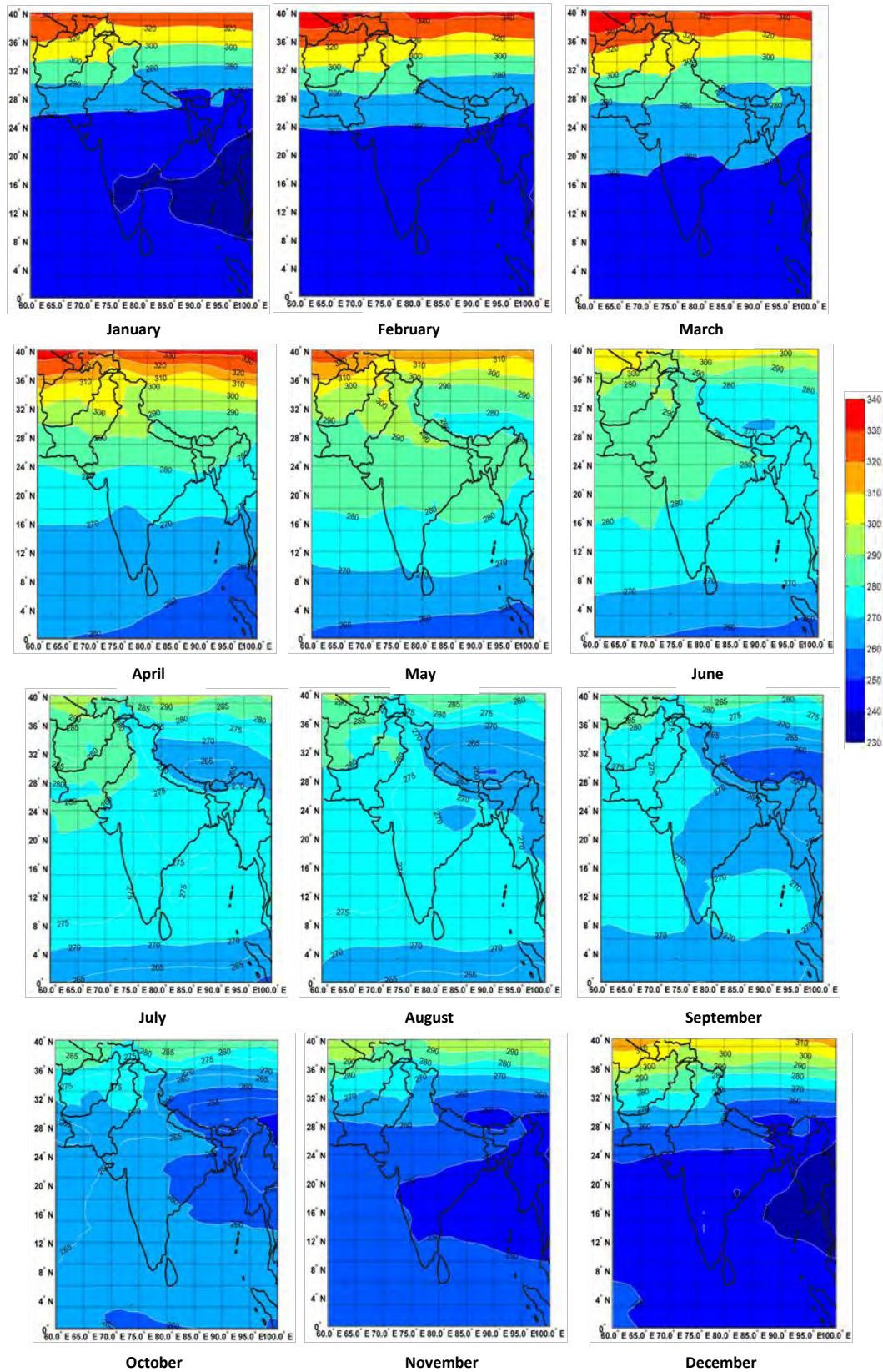
Fig.3.1. Climatology of total ozone over India from 1979 to 2008

Prabhakara and Rodgers (1976) stated that the geographic extent of the tropical ozone minimum over Southeast Asia associated with wave number 1 in the lower stratosphere seems to grow in size in July, extending over the Tibetan plateau to the north. The low ozone area which started its development in June increases in extent with the progress of the monsoon season and is known as' Ozone valley'( Zhou and Luo, 1994, Zhou et al., 1995, Zou,1996, Zou and Yongqui, 1997, Liu et al., 2003, Bian et al., 2006). The lower values of ozone column during this season are accompanied by upper level monsoon anticyclone (Tobo *et.al,* 2008, Ye and Xu, 2003).  By the end of September, this low ozone area develops a limb towards the tropical region. Low total column ozone over Tibet is due to the seasonal and longitudinal variations in tropopause height and the variations can be due to convective activity, air expansion or the monsoon system (Tian et al, 2008). By October the low ozone concentration spreads to the latitudinal region from 0°N to 28°N.

The region from 16°N to 30°N is showing the highest of ozone values in this region of about 280-290 DU from April to June. After that the ozone values again drops by about 5DU during July and August. Another area with the lowest ozone concentration can be seen from 85°E to 100°E and 8°N and 24°N during December and January. High latitude zone from 28°N to 40°N shows the highest concentration of ozone from mid winter to early spring while the lowest of the values over this region is seen during July, August, September and October. At northern mid latitudes, ozone amounts will be larger in winter and early spring and smaller in summer and fall (Stratospheric Ozone: An Electronic Textbook, NASA, GSFC).  Higher ozone values spread southwards from 30°N during April and May with an increase of about 10 to 20 DU. Latitudinal band from 35°N to 40°N shows a decrease of about 10 DU concurrent with this increase and reaches a value of about 310 DU.

**3.3.2. Temporal evolution of Ozone over tropical and subtropical regions of India**

The temporal variation of monthly mean total ozone over India in latitude bands 0°N-20° N and 20-40° N in longitudinal region 60°E-100°E is given by Fig 3.2. The figure shows high values in subtropical Indian region compared to tropics as expected. The two latitudinal bands display an out of phase relation during most of the study period. For the 20°N-40°N latitude band, a decrease in ozone concentration from 1979 to mid

1990s is obvious from the figure. From 1993 onwards ozone is displaying a slight increase. This may be due to the commencement of recovery in atmospheric ozone concentrations caused by the decrease of ozone depleting substances (WMO Scientific Assessment of Ozone Depletion, 2010). Also amplitude of fluctuations in total ozone for the 20°N-40°N band is higher during the first half of the study period (from 1979-1993). The region from 0°N-20°N is showing biennial behaviour after 1995. Minimum value of ozone concentration around 261 DU occurred during years 1984 and 1996. Maximum amount of ozone in 20°N-40°N is about 278 DU that occurred in 1990 and 1999. Subtropical region exhibits large interannual variability compared to 0°N-20°N region. The variability is more pronounced in the first half of the study period. The highest value of ozone concentration can be observed during 1982 and lowest during 1993.
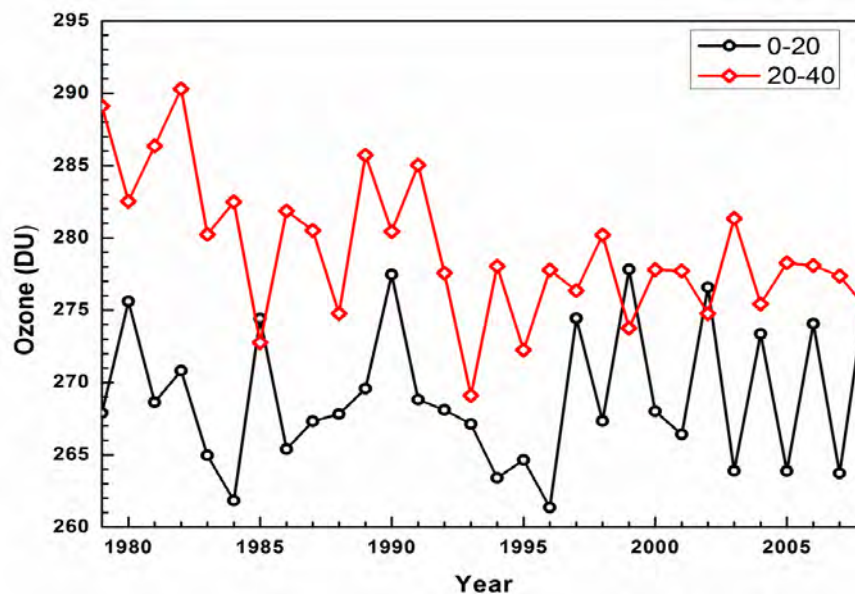


Fig.3.2. Time series of ozone concentration over India from 1979-2008. The black line represents latitudes from 0°N -20°N and redlines represents latitudes from 20°N-40°N.

### 3.3.3. Latitudinal distribution of Ozone

Figure 3.3 represents the distribution of total column ozone during various months of the year. During winter season (Fig.3.3. a) the latitudinal distribution of ozone column shows high variability across the latitudes. Total ozone amount is around 250 DU from

0 to 5°N and it shows a slight decrease from 5°N to 15°N. From 20°N onwards ozone shows a continuous rise of about 90 DU when it reaches 40 °N. The month of February shows comparatively higher concentration during winter season followed by January and December respectively. The latitudinal gradient is higher during winter season. From about 5°N to 15 °N a constant increase of about 2 DU is observed from January to February.  The value of total ozone remains roughly the same around 23°N for December and January. The region above this latitude shows an increase of about 3 to 5 DU during midwinter i.e. between December and January.

During spring season (Fig.3.3.b) the concentration of ozone in the lower latitudes increases by about 5 DU in the near equatorial Indian region from 0 to 5°N compared to the winter season. A small dip in ozone values of about 1-2 DU can be seen from 5°N-20°N for March (black squares) similar to that of winter season. The steepness of latitudinal gradient is slightly lesser compared to that of the winter season.  Ozone increasing steadily from 0°N to 40°N is for the month of April. But for May the Ozone concentration is showing a dip of 2-3 DU nearly 30°N.  For spring season the behaviour of ozone amount over 0°N to 30°N is opposite to that from 30°N-40°N. The month of May has the highest concentration followed by March and April in the former region whereas over the latter region the ozone concentration for earlier spring (March) is the highest compared to that of the later spring.

Column amount ozone during summer season (Fig.3.3.c) shows a range of variability from 260 to 300 DU over India.  For the latitudes from 0°N to 7°N the concentration increases by about 5 DU from the initial values around 260-265 DU for the three months. The latitudinal amount of ozone remains steady until 20°N especially for the month of June.  From 20°N to 28°N there is a slight decrease in ozone amounts for July and August while the month of June is showing a slight increase. Above 30°N the values of total ozone shows an increase of about 20 DU till 40°N. The variability of ozone concentration over equatorial latitudes is high during autumn season (Fig.3.3.d). From 0 to 20°N, September has the highest ozone concentration of 265 DU followed by October with 260 DU and November with 253 DU.  There is a slight decrease of 2-3 DU for November from 10°N to 20°N. The concentration of ozone remains more or less unchanged from 0°N to 30°N latitudes for autumn season.  Total amount of ozone

becomes same for the three months at 33°N. Thereafter the values rise by 30 DU when it reaches 40°N. Higher latitude variability of ozone is very less during autumn.

Considering the four seasons, the winter and spring seasons show comparatively large variability of about 90 DU for the entire latitude range from 0-40°N. Summer and autumn seasons display a variation of around 50 DU. Winter season is exhibiting the highest and lowest of ozone values during the entire year. The lowest value of about 235 DU occurs during January at nearly 15°N and the highest values can be seen at 40°N during February. The role of shortwave radiation in inducing seasonal variability of ozone is examined in next section.
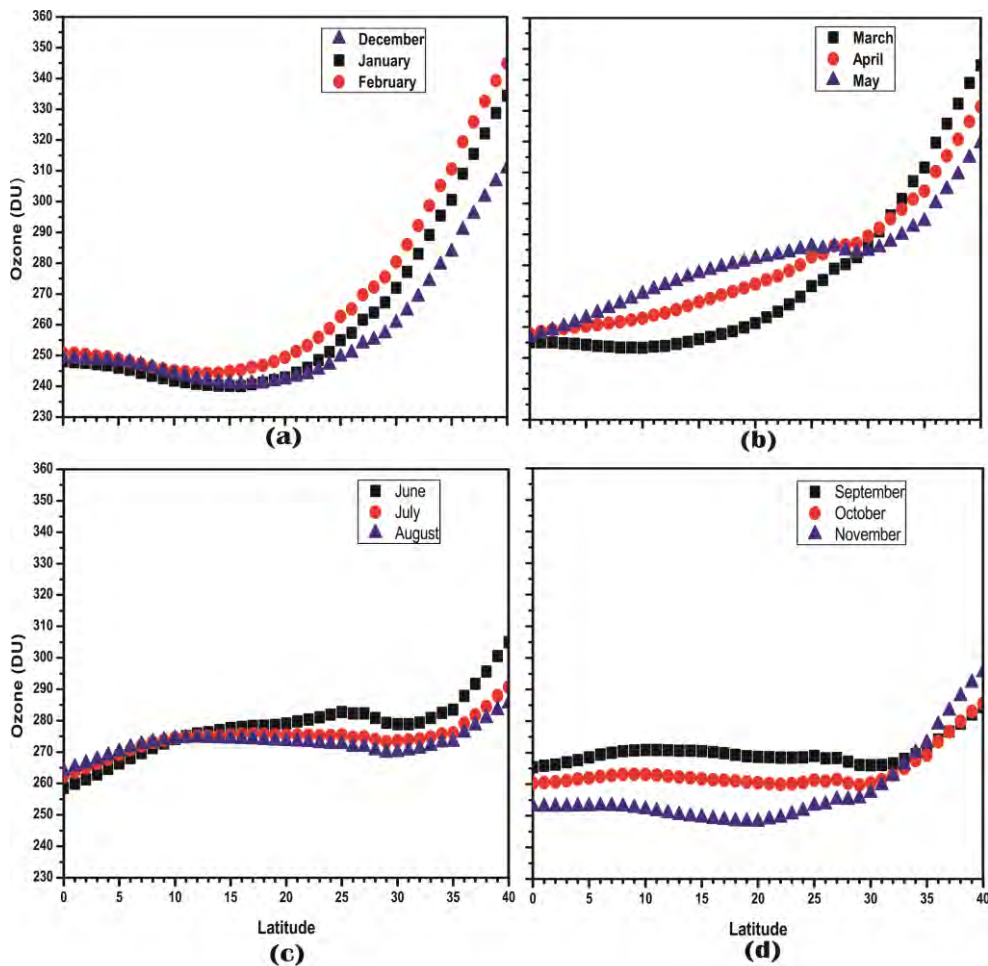


Fig 3.3.Latitudinal distribution of Total Column Ozone during months (a) December, January, February (b) March, April, May (c) June, July, August (d) September, October, and November.

### 3.3.4. Relation between ozone and shortwave radiation flux at the top of the atmosphere

Fig 3.4. shows the seasonal cycle of the latitudinal distribution of ozone for each ten degree latitude bands from 1979 to 2008. One of the major factors that influence the ozone concentration over a region is the incoming shortwave radiation. The region from 0°N to 20°N is the region that receives large amount of solar radiation over the entire year with slightly higher amounts during spring and autumn seasons. Figure 3.4. (a) represents the seasonal cycle of incoming shortwave radiation at the top of the atmosphere for 0°N to 10°N from 1983 to 2007. From Figure (a) it can be seen that the region from 0°N to 10°N receives shortwave radiation in the range of 395 Wm$^{-2}$ and 435 Wm$^{-2}$. Because of the presence of the sun directly above this region almost all the time of the year since the sun moves from 0°N to 20°N from equinox to solstice and back.
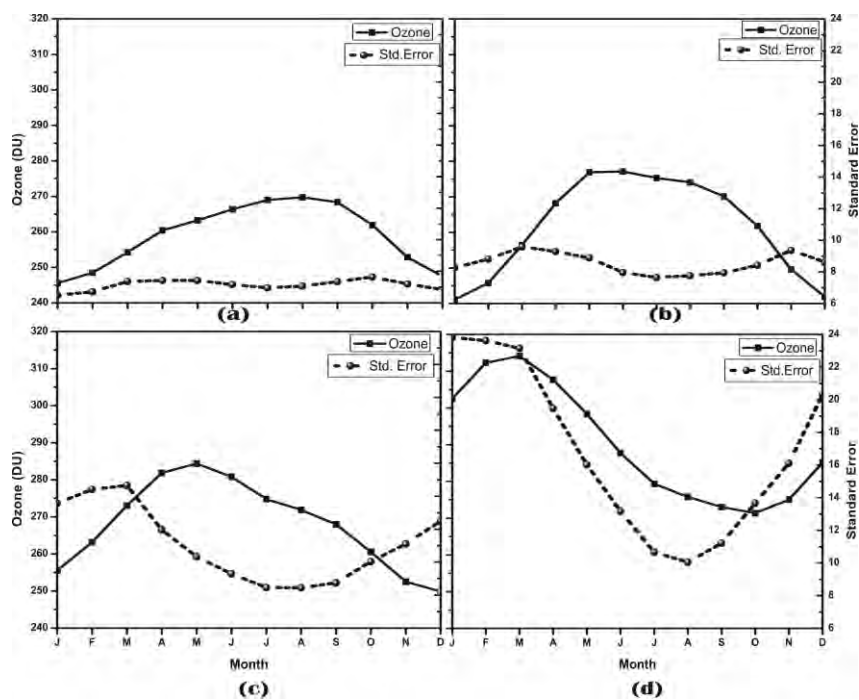


Figure 3.4.  Latitudinal average of Total Ozone (solid line) and standard error in Ozone measurement (dashed line) from1979 to 2008 for longitude 60°E to 100°E and latitudes (a) 0°N -10°N (b) 10°N-20°N (c) 20°N-30°N (d) 30°N -40°N.

Shortwave flux is slightly higher during the spring and autumn seasons with values of 435 Wm$^{-2}$ and 430 Wm$^{-2}$ respectively (Fig. 3.4. (a) ). This is due to the proximity of the sun during the equinoxes. Figure 3.4.(a) shows the total ozone values averaged over 60°E to 100°E and 0°N to 10°N for the time period from 1979-2008. The distribution of ozone in the region from 0°N to 10°N shows concentration in the range from 245 DU to 270 DU with the highest value during August. The annual maximum value of ozone occurs from mid-summer to early autumn period. The amount of ozone shows comparatively lower values during spring season when the region is receiving largest magnitude of radiation. The standard error of ozone data is minimum during the month of July and maximum during October for 0°N to 10°N band.

The region from 10°N to 20°N (Fig 3.4. (b)) shows the maximum value of ozone concentration during the month of May. The value of ozone varies from 241 DU during the month of December to 278 DU during May. Figure 3.4.(b) shows the maximum solar radiation during the month of May. The value of minimum standard error is during the month of July.
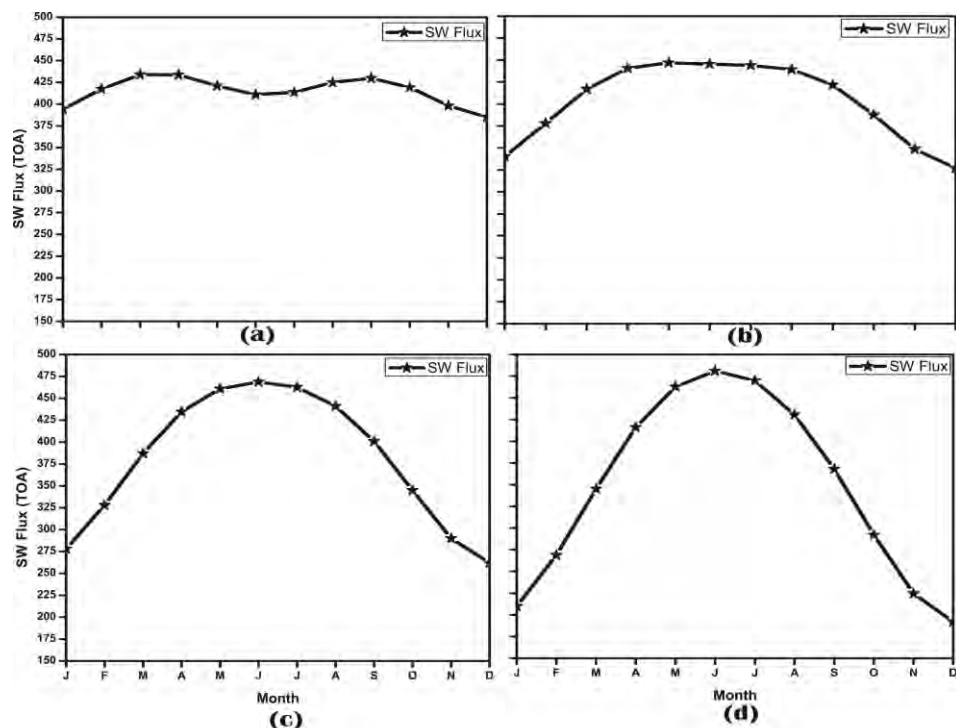


Fig. 3.5. Shortwave Radiation flux at the top of the atmosphere for from1983 to 2007 for longitude 60°E to 100°E and latitudes (a) 0°N -10°N (b) 10°N-20°N (c) 20°N-30°N (d) 30°N -40°N.

The region receives minimum shortwave flux during December, the month with the lowest ozone concentration. The total column ozone over 10°N to 20°N nearly follows the fluctuations in solar flux. The region from 20°N to 30°N (Fig. 3.5. (c)) receives maximum amount of solar radiation during late spring and summer season, the time close to the summer solstice. The solar flux during this time is around 465 $Wm^{-2}$. From Figure 3.5.(c) it can be observed that the region shows the maximum amount of ozone during the month of May and minimum during the month of December. The value of Total column ozone (TCO) ranges from 255 DU to 285 DU.

The annual minimum value also coincides with the lowest value of solar radiation. Standard error of ozone data is highest during March. Although the solar flux is maximum during June the highest ozone values occur during the month of May. The latitudinal band that extends from 30°N to 40°N gets maximum amount of solar radiation during summer season (Fig 3.5. (d)). The Total ozone values at this region are from 310 DU to 272 DU during March and October respectively. Standard error for this area is also highly variable with values from 9 to 24. The standard error varies in the same direction as the variation in the concentration of ozone over this latitudinal band.

From Figure 1.2 it is evident that the range of variability of total column ozone increases towards higher latitudes. The overall fluctuation in ozone is about 25 DU in the 10°N -20°N over a year. The range increases to about 30-35 DU in the latitudes from10°N to 30°N. The region from 30°N to 40°N shows the range of variability of 45 DU. Even though solar radiation is an important criterion for ozone fluctuation, the ozone variation is not exactly following the variation in solar radiation in all the latitudinal regions considered except the 10-20°N region. The extratropical region from 30-40°N shows the least concurrence to the variations in incoming solar flux. The region is showing large ozone concentrations during March despite the highest amount of solar radiation during June. The role of atmospheric dynamics could be a reason for this behaviour of ozone concentration.

### 3.3.5. Coefficient of Relative Variation

Figure 3.6. represents the coefficient of relative variation (CRV) of Column amount ozone over India divided into eight latitude zones of 5° latitude width. Fig.3.6.a gives the CRV of about 2.5, for years from 1979 to 1983. The equatorial band 0-5°N shows the lowest value of CRV in the whole year. The zones further north displays an increasing variation throughout the year and the value reaches about 5.5 at 10-15°N and again decreases to about 3.5 in 25 to 30°N. From there the values increases steeply towards 40°N with values as high as 9.5.
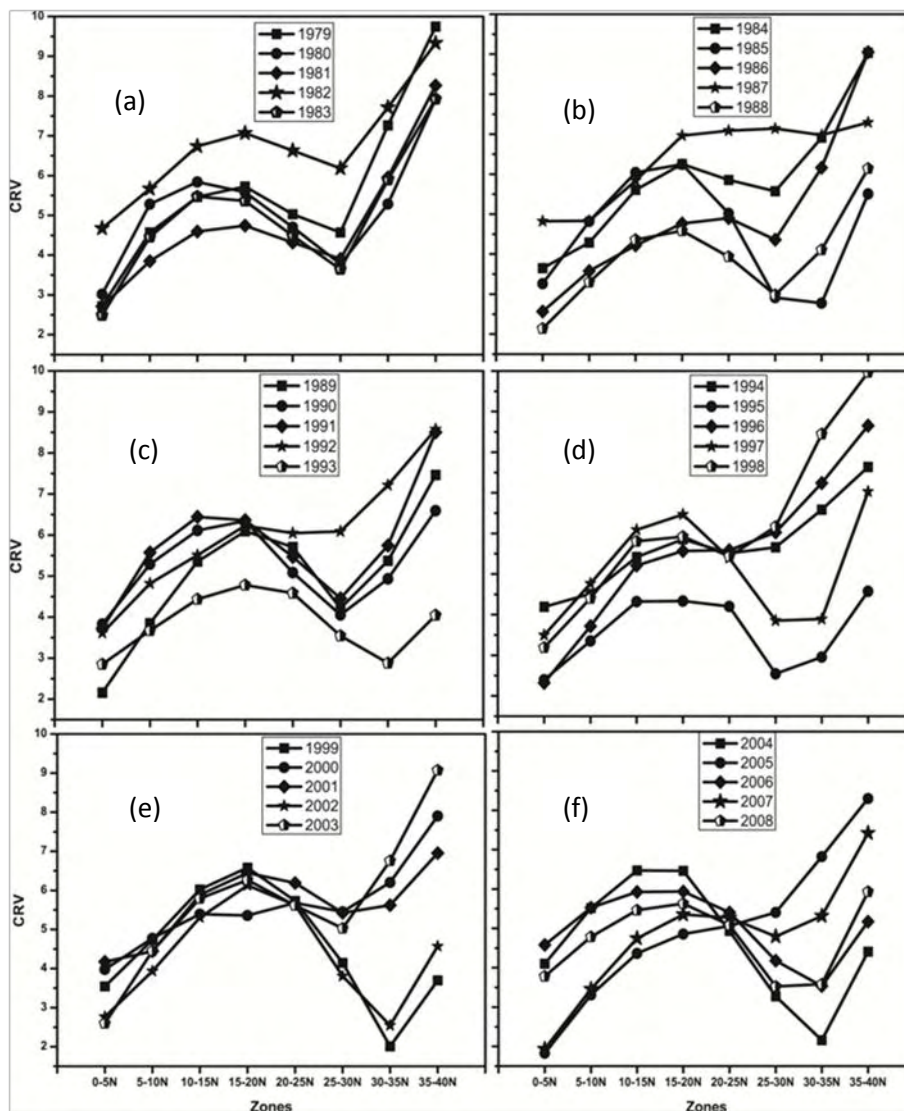
Fig 3.6. Coefficient of relative variation of ozone over the eight latitude zones (longitude 60-100°E) over India from 1979 to 2008.

From the figure it can be seen that year 1982 has the highest value of CRV in all the period from 1979 to 1983 and the highest variation during this year occurs in 15-20°N band. From 1984 to 1988 (Fig.3.6.(b)) the peak value of CRV over tropical region shifts to 15-20°N zone. But the variation over 25 to 30°N is not as low as in previous years and displays a value of about 5.5. The coefficient shows the same values of previous years over subtropical regions. In 1985 the annual variation in the tropical region was the same with lowest in the equatorial band and highest in 15 to 20°N. But in the region north of this zone the coefficient of variation values shows a steep decrease in the next three latitude zones reaching about 2.5 which is same as the equatorial variation. Year 1987 shows a gradual increase from equator to 40°N without any drop off in between.

Period from 1989 to 1993 (Fig.3.6.c) displays the same general pattern of variation as in previous years. Year 1993 shows the lowest variation during this period. From Fig. 3.6. (d) it can be seen that years 1995 and 1997 shows the general pattern of increase from equator to 20°N and decrease towards 30-35°N and an increase thereafter. Years 1994, 1996 and 1998 show steady increase of CRV from equator to 40°N. Years 1999, 2000 and 2003 (Fig.3.6. (e)) also exhibit a steady increase from equator towards north. The pattern of annual variation during 1999 and 2003 displays departure from the other years by showing lowest values of CRV about 5. Coefficient of relative variation is also showing lowest values during 2004, 2006 and 2008 (Fig.3.6. (f)).

### 3.3.6. Percent of variability of Total Ozone Over India

Magnitude of ozone variations that occurred during the period 1979-2008 is expressed as percentages in Fig.3.7. The subtropical Indian region is showing large variability during winter and spring seasons come next in the extent of variability. Seasonal variation of solar radiation, transport due to planetary wave propagation during winter (Fusco and Salby, 1999) and the passage of weather systems like western disturbances can account for the high amount of variability during this season at subtropical latitudes.
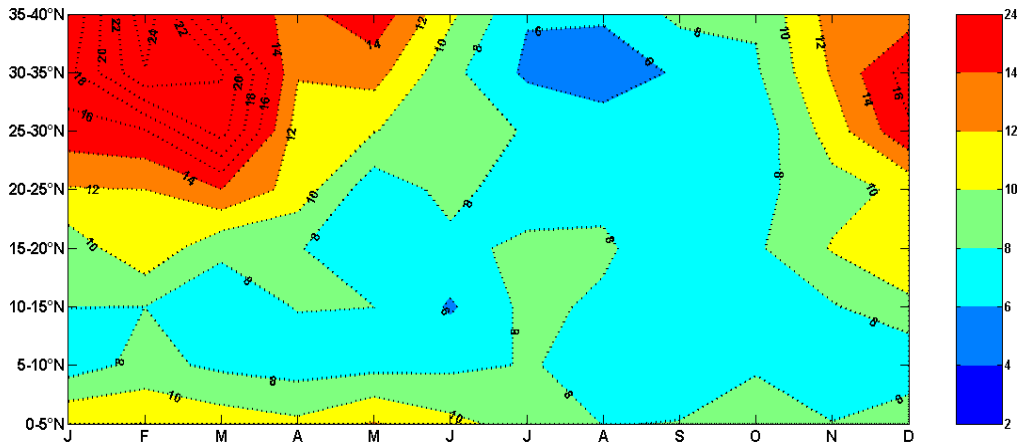
Fig.3.7. Percent of variability of ozone over the eight latitude zones from 0 to 40°N from January to December for the period 1979-2008.

Late winter season exhibits the highest amount of variability with ozone amounts changing as high as 24% .When it comes to spring season the percent of variability is from 10 to 14%. Entire Indian region exhibits the lowest variability during August, September and October. The subtropical region is showing high seasonal variability with highest variation during winter and lowest about 6 percent during summer season. It is obvious from the figure that the equatorial region is also showing a medium amount of variability especially during the first half of the year.

### 3.3.7. Trends in column amount ozone from 1979 to 2008

Trend in annually averaged ozone over India region is given in Fig. 3.8. (a). The region is exhibiting near zero (between 0 and 0.05) and negative trends with progressing negative trends from equator to higher latitudes. The near equatorial region from 0°N to 12°N is displaying near zero trend during 1979 to 2008. The area further north of this show declining trends. The latitudes from 12°N to 24°N display a declining trend of -0.05 % per year. Region extending from 24°N to 32°N exhibits a negative trend of 0.1% per year and the area from 32°N to 40°N shows a decreasing trend of 0.15 percent per year. Fig.3.8. (b) represents the trend in column amount ozone for spring season over the entire period of study. This season shows slightly higher values of trend compared to annual values over the entire region but the spatial distribution of trends resembles the annual pattern. The near zero (from -0.05 to 0.05) extends to more area in

the tropical Indian region during spring season from equator to about 22°N. The region from 22-27 °N and region from 27-32°N have trend values of -0.1 percent and -0.15 percent respectively. The region from 32-40°N shows highest value of negative trend about -0.2 percent.

Trend in seasonally averaged column ozone amounts during summer season is given by Fig.3.8. (c). Summer season is showing lower values of negative trend when compared to other seasons with trend values nearly -0.05 per year almost everywhere the entire subcontinent. The subtropical region from 32-40°N and 80-100°E shows trend values between -0.1 and -0.15 percent per year. During autumn season (Fig.3.8. (d)). approximately all part of the region from 20-40°N displays the lowest negative trend compared to other seasons. The value of trend drops to about -0.06 over the subtropical region. In contrast, the region from 12-24° N showed slight positive values. Positive trends total ozone is displayed by this latitudinal region during autumn season only and the trends over the region from 0-12°N exhibits slight negative behaviour during autumn. Spatial distribution of trends during winter season (Fig.3.8. (e)) also resembles the annual averaged trend distribution as well as the trend during spring season. From figure it is clear that the interannual variation during winter and spring is larger compared to the other seasons and thus can significantly influence the annual averaged trend.

### 3.3.8 Amplitude of daily variation in column amount ozone over two Indian stations

#### 3.3.8.1. New Delhi

Daily fluctuations in ozone amount over two Indian stations were examined to understand the seasonal nature of daily fluctuations. The frequency distribution of various amplitudes for daily variation for New Delhi is shown in Fig 3.9. This picture is obtained using the data from 1957 to 2011. It is obvious from the figure that most of the daily fluctuations fall within 0 to 5 DU range. The difference in ozone concentration between two consecutive days can go up to 80 DU for New Delhi. The daily variation of ozone in 5-10 DU also occurred nearly half of the total number of days considered.
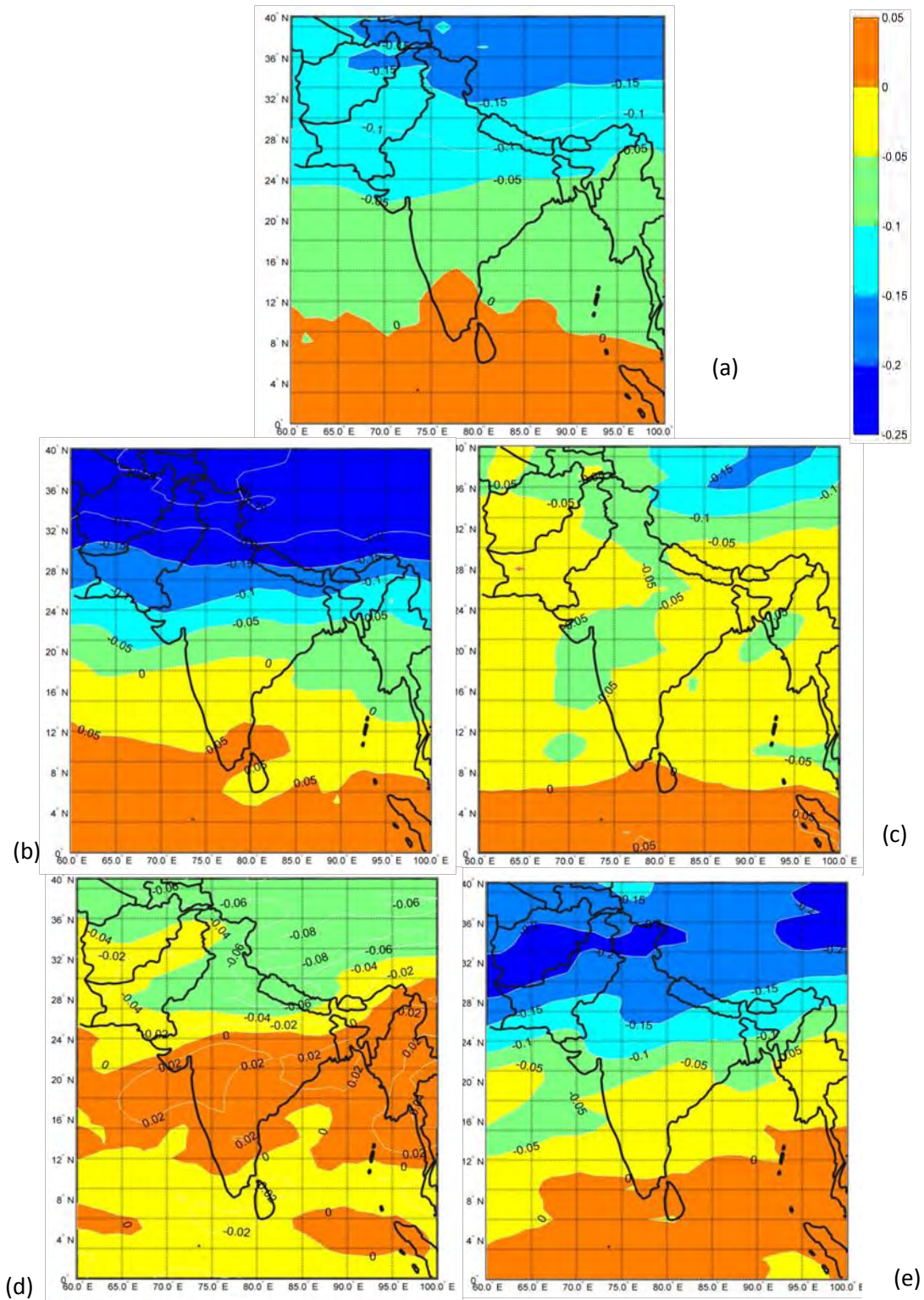
Fig.3.8. Trend (percent per year) in total column ozone over India from 1979 to 2008 (a) Annual, (b) Spring (c) Summer (d) Autumn (e) Winter.

One of the possible causes for the daily fluctuations in ozone is the passage of weather systems. Ozone distribution in the atmosphere reflects the pattern shown in weather maps. The concentration of ozone can change up to ten percent due to the passage of frontal and low pressure systems (Stratospheric Ozone: An electronic text book, NASA, GSFC). Besides Delhi is in the sub tropical region where there is more possibility of daily weather variations like the passage of western disturbances.
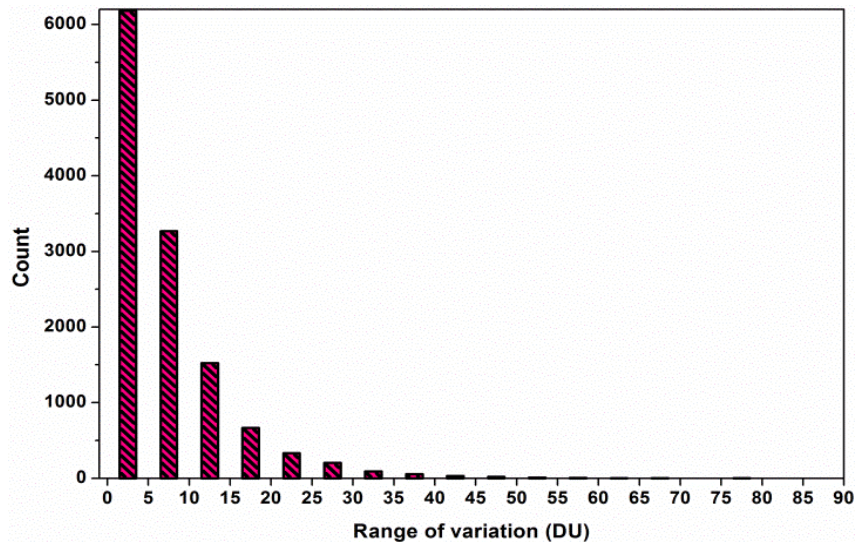


Fig.3.9. Frequency distribution of daily fluctuations for New Delhi for the total ozone data from 1957 to 2011.

The seasonal occurrence of various amplitudes of daily ozone fluctuation is given in Figure 3.10. For New Delhi autumn season shows minimum amplitude (0-5 DU) of daily fluctuations more. Fluctuations with amplitudes 10-15DU, 15-20 DU, 20-25DU, 25-30DU takes place more during winter and spring seasons. Amplitudes higher than that like 30-35 DU and 35-40 DU occurs during January and February. Daily variations reaching 40-45 and 45-50 DU (Fig 3.10-lowermost panel) have a very small frequency and they are found to happen during spring and a few in summer.

Fig. 3.10. Frequency distribution of daily fluctuations during all months of the year for New Delhi for the total ozone data from 1957 to 2011.

### *3.3.8.2. Pune*
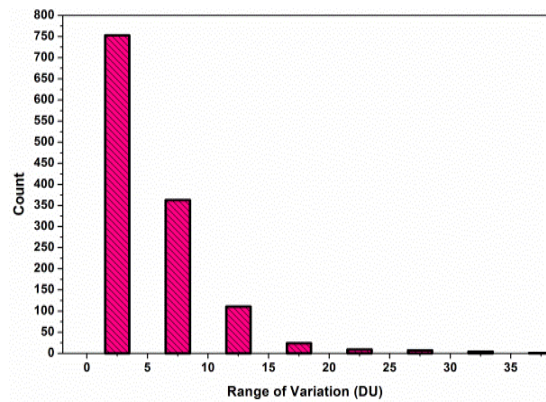


Fig. 3.11. Frequency distribution of daily fluctuations for Pune for the total ozone data from 2005 to 2009.
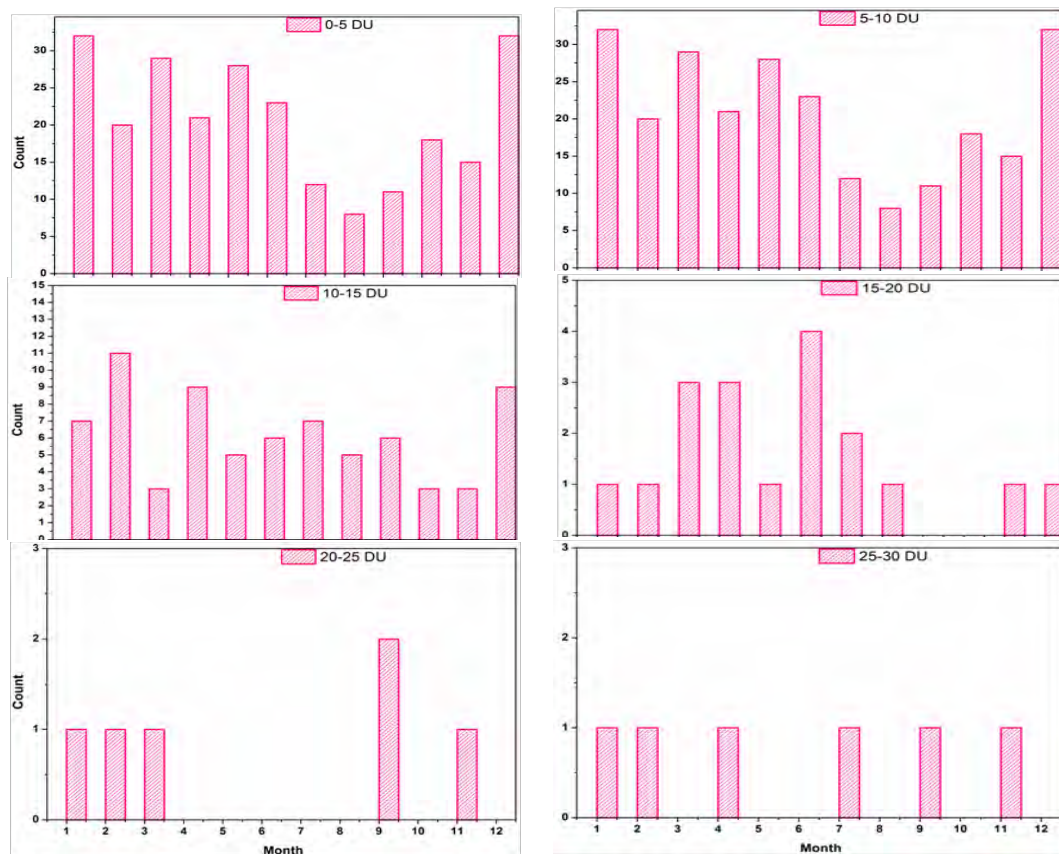


Fig. 3.12. Frequency distribution of daily fluctuations in different range of values during all months of the year for Pune using the total ozone data from 2005 to 2009.

Frequency distribution of ozone daily fluctuations is displayed in Fig.3.11. The distribution of different range of fluctuations during various months is given by Fig.3.12. The daily variations were calculated using data from 2005 October to 2009 December. Large scale daily fluctuations are only up to 40 DU. Compared to this New Delhi displayed large amplitude daily fluctuations reach up to 70 DU. For this tropical station large amplitude fluctuations occur during winter and spring seasons. UV-b irradiance is linked with the day-to-day ozone changes. A 1% decrease in total ozone can cause about 1.5 to 2% increase in damaging UV dose at ground level (Pyle and Derwent, 1980).

**3.3.9. Variation of ultraviolet radiation and total ozone over two stations**

Variations in total ozone and erythemal ultraviolet irradiance for New Delhi and Pune are shown in Figure 3.13 (a) and (b). Total ozone is given in black and UV irradiance is represented by red lines respectively. Erythemal UV irradiance display a clear annual cycle with peak values during summer months (mostly July) and the lowest is found during early and midwinter (December and January). The annual range of UV irradiance at the surface ranges from 100 to 310 mW/m$^2$ for New Delhi. The peak values of UV irradiance appear to be decreasing during 2009 and 2010. Total ozone over the station shows annual maximum during spring season (April and May) and many years have minor secondary peaks during winter season. The range of ozone variation fluctuates over various years. The period from 2009 to 2010 has larger amplitude of ozone variations when the range of UV irradiance is relatively small from previous years.

Total ozone data for Pune is not continuous. UV radiation is taken for analysis in the corresponding period only. The UV irradiance is not showing sharp increase from winter to summer as in New Delhi. The magnitude of annual UV radiation is also comparatively large as expected from a tropical station. The range of annual variation is from 180 to 360. Ultraviolet irradiance is showing higher values during spring and summer.

### 3.3.10. Radiation Amplification factor

The radiation amplification factor (RAF) computed for the eight latitudinal zones by taking the difference between corresponding months of 1999 and 2000 is given in Fig.3.14. These two years showed obvious difference in the pattern of coefficient of relative variation of ozone. Radiation amplification factor is defined as the percentage increase in erythemal UV radiation that would result from a one percent decrease in column amount atmospheric ozone (McKenzie, 1991). Simultaneous and independent measurement of total ozone and UV irradiance is necessary for the computation of RAF (Serrano et al, 2007).
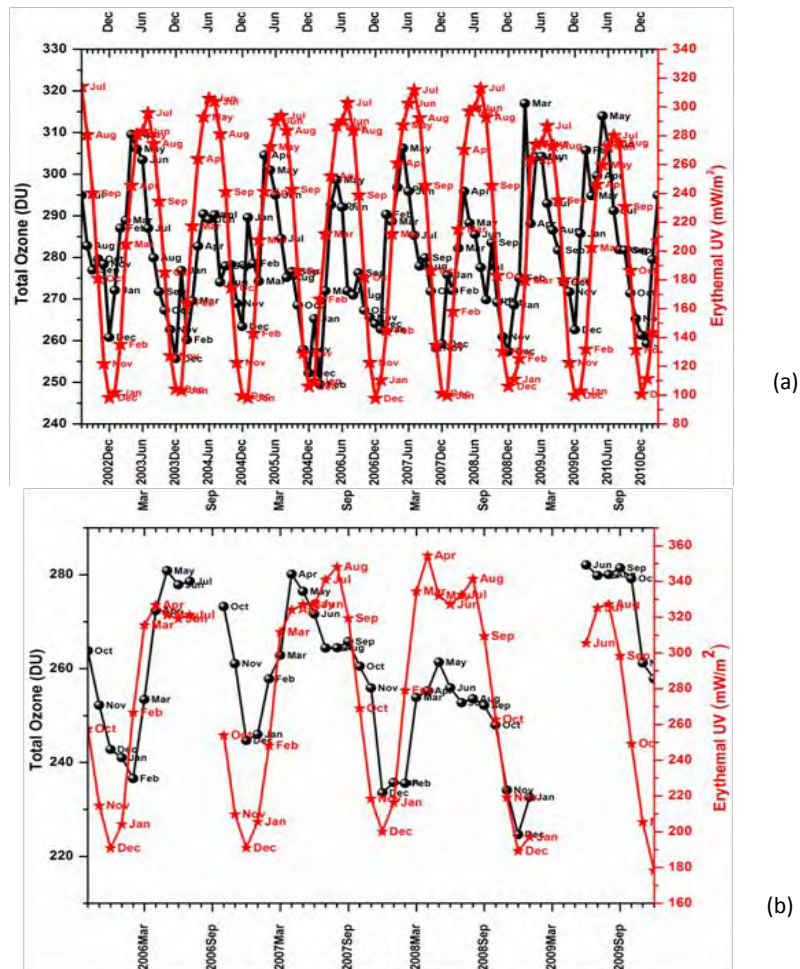


Fig.3.13. Time series of monthly averaged values of Total Ozone (black) and Erythemal UV radiation at the surface (a) New Delhi (b) Pune.

Most of the region is showing values between 0 and 1 with some isolated lower and higher values. Here satellite datasets for UV irradiance and Total ozone values from multisensor reanalysis are used for computing RAF. Since the multisensor ozone dataset includes TOMS total ozone values, it can influence the calculation of RAF using TOMS ultraviolet measurements (Since the algorithm of TOMS uses ultraviolet measurements from the satellite to calculate ozone).

The response of ultraviolet wavelengths to atmospheric ozone is more pronounced in UV-B wavelengths (280-315nm). Quantification of this wavelength band is more important due to its biological effectiveness. Apart from ozone atmospheric aerosols and total fraction of clouds can also influence the intensity of UV radiation reaching the surface. Isolation of ozone effects on UV is necessary (WMO Scientific Assessment of Ozone Depletion, 2010). The highest value of RAF is obtained during autumn season (August) in the tropical Indian region (5°N-10°N). The lowest value of RAF can be seen during summer season (June) subtropical region. During June all the latitude zones are showing values less than 1.
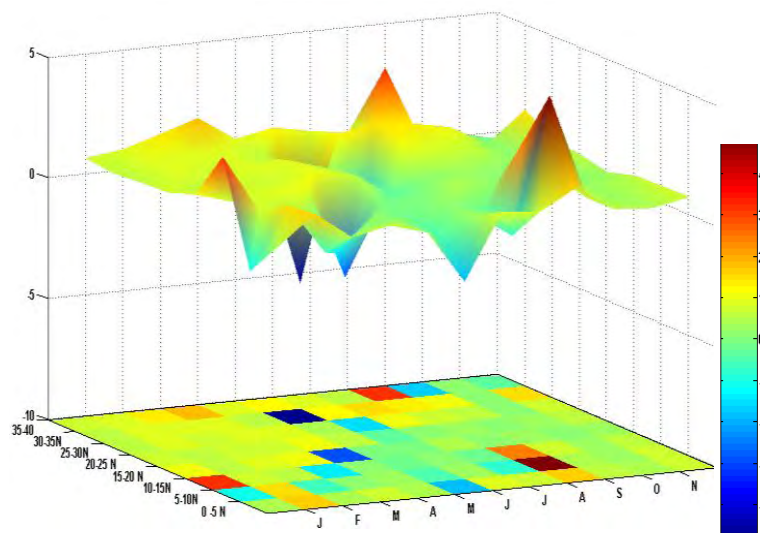


Fig.3.14. Radiation Amplification Factor over eight latitude zones of Indian region for years 1999-2000.

The sensitivity of UV radiation to ozone changes from 2002 to 2010 is represented as Radiation Amplification Factor for Pune and New Delhi in Figure 3.15. (a) and (b) respectively . For New Delhi the intra annual variation of RAF shows sharp peaks similar to the nature of the time series of UV irradiance for the same station given in Figure 3.13. The curve shows a see saw shape which is the typical characteristic of radiation curves. The range of variation is from 0.92 to 1.10 with minimum during October and maximum during January or February. Thus UV irradiance at the surface is more sensitive to ozone changes in winter. The daily variation of ozone showed its maximum during winter and minimum during autumn. Even though the ozone peaks annually during spring and erythemal UV peaks during summer, UV irradiance is more sensitive to ozone during winter when the daily fluctuations of ozone are more.
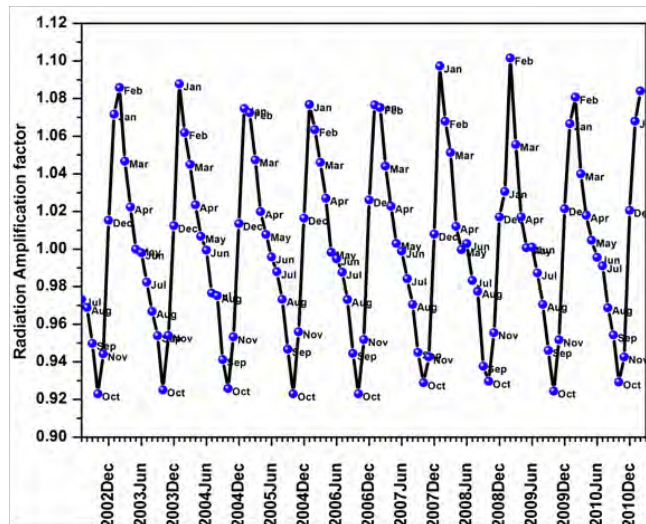


(a)
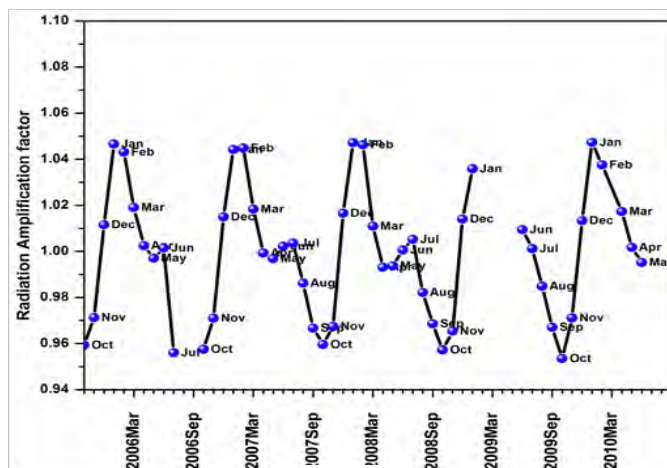


(b)

Fig.3.15. Radiation Amplification Factor for (a) New Delhi and (b) Pune.

Radiation Amplification factor shows lesser amplitude in seasonal variation over Pune with values ranging from 0.96 to 1.05. The lowest values are during October and highest during January or February. RAF values are showing minor secondary peaks during spring season when total ozone is showing its highest values over a year. This is absent for New Delhi. From the analysis of RAF it can be deduced that the extent of UV irradiance response differs for different locations depending on their latitude. The amplitude of response is more for New Delhi which is more distant from the equator compared to Pune. But the seasonal variations of both the stations are same. This analysis is carried out using satellite data for UV irradiance. Long term data for more stations are required to further clarify the effect of total column ozone on surface UV. Also isolation and attribution of UV irradiance anomalies due to column ozone variations can be done more effectively in the frame work of a radiative transfer model (because UV irradiance is affected by aerosols, clouds etc).

## 3.4. Summary

The season of winter and early spring is the time of extreme values in total ozone over India. The highest values of the entire year during the subtropical region from 28°N to 40°N and the lowest values of the entire year over the region from 0-28°N during these seasons. The study area can be divided into two zones on the basis of total ozone concentrations during months of January to March and October to December. Region 0°N-28°N having low ozone values (260-280 DU) and 28-40°N (300-340 DU) is having high ozone values. During April, May and June the study region can be divided into three zones with lowest values in the tropical region from about 0 to 16°N (260-270 DU), medium values from 16 to 30°N(280-300) and high values from 30 to40°N (300-320 DU). During these period ozone values increase in increments of 10 DU from tropics to higher latitudes. During July, August and September the entire Indian region is showing comparatively moderate values of column amount ozone. The origin of low total ozone values over Tibetan anticyclone during monsoon season and subsequent spread to higher and low latitudes is obvious from the study of total ozone climatology during this season.

Study of the ozone variations from 0-20°N and 20-40° N shows an out of phase relation between the two regions. The latitudinal variability is higher during winter and spring

months while it is lower during winter and autumn months. Annual cycle of near equatorial total ozone (0-10°N) is showing peak values during late summer and autumn season and lowest values during winter. Total Ozone in the latitude bands from 10-20°N and 20-30°N is displaying highest values May (late spring) and lowest during winter. Ozone column over 30 -40 °N shows highest values in late winter-early spring and lowest during autumn season. Ozone over this latitude band shows least concurrence to solar radiation at the top of the atmosphere. Coefficient of relative variation (CRV) is higher over subtropics and lower over near equatorial region. A secondary high in CRV is observed over 15-20°N latitude band. Ozone variation during winter and spring is influencing the overall trend of total ozone over India. From the study of Radiation Amplification factor it was deduced that a one percent decrease in column amount ozone can give rise to an increase in ultraviolet radiation between 0 and 1 percent. The computed RAF using different sources i.e. in situ total column ozone and satellite UV irradiance also shows similar values for Indian region. It was also found that the sensitivity of UV to ozone occurs during winter season which is the time of maximum daily variation in column amount ozone.

# Principal Modes of Variability in Atmospheric Ozone over India

## 4.1. Introduction

The atmosphere is in perpetual motion. Due to the turbulent nature of the atmosphere it becomes difficult to identify the impact of anthropogenic factors on the concentration of atmospheric ozone. Hence it becomes necessary to quantify the relation between various atmospheric dynamical phenomena and ozone abundance. Variations in ozone amount due to fluctuations of solar irradiance in ultraviolet (UV) wavelengths which is the primary factor that can directly alter the production and destruction of ozone should be identified. Output of UV wavelengths from the sun depends on the formation of magnetically active regions of the sun known as sunspots. The number of sunspots exhibits a in cyclical pattern with a period of around 11 years known as 11 year solar cycle. Incoming ultraviolet radiation from the sun induces ozone changes on decadal scale. The time in which the sunspot activity is highest is called solar maximum. Usually during solar maxima the sunspots occur in clusters on both hemispheres of the sun. When the sun rotates with a period of 27 days the effect of sunspots gets reflected in the quantity of atmospheric ozone. Incoming solar radiation changes about 0.1% from solar minimum to solar maximum.

Zerefos (2005) studied the effect of solar activity on ozone profiles and deduced that the amplitude of solar activity on ozone is more pronounced in the tropics amounting to about 1-2% of the total variability. Chandra and McPeters (1994) examined ozone observations from Solar Backscaterred Ultravilolet Radiometer (SBUV) covering more than one solar cycle and inferred that 5-7% of the change in upper stratospheric ozone is attributable to solar UV flux. Herman et.al (1991) quantified the effect of solar cycle

on ozone and found that the removal of apparent solar cycle reduces the net ozone loss to $2.66 \pm 1.4\%$ per decade. Angell (1989) found that ozone increases significantly with the sunspot number with very strong relation in the north tropical and temperate zones. Ozone can act as a modulator. The temperature change due to 11 year solar cycle was primarily controlled by ozone. (Austin et. al, 2007). Shindell (1999) showed that stratospheric ozone changes can amplify the irradiance changes due to solar cycle to affect climate.

Variability of ozone distribution due to Quasi Biennial Oscillation (QBO) is the most important dynamical factor that can affect ozone amounts. QBO develops as a consequence of the upward propagation of disturbances or waves produced in the tropical troposphere. Funk and Garnham and Ramanathan (1963) reported the presence of Quasi Biennial Oscillation in Total Column Ozone. QBO is a feature with successive wind regimes propagating smoothly downwards with a spectral peak near 28 months (Fraedrich et.al, 1993). Although the QBO is a tropical phenomenon, it affects the stratospheric flow from pole to pole by modulating the effects of extratropical waves (Baldwin et.al, 2001). Wave drag associated with the QBO induces a circulation between the lower stratosphere of the tropics and the middle latitude of the extratropics and this causes the transport of ozone rich air out of the tropics and ozone poor air to the tropics during different phases of the QBO. Many studies have attempted to analyse the variation of ozone in response to QBO (Randel and Wu, 1996, Witte et.al, 2008). Gray and Dunkerton (1990) showed that the QBO exhibits a zonal asymmetry about the equator. Tung and Yang (1994)examined the frequency spectrum of anomaly changes in ozone and found that the extratropical anomaly has two spectral peaks compared to one in the tropical anomaly and suggested that the second spectral peak is the difference combination of QBO and annual frequency.

Camp et.al (2001) explored the spatial and temporal patterns in the interannual variability of ozone in the tropics and found that the major modes of variability are the QBO, QBO interaction with decadal cycle, combined effect of QBO and annual cycle and El Nino Southern Oscillation. Fadnavis and Beig (2008) studied the latitude – altitude structure of QBO over the tropical stratosphere and showed that the equatorial maxima of both the hemispheres are out of phase with each other. Hamilton (1989) demonstrated that the dynamical QBO acts to modulate strong seasonal transport from

the midlatitude to the tropics. Wang et.al (2011) examined the tropical and midlatitude total column ozone using a chemistry climate model in which solar cycle, QBO and volcanic forcing were not included. They found that ENSO signal was dominating the tropical total column ozone variability. Kayano (1998) performed empirical orthogonal function study of TOMS data and found ENSO related wave number one in the tropics and southern hemisphere extratropics. Contributions of all the dynamical modes to total ozone over a region should be interpreted to have a better understanding of its future evolution. Recognizing the effects of various atmospheric phenomena in the spatial and temporal distribution of ozone can be accomplished using principal component analysis. Lack of long term datasets of ozone for climatological studies is one of the main factors that restrain the identification of the dynamical phenomena affecting ozone. Ozone observations at the stations give data over a selected number of points. Hence this study aims to identify the major modes of variability in column amount ozone over India with a dataset of adequate spatial frequency and temporal extent.

## 4.2. Data and Methodology

Monthly values total column ozone data over India (0°N-40°N, 60°N-100°E) from Multisensor reanalysis for the period from 1979-2008 is used in the present study . Long term trends were found by the least squares fit and removed from the data. Mean values of total ozone were computed for each month of the year for the 30 year time span of the dataset. This average was removed from each individual month in order to de-seasonalize the data. The detrended and deseasonalized data were subjected to Principal Component Analysis (PCA). PCA is an effective method to extract significant information from a dataset, invented by Carl Pearson in 1901.  The purpose of the principal component analysis is to formulate the most meaningful basis to re-express a noisy dataset (Shlens, 2005). Climate data sets vary multi-dimensionally through space and time. PCA is one of the most useful statistical tools to reduce the dimensions for valuable interpretation of data.

PCA expresses the dataset as the linear combination of its basis vectors. Let X is an m × n matrix that represents the original dataset. Let Y be another m × n matrix related by

a linear transformation by P. X is the original dataset and Y is the re-representation of the dataset.

$$PX = Y \qquad \text{... (4.1)}$$

P is a rotation and a stretch which transforms X in to Y

Equation (4.1) can be written as

$$PX = \begin{bmatrix} p_1 \\ \vdots \\ p_m \end{bmatrix} \begin{bmatrix} x_1 & \cdots & x_n \end{bmatrix} \qquad \text{... (4.2)}$$

$$Y = \begin{bmatrix} p_1 & \cdot & x_1 & \cdots & p_1 & \cdot & x_n \\ & \vdots & & \ddots & & \vdots & \\ p_m & \cdot & x_1 & \cdots & p_m & \cdot & x_n \end{bmatrix} \qquad \text{... (4.3)}$$

Hence each column of Y

$$y_{i=} \begin{bmatrix} p_1 & \cdot & x_i \\ & \vdots & \\ p_m & \cdot & x_i \end{bmatrix} \qquad \text{... (4.4)}$$

From above it is obvious that $j^{th}$ coefficient of $y_i$ is a projection on to the $j^{th}$ row of P.

Inorder to reduce noise in the dataset the principal component analysis appropriately rotates the naïve basis towards the direction of maximum covariance. For reducing the dimensions method should be applied such that redundancy is eliminated. This is done by choosing the variable that are directly related and considering only one of them for analysis. Variables with minimum covariance should be selected for attaining minimum repetition.

If A and B are two sets of measurements with zero means given by

$$A = \{a_1, a_2, \dots, a_n\}$$

$$B = \{b_1, b_2, \dots, b_n\}$$

$$\text{Covariance of A and B } = \sigma^2{}_{AB} = \langle a_i b_i \rangle_i$$

Where the expectation is the average of n variables

$\sigma^2{}_{AB} \geq 0$ if A and B are entirely uncorrelated

$\sigma^2{}_{AB} = \sigma^2{}_A$     If A=B

Converting A and B into corresponding row vectors

$$A= [a1,a2....an]$$

$$B= [b1,b2,...bn]$$

Covariance can be expressed as the dot product of matrix computation

$$\sigma^2{}_{ab} = \frac{1}{n-1} ab^T \qquad\qquad \textbf{...} (4.5)$$

Renaming the row vectors $x1 \equiv a, \ x2 \equiv b$ and considering other row vectors $x_3 \ .....x_m$, a new m X n matrix can be defined as

$$X = \begin{bmatrix} x_1 \\ \vdots \\ x_m \end{bmatrix} \qquad\qquad \text{... (4.6)}$$

Each row of x can be considered as measurements of a particular type and columns to the set of measurements. The definition of the covariance matrix is

$$C_X = \frac{1}{n-1} XX^T \qquad\qquad \text{... (4.7)}$$

The ij[th] element of $C_x$ is the dot product between i[th] measurement type with the jth measurement type.

The properties of $C_X$ are

1. $C_x$ is a square symmetric m x m matrix
2. The diagonal terms of $C_x$ are the variance of particular measurement types
3. The off diagonal terms of $C_x$ are the covariance between measurement types

The large values of the diagonal terms can be assumed to be related to interesting dynamics (or noise) and the large values (small) of diagonal terms represent high (low) redundancy.

The covariances are non negative by definition and the minimum value of co variance is zero. The off diagonal terms should be reduced to zero to get an optimized matrix that represents maximum variance and minimum covariance. PCA assumes all basis vectors $\{p_1,\ldots,p_m\}$ are orthonormal that is P is an orthonormal matrix. PCA also assumes the directions with the largest variances the signals are most principal or important. PCA could be performed in the following steps

1. Select a normalized direction in m-dimensional space in which the variance in X is maximised. Take this vector as $P_1$.
2. Find another direction in which is perpendicular (orthonormality condition) to the initial direction in which the variance is maximized. Consider this vector as $p_i$.
3. Repeat this procedure until m vectors are selected.

The resulting ordered set of p's are the principal components.

Principal components can be solved either by empirical orthogonal function (EOF) method or singular value decomposition (SVD) method. The method of SVD is used in this chapter.

Let X be an arbitrary n x m matrix. The form of singular value decomposition is given as

$$X = U \sum V^T \qquad\qquad \text{... (4.8)}$$

Where U is a n x n matrix containing left singular vectors, V is m×m matrix containing right singular values. And $\Sigma$ is a diagonal matrix of the same size as X i.e. n × m non negative diagonal elements.

Here the spatial structure of principal components (PC) can be considered as two dimensional standing waves while the time series of the PCs represent the temporal evolution of the amplitude of these waves. In order to represent the pattern in

dimensional units the spatial map of principal components were multiplied by the standard deviation of the PCs. The PCs were divided by their standard deviation. The peak-to-low amplitudes of the oscillations at any grid point can be recovered by taking the product of value at that grid point from the spatial structure and the peak-to-low amplitude of the associated PC time series.

Harmonic analysis for the monthly mean total ozone data is done using Fourier expansion. This is a method of representing the signal in time frequency domain. Fourier analysis represents a signal as a set of amplitude and phase information pairs for a number of frequencies embedded in the signal. This is done by representing the signal in to pairs of sines and cosines. A periodic function which is piecewise-continuous and monotonic and absolutely integrable can be expressed as a Fourier series with harmonically related sine/cosine terms

$$s(t) = a_0 + \sum_{k=1}^{+\infty}[a_k.\cos(k\omega t) - b_k.\sin(k\omega t)] \qquad \text{... (4.9)}$$

Where $a_0$, $a_k$, $b_k$ are Fourier coefficients, K is the harmonic number and T the period

## 4.3. Results and Discussion

### 4.3.1 Principal Component Analysis of total ozone

The first four principal components of total ozone from multisensor reanalysis capture more than 85 percent of the variance. Fig.4.1. represents the spatial distribution of the first four principal components. Corresponding time series of PCs and their Fourier spectra are shown in Fig.4.2. The powers of the spectra are not represented in the same scale for all the PCs to visualise the extent of the fluctuations in power more clearly. X axis of the power spectra is expressed in linear scale. Red noise spectrum displaying 95 percent significance level using F test is shown as purple line. The red line represents above 50 percent significance level. The first principal component captures about 50 percent of variance in total column ozone. The values (Fig.4.1. a) range from a high of about 8.5 DU at the subtropics to a low of about -2 DU at the tropics. The associated PC time series show the amplitude of this oscillation. A maximum peak to trough amplitude of about 22 DU occurs at the subtropical Indian region (28°N -38°N, 60°E-80°E). The spectrum of the PC shown in figure 4.2.b shows a dominant peak at 28

months and a secondary one at 21 months. There are additional peaks at 32, 52 and 90 months. It is obvious from the figure that the 28 and 21 month oscillations are significant above 95 percent.
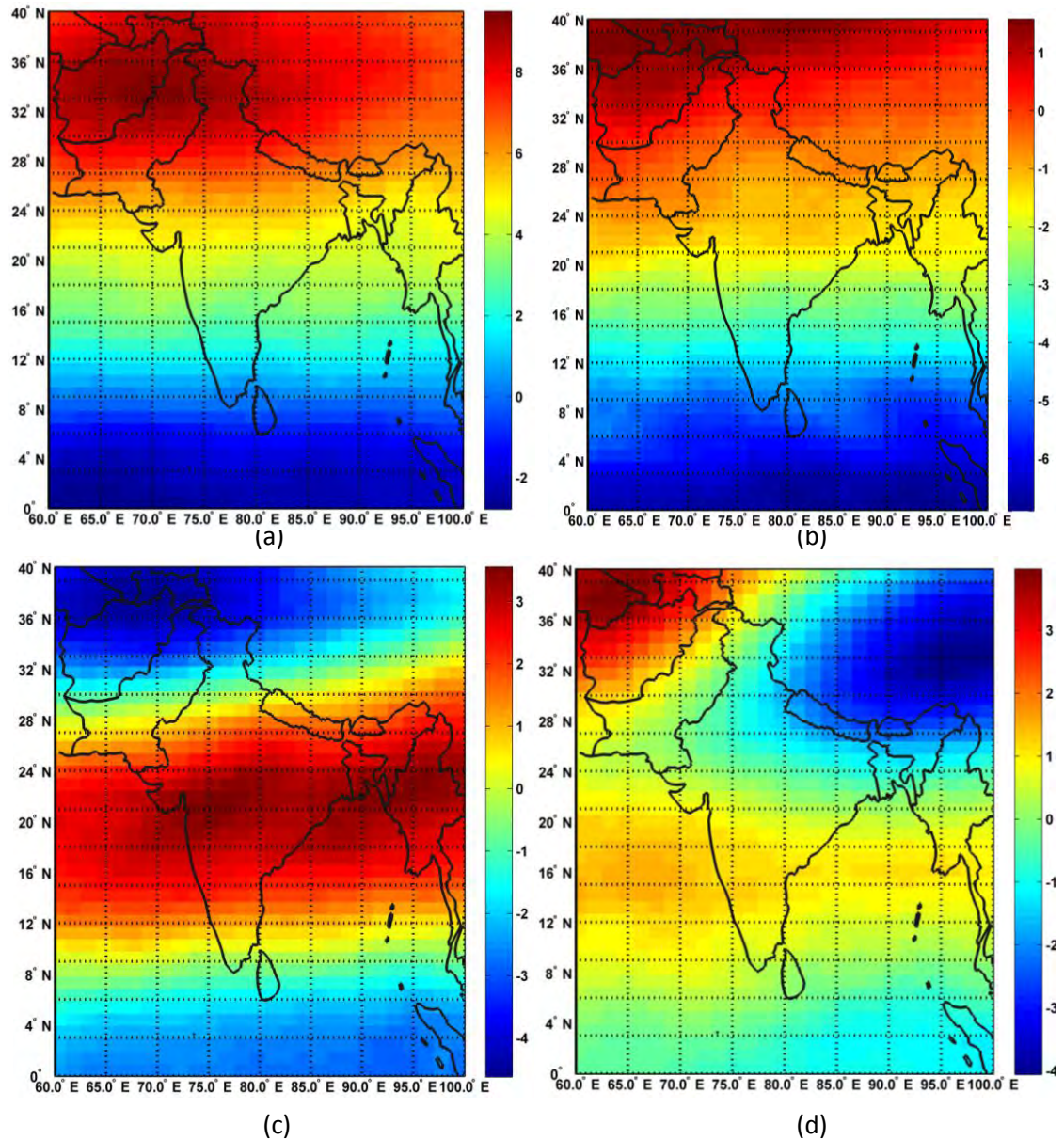


Fig.4.1. Spatial patterns of first four Principal Components

The spatial structure of the second PC resembles the first one in with the lowest values in the tropical and highest values in the subtropical region. It captures about 21% of the total variance. However the pattern is almost entirely negative from 0 to 28°N and positive in the region further north. It is similar to PC 1 except for the negative value in the region from 0°N to 28°N as well as the dispersed structure of positive values in the

region from 28°N to 40°N compared to PC 1. The associated PC is shown in Figure 3.2. c. The spectrum of the PC (Fig.4.2. d) has two primary peaks-28 months and decadal. Both the oscillations show significance above 95 percent. But the decadal is clearly dominant.

The third principal component capturing 10 percent of the variance is roughly symmetrical about the middle of the Indian region. The values range from -4.5 to -3.5 DU in the northern and southern portions and about 2.5 to 3.5 in the mid Indian region. The Fourier spectrum shows a significant (above 95 percent) double peak with the peaks having periods of 28 and 32 months respectively. The fourth principal component capturing more than 4 percent of the variance displays pattern with zonal structure in the subtropical Indian region. The standing wave exhibits positive values in the western part and negative values in the eastern part of the subtropical Indian region. The corresponding spectrum contains prominent peaks at 24, 30, 40 and 120 months. The patterns exhibited by the principal components can be closely related to the dynamical processes in the atmosphere.

Most of the structures exhibited by the first four principal components can be attributed to four physical processes-QBO, interaction between QBO and annual cycle, decadal solar cycle and ENSO. The dominant pattern seen in the first three principal components is the QBO. Quasi-biennial oscillation (QBO) in stratospheric winds is a quasi-periodical reversal in zonally symmetric easterly and westerly wind regimes between 30– 50 hPa (Holton, 1992). It is believed to be caused primarily by vertical displacements due to the meridional circulation associated with the equatorial temperature QBO (Holton, 1989). The variations of the amplitude of the first principal component bear a resemblance to the total ozone variations in the 20°N-40°N latitude band (as observed in chapter 3). The PC1 amplitude has highest values in 1979 which decreases gradually to reach a minimum during 1994 and thereafter a gradual increase until 2008. The maximum amplitude of the principal component is 2 and minimum is -1.6. Since most of the variation over Indian region occurs at the subtropics the resemblance with the subtropical ozone trend and the capturing of more than 50 percent of the variation can be expected in the first principal component.
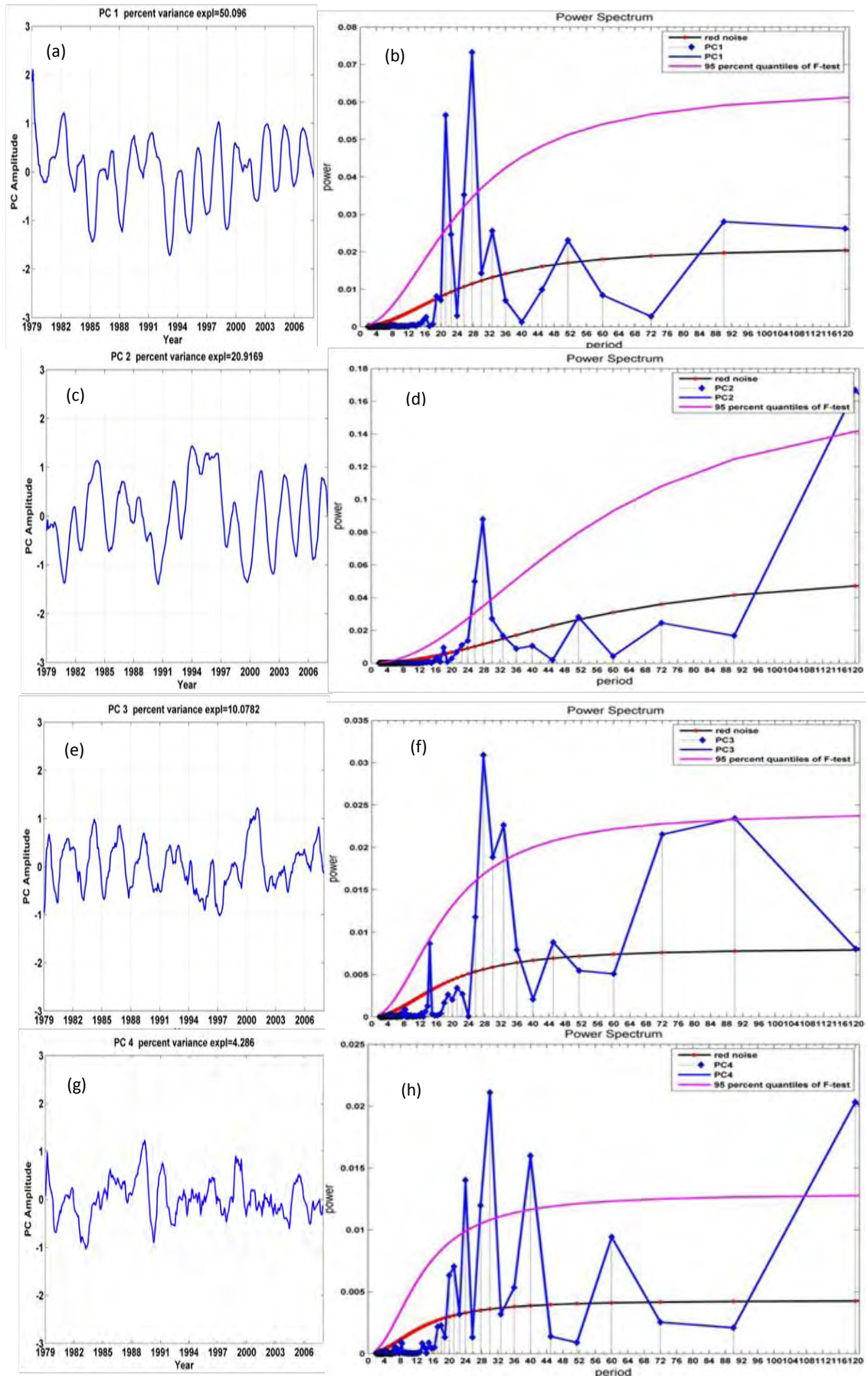
Fig 4.2. Time series (left column) and spectra (right column) for first four principal components.

The power of the spectral peaks at 28 and 21 months are 0.074 and 0.058 respectively and corresponds to the QBO and the interaction of QBO with annual cycle (QBO-Annual beat). Correlation between 30 hPa Singapore wind and Principal component 1 gives a negative value of -0.21. This unexpected result may be due to the presence of the QBO annual beat component. The time series of principal component 1and QBO index is given in Figure 4.3. From the figure it is obvious that QBO index (Singapore 30 hPa wind) and PC 1 are not in phase. To explore the temporal association between Ozone distribution and QBO, lag correlation between anomalies in ozone column amount for Indian region and zonal component of wind at Singapore was performed.
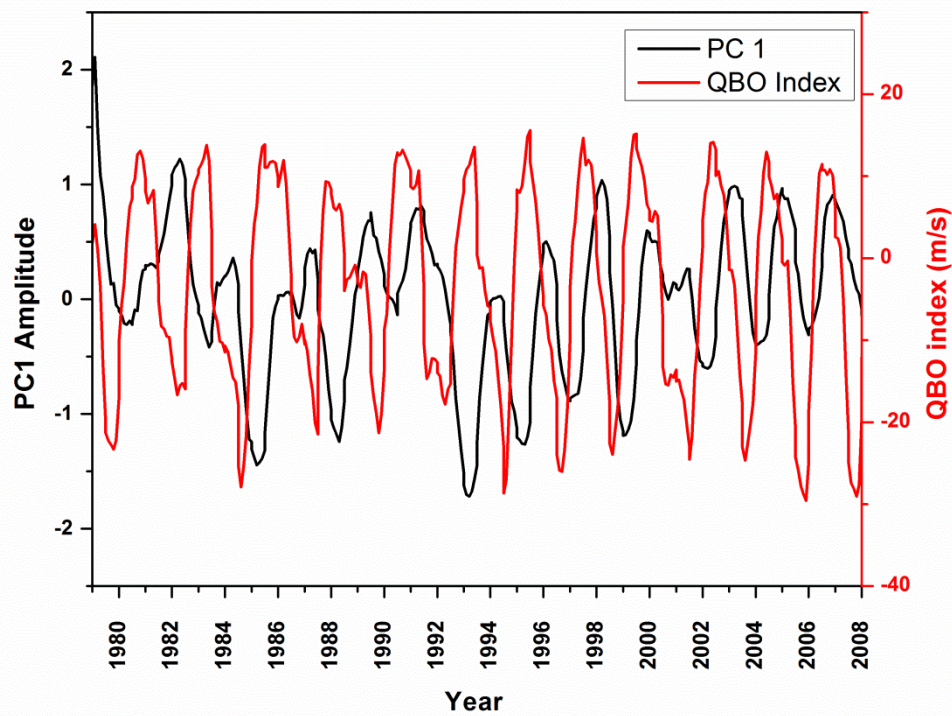


Fig.4.3. Time series of principal component1 (black line) and QBO index (red line) from 1979 to 2008.

The lag correlation for the 0-20°N is given in Fig.4.4. (a) Values of correlation for this band peaks at the lag values of 0 and 26 (when the Singapore wind lags behind ozone). The minimum value of the correlation coefficient -0.45 is at a lag of 12 months. But for the 20°N-40°N latitude band (Fig.4.4. (b)) maximum correlation occurs at a lag of 7-8 months and the lowest value occurs during 21 months. The occurrence of maximum negative correlation occurs at the period of QBO annual beat whereas maximum positive correlation occurs at the difference in the period of QBO and QBO annual beat

(28 months – 21 months = 7 months). Significant oscillations in the spectra of the first principal component are QBO and QBO annual beat.
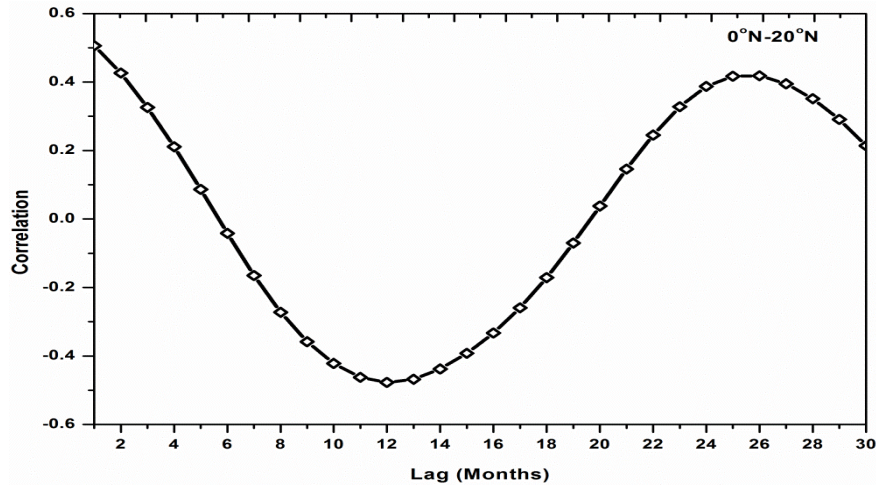


Fig.4.4.(a) Correlation coefficients between total column ozone for the region 0°N-20°N, 60°E-100°E and Singapore wind at 30hPa with negative lags from 0 to 30 months.
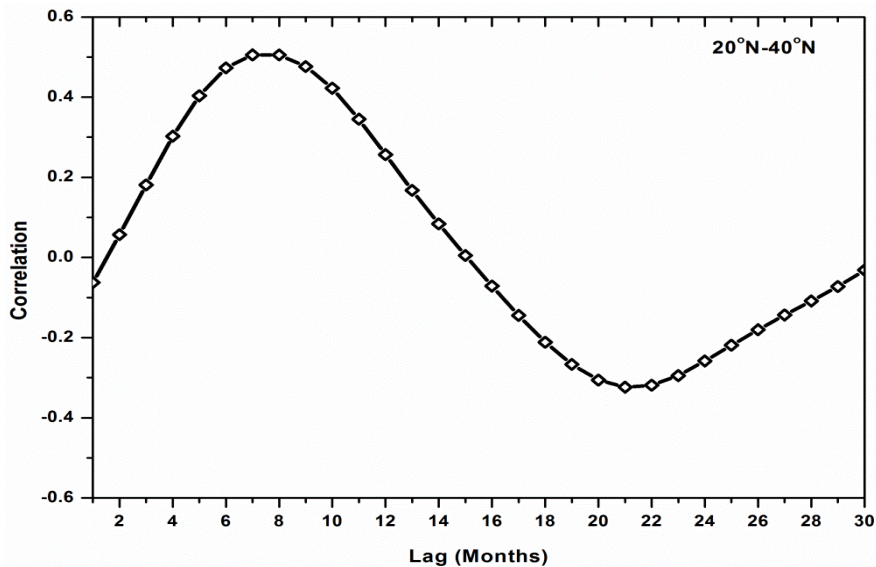


Fig.4.4.(b). Correlation coefficients between total column ozone for the region 20°N-40°N, 60°E-100°E and Singapore wind at 30hPa with negative lags from 0 to 30 months.

The influence of Quasi biennial Oscillation on annual meridional transport can lead to the occurrence of two beat oscillations due to the sum and difference of the QBO and annual frequencies that is at periods 21 and 8.4 months (Tung and Yang, 1994, Camp et.al, 2001).Due to the close similarity between the time series of the first principal component and that of the 20N°-40°N column amount ozone there is the possibility of

maximum correlation between principal component1 and QBO index at the time scale expressed by the lag correlation analysis of 20°N-40°N.

The time series of principal component 1 and Singapore u wind at 30 hPa lagged behind 7 months is expressed below (Fig.4.5.). From the figure it can be seen that column amount ozone and equatorial wind are approximately in phase with each other when a lag of seven months applied to Singapore wind..  It can be seen that the two time series are more synchronised after 1994. This time is regarded as the beginning of the recovery of ozone column amount from the low values during previous years. The correlation between the lagged QBO index and principal component 1 is found to be 0.4968.
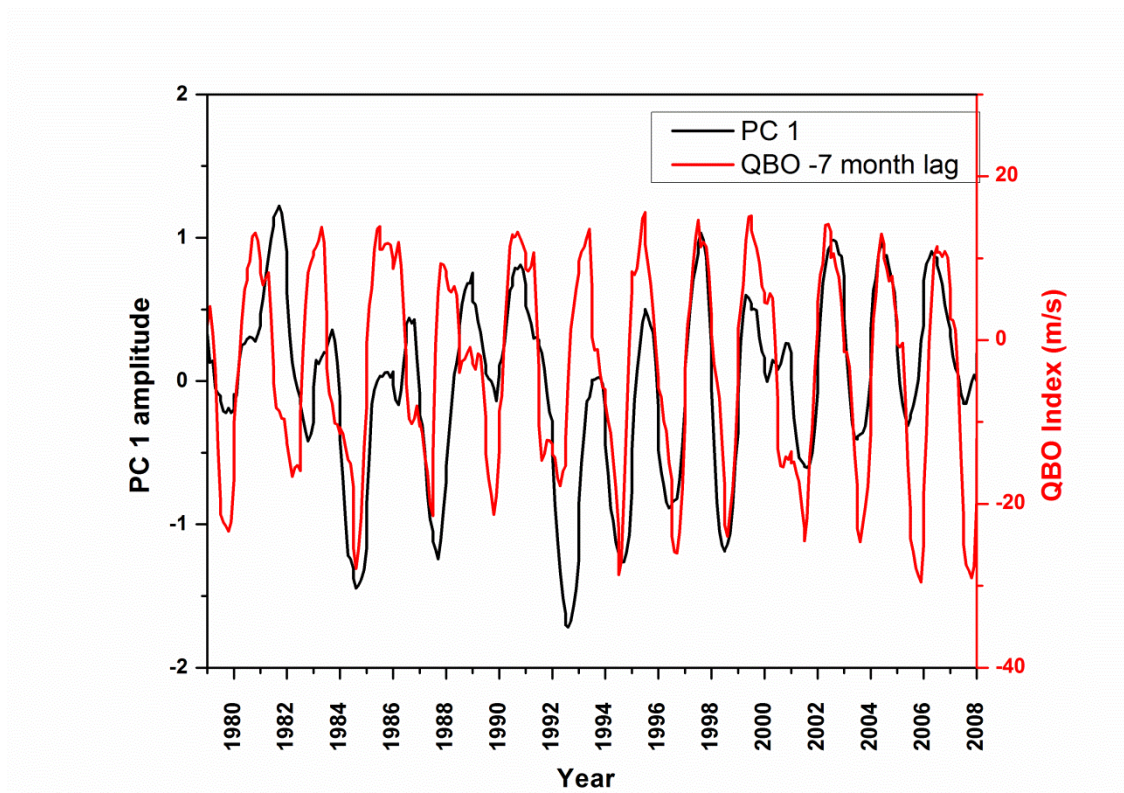


Fig.4.5. Time series of principal component 1 from 1979 August to 2008 December and Singapore wind at 30 hPa from 1979 January to 2008 April (Singapore wind lagging principal component 1 by 7 months).

From this study it is obvious that the principal component 1 captures the variability in the latitudes from 20°N-40°N. This is evident from two facts. (1) the time series of the principal component resembles the time series of the 20°N-40°N column amount ozone

values. (2) the principal component 1 and QBO index becomes in phase with each other when the lag with maximum correlation (7 months) for 20-40°N is applied to QBO index. The analysis also shows that ozone fluctuations in the subtropical Indian region (20°N-40°N) are due to QBO and QBO annual beat.

The fluctuations in the amplitude of the principal component 2 are small compared to that of PC1. The amplitude varies from -1.4 to 1.4. But the power spectrum of this principal component shows higher values for the 28 month oscillation than the principal component1. The value of power for QBO (28 month oscillation) is 0.09 compared to the value 0.075 in the first principal component. The correlation between the second principal component and QBO index is about 0.5798. The other dominant component is the decadal cycle which has amplitude of about 0.17. One possible cause for the presence of the decadal oscillation is the solar cycle. In order to analyze the contribution of the solar cycle, solar radio flux at 10.7 cm is obtained and compared with the variation of principal component 2. It was found that the principal component is positively correlated with (inverted axis) solar flux (Fig.4.6). This is similar to the result obtained by Camp et.al (2001) in the tropical total ozone variations. Correlation coefficient between inverted solar flux and PC 2 has a value of 0.430. Angell (1989) obtained zero lag correlation values of about 0.480 between total ozone values and sunspot number.

The time series of the solar flux used in this study covers half of solar cycle 21 and full extent of solar cycles 22 and 23. Amplitude of PC2 shows maximum value at the end of solar cycle 22 and the beginning of the solar cycle 23. It can be seen from the figure that PC2 is not exactly in phase with the inverted solar flux especially in the beginning during solar cycle 23. The pattern of QBO can be clearly seen in the figure 4.6 especially during solar cycle 23. This can be attributed to higher power and correlation coefficient of QBO with principal component 2.
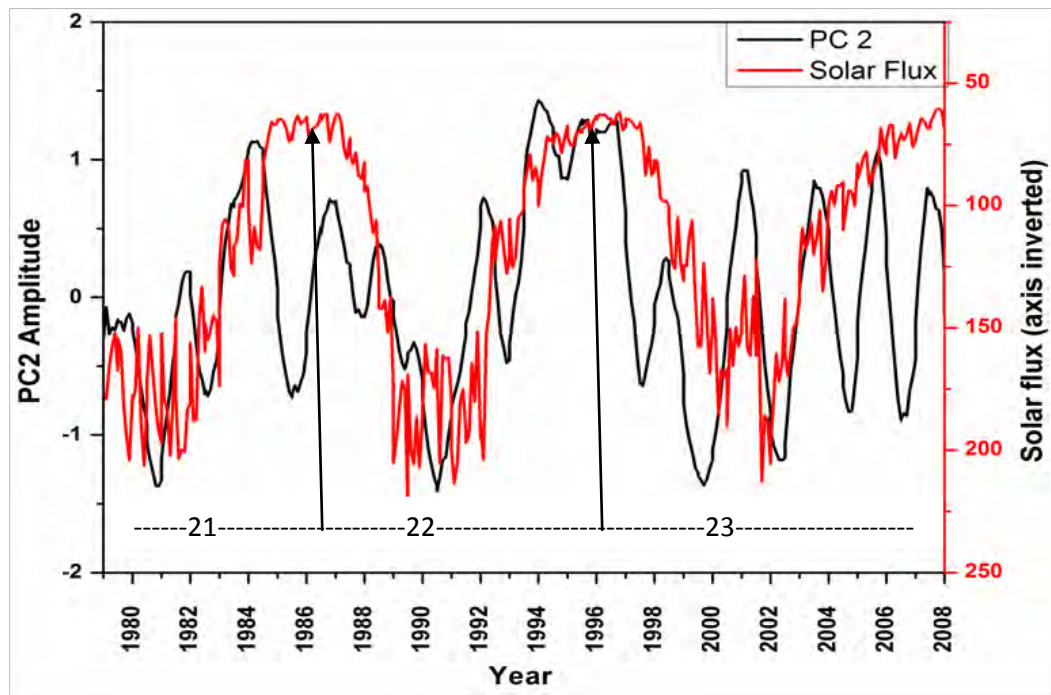
Fig. 4.6. Amplitude of principal component 2 and 10.7 cm solar radio flux (inverted) from 1979 to 2008.

Principal component 3 shows an amplitude variance from -1.0 to 1.2. The power of the QBO in the spectra is about 0.032. Other significant oscillation with period of 32 months has power 0.022. Correlation of qbo index and principal component 3 yields a value of about -0.406. The amplitude of the fourth principal component varies from -1.0 to 1.1. Power of the associated spectrum for 24, 30 and 40 month oscillations are 0.014, 0.022 and 0.016. There is another peak with 60 months with significance below the 95 percent level. Principal component 4 does not show any considerable correlation with Quasi Biennial Oscillation and Solar flux with the values of correlation -0.0753 and 0.0257 respectively. But it exhibits positive correlation with Southern Oscillation Index (SOI) with a value of 0.3585. Interannual variations in the equatorial ozone are dominated by the QBO above 20 km and the ENSO-related variation below 20 km (Shiotani and Hasebe, 1994). Variation of total ozone by ENSO can be attributed to the tropopause height changes associated with convection due to ENSO circulation (Hasebe, 1993). The time series for principal component 4 and SOI is given by Fig 4.7. From the figure it can be observed that the fluctuations of PC4 are approximately in phase with the variations of SOI.
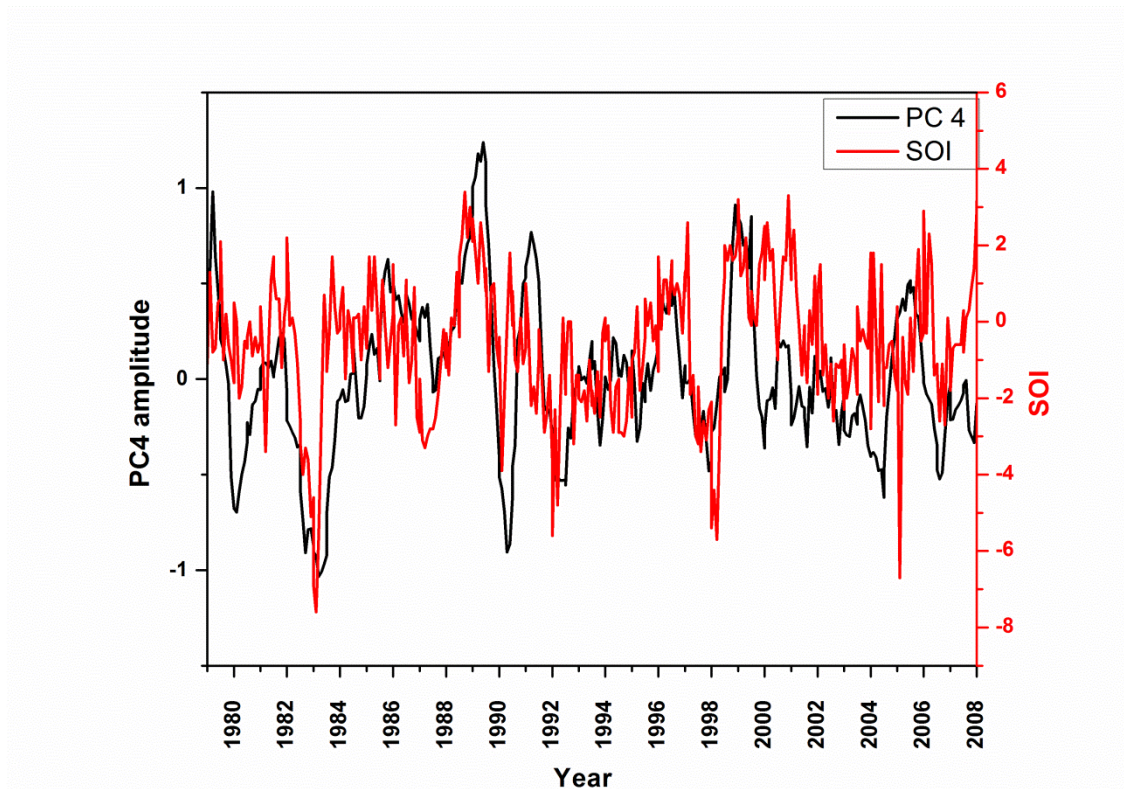
Fig.4.7. Amplitude of the principal component 4 and Southern Oscillation Index (SOI) from 1979 to 2008.

## 4.3.2. Harmonic Analysis of total column ozone over India

Harmonic analysis of unfiltered total column ozone data over India yields the oscillations displayed in Fig.4.8. Since the data is not de-seasonalized, the maximum amplitude oscillation is the annual cycle with a period of 12 months displaying amplitude of about 17.5. The second dominant oscillation is semi annual oscillation with a period of about 6 months and displays amplitude of 3.8. The most prominent oscillation possessing almost the same amplitude as semi-annual cycle is the quasi biennial oscillation. Next prominent harmonic displays a period of about 20 months. This corresponds to QBO annual beat (QBO-AB) which shows amplitude of about 3.3. Decadal scale oscillation exhibits amplitude of about 3.2. Other harmonics which showed prominence are at 36, 40, 45, 52, 60 months and they displayed harmonic amplitude 1.
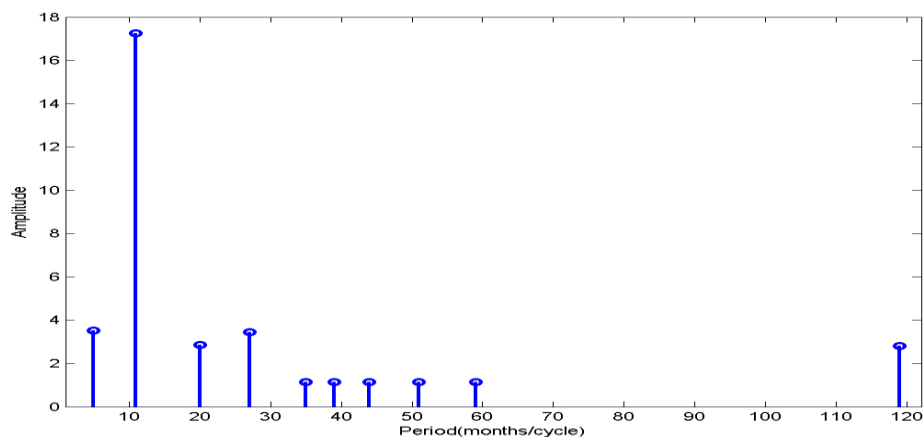
Fig.4.8. Major harmonics of total column ozone over India

Fig. 4.9. shows the spatial distribution of annual oscillation amplitudes over the Indian region. It is clear from the figure that the amplitude of annual oscillation is highest in the subtropical region and lowest in the near equatorial region. The values of the amplitude range between 10 and 30. Amplitudes increases northwards displaying same values along the same latitude band. An exception to this can be observed in the region 87°E -100°E and 14°N to 24°N. The amplitude is higher by 5 compared to other regions in the latitude band.
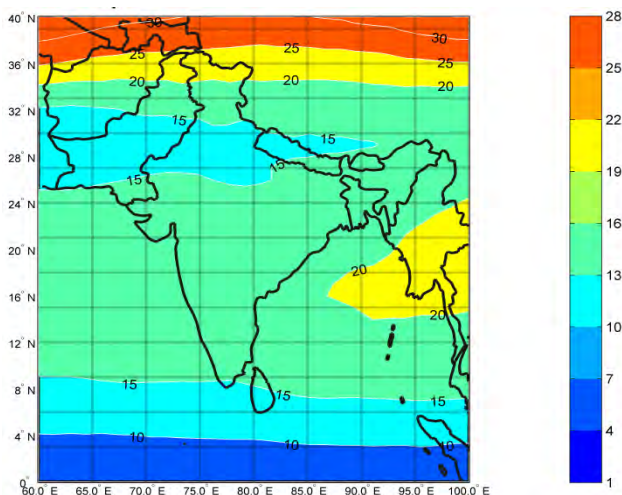


Fig.4.9. Amplitude of annual oscillation over Indian region (0-40°N and 60-100°E)

The spatial structure of annual harmonic displays the same structure as the spatial distribution of monthly climatological ozone during the months of April and May *i.e.,* spring season. Annual oscillation displays the same phase throughout the entire Indian region (Figure not shown) Amplitude values of semi annual oscillation (Fig. 4.10) ranges between 2 and 6 DU. It displays the highest amplitude in the subtropical Indian region from 32°N to 40°N and 60°N to 70°E. The oscillation shows comparatively lower values from 4°N-12°N, 60-100°E. Tropical semi annual oscillation (SAO) was discovered by Reed (1962, 1966) in zonal wind and temperature. The photochemical lifetime of ozone in the tropical upper stratosphere is related inversely to temperature. Hence ozone responds to the SAO in temperature which gives rise to SAO in ozone concentration. Fadnavis and Beig (2010) studied the spatio-temporal variations of semi annual oscillation in the tropical subtropical region and found an anti phase relation between ozone and temperature in the upper stratosphere and an in-phase relation in the lower stratosphere.
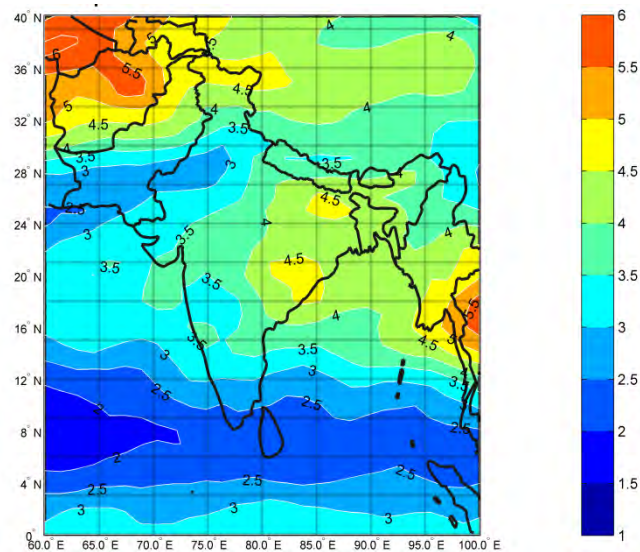


Fig.4.10. Amplitude of semi annual oscillation over India

The amplitude of QBO and QBO annual beat is shown in Fig.4.11. (a) and (b) and. The amplitude of QBO annual beat is in the same range as the amplitude of QBO. But the annual beat shows higher frequencies in subtropical region only. The amplitude of QBO (Fig.4.11.a) is higher in both the tropical region from 0°N-7°N and subtropical

region from 28°N-40°N and 60°E-85°E. Other longitude region (85°E-100°E) in this latitude band is showing lesser amplitude for QBO. The northern portion of the tropical region from 8°N-20°N is showing the lowest values for QBO. In the tropical region where QBO shows its highest amplitude (0°N-8°N), the annual beat shows its lowest amplitude. The phase of total ozone variations and QBO wind depends on latitude (Zerefos et al., 1992; Kane et al., 1998). By the application of principal component analysis of total column ozone over tropics, Jiang *et.al,* (2005)*,* studied the vertical propagation aspects of both QBO and annual beat and found that QBO-annual beat is an upward propagating feature.

Fig.4.12 (a) shows the phase of QBO over Indian region. It can be seen that the oscillation is showing 28 month periodicity over most of the Indian region. The regions from 9°N-18°N and 72°E-100°E and 24°N-40°N and 24°E-90°E are showing a periodicity of 26 months. Fig.4.12 (b) displays the phase of QBO and QBO-annual beat whichever is dominant at each grid point. The tropical region from 12°N to 20°N and the whole subtropical Indian region is dominated by QBO-annual beat frequencies. This agrees with the previous studies that the strength of QBO annual beat increases as one move from tropical to extratropical region.
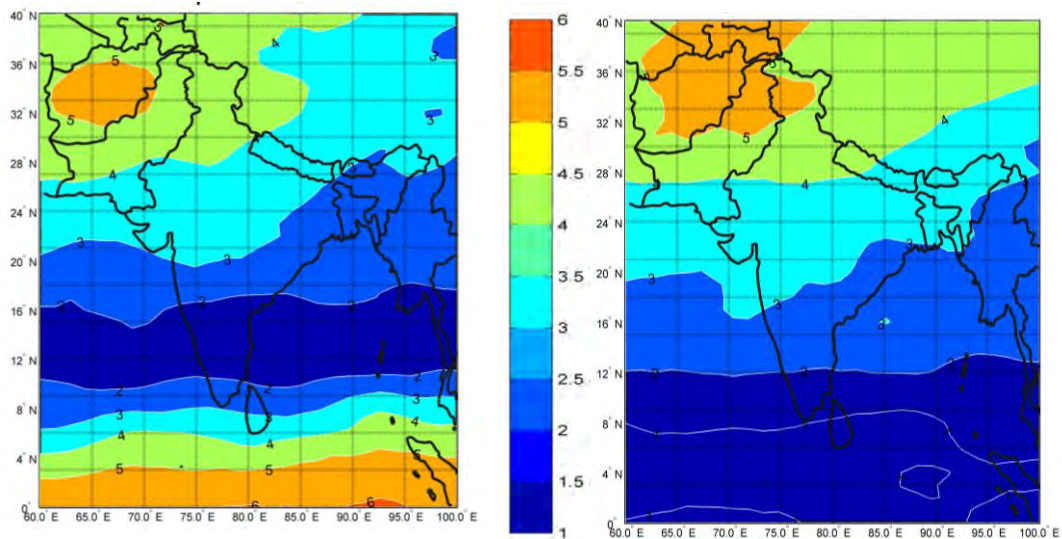


Figure 4.11. Amplitude of (a) Quasi biennial oscillation and (b) Quasi biennial oscillation annual beat (QBO Annual beat).

Amplitude and phase of 36, 40, 45, 52, 60 scale frequencies which were present in the harmonic spectra are shown. These are considered as representative frequencies of El

Nino Southern Oscillation. The spatial distribution given in Fig.4.13.(a) shows the amplitude of the oscillation which is maximum among the five frequencies given above at each grid point. The phase distribution given in Fig.4.13. (b) also shows the phase of the corresponding frequencies with highest amplitude. Subtropical Indian region from 28°N to 40°N is exhibiting higher values of amplitude. Lowest amplitude lies in the region from 8°N to 28°N.
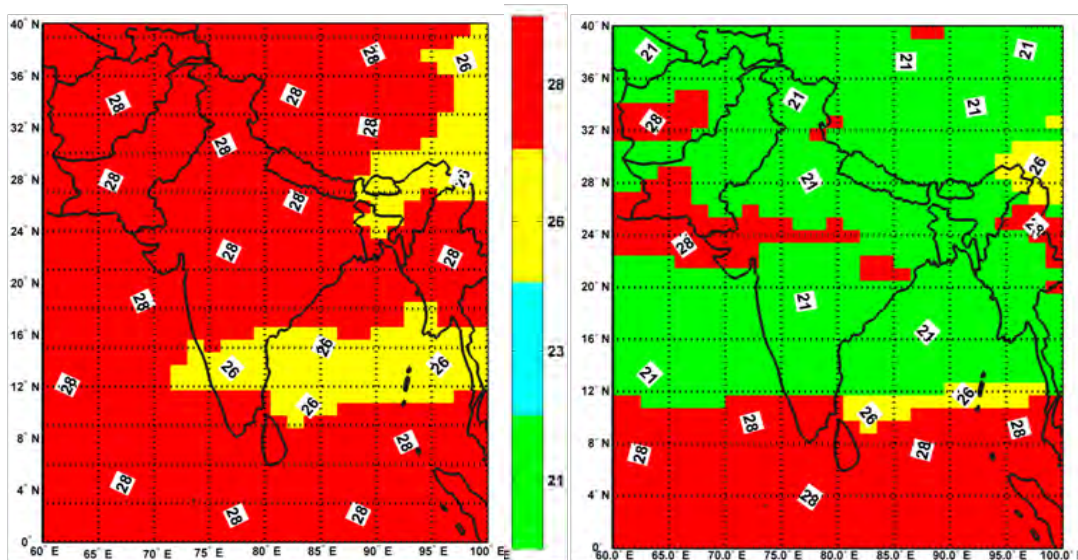


Fig. 4.12. Phase of (a) QBO and (b) Combined Phase of QBO and QBO Annual beat (Phase of the dominant pattern among the two at each grid point).

The oscillation with 60 month period is present over most of this low amplitude region. The region from 0 to 8°N shows intermediate amplitudes of about 1.5. The oscillation dominant over this region is 52 month oscillation. The region from 28 to 40°N shows the highest amplitudes. The periods of oscillations present over this region are 36 months and 45 months.

The spatial structure of decadal scale (which is inferred as solar cycle here) is given in Fig.4.14. The range of amplitude value is between 1.5 and 2.5. The lowest value of solar cycle amplitudes can be observed at latitudes from 28°N to 40°N and from 60°E to 80°E. Highest values are displayed by the region from 34°N-40°N and 60°E-100°E.
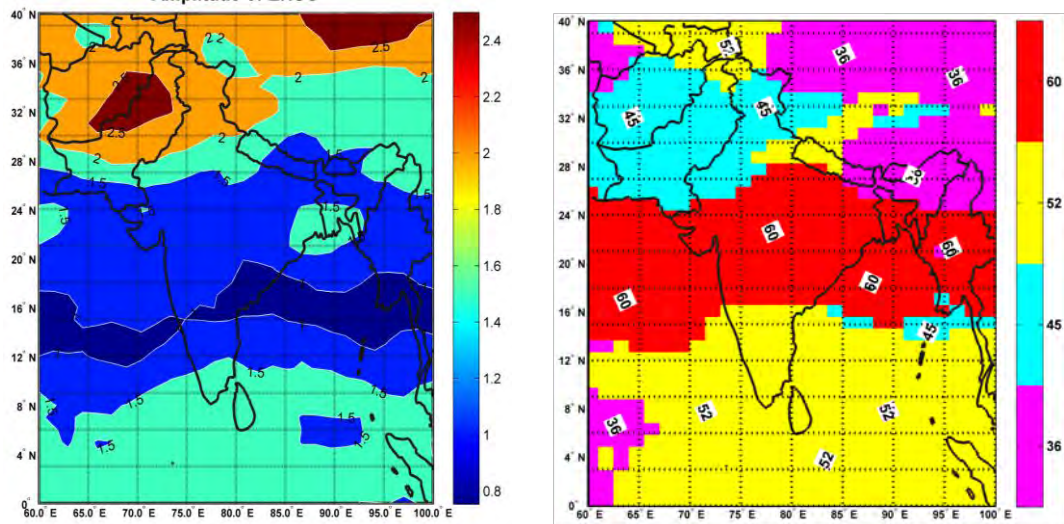
Fig.4.13. (a) Amplitude and (b) Phase of El Nino Southern Oscillation over India
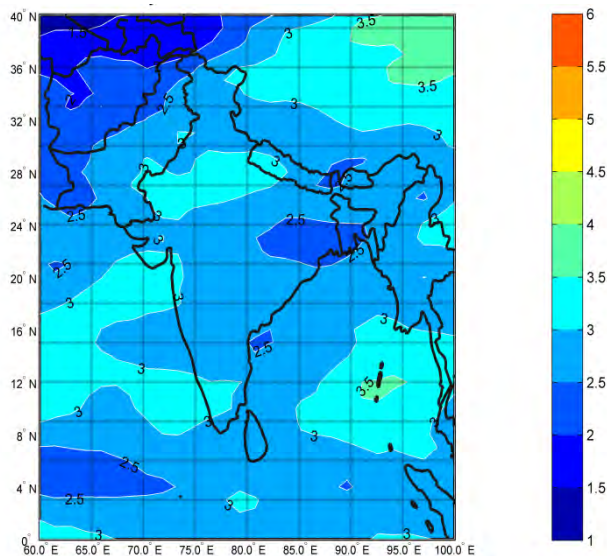


Fig.4.14. Amplitude of Decadal cycle harmonic.

Fig 4.15. illustrates the ratio of the harmonic amplitudes of QBO and solar cycle. This gives a picture of the relative contribution of the role played by QBO and solar cycle. It is clear from the figure that QBO plays comparatively dominant role in ozone concentration in the tropical region from 0°N to 7°N and the region from 24°N to 40°N and 60°E to 75 °E. The area from 8°N to 20°N shows that the contribution from both the solar cycle and QBO is roughly the same.
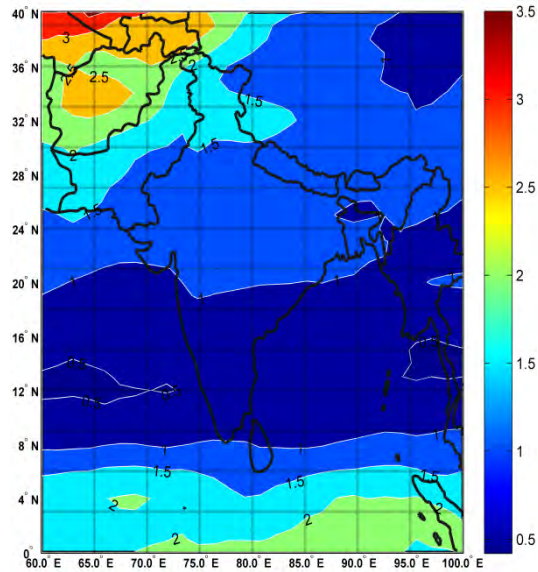
Fig.4.15. Relative contribution of QBO and Solar cycle to total ozone variability.

### 4.3.3. Correlation between total ozone and equatorial wind

The influence of QBO on total ozone concentrations over India is further explored by analysing the correlation between ozone and QBO index (Singapore u wind at 30 hPa) during every month for 30 years from 1979 to 2008. The influence of QBO zonal wind on the total ozone concentrations with zero lag is illustrated in Fig.4.16. It is obvious from the lag correlation analysis shown in Fig.4.4. (b) that Singapore wind at 30 hPa shows maximum positive correlation with total ozone during zero lag and then with a lag of 26 months. The spatial distribution of the correlation coefficients demonstrates that behaviour. Zossi and Campra (2010) examined the spatial correlations between total ozone and equatorial zonal wind and found that the highest correlations appear in tropical zone. From Fig. 4.16 it can be observed that the area from 0 to 12°N is the area of positive association. The region above 15°N shows near zero or negative correlation except during the months of October and November.

During the month of October the region from 32°N to 38°N and 75°E to100°E shows largest positive correlation. Subtropical region from 16°N-40°N shows highest anticorrelation between ozone and Singapore wind, with values between -0.4 and -0.6 during spring season. The nature of association is always positive in the tropical region

with values as high as 0.8, whereas it changes from near zero, negative and positive during different seasons for area from 16°N to 40°N.

Echer (2004) and Bowman (1989) showed that ozone is nearly in phase with QBO signal in the equatorial region whereas an out of phase relation exists among the two in the region from 10-55°. The study by Hollandsworth *et.al* (1995) and Fadnavis *et.al* (2008) also state that the subtropical temperature and total ozone anomalies are dependent on season. The ozone QBO is strongly tied to the seasonal cycle, with anomalies centered in the winter-spring season irrespective of QBO phase (Gray and Dunkerton, 1990). Holton (1989) used a single one layer model to demonstrate that the gross features of the observed features in QBO can be attributed to the meridional advection of ozone perturbation by the annually reversing mean meridional Hadley cell circulation. Logan *et.al* (2003), showed that the influence of QBO on equatorial ozone dominates between 10 and 45 hPa. They also observed that there is an altitudinal three cell structures in ozone anomalies at 20°N and 20°S with two cells above 50 hPa related to QBO.

## 4.4. Summary

Principal component analysis of deseasonalized total ozone over India gives four major principal components capturing about 85 percent of variations. More than half of the total variance is caused by QBO and the interaction of QBO with annual cycle (QBO-AB). The effect of QBO is more pronounced in the region and that of QBO-AB in the subtropical region. Lag correlation between QBO and zonal wind Index shows the highest values at zero and 26 month lags for the equatorial region. For the subtropical region maximum values of lag correlation occurs at a lag of seven months. The first principal component is dominated by QBO-AB. It shows an in phase relation with QBO index when a lag of seven months is applied.
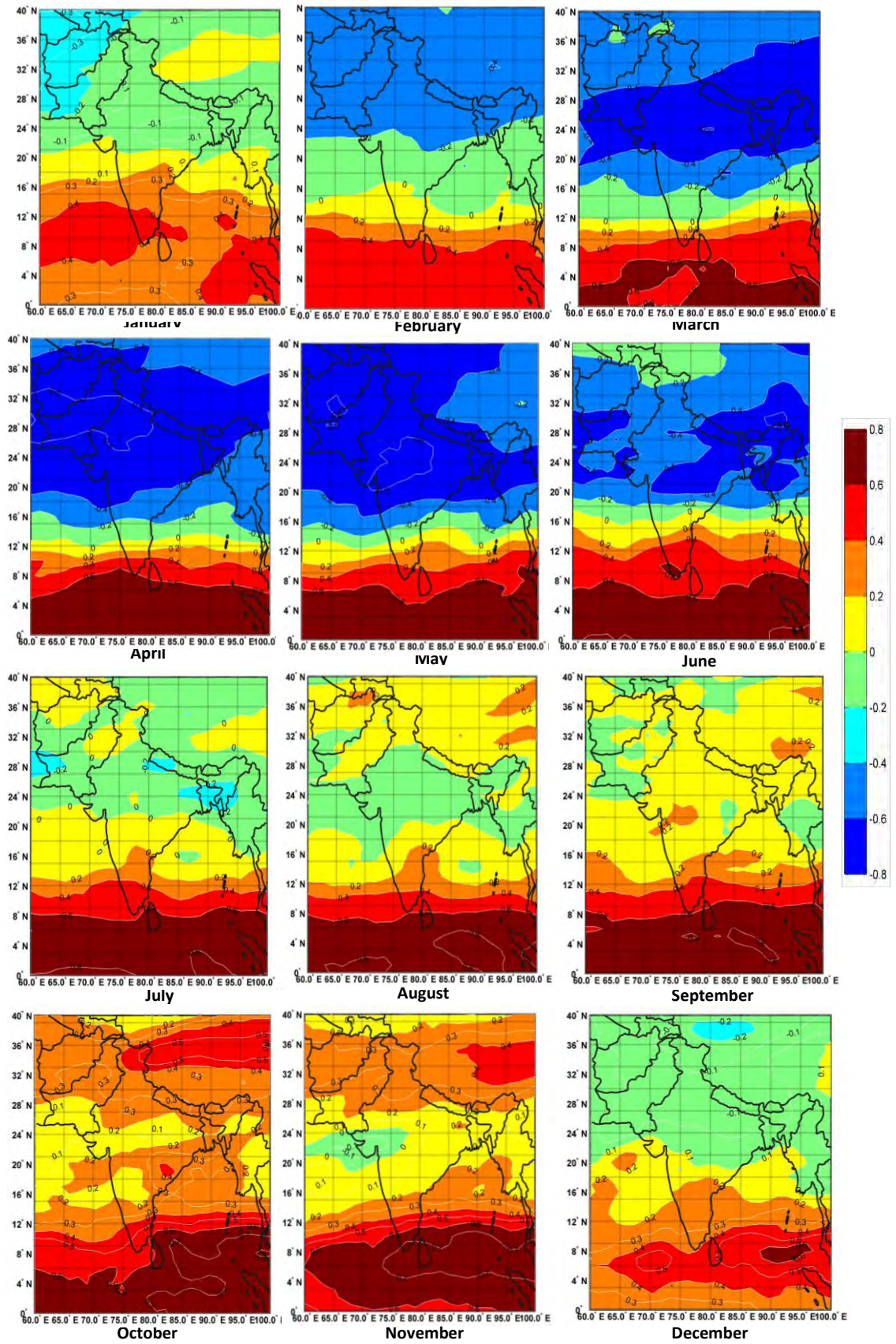
Fig.4.16. Zero lag correlation coefficients between total ozone anomaly and Singapore wind at 30 hPa from January to December for the period 1979-2008.

The second principal component shows significant oscillations in QBO and decadal scale. This principal component shows an in phase relation with the inverted solar flux. QBO makes its appearance in the third principal component as well. Principal component 4 shows significant peak at 40 months apart from QBO scale frequencies. This can be due to the influence of ENSO over total ozone which can cause fluctuation to ozone in the tropospheric region. This principal component shows comparatively higher association with Southern Oscillation Index.

Harmonic analysis of unfiltered column amount ozone over India demonstrates the annual and semi annual oscillations apart from the other oscillations given by principal component analysis. The strength of the annual oscillation is lower in the equatorial region and higher in the northern part of the subtropical region (34°N-40°N). The spatial structure of this harmonic resembles the ozone distribution during spring season. Amplitude of annual oscillation is very high compared to that of other oscillations in total ozone. Semi annual oscillation and QBO comes next in strength to annual oscillation. The semi annual oscillation displays lower values in the tropical region and higher values in major portion of the subtropical region.

Harmonic corresponding to QBO shows more strength at the near equatorial and a major part of western subtropical Indian region. The period of QBO is 28 months over most of the region. Time period of 26 months is shown by regions displaying low amplitude values for QBO. Annual beat of QBO exhibits the same strength as that of QBO. But it shows lowest values over the equatorial region in contrast to the higher values shown by QBO. This is because ozone is directly influenced by QBO circulation in the equatorial region. But in higher latitudes seasonal variations in circulation induces changes in total ozone anomalies along with the QBO. This interference of annual cycle is giving rise to QBO annual beat as is evident from many studies. The combined phase diagram of QBO and QBO-AB clearly displays its dominance in the subtropical region.

Considering the ENSO scale frequencies we can see that 52 month oscillation is predominant over the tropical region and 60 month oscillation is leading in the region from 16 to 24 °N and 36 and 45 month oscillations dominate in the subtropical region. The amplitude of the oscillation is higher in the subtropical region. The amplitude of

decadal scale oscillation is almost the same everywhere in the study region. It shows comparatively lower values in the western part of the subtropical region. From the analysis of the relative contribution of QBO and solar cycle to total ozone variability it is apparent that QBO is playing a major role in the equatorial and subtropical region. The spatial correlations between QBO index and total ozone anomalies show a positive association in the equatorial region and seasonally dependent relation over the subtropical Indian region. The application of principal component and harmonic analysis to the total ozone data delivers almost same kind of output. Thus the studies reported in the chapter successfully explored the major patterns of variability in atmospheric ozone over India.

# Vertical Distribution of Atmospheric Ozone over Indian Subcontinent

## 5.1. Introduction

The vertical distribution of ozone in the atmosphere is one of the key factors that determine the thermal structure of the atmosphere. The amount of shortwave radiation reaching the surface of the earth depends mainly on the amount of ozone and water vapour present in the atmosphere. Most of the ozone in the atmosphere is formed in the middle to upper stratosphere of the tropics. The availability of intense ultraviolet radiation which can break the diatomic oxygen molecules makes this possible. Ozone maximum in the atmosphere is roughly from 20- to 40km altitude (lower to mid stratosphere).

The existence of this ozone maximum is due to the optimum amount of oxygen molecules and extreme ultraviolet (EUV) radiation in this layer. Below this region the UV radiation decreases down to the surface due to absorption by ozone and other atmospheric constituents. This is because the ozone molecules present in the upper layers absorbs the uv radiation passing through it. If there is more ozone molecules present in the upper layers lesser will be the UV radiation passing to the lower layers and this causes the formation of lesser amount of ozone. Exploring the vertical distribution of ozone will help to get better knowledge about the diverse roles played by ozone at different altitudes of the atmosphere.

Atmospheric ozone can vary over different timescales. Short term variablilty can be due to day to day fluctuations of weather like the passage of a weather system. Seasonal variability is due to the varying position of the sun for different seasons and the resultant

change in circulation. Interannual variability occurs due to cyclical oscillations in the atmosphere like QBO and solar cycle. Long term variability is the gradual variation due large period fluctuations in solar input or the development of a trend due to the gradual build up of chemicals like Chlorofluorocarbons in the atmosphere. The regional, seasonal and day-to-day variations of ozone can be identified if we separately consider the contributions to total ozone content over any place from the photo-chemical action of sunlight and from transport in the horizontal and vertical directions of the accumulated ozone below the level of primary ozone formation (Karandikar and Ramanathan, 1949). Ramanathan and Kulkarni (1949) studied the vertical distribution of ozone over Mount Abu (Latitude-24°26', Longitude-72°43' E) and found that most of the changes take place in the layer between 18 and 27 km.

Mani and Sreedharan (1973) reported that in the equatorial atmosphere represented by Trivandrum and Pune, the vertical distribution of ozone in the stratosphere remains practically unchanged throughout the year while the tropospheric ozone exhibit marked seasonal variations. There is a strong seasonal variation in trends in northern midlatitudes in the altitude range from 10-18km, with the largest ozone loss during winter and spring. In the dynamic sector, the ozone transport is controlled by atmospheric tide and Kelvin wave above 50 km, by planetary waves in 15-50 km and by synoptic scale motions, planetary waves, cumulonimbus, walker and Hadley cells below 15 km (Han and Yongqui, 1997).

One of the main factors that obstruct the detailed study of altitudinal variations in atmospheric ozone is the lack of evenly spaced and long term data. Ozone soundings has been available for a few and widely scattered stations around the globe for a long time period. Ozonesondes can be considered as a reliable source of information about the vertical distribution of ozone over a region. A number of studies before the advent of satellite era (Dütch, 1964; Bojkov, 1968) attempted to compute the vertical distribution of ozone from total column ozone measurements since there are comparatively limited numbers of observations for the altitudinal distribution of ozone. Satellite measurements of atmospheric ozone can give more spatial coverage but they have very short time span. Many studies (Mclinden et.al, 2009) have attempted to combine ozone measurements from various sources in situ or satellite, to create long term data records for ozone. Large interannual variability and uncertainty of ozone measurements causes uncertainties in

understanding ozone trends (Tilmes et.al, 2012). The construction of long term climatology is necessary for model evaluations and comparison of ozone measurements from various sources.

 Klenk et al. (1983) derived standard ozone profiles from upper level averaged profiles from back scattered ultraviolet (BUV ) and lower level averaged profiles from balloon measurements. The occurrence of laminae in ozone profiles are extensively studied by many researchers (Appenzeller and Holton,1997; Mariotti et.al, 1997; Kar et.al,2002;Lemoine, 2004; Krizan and Lastovicka, 2005). Paul et.al (1998) constructed an ozone climatology based on satellite and ozone sonde measurements for the period from 1980 to 1991. Chan et. al. (2004) studied variation in tropospheric ozone profiles over China due to long range tranport using Pacific Exploration of Asian Continental Emission (PEACE) data. Gupta et.al (2007) anlayzed vertical ozone distribution over Kanpur using ozonesonde data due to long range transport and intrusions from the stratosphere. McPeters et.al (1997) constructed a satellite based ozone climatology to estimate total column ozone from balloonsondes. It is very crucial to have a clear picture of the altitude variations in ozone since the radiative forcing of ozone is sensitive to changes in ozone at different heights (Scwarzkopf and Ramaswamy, 1993, Wang et al., 1993).

Data records by satellites are regular in time but cannot provide long term information. Sensors using solar occultation like Stratospheric Aerosol and Gas Experiment (SAGE) and Halogen Occultation experiment (HALOE) as well as limb viewing instruments like High Resolution Dynamics Limb Sounder (HiRDLS), Troposphere Emission Spectrometer (TES) and Microwave Limb Sounder (MLS) can give data with high vertical resolution. But these instruments have small horizontal resolution. Nadir viewing instruments like SBUV (Solar Backscatter Ultraviolet), OMI (Ozone Monitoring instrument) are capable of giving fine horizontal resolution but comparatively coarse vertical resolution. Interaction of ozone with atmospheric circulation can be better understood if regular gridded data is available. OMI possesses good spatiotemporal resolution. Ziemke et.al (2011) derived a global climatology of tropospheric and stratospheric column ozone by combining OMI and MLS data. This chapter attempts to study the vertical structure of ozone over Indian region using ozone profile data from OMI.

## 5.2. Data and Methodology

Atmospheric ozone profile data from ozone monitoring instrument over Indian region ( 0-40°N and 60-100°E) was subsetted and retrieved from the site http://mirador.gsfc.nasa.gov. The daily data files in swath form was regridded in to 1° latitude × 1° longitude grid intervals and averaged to obtain monthly ozone profiles. The spatial resolution of the dataset is 13×48 km and temporal resolution is 1 hour. Each profile consists of 18 pressure levels and the unit for ozone concentration was expressed as partial columns between layers in Dobson Units (DU). Data was obtained for the time period from 2004 October to 2012 May. Every profile unanimously contains data from lower mesosphere to upper troposphere (0.5-0.3 hPa, 1-0.5 hPa, 2-1 hPa, 3-2 hPa, 5-3 hPa, 7-5 hPa, 10-7 hPa, 20-10 hPa, 30-20 hPa, 50-30 hPa, 70-50 hPa, 100-70 hPa, 150-100hPa, 200-150 hPa, 300-200 hPa) in the first 15 levels. But in the lower troposphere the layers measured by the instrument are not uniform. Hence three layers (550-450 hPa, 750-650 hPa, 1000-950 hPa) representing upper to lower stratosphere are selected and portions of profiles containing this three layers are taken for gridding. Thus each resulting monthly files consist data from 0°N to 40° N and 60°E to 100°E.

Time series of each atmospheric layer for the entire study period was constructed to study the temporal evolution of ozone over different layers. Seasonal cycle of each layer was obtained by taking the average of the same month from each year for the 2005-2011 and subtracting individual month from its seven year average. Solar Irradiance data in the ultraviolet wavelengths (200-400 nm) was extracted from Solar Radiation and Climate Experiment (SORCE). Irradiance data for the wavelengths from 320-400 nm was taken from October 2004 to September 2010 and data for wavelengths from 200 to 320 nm was selected from December 2004 to May 2012. Timeseries for 200nm, 240nm, 280nm, 340, 360 and 380nm was constructed to study the variation of ultraviolet wavelengths.

Time -pressure plots of ozone were constructed for three atmospheric layers (300-70 hPa, 70-7 hPa, 7-1 hPa). Seasonal climatology of ozone over different layers was calculated by averaging for eight consecutive spring and winter seasons as well as seven consecutive summer and autumn seasons over the entire study period and represented as slice plots. Ozone profile climatology for all the months of the year was also plotted. Climatological deviations of ozone over selected pressure levels representing distinct

portions each atmospheric layer (1-0.5 hPa, 10-7 hPa, 100-70 hPa, 300-200 hPa, 550-450 hPa and 100-950) were also performed. Monthly values of ozone mass mixing ratio and meteorological parameters from ECMWF is taken and correlation coefficients were computed between ozone and various parameters at each vertical layer. This is done separately for 0°N-20°N, 60°E-100°E and 20°N-40°N, 60°E-100°E region. Ozone mixing ratios from ECMWF were chosen to get the ozone mixing ratios at the same vertical level as the meteorological parameters.

Table.5.1. Pressure levels at which OMI ozone measurements are available and corresponding altitudes.

| Layer | Pressure boundaries (hPa) | Approximate altitude at the bottom of the layer (km) |
|---|---|---|
| 1 | 0.5-0.3 | 53 |
| 2 | 1-0.5 | 50 |
| 3 | 2-1 | 42 |
| 4 | 3-2 | 39 |
| 5 | 5-3 | 36 |
| 6 | 7-5 | 33 |
| 7 | 10-7 | 30 |
| 8 | 20-10 | 26 |
| 9 | 30-20 | 23 |
| 10 | 50-30 | 20 |
| 11 | 70-50 | 18 |
| 12 | 100-70 | 16 |
| 13 | 150-100 | 14 |
| 14 | 200-150 | 12 |
| 15 | 300-200 | 10 |
| 16 | 500-300 | 6 |
| 17 | 700-500 | 3 |
| 18 | 1000-700 | 0 |

## 5.3. Results and Discussion
### 5.3.1. Temporal evolution of ozone at various atmospheric layers

Fig. 5.1 (a-i) shows the temporal evolution of ozone for the the region from middle stratosphere to lower mesosphere (0.3 to 30 hPa) from 2004 December to 2012 May whereas Fig.5.2. displays the ozone time series for the same period for the 30 hPa to 1000 hPa layer. The amount of ozone over each layer is represented as partial columns in Dobson Units. The lowest amount of ozone is found in the lower mesospheric layer 0.5 to 0.3 hPa with values ranging from 0.27 DU to about 0.33 DU.
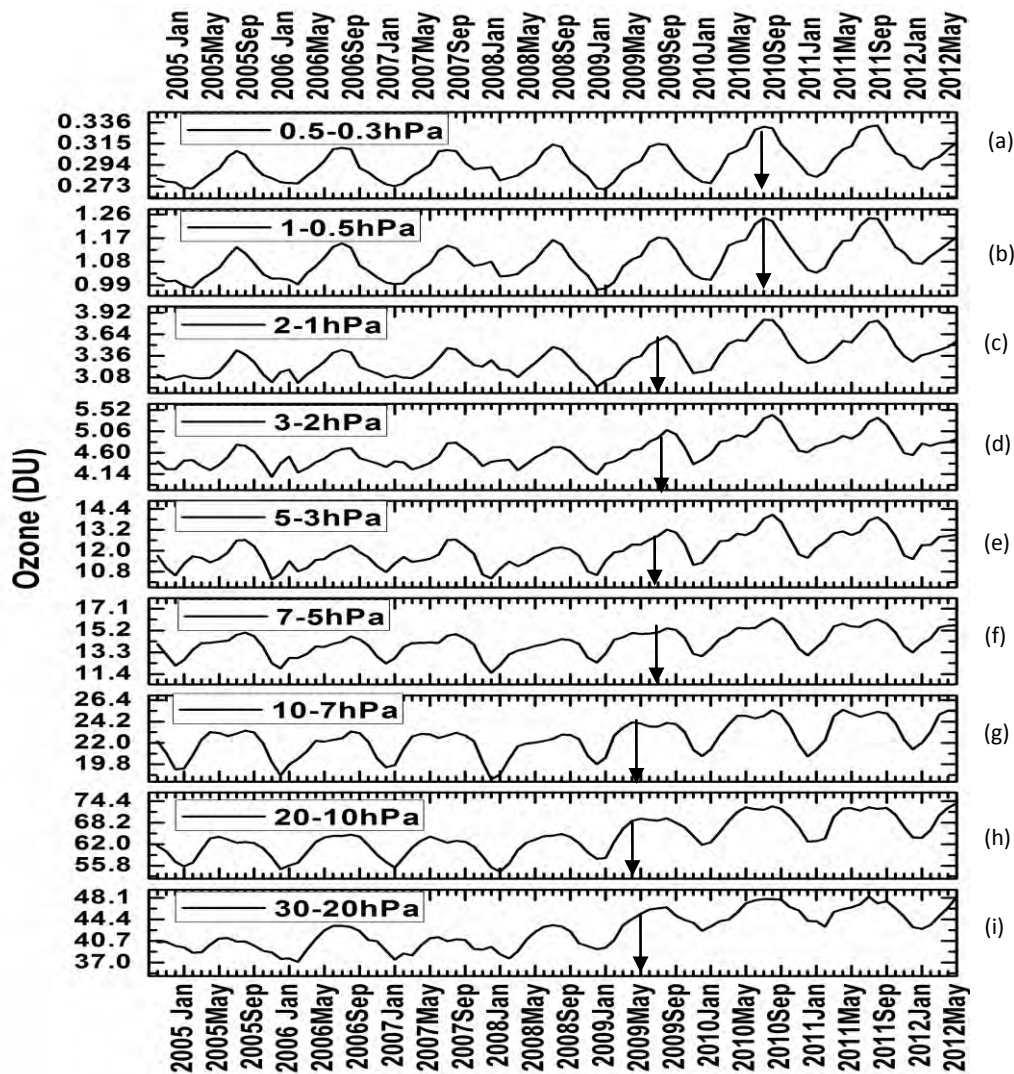


Fig.5.1. Time series of ozone concentration over different layers from 0.3 to 30 hPa

The concentration of ozone increases further down with 0.99 to 1.26 DU in the layer 1-0.5 hPa, 3 to 3.92 DU in 2-1 hPa, 3.1 to 5.5 DU in 3-2 hPa, 10.4 to 13.8 in 5-3 hPa, 11.4 to 16.1 in 7-5 hPa, 18.8 to 25.3 DU in 10-7 hPa, 55.8 to 71.3 DU in 20-10 hPa, 38.4 to 48.1 DU in 30-20 hPa. Highest amount of ozone in the entire atmosphere is seen between 20-10 hPa.
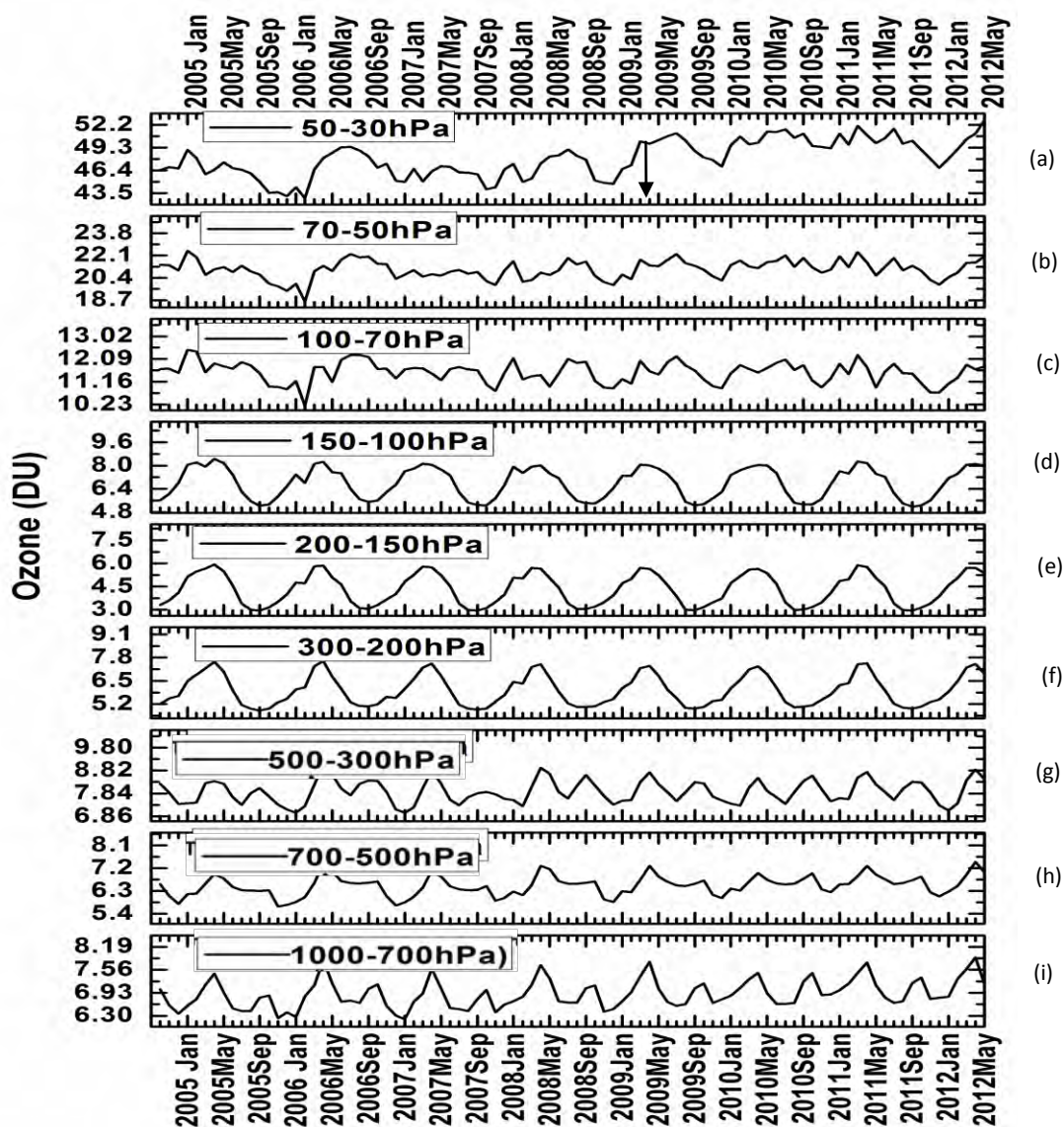


Fig.5.2. Time series of ozone concentration over different layers from 30 to 1000 hPa

In figure 5.2 the (a) 50-30 hpa layer has ozone values ranging from 43 to 52.2 DU, (b) 70-50 hPa layer has 18.7 to 22.2 DU, (c) 100-70 hPa 10.2 to 12.2 DU, (d) 150-100 hPa shows 5.4 to 8.1 DU, (e) 200-150 hPa shows 3-6 DU, (f) 5.2 to 7.8 DU in 300-200 hPa,

(g) 6.8 to 8.8 DU in 550-450 hPa,(h) 5.6 to 7.6 DU in 750-650 hPa,  (i)6.3 to 7.7 in 1000-950 hPa.  Ozone displays a maximum at 20-10 hPa (betwen 26 and 30.5 km) and a secondary maximum at 50-30 hPa( 20-23 km).  Ozone  variation exhibits  regularity in the annual and semiannual timescales in the respective layers except in the layers 50-30 hPa, 70-50 hPa and 100-70 hPa that is for the altitude  16.5 to 23.5 km.

The mesospheric  region represented by 0.5 to 0.3 hPa and 1-0.5 hPa Fig.5.1. (a) and (b) displays an increase in ozone concentration from 2010 June till May 2012.   In the upper stratospheric region below 1 hPa till the mid stratospheric region  30 hPa (Fig 5.1. (a)-(i)) the ozone amount increases in the middle of 2009 roughly an year before the ozone increase in the layers above. The degree of increase   becomes higher in the lower layers.The layer from 50-30hPa   also shows an increase in ozone amount from 2009 May. An anomaly in OMI measurements has also been reported during the period of its measurement. But the ozone increase in the above figures is observed in the middle and upper stratopsheric layers only. One of the possible reasons for ozone increase in the middle and upper stratosphere is the variation in the incoming solar irradiance from sun. Solar activity signal was identified in the middle and upper tropopshere in many studies (Varotsos, 1989, Hood, 1997). The presence of solar cycle variation in atmospheric ozone has been studied extensively (Soukharev and Hood, 2006) .

 Even though  the change in total solar irradiance during solar cycle is very small ,the variability in ultraviolet wavelengths (that influence ozone production and loss) are large enough to influence the temperature profile of the atmosphere and hence the tropospheric processes indirectly (Austin and Hood ,2007).  The variability ranges about 70% in the far ultraviolet region to  about  10 % in the middle ultraviolet wavelenghs (200-300 nm). Ozone displays a variation in response to the UV-A wavelengths of 200, 240 and 280 nm. The wavelengths less than 240 nm are responsible for the breaking of oxygen molecules into oxygen atoms which take part in the formation of ozone.

 Here Solar Spectral Irradiance (SSI) in ultraviolet wavelengths from SOlar Radiation and Climate Experiment (SORCE) are plotted as time series.  Fig.5.3. (a) displays the variation of 200 nm, 240 nm and 280 nm wavelengths  from 2004 octber to 2012 May.
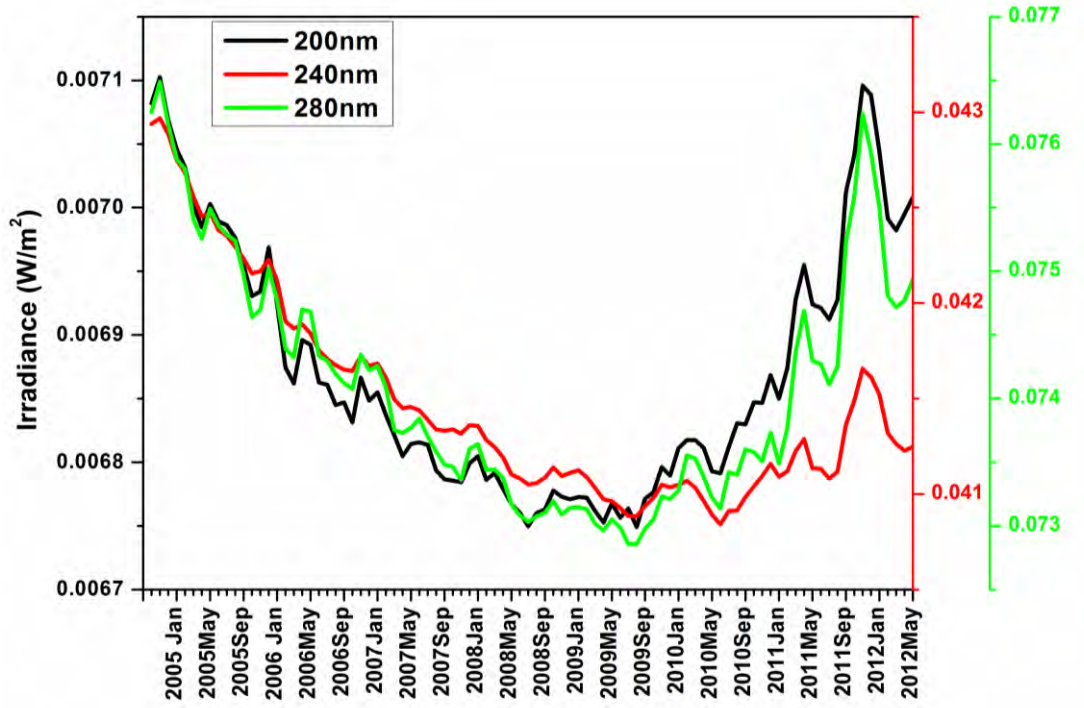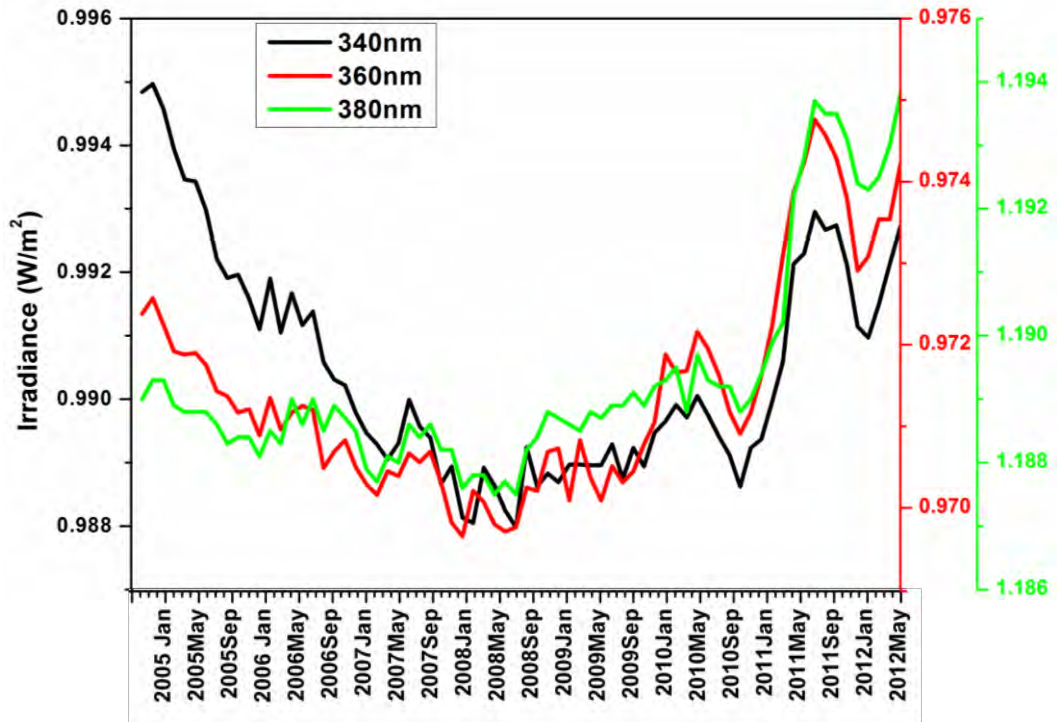
Fig. 5.3. (a) Solar Spectral Irradiance for (a) 200, 240, 280nm and (b) 340, 360, 380 nm

Period from 2008 to mid 2009  is the transition period from solar cycle 23 to 24 with the minimum solar activity. Wavelengths  200,240 and 280 nm are showing  a decrease in irradiance  from 2004  to mid 2009 July. Thereafter an increase in irradiance can be observed  towards May 2012. The peak of  solar cycle 23 is known to have  occured in 2002-2003 and the peak of the solar cycle 24 is expected to be in 2013. The spectral irradiances of 200 and 280 nm shown in the figure shows a  decrease from 2004 to 2009.

Thereafter it is seen increasing upto 2012. The rate increase of irradiance from 2009 to 2012 is found to be steeper than the decrease 2004 to 2009. This steepness of increase in solar irradiance may be the reason for sudden increase in ozone seen in OMI upper and middle stratosphere ozone measurements. Panel (b) of figure 5.3 shows the changes in irradiance for the three wavelengths in the near UV region - 340 nm, 360 nm, 380 nm. These wavelengths show a decrease from 2004 October. The minimum values occur during 2007 December. Thereafter it shows slight increase until 2010 January and a steep increase towards September   2012.

**5.3.2. Seasonal cycle of ozone at different heights of atmosphere**

Figure 5.4. shows the seasonal cycle of ozone over different layers for the period from 2005 to 2011. The lower and mid tropospheric layers show semiannual cycle with two ridges (during  spring and autumn) and two troughs (during summer and winter) over an entire year. The near tropopause layers in the troposphere (150-100 hPa, 200-150 hPa) shows annual cycle with highest values in summer and lowest in autumn. The near tropopause layers in the stratosphere (70-50 hPa and 100-70 hPa) the seasonal variation more or less follows the semiannual cycle with two faint peaks during spring and summer seasons).  Intraseasonal variation for the layers from 3 to 30 hPa the is very low except for winter season. Mesospheric and uppermost stratospheric layers from 0.3 to 3 hPa (Figures 5.4 (o) to (r)) show typical annual cycle with minimum in winter season and maximum in summer (June, July, and August).
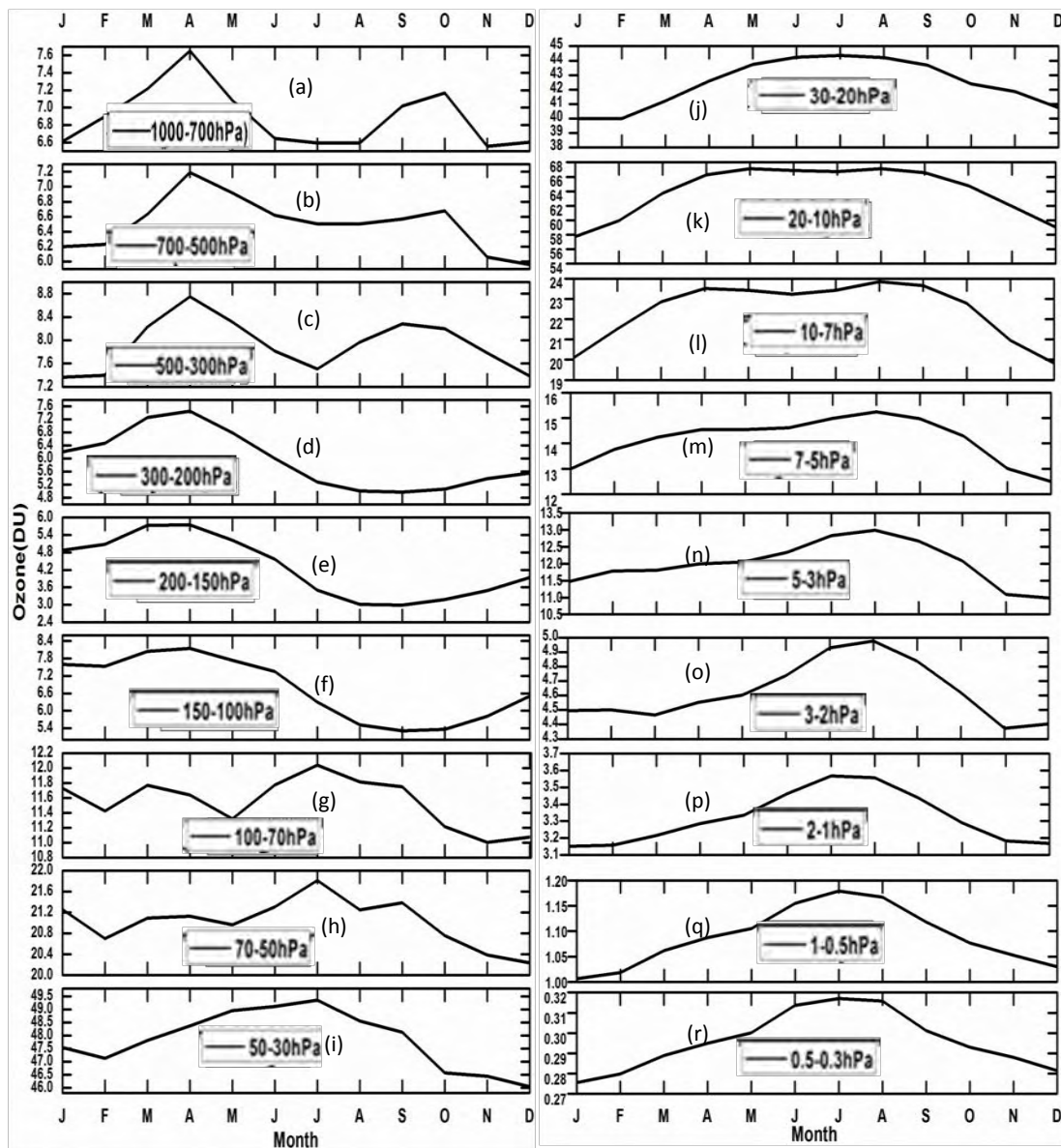
Fig 5.4. Seasonal cycle of ozone at various layers from 0.3 hPa to 1000 hPa

### 5.3.3. Vertical Distribution of ozone during the period of study

Figure.5.5.a. shows the temporal variation of spatially averaged ozone values over Indian. region in the middle to upper stratospheric layers from 7to 1 hPa. An increase in ozone columns for the layers 7-3 hPa and 2-1 hPa is obvious in the figure. In Figure 5.5.b. also an increase of about 5-10 DU observed in the ozone layer 20-10 hPa.

An increase of about 5 DU occurs in 30-20 and 50-30 hPa. The increase can be attributed to variations in solar activity and the increase occurs even in the lower stratosphere up to 50 hPa.
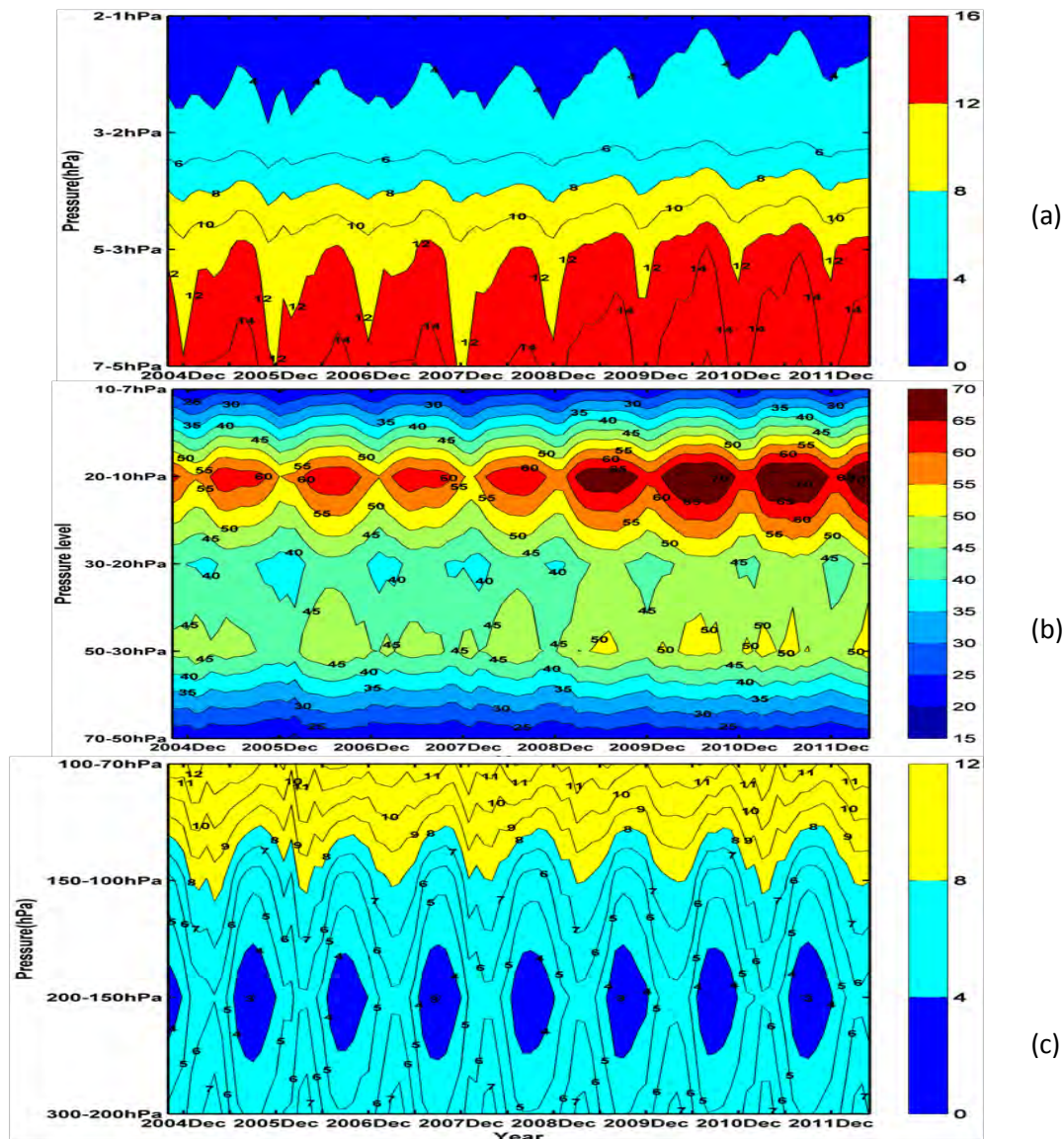


Fig.5.5. Vertical distribution of ozone over the period from 2004 October to 2012 May.(a) 7-1hPa, (b) 70-7 hPa, (c) 300-70 hPa

## 5.3.4. Seasonal Climatology of ozone vertical distribution over India

Vertical distribution of ozone differs from season to season due to the variation in solar radiation as well as the circulation pattern of the atmosphere. In some layers of the stratosphere ozone amounts are dependent on photochemical formation and destruction

of ozone while in some other layers it is dependent on transport.  Seasonal pattern of ozone concentration over 0°N to 40°N and 60°E to 100° E in different layers from 1000 to 0.3 hPa is shown in Figures 5.6 to 5.9. Colorbars and name of the layer for each pair of planes is given in the centre. Figure 5.6. represent the spatial distribution of ozone from the lower stratosphere to lower mesospheric region for spring  and summer.  In the middle and upper stratospheric layers ozone concentration is highest during summer season 0.5 to 5 hPa (the layers .5-0.3 hPa, 1-0.5 hPa, 2-1 hPa, 3-2 hPa, 5-3 hPa). This is due to increased photochemical production of ozone due to large amounts of UV radiation during summer.  These are the regions where ozone amount is controlled by phtochemical processes caused by solar radiation.

 For the 7-5 hPa region the summer and spring seasons are showing approximately same ozone values. For the layers 10-7 and 20-10 hPa which is the region of ozone layer there is barely any variation in total ozone values in the tropical and the equatorward subtropical region from spring to summer. But for the layer 30-20 hPa there is a small increase in ozone column from spring to summer. But for the layers below  (50-30 hpa and 70-50 hPa-for spring and 70-50 hPa-for summer) the subtropical Indian region is showing higher values during spring season while the equatorial region is showing lower values. Stratospheric circulation can transport higher amounts of ozone created in the tropics to higher latitudes.

Thus the effective ozone distribution over this layer  can be  due to the dominance of dynamics compared to photochemistry in controlling ozone concentrations. The ozone at higher latitudes absorb more ultraviolet radiation and hence less radiation reaches the lower stratosphere. Thus the time for the photochemical production and destruction of ozone at these altitudes is slow compared to the transport caused by circulation in the stratosphere.  Among the two seasons considered in Figure 5.6., the effect of tranport processes seen below 50-30 hPa layer is more observed during spring season compared to summer. Vertical distribution of ozone from OMI during autumn and winter is shown in figure 5.7.  Winter season shows lowest amounts of ozone in the middle and upper stratospheric and lower mesospheric layers. As said earlier these layers have photochemically controlled ozone values and thus show the lowest values during winter due to less solar radiation.  The autumn time concentrations resemble spring time values for the layers from 0.5-0.3 hPa to 5-3 hPa.
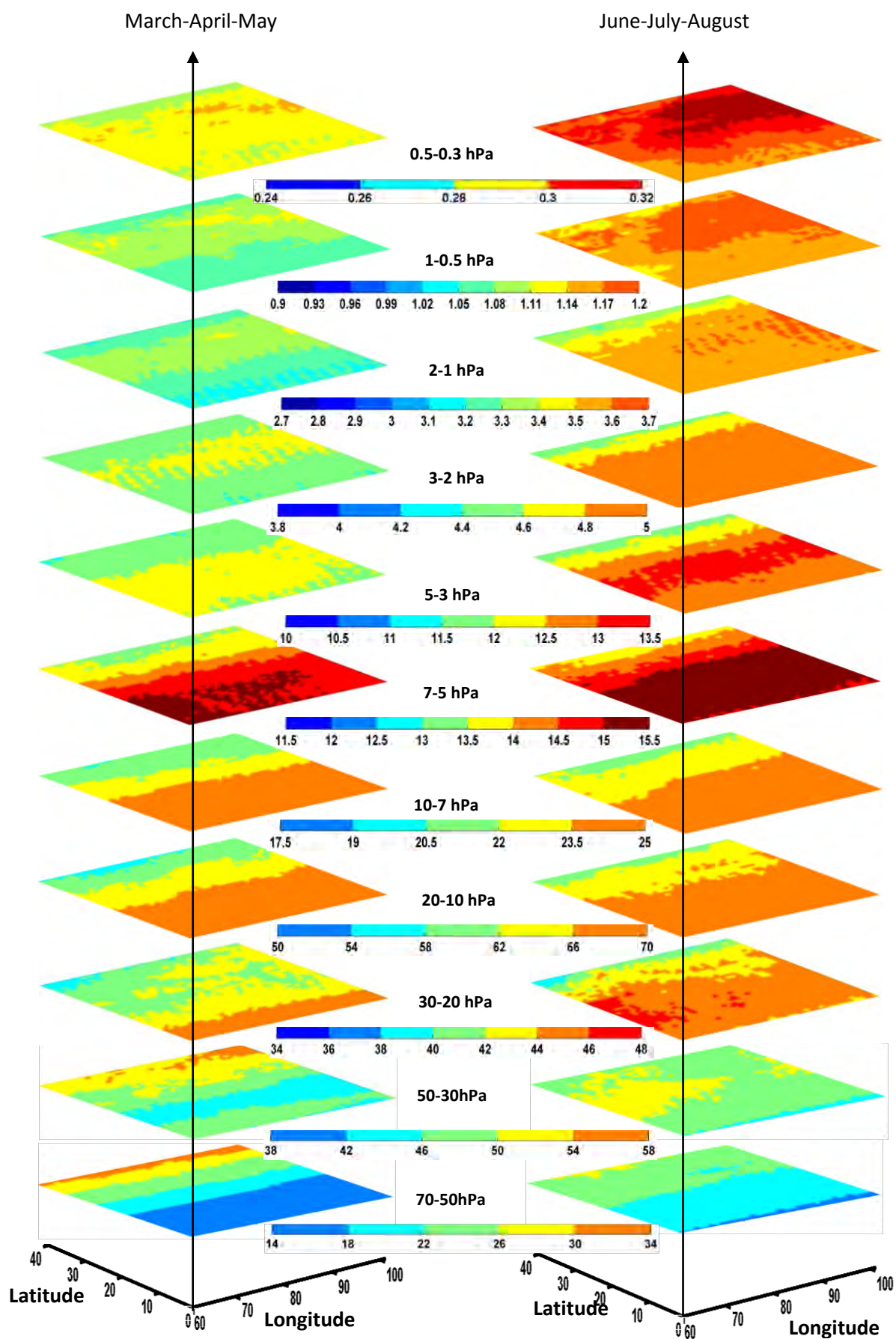
Fig. 5.6. Vertical distribution of ozone in partial columns (DU) for (a) spring and (b) summer seasons from 70 to 0.3 hPa.

Latitudinal variations in ozone amounts appear more clearly below 7-5 hPa. This layer shows large ozone amounts in tropics and lesser amounts in high latitudes for both autumn and winter season. But in the 30-20 hPa layer there is no well defined latitudinal variation over the entire region as observed from the spring and summer seasons as well. But there is difference between ozone amounts between the two seasons (autumn and winter). The layer of ozone maximum occurs due to the optimum amounts of solar radiation and oxygen molecules in this region that causes the production of high amounts of ozone. In the layers above this there is plenty of solar radiation but the atmospheric density becomes less causing fewer amounts of oxygen molecules. For the layers below ozone maximum there is comparatively less amount of solar radiation for ozone production due to the absorption by ozone molecules present above (Stratospheric ozone: An electronic textbook, NASA, GSFC).

Below the layer of secondary ozone maximum (30-20 hPa) the effect of dynamics becomes more prominent during winter as seen in the spring and summer seasons. In the 70-50 hPa layer there is more ozone in the higher latitudes compared to spring. The effect of circulation is more seen during winter season as expected. This is due to the increased planetary wave activity during winter season which causes the transport of ozone from tropics to mid and high latitudes. The spatial distribution of ozone from lower stratosphere to surface (100-70 hPa to 1000-700 hPa) for spring and summer seasons is represented by the Figure 5.8. Both the seasons show higher values of ozone over high latitudes. For higher latitudes spring season is showing higher ozone amounts compared to summer season. For lower stratosphere and troposphere the influence of circulation is more obvious during spring season.

The tropospheric layers 500-300 hPa, 700-500 hPa and 1000-700 hPa has more amount of ozone in the tropical and equatorward subtropical region during spring. But spring season shows higher amount of ozone in the high latitude region from about 30°N to 40°N. Middle and lower tropospheric ozone concentration appears to be governed by circulation during the spring season that causes the high ozone amounts in higher latitudes. But during summer more radiation reaching the surface can bring about the formation of more ozone in the tropical tropospheric layers.
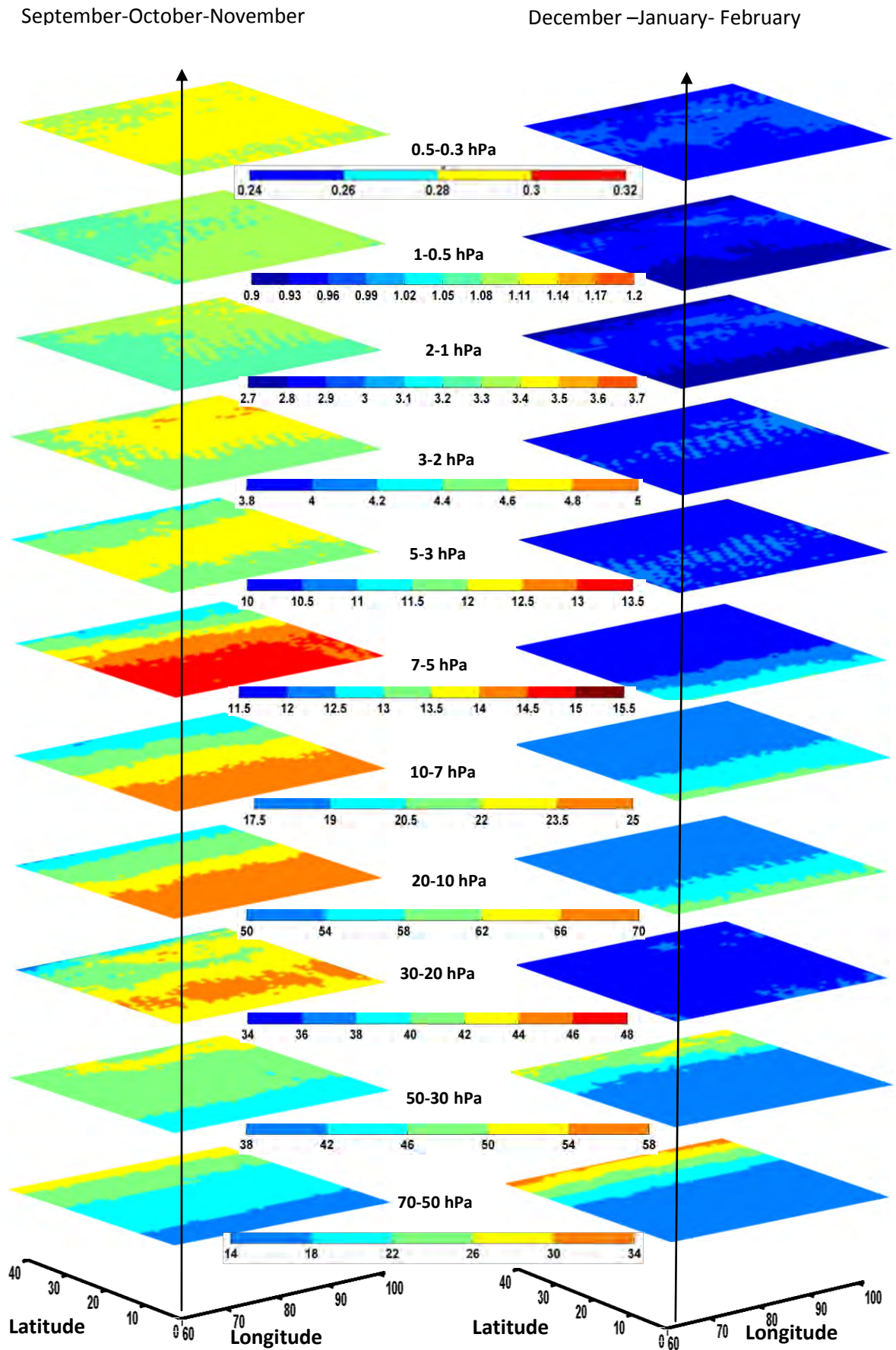
Fig. 5.7. Vertical distribution of ozone in partial columns (DU) for (a) autumn and (b) winter seasons from 70 to 0.3 hPa.
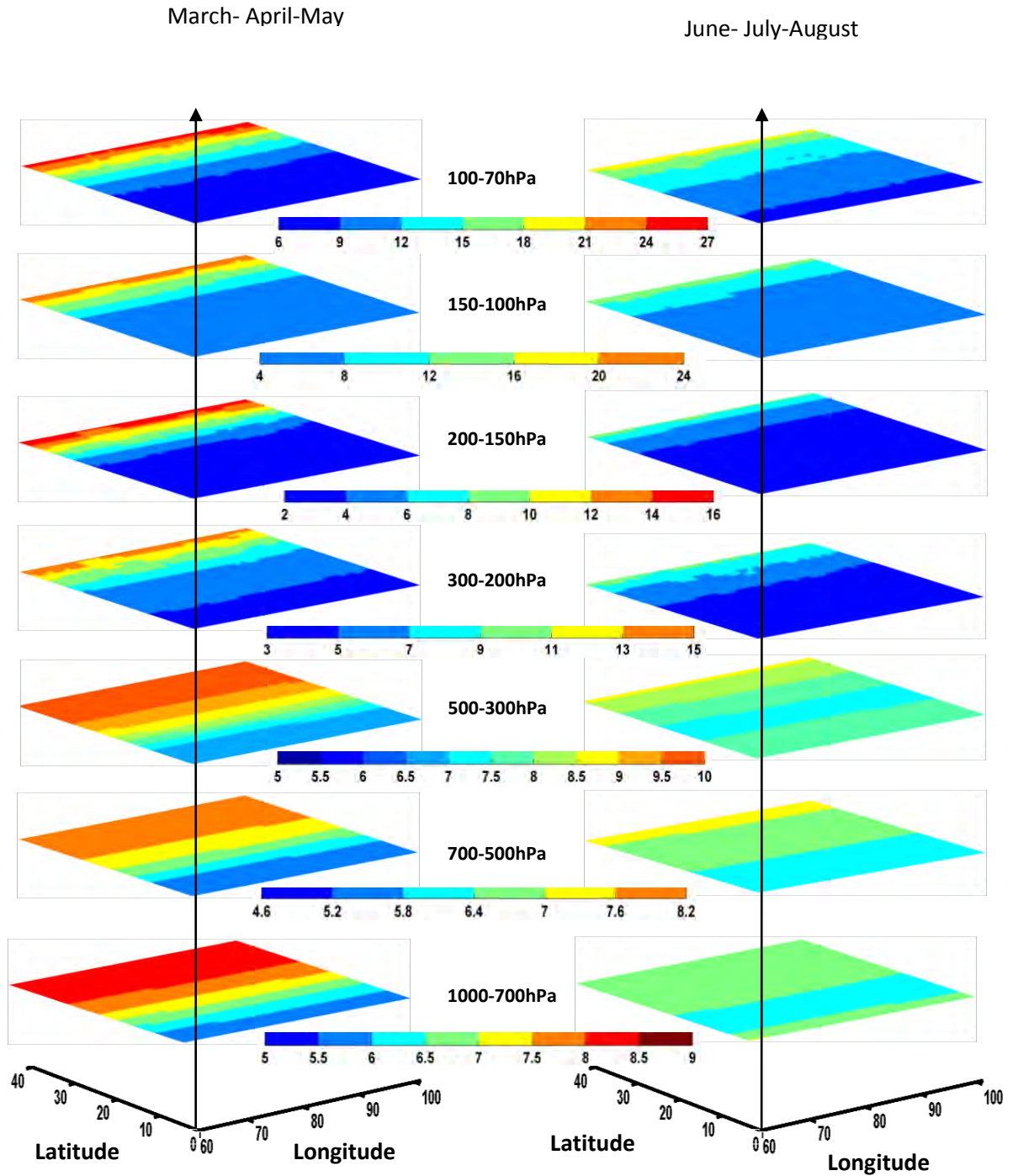
Fig. 5.8. Vertical distribution of ozone in partial columns (DU) for (a) spring and (b) summer seasons from 1000 to 70 hPa.

Autumn and winter ozone distribution over Indian region is given in Figure 5.9. During autumn upper troposphere lower stratospheric layers (100-70 hPa, 150-100 hPa) are showing high ozone at high latitudes. For upper tropospheric layers (200-150 hPa, 300-200 hPa) during autumn season the effect of meridional circulation is comparatively small compared to the levels above that. Winter season high latitude ozone values over

UTLS region is higher compared to that of autumn. The effect of meridional circulation can be observed in more upper tropospheric levels during winter compared to autumn season. The middle and lower tropospheric layers (500-300 hPa, 700-500 hPa and 1000-700 hPa) layers show the same range of values during summer and autumn seasons. Winter values are lowest over these layers the entire season. The presence of lowest values over the tropical region and higher values over subtropical region shows the influence of tropospheric circulation on ozone values.

The influence of ozone present in each vertical layer on total ozone concentrations is given in Table 3.2. as correlation coefficients between total column ozone and ozone at each vertical layer. Radiative forcing by ozone is sensitive to the altitude of ozone changes (Myhre et al., 1996). It can be observed that middle and lower stratospheric regions (50-30 hPa, 70-50 hPa, 150-100 hPa) where the ozone concentration is determined by transport processes shows more correlation with total ozone in the tropical region (0-10°N, 10-20°N). Total ozone of the subtropical region shows high correlation with upper tropospheric layers along with the lower stratospheric layers. Thus the value of total ozone is determined by the ozone concentrations in the transport dominated layers.

### 5.3.5. Vertical distribution of ozone over various latitude bands

The extent of seasonal fluctuations at various vertical levels over Indian region is given by Figure.5.10 (a) to (d). The graphs are constructed by averaging seven years of OMI profile data from 2005 to 2011. Each line of the figure represents the vertical profile of a month. The spread of the line graphs indicate the seasonal fluctuations at various levels. Ozone maximum layer shows a value up to 70 DU for the tropical region (0-10°N, 10-20°N). For 20-30°N and 30-40°N ozone maximum shows values in the range 60 to 65 DU. Seven year averaged ozone values show little variability in the uppermost stratospheric and lower mesospheric layers (3-2 hPa, 2-1 hPa, 1-0.5hPa, 0.5-0.3 hPa i.e. from 39 to 53km). Below 3 hPa (about 39 km) seasonal variability occurs in ozone amounts at each layer in various degrees over different latitudes.
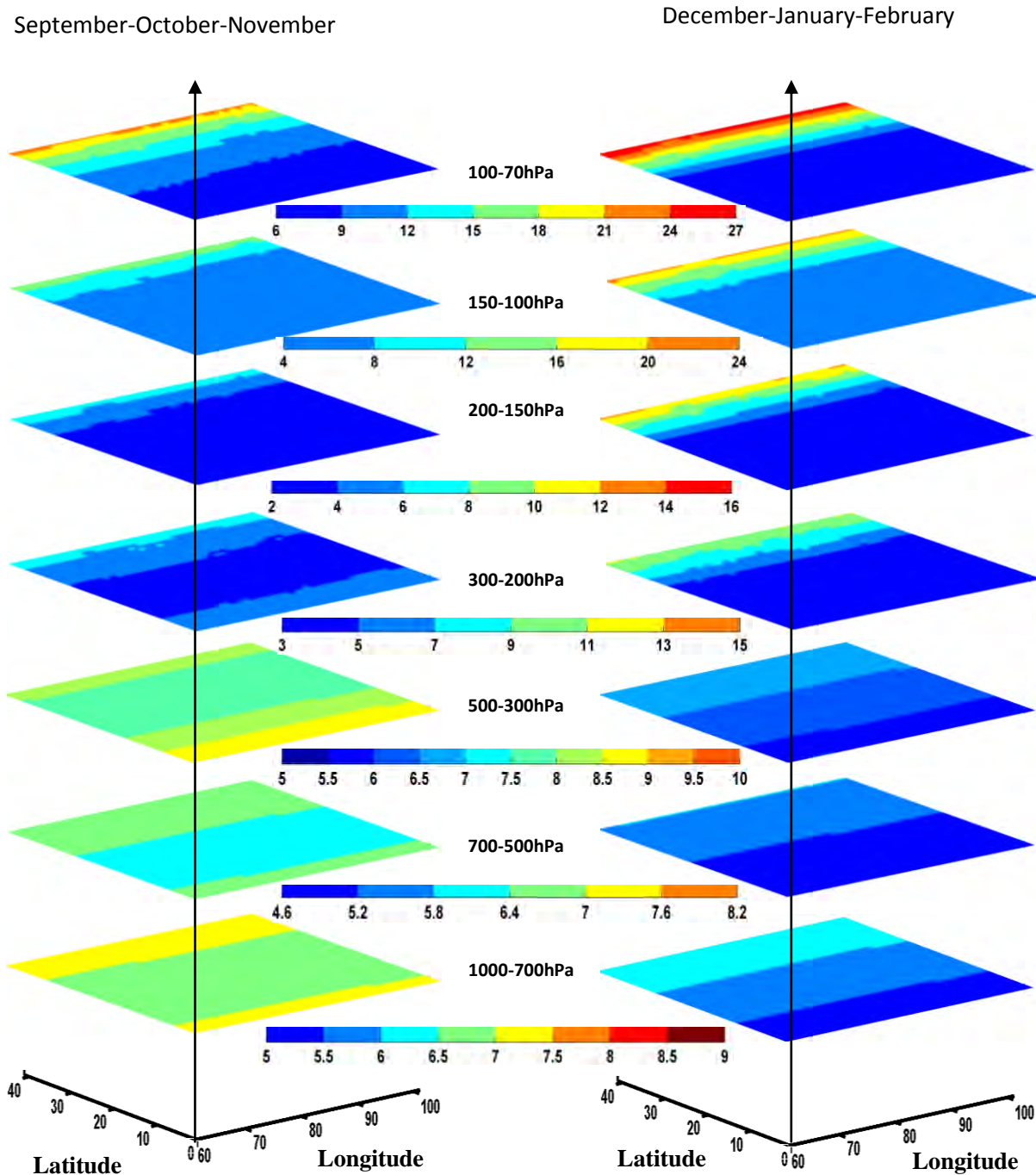
Fig. 5.9. Vertical distribution of ozone in partial columns (DU) for (a) autumn and (b) winter seasons from 1000 to 70 hPa.

Table 5.2. Correlation coefficients of total ozone and ozone at each vertical layer. Significant
correlations are highlighted.

|  | 0°N-10°N | 10°N-20°N | 20°N-30°N | 30°N-40°N |
|---|---|---|---|---|
| 0.5-0.3 hPa | 0.6035 | 0.6827 | 0.3754 | -0.1637 |
| 1-0.5 hPa | 0.5265 | 0.6334 | 0.4403 | -0.1225 |
| 2-1 hPa | 0.2932 | 0.4860 | 0.4423 | -0.15641 |
| 3-2 hPa | 0.1065 | 0.3569 | 0.4311 | -0.1558 |
| 5-3 hPa | 0.1956 | 0.4625 | 0.5043 | -0.1314 |
| 7-5 hPa | 0.3872 | 0.6228 | 0.5968 | -0.1119 |
| 10-7 hPa | 0.3834 | 0.6356 | 0.6269 | -0.1199 |
| 20-10 hPa | 0.3394 | 0.5358 | 0.5549 | -0.1362 |
| 30-20 hPa | 0.5431 | 0.5503 | 0.4730 | 0.2015 |
| 50-30 hPa | 0.8137 | 0.7501 | 0.5952 | 0.7070 |
| 70-50 hPa | 0.8412 | 0.7742 | 0.6856 | 0.7538 |
| 100-70 hPa | 0.7287 | 0.7603 | 0.6998 | 0.7347 |
| 150-100 hPa | 0.7509 | 0.8381 | 0.7479 | 0.8262 |
| 200-150 hPa | 0.5203 | 0.6030 | 0.6447 | 0.8242 |
| 300-200 hPa | 0.2364 | 0.4428 | 0.6204 | 0.8365 |
| 500-300 hPa | 0.4116 | 0.5007 | 0.6065 | 0.4434 |
| 700-500 hPa | 0.4709 | 0.7298 | 0.7596 | 0.4761 |
| 1000-700 hPa | 0.3053 | 0.2892 | 0.5193 | 0.5336 |

For the layers from 5-3hPa to 20-10 hPa seasonal variability of ozone increase from tropics to high latitudes. The layer just below the profile peak region (30-20 hPa), spread is less for subtropical region compared to tropics. Seasonal variation of ozone is roughly same for 0 -10°N, 10-20°N and 20-30°N. But the change in monthly values is less for 30-40°N.

In the 50-30 hPa layer seasonal variation is same for the two latitude bands in the tropical region. The spread becomes slightly less in this layer in the equatorward subtropical region (20-30°N), but it becomes the highest in the subtropical region. In the 50-30 hPa layer the seasonal variability becomes higher during winter months to the extent of values reaching near 20-10 hPa (ozone maximum layer) values. In the lower stratospheric region (100-70 hPa and 70-50 hPa), the tropical region is showing comparatively moderate seasonal variability. But the equator ward subtropical region is showing lesser seasonal spread in ozone values compared to the tropical region. Subtropical lower stratosphere is showing highest variability among the four latitude bands considered.
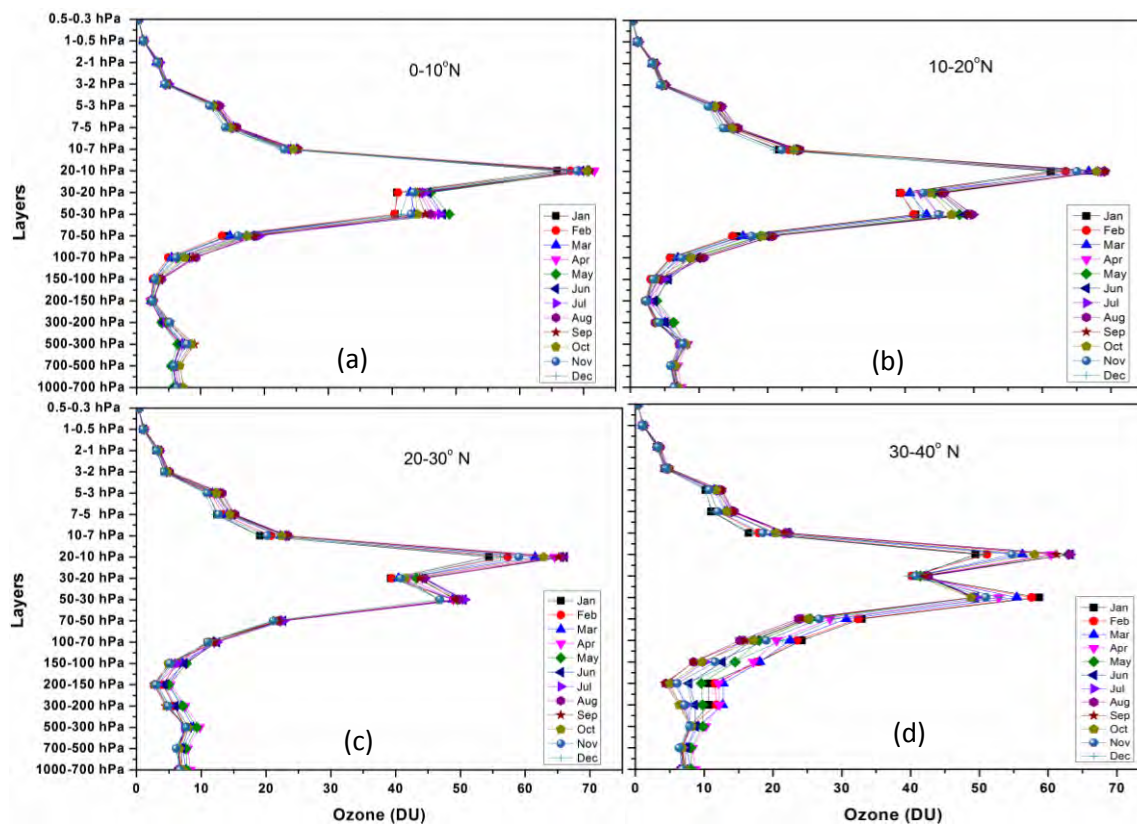
Fig.5.10. Seasonal variation of ozone profile over four latitude bands over India (a) 0-10° N (b) 10-20°N (c) 20-30°N (d) 30-40°N.
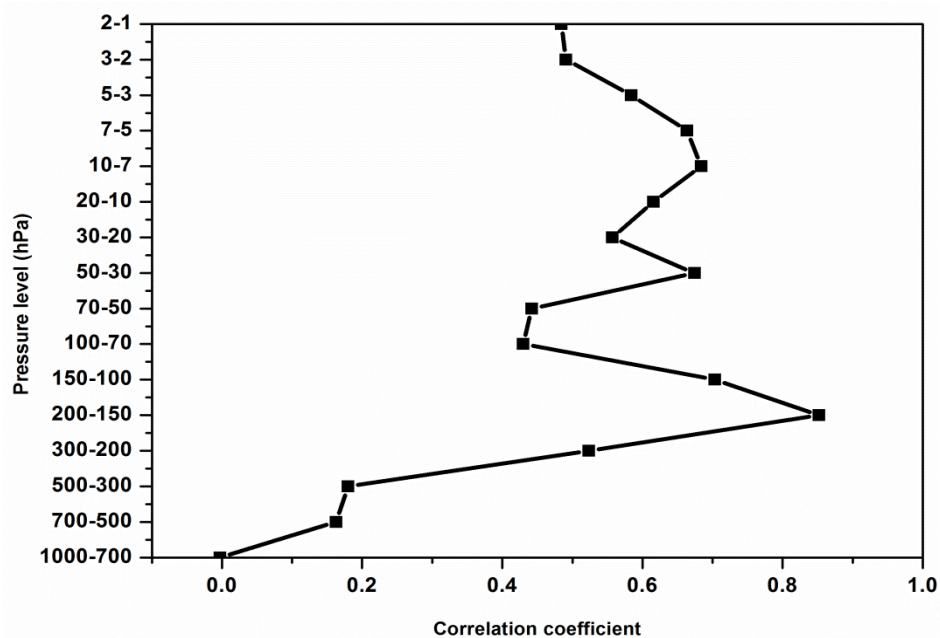


Fig.5.11. Correlation coefficients between OMI ozone and ECMWF ozone at various levels.

The tropopause (150-100 hPa) and upper (200-150, 300-200) tropospheric layers the seasonal variability of ozone increases from tropics to subtropics. For the mid and lower troposphere (500-300 hPa, 700-500 hPa, and 1000-700 hPa) there is little seasonal variability in ozone concentrations in all the latitude bands. Correlation of OMI ozone profile data with ECMWF ozone data at various levels is represented in Figure 5.11. The tropospheric ozone values from both show near zero correlation. But the UTLS region shows highest values of correlation with the 200-150 hPa layer showing values of correlation coefficients nearly equal to 0.9. Ozone amounts at the 50-30 hPa also have a correlation of about 0.7 with ECMWF ozone values.

### 5.3.6. Seasonal deviation of vertical ozone from seven year mean for different atmospheric layers

Seasonal deviation from the seven year seasonal mean values for different atmospheric layers are given in Figures 5.12 and 5.13. Left panels represent the tropical and those on the right represent the subtropical region. In the layer 1-0.5 hPa of the tropical Indian region the deviations of all the seasons follow roughly the same path. The values exhibit an increase starting from the solar minimum year 2008. For the subtropical 1-0.5 hPa layer all the seasons except spring season shows the same variation but the anomaly values are more dispersed compared to the tropical region. Ozone partial column values during spring season show high positive anomalies in the beginning of the solar cycle. But the anomalies become negative for the years 2009 and 2010 during the progression of the solar cycle. For the 3-2 hPa layer also the subtropical region is showing more dispersion compared to the tropical region. From the figures (5.12.a and 5.12.b) it can be seen that spring season  sub tropical upper stratospheric region is not displaying parallel response to solar activity in OMI profile data.

For the mid stratospheric layers (10-7 hPa, 30-20 hPa), the tropical (Figures (c), (d)) and subtropical regions (Figures (h), (i)) show similar range of seasonal variations.  Ozone concentrations in these layers also exhibit approximately equal response to solar activity. The pressure layer below the peak profile region (50-30 hPa) of both the tropical and subtropical region displays similar range of variations and also shows response to solar activity.
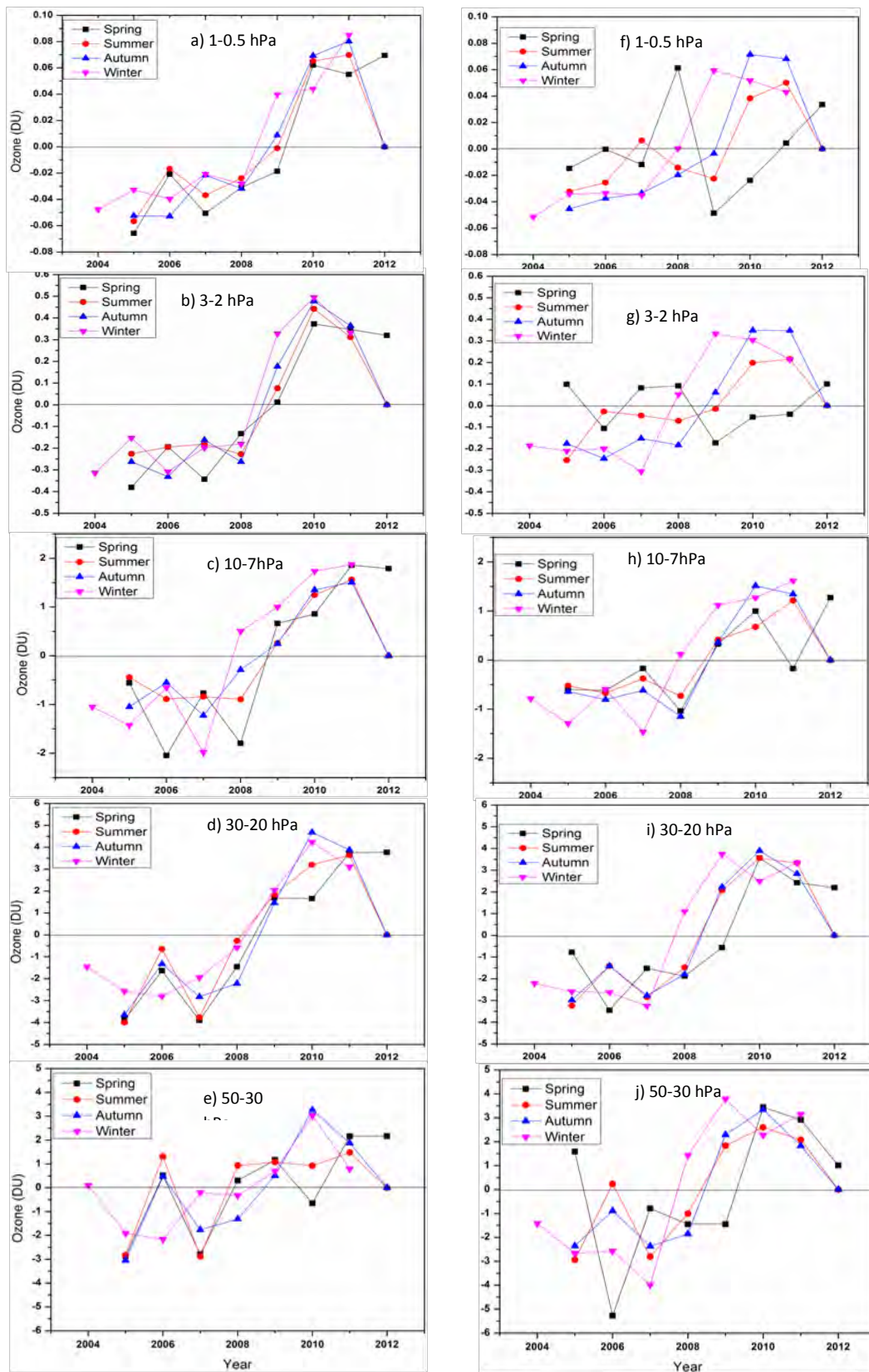
Fig.5.12. Seasonal ozone anomaly (DU) for tropical (0-20 °N, 60-100 ° E-left) and subtropical (20-40 °N, 60-100 ° E-right) Indian region for layers from 0.5-50 hPa.
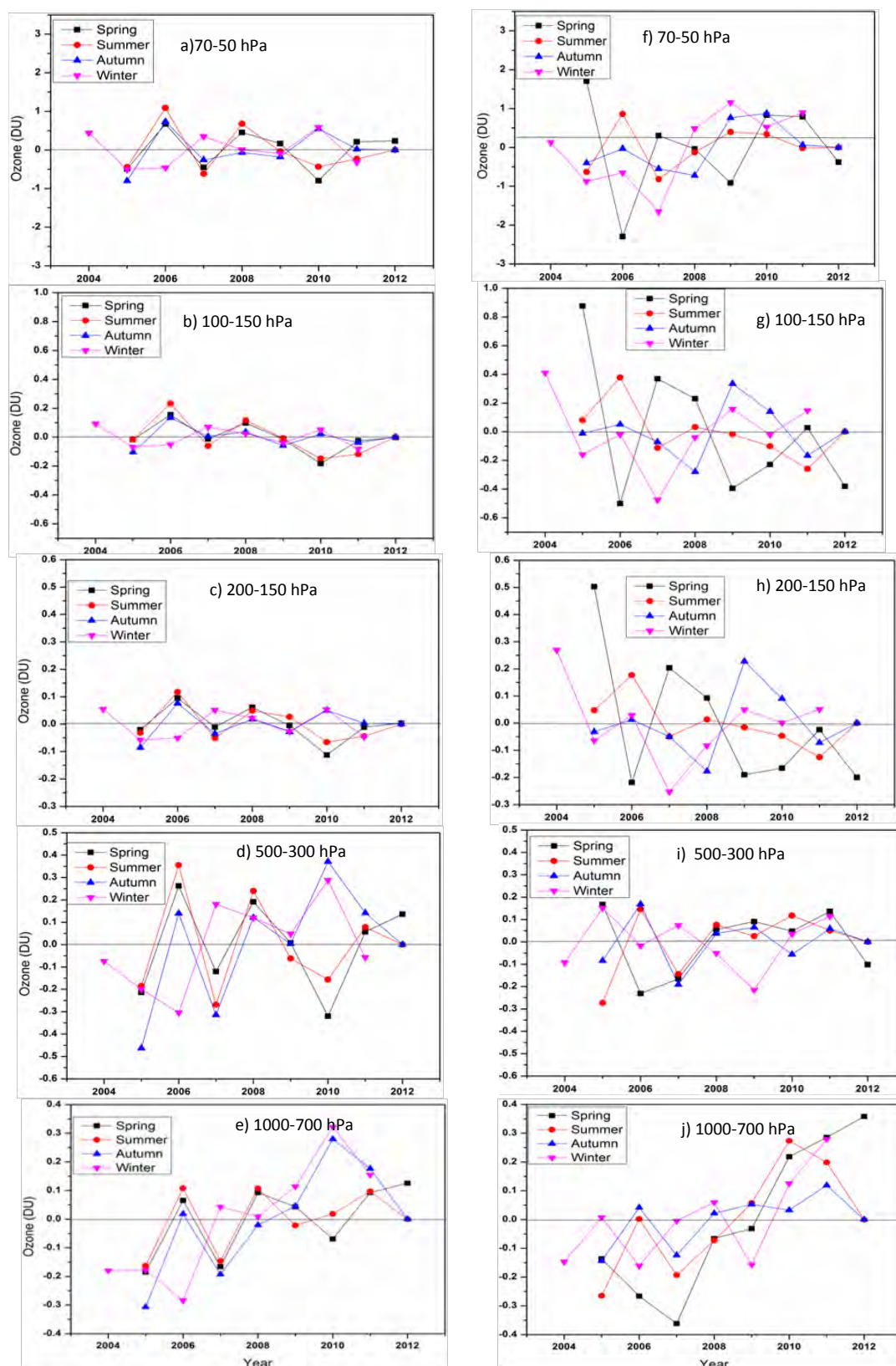
Fig.5.13. Seasonal ozone anomaly (DU) for tropical (0-20 °N, 60-100 ° E-left) and subtropical (20-40 °N, 60-100 ° E-right) Indian region for layers from 50-1000 hPa.

Lower stratospheric and upper tropospheric layers (70-50 hPa, 100-70 hPa, 150-100 hPa, 200-150 hPa) shows marked differences in ozone anomalies for both the tropical and subtropical regions. Summer season of both the regions show matching variations in the two latitude regions whereas winter and spring seasons show contrasting variations in the two latitude regions. In the 500-300 hPa layer the range of variations is more for tropical region. Winter season is showing an out of phase behaviour with other seasons over most of the time in seven years for this layer. The lower most tropospheric layer (1000-700 hPa) shows positive ozone anomalies from the year 2008 similar to the upper stratospheric layers.

## 5.3.7. Relation between vertical ozone distribution and meteorological parameters

Stratospheric ozone is strongly influenced by meteorological variability on both short and long time scales (Wang and Wang, 2010). Correlation coefficients between deseasonalised ozone and meteorological parameters over different pressure layers are represented in Figures 5.14 and 5.15. All the correlation coefficients computed exhibited statistical significance. ECMWF ozone mass mixing ratios and meteorological parameters over different layers from 1979 to 2012 has been used for the study. Hence the study can give a general outcome of the assimilated data and the model equations used for creating the data. Figures on the left represent the 0-20°N and those on the right represent the 20-40°N regions.

Ozone in the midlatitudes is showing a more association with temperture as can be seen from Figure. 5.14 (a) and (b). Many studies have emphasized the coupling between ozone and temperature (Stahelien et al., 2001; Austin et al., 2008). The nature of association i.e. the sign of correlation coefficients is nearly the same at all vertical levels except at the near tropopause (125-250) hPa region where the nature of association is opposite for both latitude bands. A positive relation is displayed by ozone and temperature in the 70-125 hPa regions. The relation is stronger for the 20°N-40°N region with a correlation coefficient of nearly 0.8. Both the regions show a strong negative relation between ozone and temperature in the uppermost stratosphere.

The association between ozone and potential vorticty at different levels is exhibited in Figure.5.14. (c) and (d). The correlation is strong and positive in the 100-225 hPa region of 20°N-40°N. Same nature is shown by the 70-100 hPa region of 0°N-20°N. Potential vorticity at the 20°N-40°N region is also showing positive association with ozone at 500 hPa. Ozone-divergence correlation coefficients for 0°N-20°N and 20°N-40°Nare given by Figures 5.15.(a) and (b). The nature of correlation coefficients is roughly the same for two latitude bands above 30 hPa. At the tropopause region divergence is showing negative correlation with ozone mass mixing ratio except at 300 hPa. The UTLS region of 20-40°N shows negative association between the two parameters. But for 0°N-20°N region positive association exists in the 125-225 hPa layer.

Ozone and zonal wind relation for the two latitude regions are shown by Figures 5.15. (c) and (d). Both the latitude regions are showing out of phase behaviour at various vertical levels with large contrast at the UTLS region. The layer from 150 hPa to300 hPa is not showing near zero correlation. Meridional wind relation with ozone (Figures 5.15. (e) and (f)) also exhibits an out of phase relation at most of the vertical layers. The relation is highly negative for the tropospheric region of 20°N-40°N. Highest negative relation occurs between the two parameters in the 125-100 hPa layer of 0°N-20°N region with values of correlation coefficient near 0.7. It can be observed from the vertical distribution of correlation coefficients of the 20°N-40°N region, that 300 to 70 hPa region is showing similar behaviour in the nature of correlation coefficients. But in the 0°N-20°N region, the layer from 150 to 70 hPa is exhibiting the same behaviour. This may be due to the relatively large thickness of the transition region between troposphere and stratosphere in the 20°N-40°N region. The two regions are showing opposite behaviour in the nature of the correlation coefficients with most of the parameters.

## 5.4. Summary

Ozone profiles from OMI were gridded and the variations of ozone at different heights were visualized. It was found that gridding of OMI data yielded desirable results and it can be used for studying the vertical distribution of ozone with good horizontal resolution at various layers. Layer of ozone maximum was seen at 20-10 hPa as expected. Time series of middle and upper stratospheric layers showed an increase during the steep

increase of solar irradiance at the time of solar cycle. OMI data at these layers is not showing any decrease at the time of irradiance decrease during solar cycle.
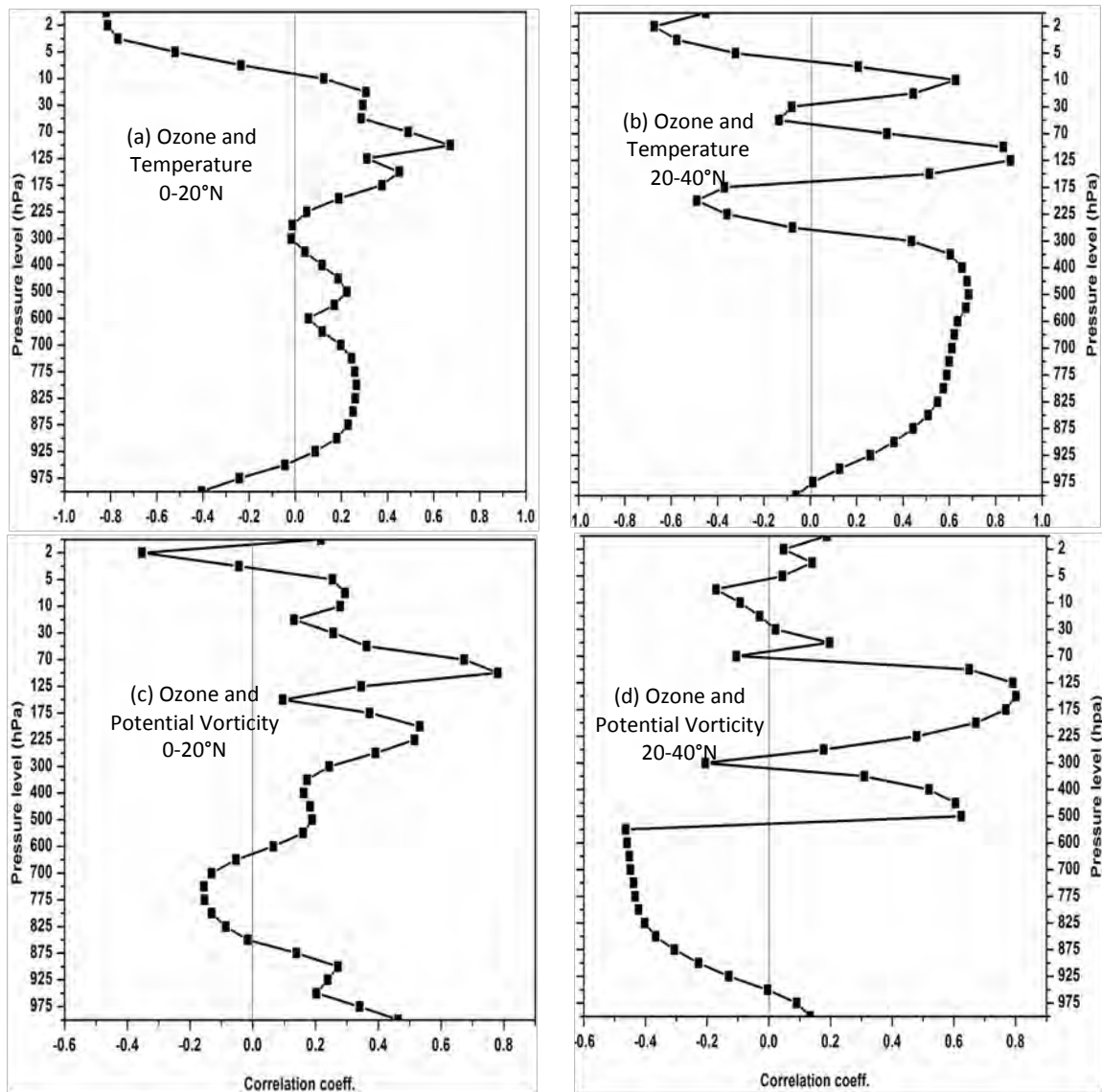


Fig. 5.14. Vertical distribution of correlation coefficients between Ozone mass mixing ratio and Temperature (top panel) and Potential vorticity (bottom panel). Figures in the left represent 0°N-20°N and those on right the 20°N-40°N region.

At the upper stratospheric layers ozone variation is following annual oscillation. The ozone at the lower troposphere and near tropopause layers in the stratosphere also exhibit semi-annual ozone variation. All other layers display annual variation of various amplitudes. Considerable increase can be observed at the ozone maximum layer during the increase of solar irradiance during 24th solar cycle.
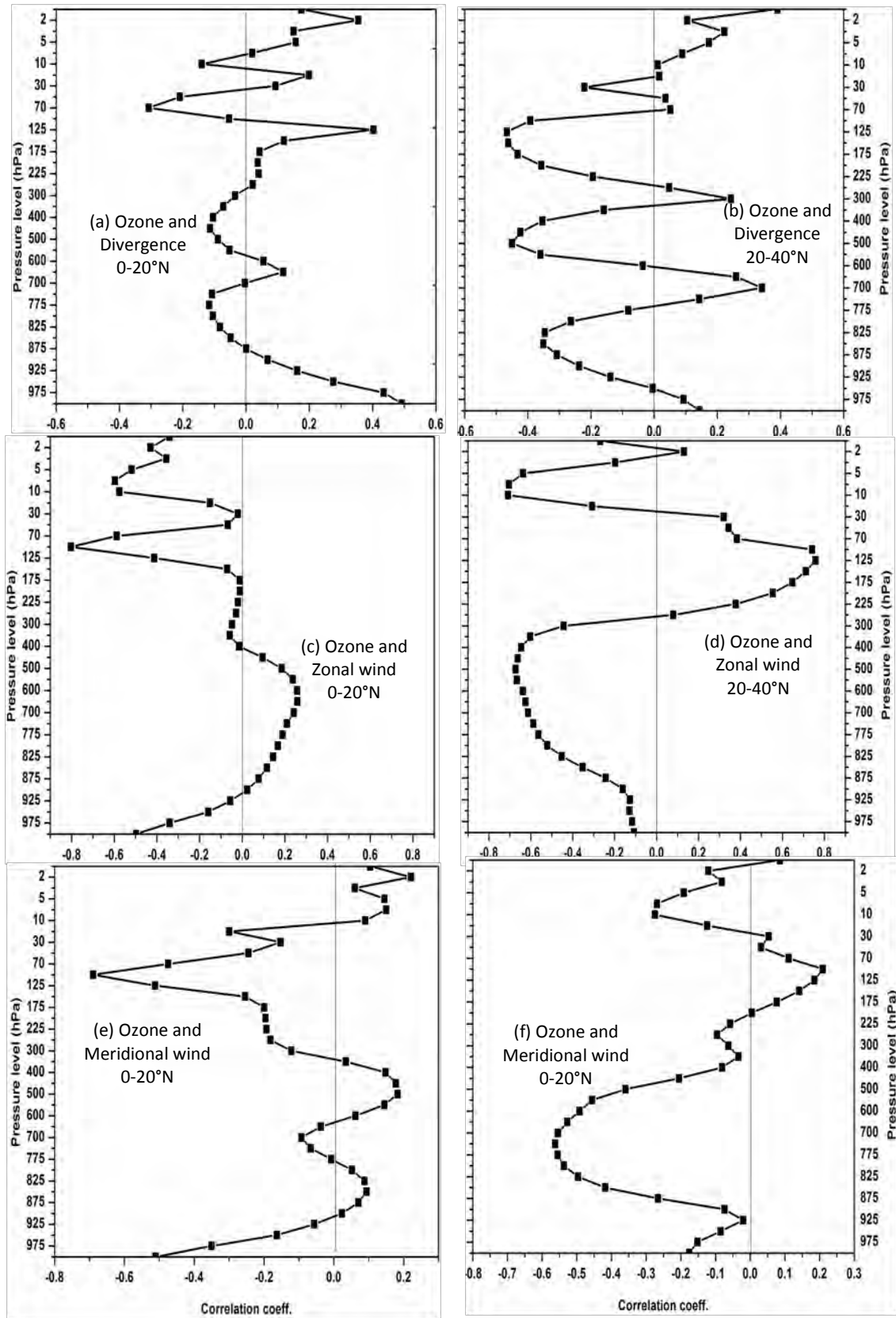
Fig. 5.15. Vertical distribution of correlation coefficients between Ozone mass mixing ratio and divergence (top panel), zonal wind (mid panel) and Meridional wind (bottom panel). Figures in the left represent 0°N-20°N and those on right the 20°N-40°N region.

Study of the seasonal vertical distribution also showed that the layers from 0.5 to 5 hPa showed highest values during summer which indicates the influence of photochemistry in this region. The ozone values at the ozone layer remained high for both spring and summer seasons. The layers below the profile peak region show comparatively high differeneces between the tropical and subtropical regions. These layers show more inclination to ozone distribution by meridional transport. Transport processes show more prominence during spring and winter seasons in the layers below profile peak region. Winter season displayed the seasonal lowest values among all the seasons in from 0.3 to 30 hPa. Also from 1000 to 300 hPa winter season is showing the lowest values of all seasons.

Correlation coefficients between total column ozone and ozone at each layer from omi showed prominent correlations in the upper troposphere lower stratosphere for tropical region from 0 -20 °N. For subtropical region correlations were high at the subtropical region. Latitudinal region from 30 to 40 ° N showed highest spread in ozone profiles among the whole Indian region. Layer to layer correlation with ECMWF data yields highest values in the 200-150 hPa region. Considering the anomalies of ozone at different layers, summer season of both the tropics and sub tropics show matching variations in the two latitude regions. But winter and spring seasons show contrasting variations in the two latitude regions. Winter season is showing an out of phase behaviour with other seasons over most of the time in seven years for 500-300 hPa layer.

# Distinction between the Variability of Upper Troposphere Lower Stratosphere Ozone in the Tropical and Subtropical Indian Region.

## 6.1. Introduction

The upper troposphere lower stratosphere (UTLS) region is a very important interface for the transport of trace gas constituents from stratosphere to troposphere and in the opposite direction. This region is associated with the large gradients of various atmospheric parameters such as temperature, ozone, water vapor and it plays a vital role in dynamics of both stratosphere and troposphere. (Rao et al., 2006). Understanding the dynamical processes and chemical composition of this region is vital to quantify the concentration of tropospheric ozone (Lelieveld and Dentener, 2000; Liang et al., 2008). In the tropical regions UTLS is the location where long lived natural and manmade trace gas species are lifted by deep convection in the upper troposphere and then into the stratosphere using the tropical tropopause layer. Hence it can help to recognize the upward transport of many anthropogenic pollutants into the stratosphere like CFCs that eventually reaches higher latitudes (Murphy and Fahey, 1994).

Ozone variation appears largely to be determined by the zonal variation of vertical convective transport of ozone poor air from the surface. (Pommereau et al., 2004). It is important to study the composition of the atmosphere at the location where the air enters the stratosphere before it is transported to poles. (Dix et al., 2004). The tropical UTLS is a highly dynamic region dominated by transport and in situ chemical processes. Major aspects controlling the UTLS ozone content are photochemical reactions, stratospheric intrusions, deep convection and in-situ chemistry. (Sembhi and Remedios, 2004).

Seasonal drift in the subtropical jet can infast changes in the vertical distribution of ozone and other chemical (Cuevas et al., 2007). Ozone in the UTLS region has an important role in global climate by regulating the photochemistry and radiation balance process (Yang, 1995, Chen et al. 2010). The overall variation in total ozone is found to be significantly correlated with the variation in UTLS ozone (see table 5.2.of Chapter 5 of this thesis). The link between UTLS ozone and temperature is very significant in determining the radiative budget of the stratosphere.

Several studies have shown ozone changes near the tropopause level have the largest climate impact (Forster and Shine, 1997; Hansen et al., 1997). Ozone at this region can also exert considerable impact on incoming UV radiation (Orsolini et al., 2003). The steep increase in ozone mixing ratios in tropical latitudes above 14 km is due to the suppression of vertical mixing associated with convective transport at the tropical tropopause layer. Low ozone concentrations in the TTL are indicative of deep convective transport from the boundary layer (Paulik and Birner, 2012). Upward tranfer by convective events transports and redistributes ozone precursors and other pollutants to the upper troposphere (Tulet al., 2002). There exists a need of more accurate and frequent measurements of trace gas species in tropical UTLS region to accurately understand about the behaviour of trace gas species during convective events (Marécal et.al. 2006). Ozone in the tropical troposphere reflects an interaction of photochemical and dynamical factors.

Alterations in the height of the tropopause (both in thermal and chemical sense) are the result of convective or wave activity taking place in the UTLS region (Thompson et al., 2010). Deep convective activity can bring about an increase in the temperature of the upper troposphere by releasing latent heat. This can change the temperature of give rise to change in the height of the tropopause (thermal). Convection can also cause the upward transport of near surface airmass to higher levels thus altering the trace gas composition of the upper troposphere. Some convective events even reach above the tropopause. This can bring about changes in the chemical composition of the UTLS region thus changing the chemical tropopause (ozonopause) heights. Lightning associated with convection can also cause changes in ozone concentrations by the release of $NO_X$ into the atmosphere.

Ozone variation in the mid latitudes depends mainly on the transport by atmospheric motions (Dobson and Harrison, 1926; Dobson, 1930). An increase in tropopause height can cause low values of total column ozone and hence the amount of UV radiation reaching the surface (Hegglin and Sheperd, 2009;Sola and Lorente, 2011). In the subtropics, the tropopause cuts steeply across isentropic surfaces (Chen, 1995). . Stratosphere- troposphere exchange through this subtropical tropopause break will ordinarily be inhibited by strong potential vorticity (PV) gradients between the troposphere and stratosphere. The subtropical tropopause is also poorly characterised in a chemical point of view (Folkins and Appenzeller, 1996). The objective of this chapter is to identify the differences in UTLS ozone over the tropical and subtropical Indian region. Also an attempt has been made to study the simultaneous variation of the chemical and thermal tropopauses of the two regions.

## 6.2. Data and Methodology

Ozone mixing ratio from 1979 to 2012 and concurrent parameters like divergence, cloud cover, vertical velocity, potential vorticity, and temperature and geopotential height for pressure levels from 300 to 100hPa were obtained from ECMWF Interim dataset. Time pressure plots were constructed for 300 to 100 hPa for divergence and 100-200 hPa for other parameters to study the seasonal and daily variation concurrent with ozone in the UTLS levels. The tropopause height data was retrieved from NCEP reanalysis. Simultaneous seasonal variations of the other parameters were also examined to look into the effect of dynamics in ozone concentrations at the UTLS. Time series of tropopause height were plotted to study the coincident variations with ozone. Annual as well monsoon time averaged plots were constructed to study the interannual variations of ozone and corresponding changes in temperature.

ERA Interim data for two locations, Trivandrum and New Delhi, were taken and analysed to examine the tropopause variations in the tropical and subtropical Indian region. The World Ozone and Ultraviolet Data Centre (WOUDC) ozone profile measurements have been converted from partial pressures in millipascals (which is an absolute unit of ozone measurement) to volume mixing ratio in parts per million volume (which is a relative unit). This is done in order to avoid the effects due to changes in

compressibility of the atmosphere. Heights of upper tropospheric ozone minimum for the ozone profiles were determined   by finding the altitude of minimum ozone concentration between 400 and 100 hPa.  Ozone gradient tropopause is determined by taking the base of the layer in which the ozone increases by 0.1ppmv or more from the layer below. Lapse rate tropopause is also computed in a similar manner –as the base of the layer in shich the lapse rate is more than 2K/km. Cold point  tropopause is obtained by taking the altitude of the lowest temperature in the 300 to 70 hPa layer.

## 6.3. Results and Discussion
### 6.3.1. Seasonal variation of ozone over UTLS region

By analysing the relation between the total ozone and ozone at each vertical layer it can be seen that UTLS ozone is playing a significant part in total ozone variability. The seasonal variation of ozone in the 100 to 200 hPa for the region from 0°N to 20°N and 60°E to 100°E is shown in Fig.6.1.  The values vary from $1 \times 10^{-7}$ to $2 \times 10^{-7}$. The 100-125 hPa layers shows higher ozone levels during summer season. Ozone concentration starts increasing from the middle of April and reaches peak values of the year during July. An increase of about $1.4 \times 10^{-7}$ can be observed during the summer season compared to the winter season. This increase can be due to the lowering of tropical tropopause during boreal summer.

The time pressure height plot given as Fig.6.2 shows the seasonal variation of 100-200 hPa ozone mixing ratios for the region from 20 to 40°N.The overall ozone amount is higher than that of the tropical region with values ranging from 1 to $7 \times 10^{-7}$. Here ozone values are more during winter season. More ozone is observed in the region during the time from January to April. The highest values were observed during February. The increase in the ozone can be closely linked to tropopause heights.  Thus it can be deduced that the ozone concentrations at the tropical tropopause region is dominated by the lowering of tropopause region during summer. This is caused by the increase in the depth of the stratosphere due to increasing temperature during the summer season. But in the subtropical Indian region the upward transport of boundary layer air with low ozone amounts by convection is the dominating mechanism in determining the near tropopause concentration of ozone.
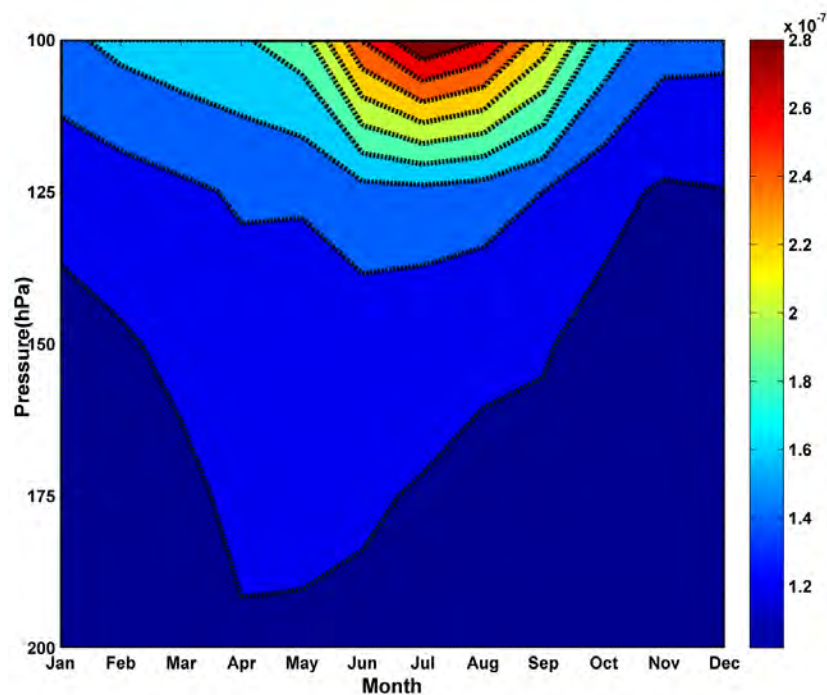
Fig.6.1.Seasonal variation of ozone mixing ratio (kg/kg) in 100- 200 hPa  layer for 0°N to 20°N and 60°E to 100°N.
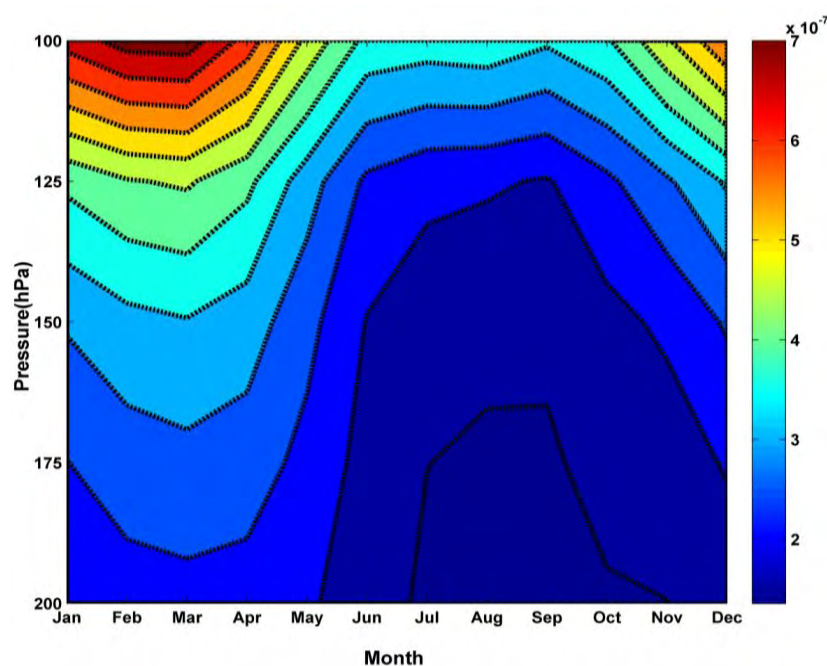


Fig .6.2.  Seasonal variation of ozone mixing ratio(kg/kg)in 100-200 hPa layer for 20°N to 40°N and 60°E to 100°N.

Daily  variations  of  UTLS  ozone  averaged  from  1979-2012  at  a  tropical  station-Trivandrum  (Figure  6.3)  and  subtropical  station-New  Delhi  (Figure  6.4)  were  also

analysed to have a clear picture of the variations. Comparing the ozone mixing ratios of Trivandrum and New Delhi the increase of ozone in the 100-125 hPa layer occurs in summer for Trivandrum and winter for New Delhi. The summertime increase over Trivandrum appears to be more organised. New Delhi is not showing similar increase during summer time. The winter time increase over New Delhi appears to be taking place as individual events of varying intensity and depth.
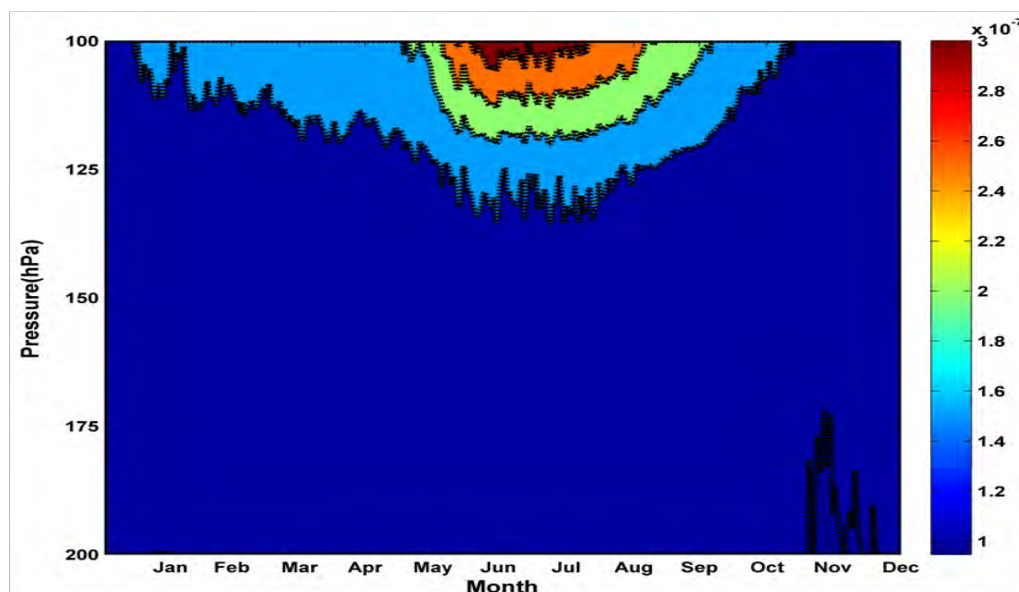


(a)
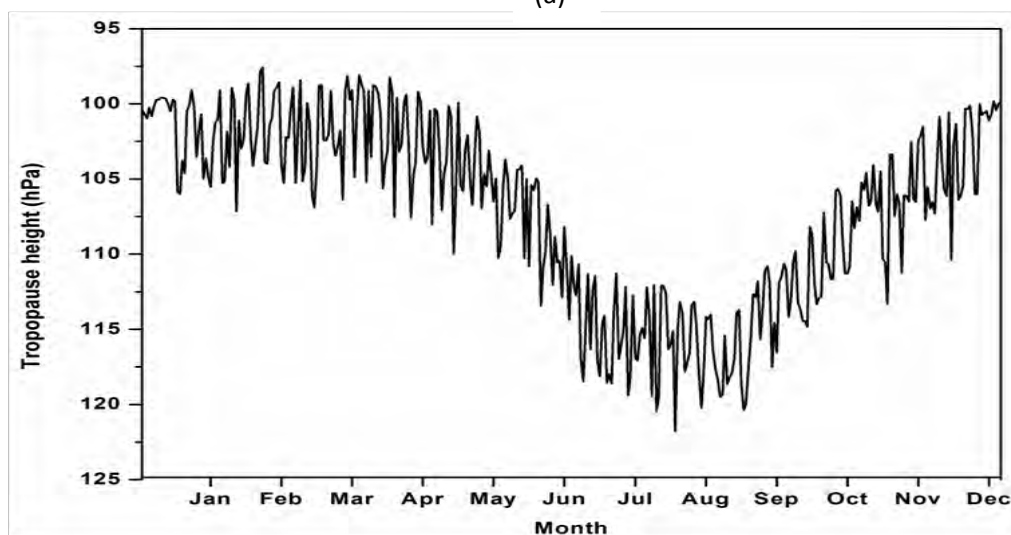


(b)

Fig .6.3. Seasonal variation of (a) ozone mass mixing ratio in 100-200 hPa layer and (b) tropopause height for Trivandrum (8.48°N,76.95°E).
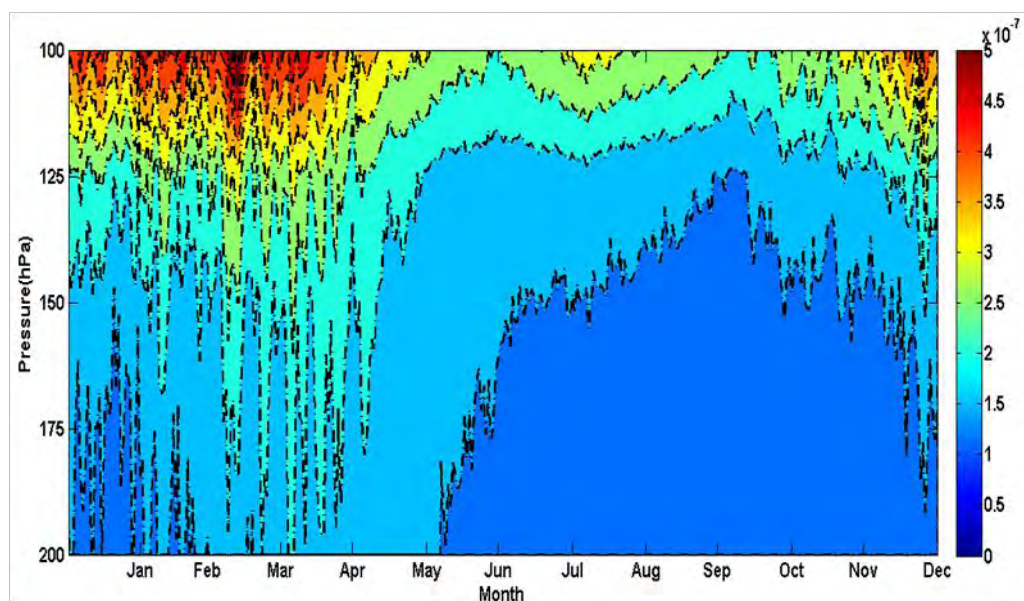
(a)
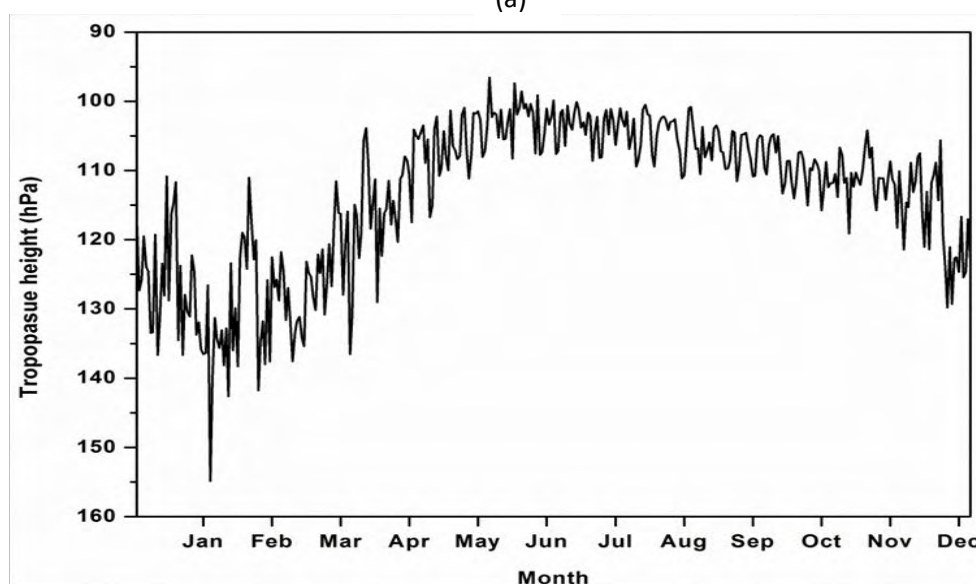


(b)

Fig .6.4. Seasonal variation of (a) ozone mass mixing ratio in 100-200 hPa layer and (b) tropopause height for New Delhi (28.3°N, 77.1°E)

The increases in ozone mixing ratio during winter can happen due to the passage of upper tropospheric troughs from middle latitudes during northern hemispheric winter (Singh, 1979). The upper tropospheric westerlies of midlatitudes shift southward during northern hemispheric winter. These waves develop into large amplitude north-south oriented troughs that can penetrate deep into South Asia (Sathyamoorthy, 2001). The passage of

this upper tropospheric troughs causes the lowering of tropopause height and hence an increase of ozone concentrations in the UTLS region. The effect on tropopause by the passage of a trough or ridge is demonstrated in Fig.6.5.

The decrease of UTLS ozone over New Delhi (Fig.6.4) during summer can be due to convection during summer monsoon and vertical transport can be attributed to gravity waves. (Pierce and Grant, 1998). Deep convection plays a major role in the vertical transport of chemical species from the lower troposphere to the upper troposphere (Wang and Prinn, 2000; Mari et al. 2003; DeCaria et al., 2005). From both the figures it is evident that the ozone mixing ratios are following the tropopause heights. Ozone trend associated with the dynamical movement of the tropopause is not a direct result of anthropogenic ozone depletion and should be considered separately in radiative forcing calculations (Ramaswamy et al., 1992, Forster and Tourpali, 2001).
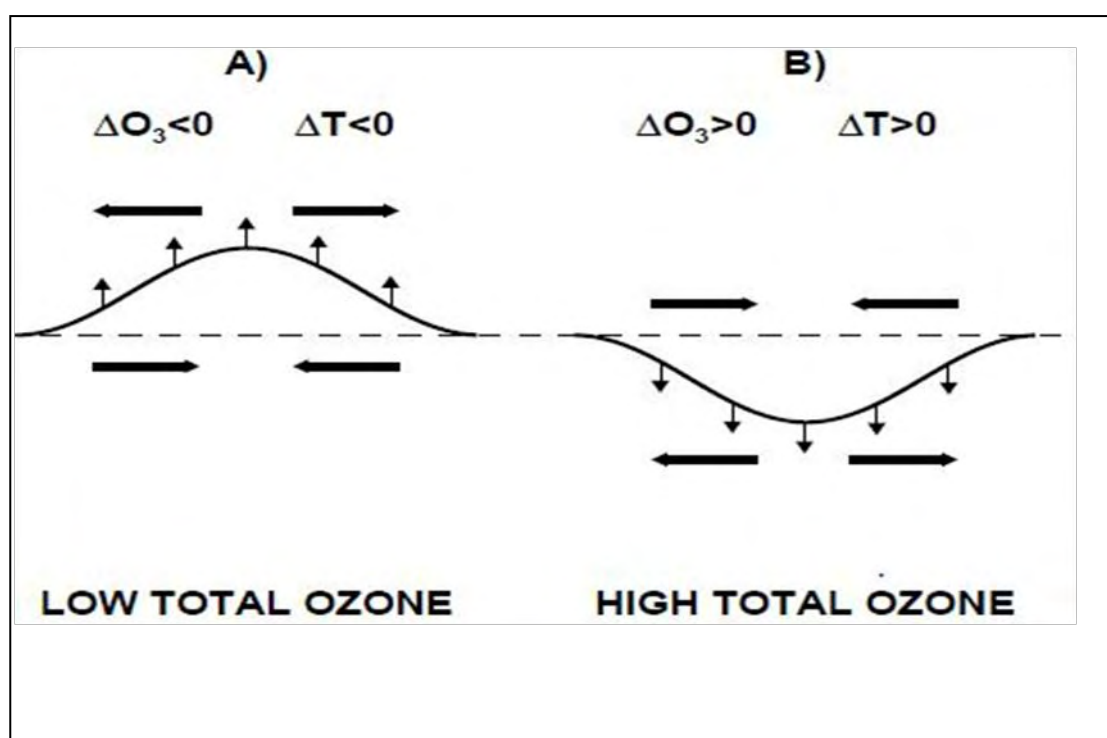


Fig. 6.5 Schematic picture showing changes in ozone and temperature associated with the passage of (a) a ridge and (b) a trough.

Inorder to inspect the role and nature of circulation in the ozone distribution over various seasons, various parameters that represent the circulation pattern over the region were examined. Fig.6.6.(a) shows the divergence of the layers from 300 to 50 hPa for 0°N to 20°N. The maximum observed at 125 to 200 hPa region can be due to upper level divergence associated with monsoon circulation. The region above 100 hPa during summer season shows a slight negative value of divergence ie convergence this is the region and the time of ozone increase occurs. But for Fig.6.6. (b) (20-40°N) the enire depth of the region shows slight positive values of divergence. This divergence is the points to the circulation that uplifts the air (or tropopause and hence ozone upwards).

Fig.6.6(c) and (d). represents the seasonal climatological distribution of cloud cover over the Indian region from 0 to 20°N and 20 to 40°N. Cloud cover is expressed in the 0 to 1 range with zero representing no clod and 1 representing full cloud cover.  The tropical Indian region exhibit a high amount of cloud cover in the 100-200 hPa level compared to the subtropical Indian region. Cloud cover is highest during the monsoon season. The highest amount of cloud cover in the subtropical Indian region occurs at the same time as the seasonal decrease  of ozone in the monsoon season as shown in Fig.6.2 and 6.4. Eventhough the cloud cover at UTLS is more stronger over the tropics the variation is not showing any concurrence with ozone vatiation.

## 6.3.2. Meteorological parameters at the UTLS region

Climatological variation of vertical velocity for both the tropical and subtropical region is represented in Figure 6.7. (a) and (b) Negative values of vertical velocity denotes ascent whereas the positive values indicates descent. Elevated values of negative vertical velocity can be noticed from spring to autumn season over the tropical region. This are the periods of the equinoxes and summer solstice for northern hemisphere. Minor positive values of vertical velocity denoting descent and hence the ozone increase can be observed during June to September near 100 hPa over a very small area in tropical Indian region.

(a) 0-20 °N

(b) 20-40 °N

(c) 0-20 °N

(d) 20-40 °N
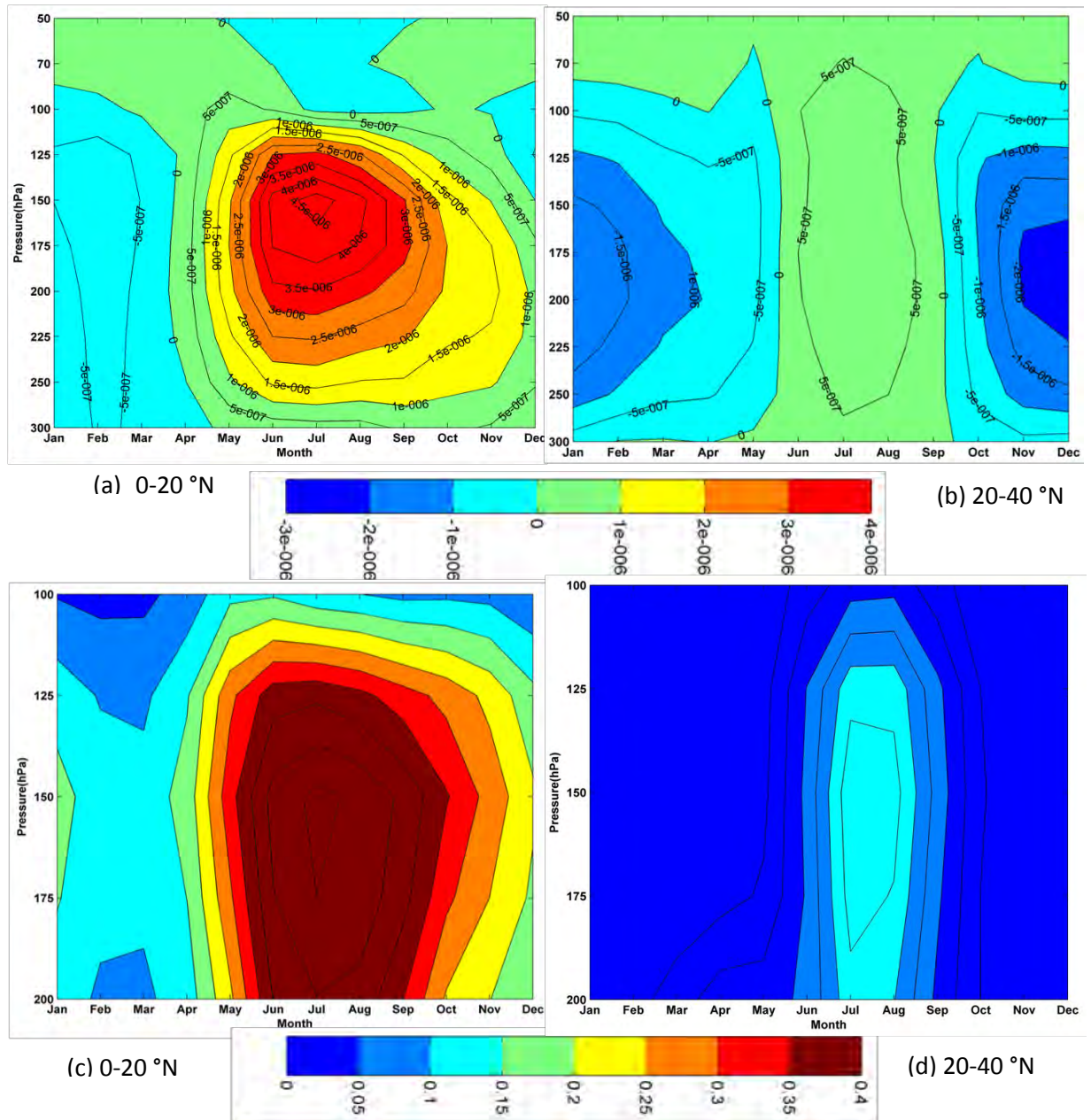
Fig.6.6. Seasonal variation of Divergence (s$^{-1}$) for 300 to 50 hPa (top) for 0 to 20°N (a) and 20 to 40°N(b ) and cloud cover 200 to 100 hPa (bottom) for 0 to 20°N(c) and 20 to 40°N(d).

For the subtropical region peak values of vertical velocity occurs only during monsoon season in the UTLS region. Highest values (blue color) of vertical velocity crosses more heights compared to that of the tropical region. This occurs during the peak monsoon months. Descending of air can be observed throughout other season in the same areas of high ozone. This reflects the occurrence of stratospheric intrusion during winter and spring months.

Potential vorticity of both the tropical and subtropical region are given in Figures 6.7. (c) and (d). Values of potential vorticity can be used to distinguish between the air of stratospheric and tropospheric origin. Dynamical tropopause is considered as the atmospheric layer that coincides with 2 PVU (Potential Vorticity Unit- 1 PVU=$10^{-6}$ Kkg$^{-1}$ m$^2$ s$^{-1}$). Ozone mixing ratios together with its maps can give information about the dynamical processes leading to ozone variations (Hoskins, 1995). The structure of variations for both the latitude regions reflects the variation of the tropopause height. Values as high as 6.5 PVU can be observed in the region between 100 and 125 hPa during winter and spring.

Seasonal variation of temperature from 200-100 hPa is depicted in Figure 6.8 (a) and (b). In the tropical upper troposphere from 200-125 hPa there is very little seasonal variation in the temperature. But there is a clear increase in the 125-100 hPa layer from June to September. This is similar in magnitude and span with the seasonal ozone variations observed during summer season over the same region (Fig.6.1 and 6.3). This increase is not concurrent with the slight increase in temperature observed from March to October near 200 hPa.

For the subtropical (Fig. 6.8) area seasonal fluctuations in temperature are comparatively high. The 125-100 hPa layer shows lower values of ozone from March to November with the lowest values from June to September which the time of seasonal decrease of ozone over the region. Also higher temperatures can be seen at the time of ozone increase over the subtropical region. From the two figures it can be seen that seasonal high temperature exists in the 100-125 hPa region at the time of seasonal increase of ozone in 0-20°N Indian region. Also a seasonal low temperature prevails at the time of ozone decrease in the 20-40°N region. Geopotential of both the latitude regions is given in Figure 6.8.(c) and (d). Seasonal fluctuation seems to be nil for the tropical region. In the subtropical region downward movement of gepotential surfaces can be observed at the time ozone decrease in the upper tropospheric region.

(a) 0-20 °N

(b) 20-40 °N

(c) 0-20 °N

(d) 20-40 °N
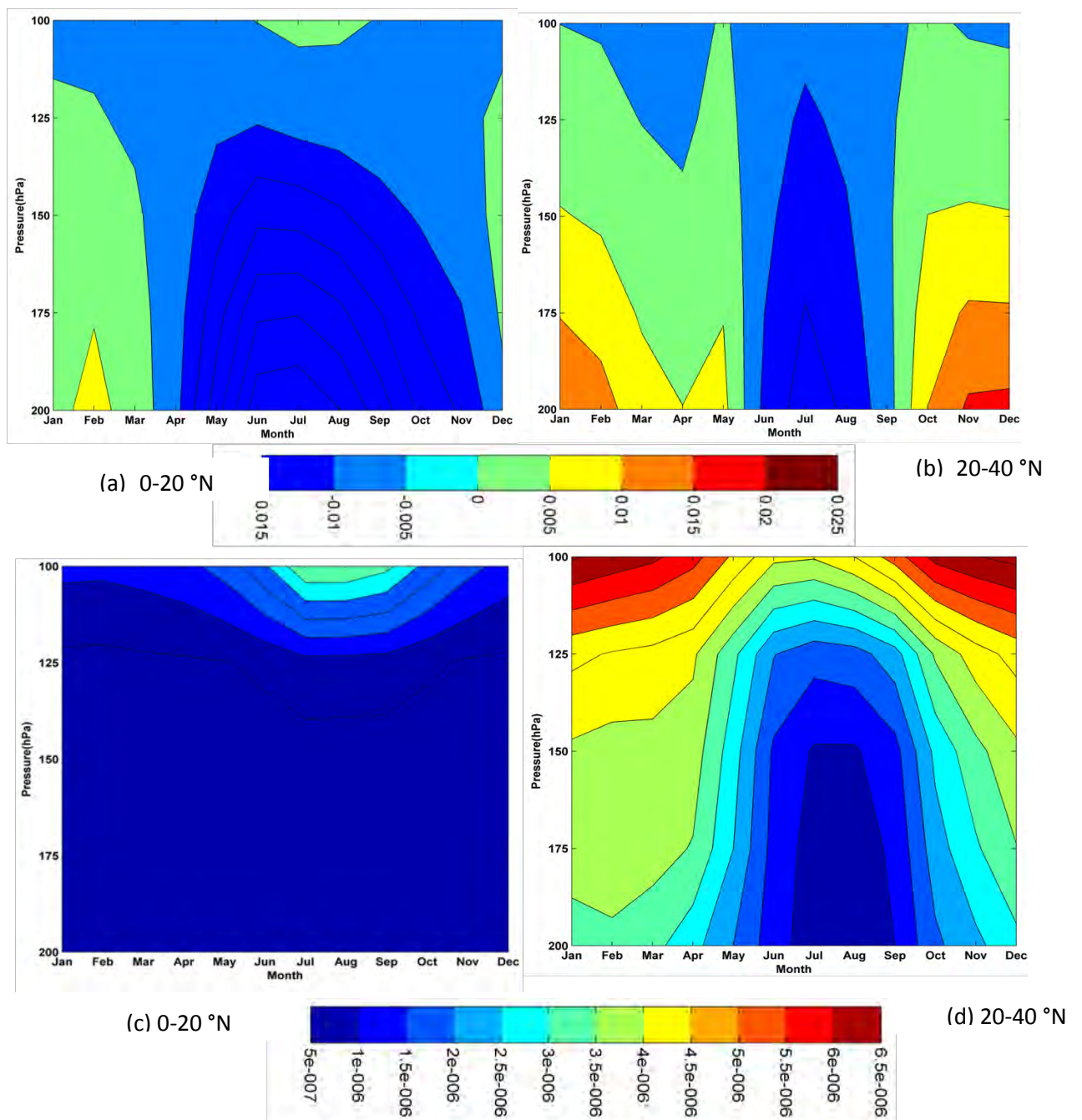
Fig.6.7.    Seasonal variation of vertical velocity (Pa s$^{-1}$) (top) and potential vorticity (K m$^2$ kg$^{-1}$ s$^{-1}$) (bottom) for the pressure levels from 200 to 100 hPa for the latitude region (a and c) 0 to 20°N and (b and d)20 to 40°N and longitude 60 to 100°E.
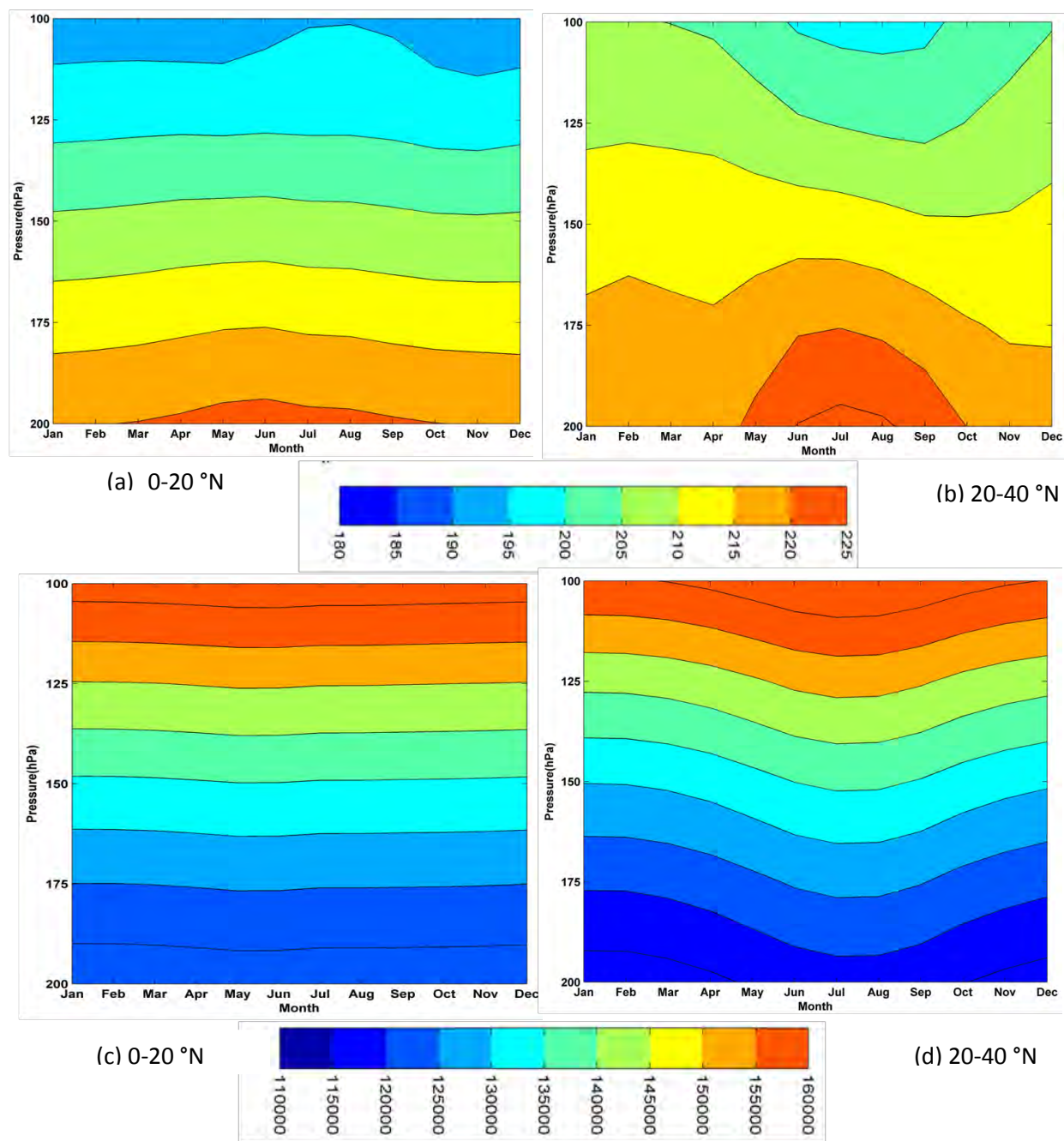
Fig.6.8. Seasonal variation of temperature (K) (top) and geopotential height (m$^2$ s$^{-2}$) (bottom) for the pressure levels from 200 to 100 hPa for the latitude region (a and c) 0 to 20°N and (b and d)20 to 40°N and longitude 60 to 100°E.

**6.3.3. Near tropopause ozone variation at the tropical and subtropical region**

Interannual variation of 100 hPa ozone for the tropical Indian region and subtropical has been examined for both annual and JJAS (June to September) average to study the effect of monsoon ozone in near tropopause. Figure 6.9. (a) represents the tropical region values with solid black lines indicating the annual average and blue dashed lines, the JJAS average. It can be recognized that the monsoon time ozone amount is higher than the annual average in the tropical near tropopause region. The amplitude of interannual fluctuations are higher during monsoon season. The amplitude of variation is highest from 1998 to 2002 with peak values during 1999 and 2001. There is a chance that higher variation of 100 hPa ozone during summer season is influencing the interannual variation of annual average from 1998 to 2009.

Subtropical region shows higher annual average than the monsoon averaged ozone values. This indicates the comparatively less influence of summer time values on the total amount of ozone in the near tropopause region (100 hPa). Influence of wave activity on winter time ozone concentrations may be the reason for the comparatively less influence of summertime ozone values on the annual average. Maximum amplitude of interannual fluctuations for annual averaged ozone is from $1.5 \times 10^{-7}$ to about $2.25 \times 10^{-7}$ kg/kg for tropical region. For subtropical region annual average varies between $5 \times 10^{-7}$ to $8.5 \times 10^{-7}$ kg/kg. Monsoon season average for tropical region is from $2 \times 10^{-7}$ to $3.75 \times 10^{-7}$ kg/kg whereas for the subtropical Indian region monsoon time average for 100hPa ozone is from $2.5 \times 10^{-7}$ kg/kg to $5 \times 10^{-7}$ kg/kg.

**6.3.4. Tropopause and Ozonopause over India**
*6.3.4.1. Trivandrum*

Typical seasonal distribution of ozone over Trivandrum is given by Figure 6.10. Data at the heights where the measurement are available are plotted (The scale is not continuous). X axis is sequenced in logarithmic scale. Near surface ozone have values from 0.03 to 0.04. A lower tropospheric minimum (around 2-4 km) and a mid tropospheric maximum (5-8 km) can be observed in the four profiles given here. Another minimum value is noticeable in the 8-12 km region for all the seasons. Ozone mixing ratio further increases up to the tropopause and the rate of increase advances when it

reaches stratospheric heights. Thus the tropospheric ozone exhibits an S-like profile (Hu et.al, 2010, Paulik and Birner, 2012). Minimum values of ozone above 8km till tropopause are examined in to know about the role of convection in the upward transport of ozone over this region. The features in tropospheric ozone can be reproduced by a model with the mean ozone mixing ratio of air detraining from convective clouds as the only free parameter (Folkins et.al, 2002).
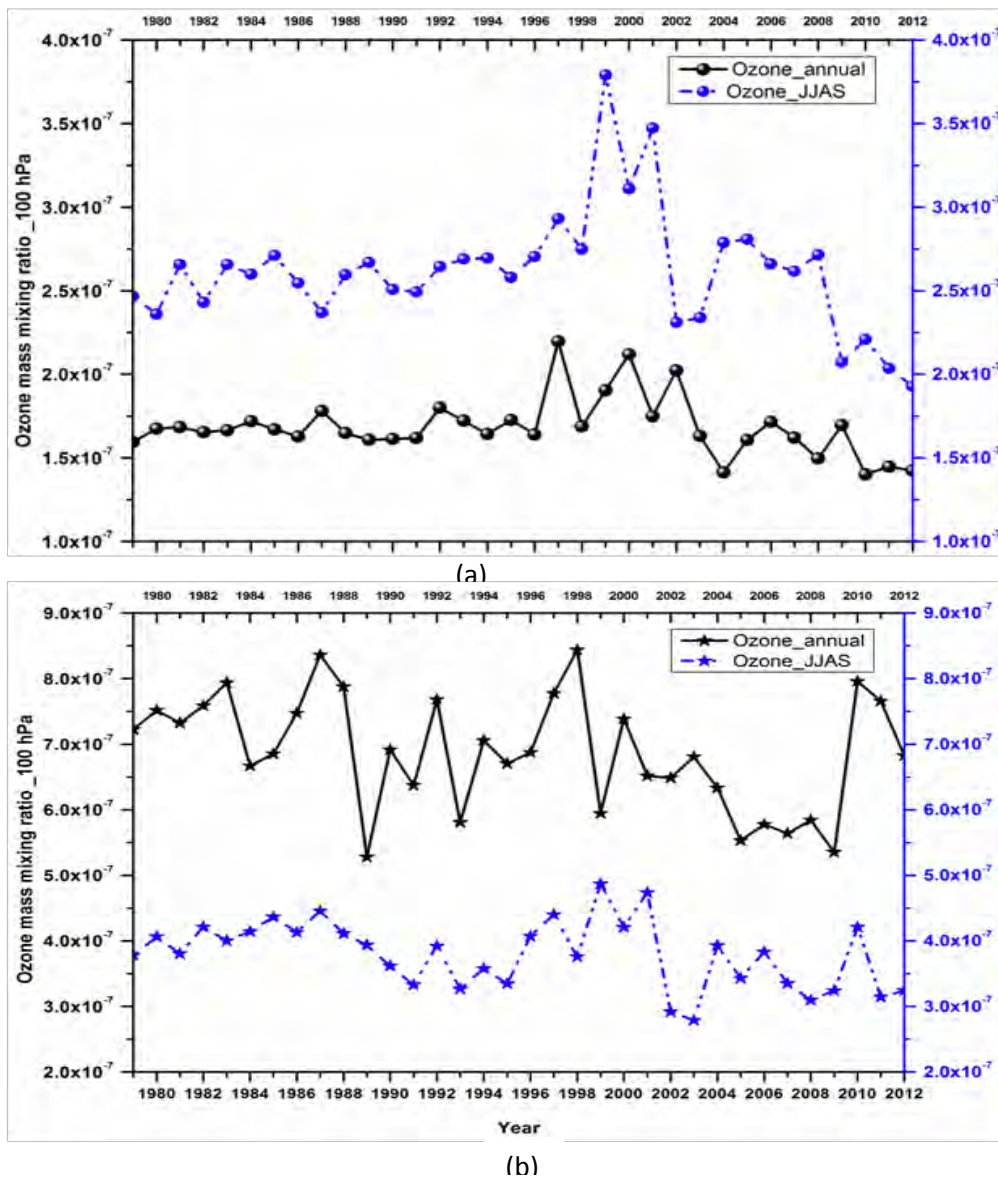


Fig.6.9. Interannual variation of near tropopause (100 hPa) ozone over (a) tropical and (b) subtropical region. Solid black lines indicate annual average and dashed blue lines indicate monsoon season average.

The behaviour of UTLS ozone variation is found to be in line with the tropopause height variations in both the tropical and subtropical Indian region (See figure 6.3 and 6.4). The NCEP reanalysis tropopause pressures represented by these figures are derived by the WMO thermal definition of tropopause. Also the dynamical tropopause represented by potential vorticity variations shows the same seasonal behaviour as ozone variations (Figures 6.6 (c) and (d)). Tropopause can be said as a transition layer from between troposphere and stratosphere in thermal, dynamical and chemical aspects. This section aims to look into the chemical aspect of tropopause height (ozone gradient tropopause or ozonopause-abbreviated here as OGT) and its simultaneous variation with the thermal tropopause since ozone is closely coupled with atmospheric temperature. Ozone tropopause may also behave like a dynamical tropopause since it is approximately conserved on synoptic timescales (Mohanakumar, 2008). Two types of thermal tropopause- Cold point tropopause (CPT) and lapse rate tropopause (LRT) are also computed using the simultaneous temperature observations from the ozonesonde.

Upper tropospheric ozone minimum (OUTM) for both the tropical and subtropical zones were also investigated in this section. Figures 6.11 to 6.12 illustrates the upper tropospheric ozone minimum, lapse rate minimum, cold point temperature and ozone gradient ozonopause for ozone profiles measured in Trivandrum station from 1994 to 2011. The upper tropospheric ozone minimum is studied to explore the presence of low ozone (from lower troposphere) at these heights. Ozone values of the upper troposphere above 12 km which is analogous to or slightly higher than those present in the surface (with values 0.01 to 0.05 ppmv) are expected to be transported from lower stratosphere upward by convection (Paulik and Birner, 2012). Ozone amounts a little higher that lower tropospheric concentration are considered because the mixing ratios will be diluted by environmental air of high ozone concentrations as the parcel travel upward. Height of ozone minimum in the upper troposphere ranges from 9.5 to 16 km for Trivandrum from 1994 to 2011.

Each part of the figure (labelled as a, b, c, and d) represents 20 profiles each. The parameters said above were computed for 160 profiles from 1994 January to 2011 November. Threshold value of ozone minimum altitude was identified as 12 km and altitudes for CPT, LRT and OGT were taken as 16 km. The threshold values of ozone minimum are indicated with black line in the figures, while those of the CPT, LRT and

OGT is shown as red line.   From the figures and tables given below it is can be figured out that altitudes of all the parameters do not cross the threshold values simultaneously. Table 6.3.1 summarises the seasonal occurrence of OUTM, CPT, LRT and OGT. From the table 6.3.1 it can be seen that the number of profiles exceeding threshold occur more during winter season for Trivandrum.
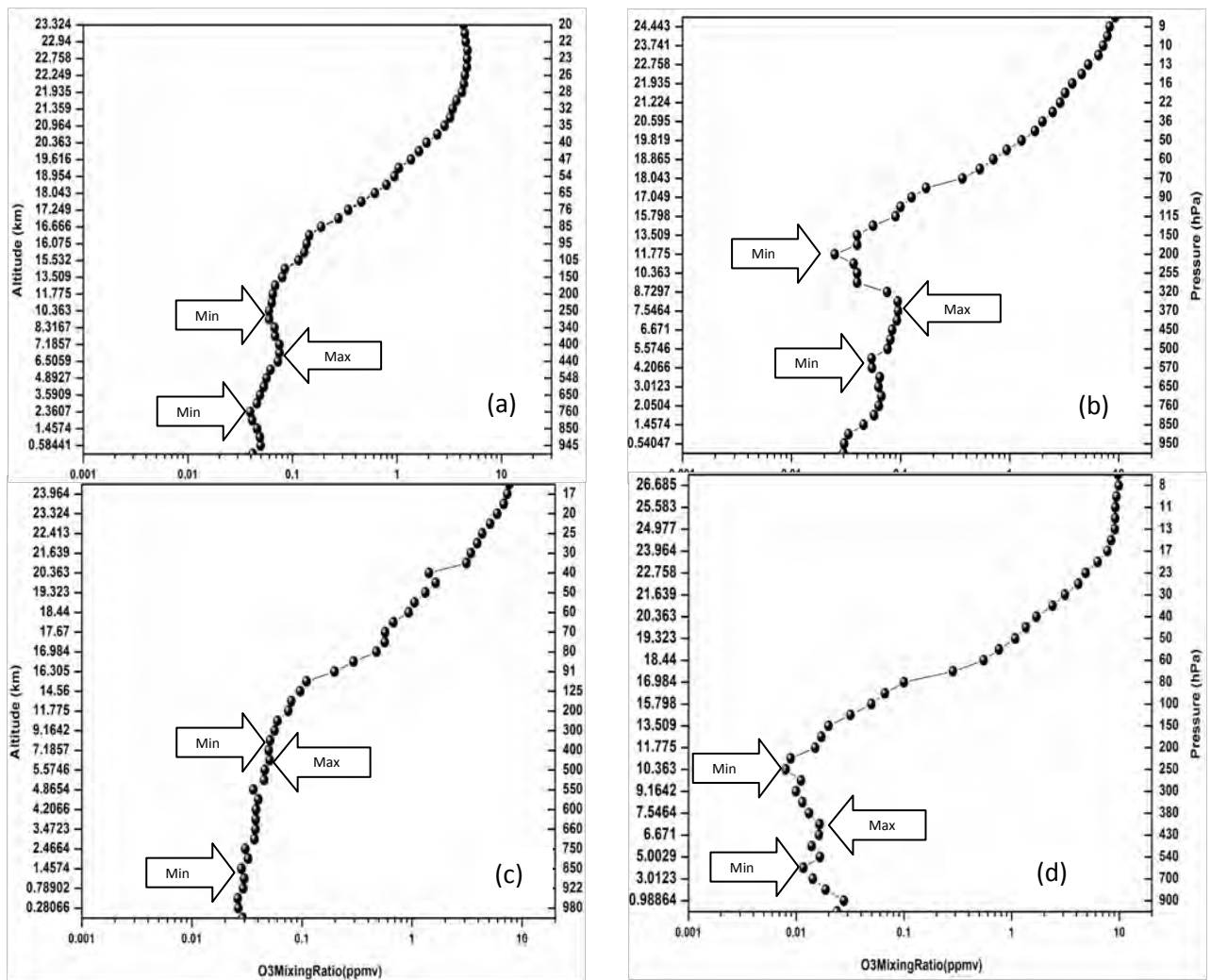


Fig.6.10: Vertical ozone profile (ppmv) over Trivandrum during 2003 (a) January (b) April (c) July and (d) November.

Ozone gradient (Table 6.5. row 16) tropopause crosses the threshold value for all the profiles taken, during winter and spring seasons. Cold point tropopause (Table 6.5. row 14) also shows large number of exceedances during winter and spring.  Taking the joint occurrence of above threshold parameters (Table 6.5 rows 2, 3 and 7) into account it can

be observed that winter and spring season shows large number of exceedances. Six years having maximum frequency of profile observations were selected and time series of OUTM, CPT, LRT and OGT were plotted and displayed as Figure 6.13. Considering the seasonal variation the OGT is showing higher values during winter and spring and lower values during summer season.



Fig.6.11: Altitude of Ozone minimum in the upper troposphere (black), Cold point tropopause (red), Lapse rate tropopause (blue) , ozone gradient tropopause (violet) from (a) 1994 January to 1995 December, (b) 1996 February to1997 July (c) 1997 July to 1999 February and (d) 1999 February to 2001 December for Trivandrum station.

Fig.6.12: Altitude of ozone minimum in the upper troposphere (black), Cold point tropopause (red), Lapse rate tropopause (blue) , ozone gradient tropopause (violet) from (a) 2002 December to 2003 April, (b) 2003 April to 2007 January (c) 2007 February to 2008 July and (d) 2008 August to 2011 November for Trivandrum station.

Table 6.1. Number of seasonal occurrences tropopauses and upper tropospheric minimum above threshold values for Trivandrum. single occurrences are given in the last four rows.

| No. | | Total | Winter | Spring | Summer | Autumn |
|---|---|---|---|---|---|---|
| 1 | **No. of available profiles** | **160** | **52** | **33** | **41** | **34** |
| 2 | Group1-All (OUTM,CPT, LRT, OGT) | 22 | 12 | 3 | 4 | 3 |
| 3 | Group2-CPT, LRT, OGT | 36 | 19 | 10 | 3 | 4 |
| 4 | Group3-OUTM, CPT, LRT | 1 | 0 | 0 | 1 | 0 |
| 5 | Group4-OUTM, CPT, OGT | 1 | 1 | 0 | 0 | 0 |
| 6 | Group5-OUTM, LRT, OGT | 0 | 0 | 0 | 0 | 0 |
| 7 | Group6-CPT, OGT | 21 | 8 | 9 | 1 | 3 |
| 8 | Group7-OUTM, OGT | 9 | 0 | 0 | 5 | 4 |
| 9 | Group8-OUTM, LRT | 2 | 0 | 0 | 0 | 2 |
| 10 | Group9-OUTM, CPT | 0 | 0 | 0 | 0 | 0 |
| 11 | Group10-CPT,LRT | 0 | 0 | 0 | 0 | 0 |
| 12 | Group11-LRT,OGT | 11 | 0 | 3 | 8 | 0 |
| 13 | OUTM in all groups | 49 | 20 | 6 | 12 | 11 |
| 14 | CPT in all groups | 87 | 42 | 23 | 11 | 11 |
| 15 | LRT in all groups | 80 | 34 | 16 | 21 | 9 |
| 16 | OGT in all groups | 134 | 52 | 31 | 30 | 21 |
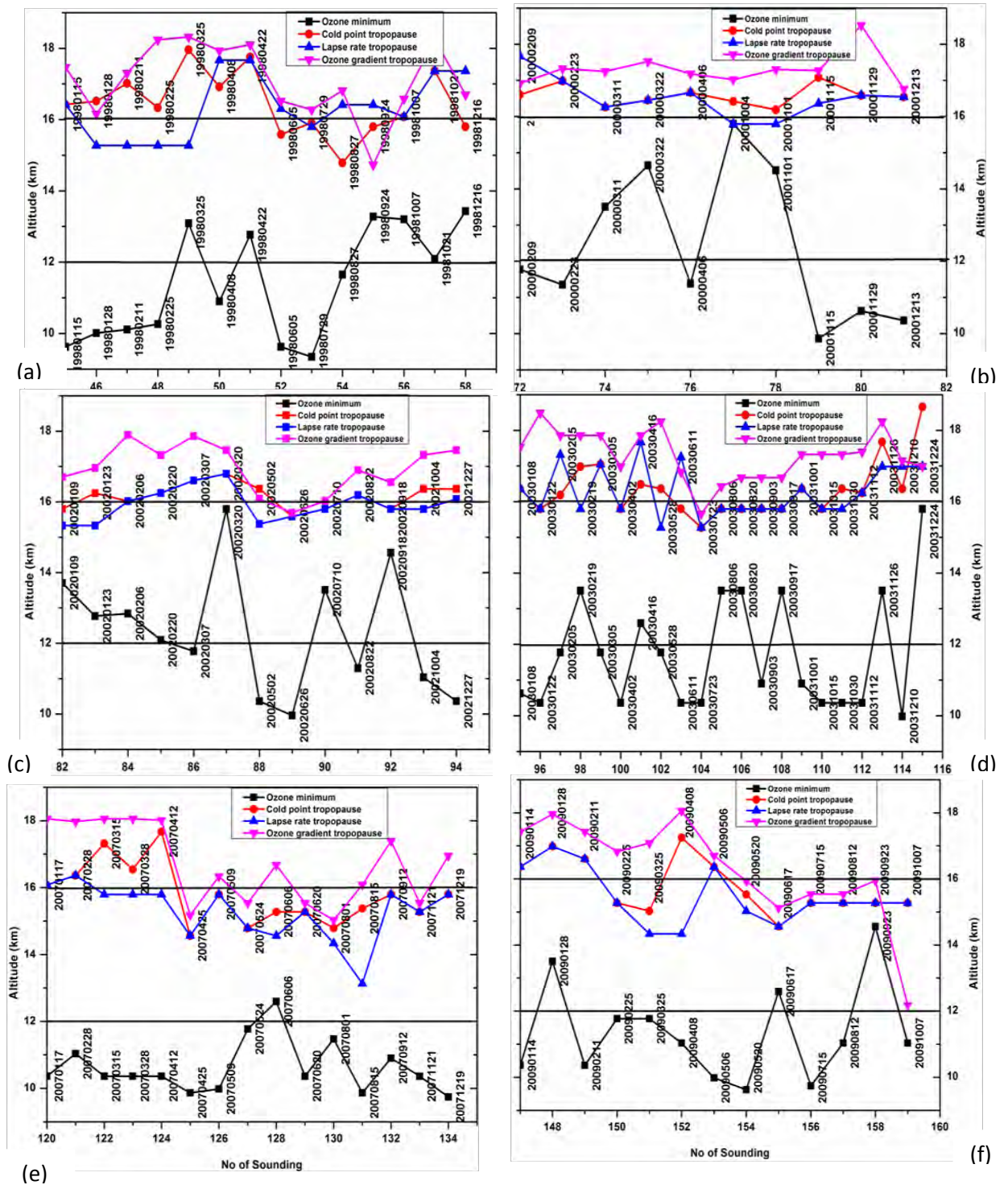
Fig.6.13. Altitudes of Upper tropopsheric ozone minimum (Black line with squares), cold point tropopause (red line with circles), lapse rate tropopause (blue line with triangles) and ozone gradient tropopause (violet line with inverted triangles) at the Trivandrum station during (a) 1998 (b) 2000 (c) 2002 (d) 2003 (e) 2007 and (f) 2009.

Ozone gradient tropopause is observed to be 0.5 to 2 km higher than the CPT and LRT. During summer, the altitude of ozone gradient tropopause nearly coincides with the heights of CPT and LRT.   From the figure it can be seen that OUTM is not showing any noticeable common seasonal variation during all the years. Cold point and lapse rate tropopauses are roughly following the same path as that of ozone gradient tropopause. The upper tropospheric ozone minimum is showing an in phase relation with ozone gradient tropopause during winter and spring. But during summer and autumn both of them shows an out of phase variation for all the years considered.

### 6.3.4.2. New Delhi

Figure 6.14 shows the seasonal ozone profiles over New Delhi. The upper tropospheric ozone minimum displays higher altitudes for New Delhi compared to Trivandrum station in some of the profiles. Figures 6.15 and 6.16 shows the  OUTM, CPT, LRT and OGT for New Delhi. The altitudes and corresponding values of the parameters are summarised in table 6.10. The number of threshold exceeding profiles is higher during spring and summer in all-OUTM, CPT, LRT and OGT (row 2) group is higher during spring and summer seasons. But when profiles surpassing threshold without OUTM (row 3) were considered, spring season shows large number of values followed by winter.   When counted individually the number of OUTM crossing threshold is higher during summer. CPTs and LRTs cross the threshold more during spring followed by winter and summer. OGTs show higher number of surpassing at the time of summer followed by spring. Highest values of OGT and OUTM together (row 8) occurs during summer.

The seasonal variation of various tropopauses and ozone upper tropopsheric minimum over New Delhi for various years can be visualized in Figure 6.14. Considering the variation of upper tropospheric minimum (black line), the number of profiles crossing 12 km is higher for New Delhi.  The surpassing of OUTM is found to occur once in every three consecutive observations for most of the years. The ozone gradient tropopause (violet line) is above the CPT (blue line) and LRT (red line) during most of the time. OUTM (black line) is not exhibiting any definite relation with OGT (violet line), showing in phase and out of phase relation during different seasons. Ozone gradient tropopause is displaying lowest values during winter season. This may be due to the

deposition of ozone in lower stratosphere by Brewer Dobson circulation and its transport into the upper troposphere. Seasonal high in OGT is different for different seasons.
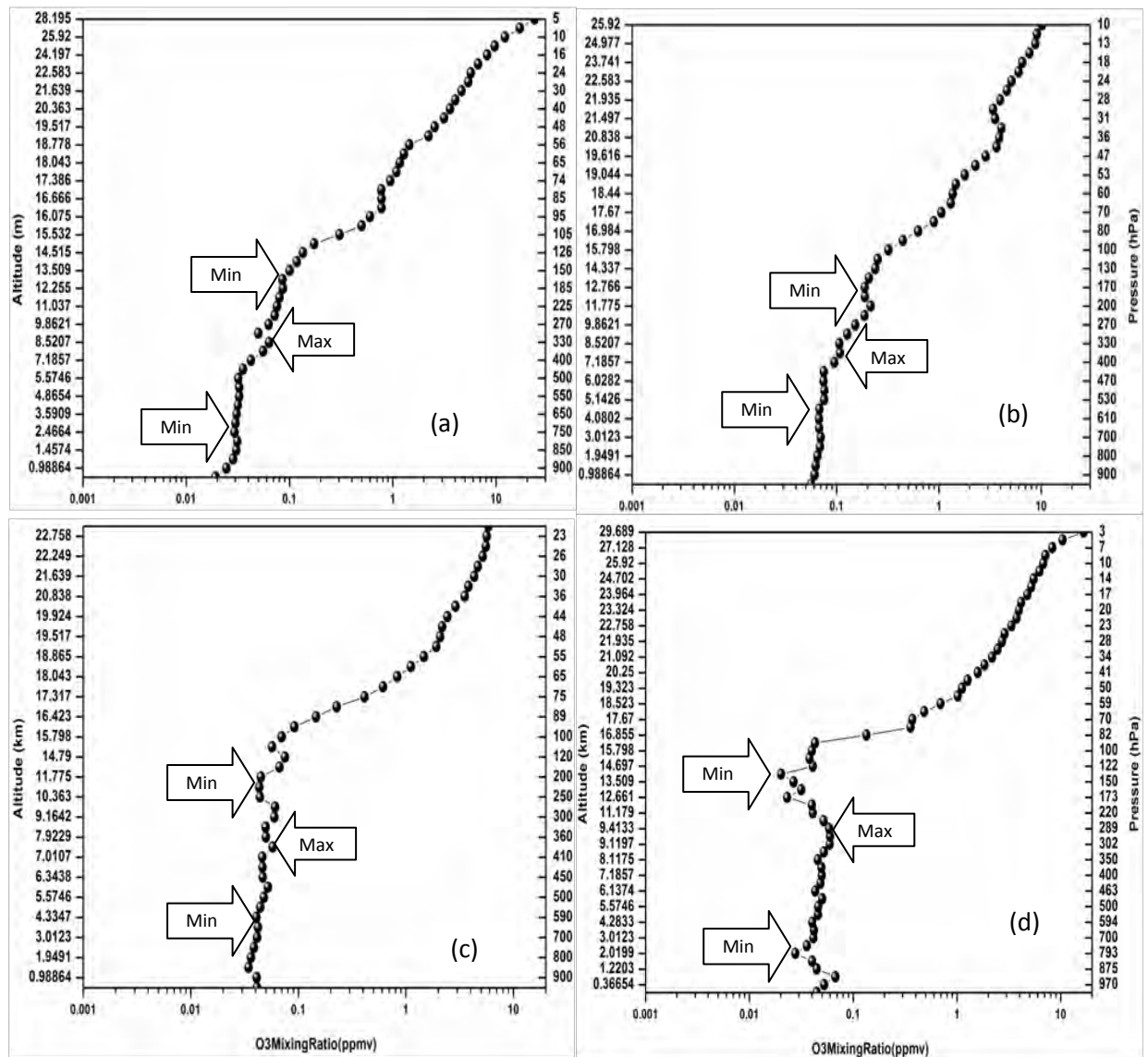


Fig.6.14: Vertical ozone profile (ppmv) over New Delhi during 2003 (a) January (b) April (c) July and (d) November.
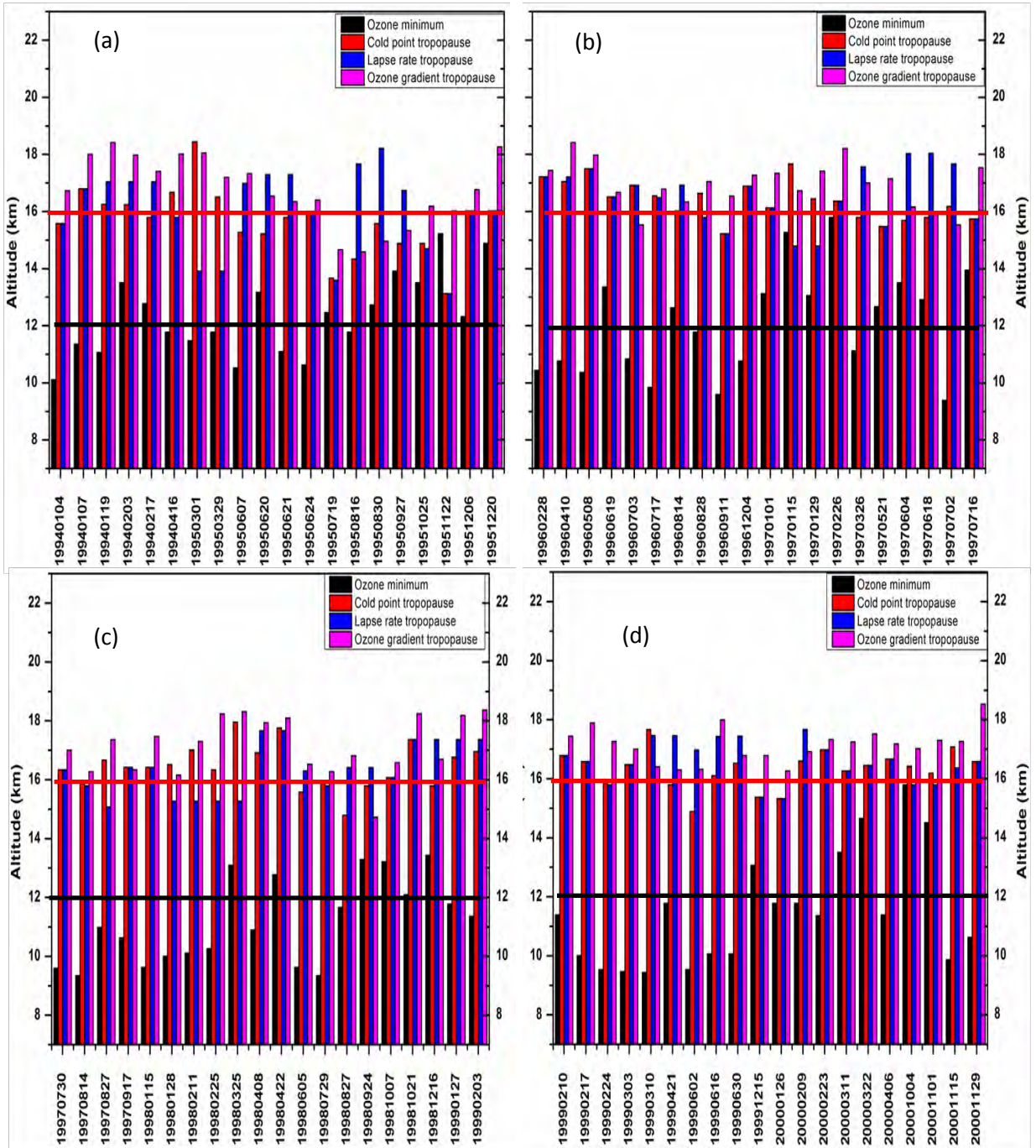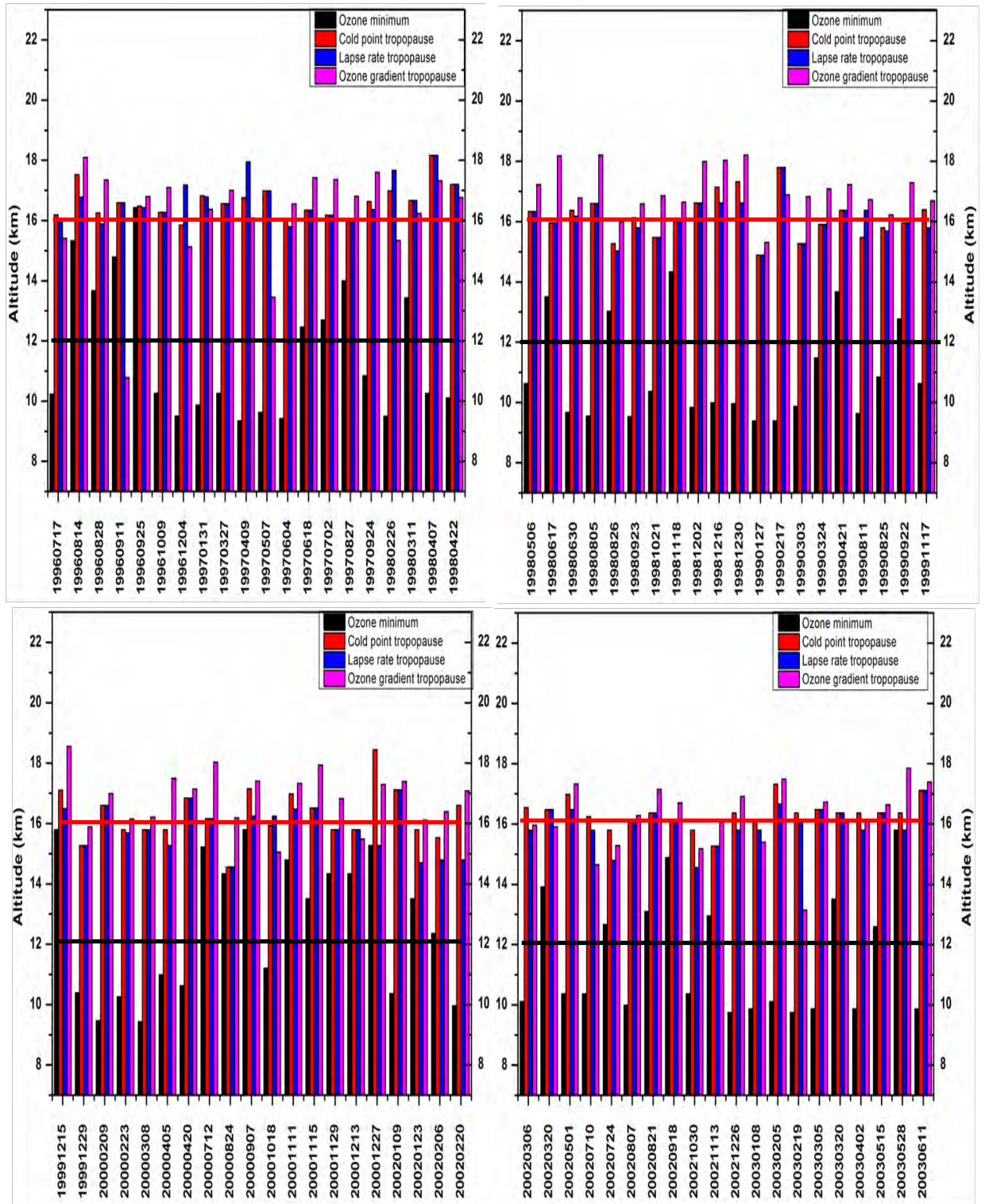
Fig.6.15: Altitude of Ozone minimum in the upper troposphere (black), Cold point tropopause (red), Lapse rate tropopause (blue) , ozone gradient tropopause (violet) from (a) 1996 July to 1998 April, (b) 1998 May to1999 November (c) 1999 December to 2002 February, (d) 2002 March to 2003 June for New Delhi station.
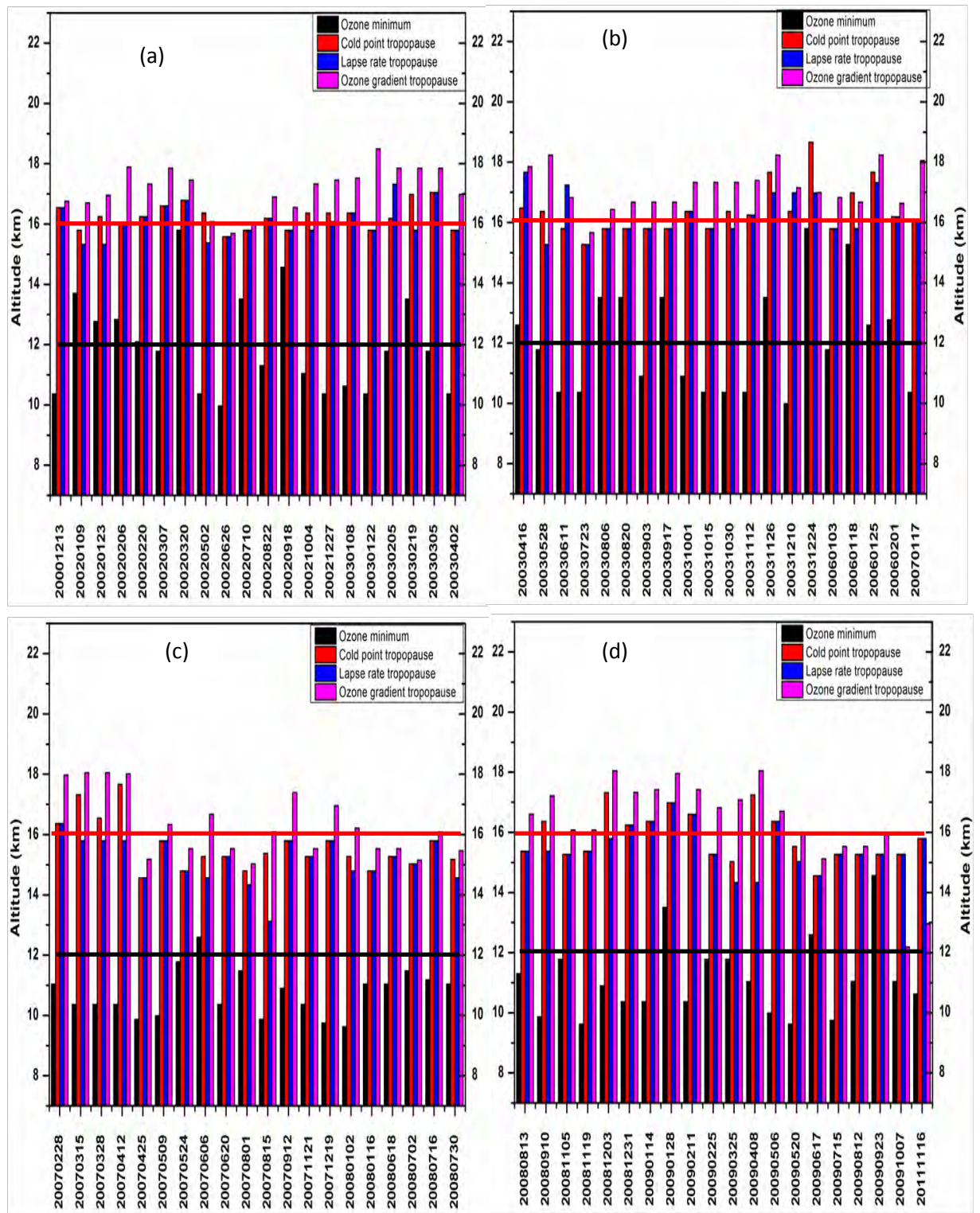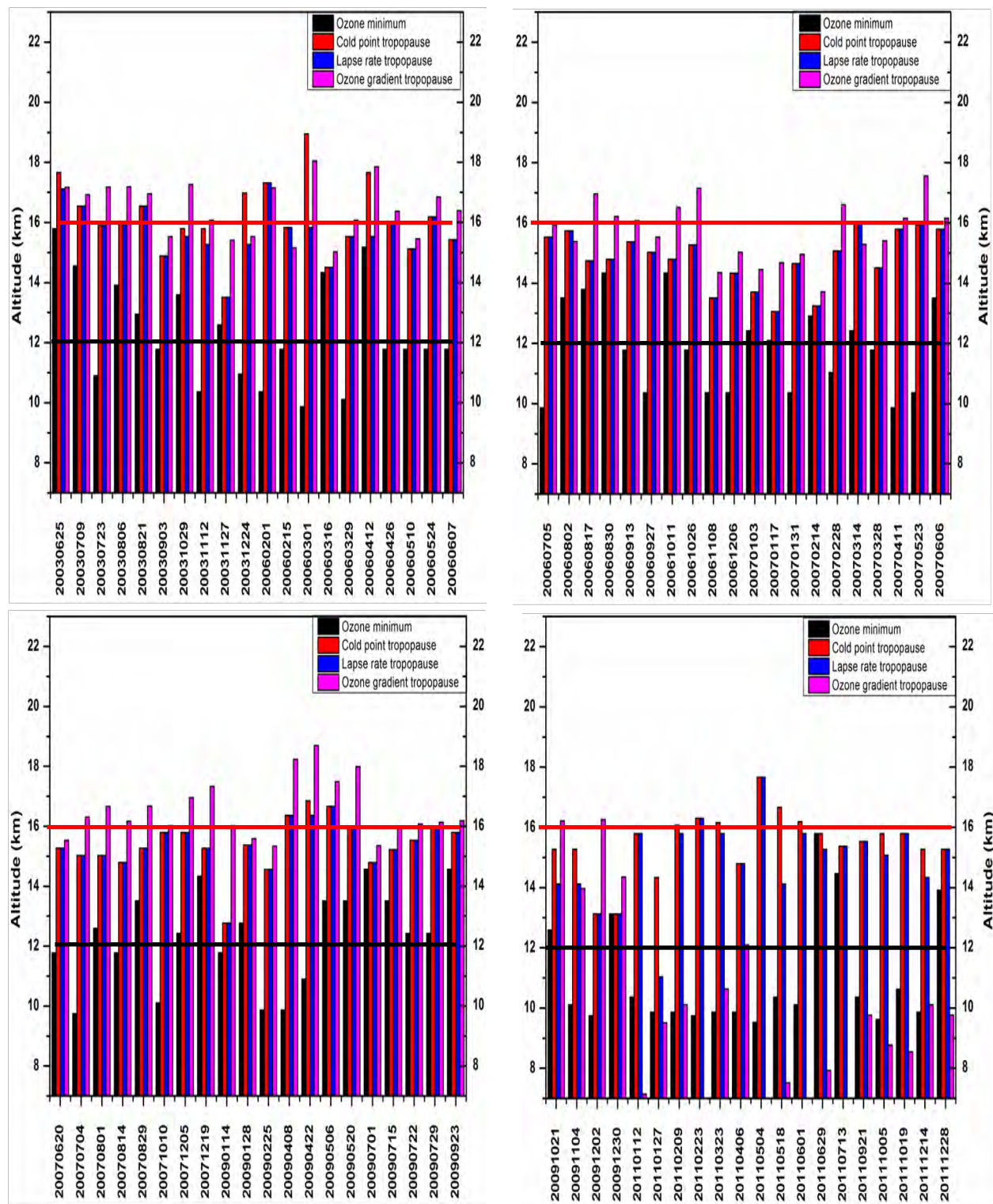
Fig.6.16: Altitude of Ozone minimum in the upper troposphere (black), Cold point tropopause (red), Lapse rate tropopause (blue) , ozone gradient tropopause (violet) from (a) 2003 June to 2006 June, (b) 2006 July to 2007 June for Trivandrum(c) 2007 June to 2009 September, (d) 2009 December to 2011 December for Trivandrum station.

Table 6.2. Number of seasonal occurrences tropopauses and upper tropospheric minimum above threshold values for New Delhi. Individual occurrences are given in the last four rows.

| No | | Total | Winter | Spring | Summer | Autumn |
|---|---|---|---|---|---|---|
| 1 | **No. of available profiles** | 160 | 32 | 44 | 41 | 43 |
| 2 | Group1-All (OUTM,CPT, LRT, OGT) | 20 | 1 | 7 | 8 | 4 |
| 3 | Group2- CPT, LRT, OGT | 30 | 9 | 14 | 6 | 1 |
| 4 | Group3- OUTM, CPT, LRT | 1 | 0 | 1 | 0 | 0 |
| 5 | Group4- OUTM, CPT, OGT | 1 | 1 | 0 | 0 | 0 |
| 6 | Group5- OUTM, LRT, OGT | 0 | 0 | 0 | 0 | 0 |
| 7 | Group6- CPT, OGT | 9 | 2 | 2 | 2 | 3 |
| 8 | Group7- OUTM, OGT | 20 | 4 | 0 | 10 | 6 |
| 9 | Group8- OUTM, LRT | 0 | 0 | 0 | 0 | 0 |
| 10 | Group9- OUTM, CPT | 0 | 0 | 0 | 0 | 0 |
| 11 | Group10- CPT,LRT | 3 | 2 | 1 | 0 | 0 |
| 12 | Group11- LRT,OGT | 1 | 0 | 0 | 1 | 0 |
| 13 | OUTM in all groups plus single | 59 | 12 | 10 | 25 | 12 |
| 14 | CPT in all groups plus single | 78 | 18 | 30 | 18 | 12 |
| 15 | LRT in all groups plus single | 62 | 14 | 22 | 16 | 10 |
| 16 | OGT in all groups plus single | 105 | 22 | 29 | 32 | 22 |
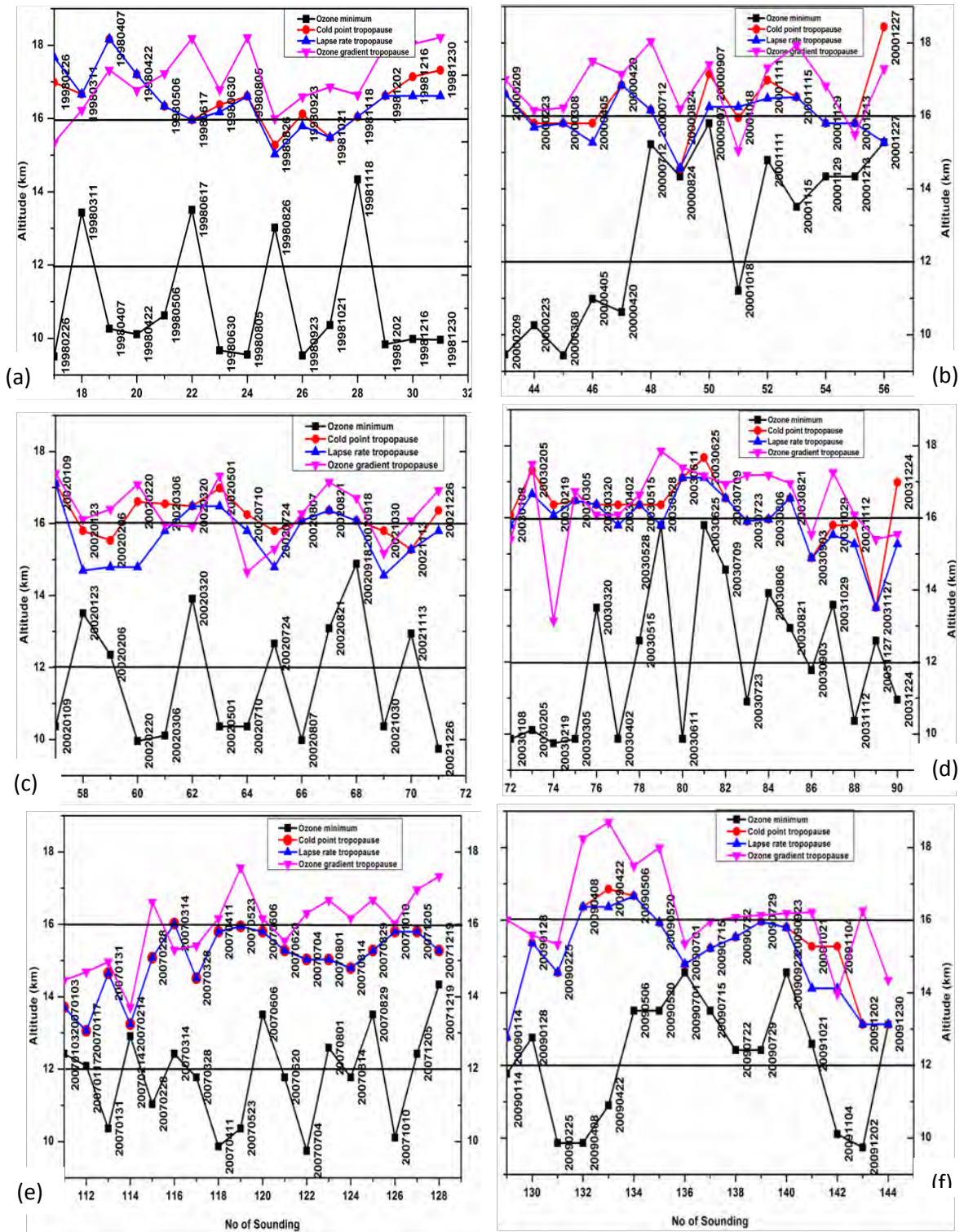
Fig.6.17. Altitudes of Upper tropospheric ozone minimum (Black line with squares), cold point tropopause (red line with circles), lapse rate tropopause (blue line with triangles) and ozone gradient tropopause (violet line with inverted triangles) at New Delhi station during (a) 1998 (b) 2000 (c) 2002 (d) 2003 (e) 2007 and (f) 2009.

## 6.4. Summary

Study of spatially averaged UTLS ozone in the tropical and subtropical Indian regions shows that the seasonal variation is concurrent with the variation of tropopause height in both the regions. The tropical region is showing an increase near the 100 hPa during summer. This is the simultaneous with the lowering of tropopause over the region. Over the subtropical region the ozone is showing lowest values in the whole 200-100 hPa. A sharp overshooting of low ozone values into the tropopause and above is visible in the peak monsoon months in the subtropical Indian region. An analysis of daily data for Trivandrum and New Delhi also shows similar results as above. But the winter time increase of UTLS ozone appears to occur in separate events. This can be attributed to the passage of upper tropospheric troughs from middle latitudes over the region. They can cause a lowering of the tropopause and more intrusion of ozone into the upper tropospheric region.

Various parameters like divergence, vertical velocity, cloud cover, temperature and geopotential over the UTLS region were analysed. It is found that divergence, vertical velocity and cloud cover are exhibiting higher values in tropical region during summer monsoon. But the structure of variations of these parameters is followed by ozone in the subtropical region even though the values of their values are lower in the subtropical region. Thus the influence of monsoon heating on UTLS ozone is more in the subtropical Indian region. Also the seasonal decrease can be ascribed to the lifting boundary layer air with low ozone to UTLS heights by monsoon updrafts. The seasonal variation of potential vorticity is showing exact variation with UTLS ozone. Temperature is also showing minute variations at a similar time of ozone variations. Geopotential contours are not showing any significant variation in tropical UTLS whereas there is a slight downward movement in the subtropical region during summer at the time of upward transport of ozone.

Analysis of interannual variation of 100 hPa ozone shows that the monsoon season average is very low for the subtropical region which again shows the influence of convection. In tropical region JJAS averages are higher than annual average. By examining the ozone tropopause (level of sudden increase in ozone gradient), thermal tropopauses (coldpoint and lapse rate) and level of upper tropopsheric minimum, it is

observed that simultaneous crossing of all the four parameters above threshold value occurs most  during summer for New Delhi and winter for Trivandrum. It was also found that the altitude of ozonopause is higher than that of the thermal tropopauses.

Chapter 7

# Summary, Conclusions and Future Work

## Summary and Conclusions

The amount of UV radiation reaching the surface depends upon total ozone column present in the atmosphere.  Estimating the column amount ozone is important to know the intensity of harmful UV radiation reaching the surface. This radiation can be influenced by other factors like clouds and aerosols. Hence it is necessary to have an awareness of the sensitivity of atmospheric ozone on UV radiation. An attempt has been made in this theis to understand the variability in the distribution of ozone over Indian region in various temporal and spatial scales and to understand the natural teleconnections that lead to ozone variability over the region.  Ozone can be influenced by many factors like variations in solar activity, atmospheric circulation patterns, Quasi Biennial Oscillation, El Nino Southern Oscillation etc.  Analysing the contribution from these natural factors is important to understand the future evolution of ozone in the atmosphere and to have an insight into the effectiveness of the ozone depleting substance limiting measures undertaken by mankind.

An analysis of the climatological spatial distribution of ozone over different seasons showed that the lower and middle latitudes of the Indian region has the largest amount of ozone during spring and summer whereas the northernmost part of the Indian subcontinent has the highest values of ozone during winter season. The variation in annual averaged ozone for the region from 1979 to 2008 showed noticeable difference the first and second half of the period. The latitudinal distribution of ozone showed comparatively large variability in the high latitude boundaries of the study area during winter season. The coefficient of relative variation of ozone has its lowest values at the 0-5° N and 30-35°N over most of the years.

Study of the ozone trends over the region gives near zero values. The seasonal trend during spring and winter is relatively large compared to other seasons. The amplitude of daily fluctuations erythemal ultraviolet radiation is found to be higher for the sub tropical station New Delhi compared to the tropical station Pune. The range of variation of ultraviolet wavelengths over a year is found to be from 100-310 mW/m$^2$ for New Delhi and 180-360mW/m$^2$ for Pune. The sensitivity of erythemal UV to ozone fluctuations is deduced by the computation of the Radiation Amplification Factor (RAF). The values of RAF are found to be higher over New Delhi. The value of the parameter is found to be in agreement when it is computed independently from both the satellite and in situ data.

Principal modes of variability in total ozone were identified. Two different methods-principal component analysis (PCA) and harmonic analysis - were used to recognise the major processes of ozone variability. Fast Fourier transform analysis was done on the principal components to make out the processes responsible for total ozone variations. Quasi biennial oscillation and the interaction of QBO with annual cycle (known as QBO annual beat) are the dominant patterns obtained from the principal components. Ozone principal components also displayed the signatures of decadal and El Nino Southern Oscillation.

To further clarify the nature of the principal components, they were compared with various indices of the corresponding oscillations. Lag correlation analysis was performed to identify the extent of lag between Principal component 1 and QBO index. The results yielded a lag of seven months between two. The Principal components showing decadal and ENSO type frequencies showed approximate in phase relation with corresponding indices. Harmonic analysis of total ozone data was performed without filtering seasonal variations and it yielded annual and semi annual cycles apart from the oscillations given by PCA.

Study of vertical distribution of ozone requires datasets with good spatial and temporal resolution. The study makes a preliminary attempt to construct an ozone dataset with good horizontal resolution. The spatial distribution in the uppermost stratospheric and mesospheric layers (above the layer 7-5 hPa) displays a seasonal variation according to changes in solar radiation with all the latitudes showing nearly the same ozone concentration. Ozone at the layers below 50 hPa exhibits different values for different

zones for the same season. This is due to the increased effect of dynamics. For upper stratospheric layers above 7 hPa summer season shows the largest values in the season and lowest were seen during winter. But for layers below 70 hPa spring season has the highest amount of ozone in the high latitude Indian region.

The seasonal cycle of ozone in various layers were also analysed. The middle and lower tropospheric layers exhibit semiannual oscillation. The layers in the stratosphere from 50 to 0.3 hPa display annual cycle. Ozone in the Upper troposphere /Lower stratosphere region is found to have the largest concurrence with the total column amount variations. A comparative study between the newly obtained data and ECMWF data was performed. Both the datasets are showing most significant relation at the UTLS region. An attempt is also made to probe into the relation with various meteorological parameters and atmospheric ozone variability.

Distinction between the stratosphere troposphere exchange and the distribution of upper troposphere lower stratosphere (UTLS) ozone between the tropical and subtropical station were also examined. The tropical station shows an increase in UTLS ozone during summer season whereas the subtropical station shows a decrease. Seasonal variations in tropopause height over the two stations were studied and the ozone concentrations are found to follow the variations in tropopause height. The origin of air is examined by means of potential vorticity. In the tropical upper troposphere air with high potential vorticity is found from mid May to September. In the subtropical stratosphere it is found during winter and early spring season. Possible causes is inspected using various parameters like divergence, vertical velocity etc as well as with tropopause height variations.

UTLS ozone in the subtropical region is found to be following the variation in divergence, vertical velocity and cloud cover. The lower concentration of subtropical UTLS ozone during summer can be due to the lifting of boundary layer with low ozone concentrations up to the tropopause height due to convective activity during monsoon season. The influence of monsoon convection over subtropical upper tropospheric ozone is analysed using variations in the height of the ozonopause (level of sudden ozone increase between troposphere and stratosphere) and cold point tropopause. It was found that the height of ozone minimum crosses 12km height during summer for New Delhi (subtropical region). Ozone minimum for Trivandrum (tropical region) crossed 12 km height during winter and

autumn season. Thus the subtropical ozonopause reflects the role of convection in transporting lower ozone values at surface to UTLS heights. Ozone gradient ozonopause is found to be at altitudes higher than that of the the coldpoint and lapse rate tropopauses for the tropical and subtropical region.

## Future Work

The work done in the thesis explored the spatial distribution and temporal evolution of ozone over India. Multisensor reanalysis data for total ozone up to 2008 is used to study the variation of total ozone. The study has to be extended to more recent period and it has to be compared with similar datasets. Higher amount of variability during winter season has to be explored further in the context of the generation and propagation of planetary waves over the region. Radiation amplification factor and sensitivity of ultraviolet radiation to ozone has to be discussed more considering the change in clouds and aerosols as well as the long term changes in climate. The major patterns of dynamical variability were identified using the primary linear method of principal component analysis. Nonlinear methods like rotational PCA or more advanced statistical tools will be applied considering the non linear nature of the problem and to isolate the nature of the oscillations more clearly.

The vertical distribution of ozone is explored by simply averaging and gridding the vertical OMI profiles. An attempt can be made to generate a more accurate dataset by applying weighted average to individual profiles. The extension of the study into the global scales and combining it with in situ and other satellite measurements could lead desirable results useful for ozone data assimilation into models. Upper troposphere lower stratosphere ozone variations observed in the study can be more clarified by looking for the wave activity occurring at the tropopause. The possible variations caused by different types of waves can be investigated using tools like wavelet analysis. The total ozone variations are found to be more associated with ozone in the UTLS region. The sensitivity of ultraviolet radiation specifically to ozone in the UTLS region can also be explored in future.

# References

Alexander, G and K.Chatterjee, Atmospheric ozone measurements in India, *Proc. Indian. Natn. Sci. Acad.*, 46(3), A, 234-244, 1980.

Andrews, D. G., J. R. Holton and C. B. Leovy, Middle atmosphere dynamics, Academic Press, 489 pp., 1987.

Angell, J. K., On the Relation between Atmospheric Ozone and Sunspot Number. *J. Climate*, **2**, 1404–1416, 1989.

Appenzeller, C. and Holton, J. R., Tracer lamination in the stratosphere, a global climatology, *J. Geophys. Res.,* 102, 13 555–13 569, 1997.

Akinyemi, L., The Influence of Some Atmospheric Phenomena on Total Ozone Concentration over the Tropics. *Aust. J. Bas. Appl. Sci..* 1(4):497 − 505, 2007.

Austin, J., L. L. Hood, and B. E. Soukharev, Solar cycle variations of stratospheric ozone and temperature in simulations of a coupled chemistry-climate model. Atmos. *Chem. Phys.*, 7, 1693–1706, 2007.

Austin, J., K. Tourpali, E. Rozanov, et al., Coupled chemistry climate model simulations of the solar cycle in ozone and temperature*, J. Geophys. Res.*, 113, D11306, doi:10.1029/2007JD 009391, 2008.

Austin, J., et al., Uncertainties and assessments of chemistry-climate models of the stratosphere, *Atmos. Chem. Phys.*, 3, 1–27, 2003.

Baldwin. M.P., L. J. Gray, T. J. Dunkerton, K. Hamilton, P. H. Haynes, W. J. Randel, J. R. Holton, M. J. Alexander, I. Hirota, T. Horinouchi, D. B. A. Jones, J. S. Kinnersley, C. Marquardt, K. Sato, M. Takahashi, The quasi-biennial oscillation, *Rev. Geophys*, 39, No. 2, pp. 179-229, 2001.

Berntsen, T. K., I. S. A. Isaksen, G. Myhre, J. S. Fuglestvedt, F.Stordal, T. A. Larsen, R. S. Freckleton, and K. P. Shine, Effects of anthropogenic emissions on tropospheric ozone and its radiative forcing, *J. Geophys. Res.,* 102, 28 101–28 126, 1997.

Berntsen T. K., G. Myhre, F. Stordal, and I. S. A. Isaksen, Time evolution of tropospheric ozone and its radiative forcing, *J. Geo- phys. Res.*, 105, 8915–8930, 2000.

Bian, J. C., G. C. Wang and H. B. Chen, et al., Ozone mini-hole occurring over the Tibetan Plateau in December, *Chinese Sci. Bull.*, 51(7), 885−888, 2003.

Bodhaine, B., E. Dutton, D. Hofmann, R . McKenzie and Johnston, P, UV measurements at Mauna Loa: July 1995 to July 1996, *J. Geophys. Res.*, 102, 19, 265–19 273, 1997.

Bojkov, R.D., Computing the vertical ozone distribution from its relationship with total ozone amount. *J. Appl Meteor.* Volume 8, 284-292, 1968.

Bojkov, R.D., The 1983 and 1985 ozone anomalies in perspective. *Mon.Weather.Rev.*, 115, 2187-2201, 1987.

Bowman, K.P., Global patterns of Quasi-biennial Oscillation in Total Ozone. *J.Atmos.Sci.,* 3328, 1998.

Brasseur, G. and Solomon, S, Aeronomy of the middle atmosphere, Reidel Publishing Company, Netherlands, 1986.

Brewer, A. M., Evidence for a world circulation provided by the measurements of helium and water vapor distribution in the stratosphere, *Q. J. R. Meteorol. Soc.*, 75, 351–363, 1949.

Butchart, N. And A. A. Scaife, Removal of chlorofluorocarbons by increased mass exchange between the stratosphere and troposphere in a changing climate, *Nature*, 410, 799–802, 2001.

Butchart, N., A. A. Scaife, M. Bourqui, J. de Grandpré, S. H. E. Hare, J. Kettleborough, U. Langematz, E. Manzini, F. Sassi, K. Shibata, D. Shindell, and M. Sigmond, Simulations of anthropogenic change in the strength of the Brewer-Dobson circulation, *Clim. Dynam.*, 27, 727–741, 2006.

Camp, C. D., Temporal and Spatial Patterns of the Interannual Variability of Stratospheric Ozone and Dynamics , *Ph.D Thesis, California Institute of Technology* , 2004.

Canziani, P.O., F.E. Malanca, and E.A. Agosta, Ozone and upper troposphere/lower stratosphere variability and change at southern midlatitudes 1980–2000: Decadal variations, *J. Geophys. Res.*, 113, 2008.

Chan, C. Y., et al., Vertical profile and origin of wintertime tropospheric ozone over China during the PEACE-A period, *J. Geophys. Res.*, 109, doi:10.1029/2004JD004581, 2004.

Chandra, S. and R. S. Stolarski., Recent trends in stratospheric total ozone: Implications of dynamical and El Chichon perturbations. *Geophys. Res. Lett.* 18: 2277–2280, 1991.

Chandra, S., R. D. McPeters, The solar cycle variation of ozone in the stratosphere inferred from Nimbus 7 and NOAA 11 satellites. *J. Geophys.Res.*Vol.99. No.D10, pp.20,665-20,671, 1994.

Chapman, S., A theory of upper atmospheric ozone. *Mem. Roy. Meteorol. Soc.* 3, 103–125, 1930.

Chen, P., Isentropic cross-tropopause mass exchange in the extratropics, *J. Geophys. Res*., 100, 16,661-16,673, 1995.

Chen, B., X.D. Xu, J. C. Bian and X.H.Shi, Characteristics of irreversible stratosphere-tropopsphere mass exchange over Asian summer monsoon region.*C.J.Geophy.,*53,310-320, 2010.

Chipperfield, M. P. and R. L. Jones, Relative influences of atmospheric chemistry and transport on Arctic ozone trends, *Nature*, 400, 551–554, 1999.

Crutzen, P. J.,The influence of nitrogen oxides in the atmospheric ozone content, *Q. J. Roy. Meteorol. Soc.*, 96, 320–325, 1970.

Cuevas. E, J. J. Rodríguez , M. Gil , J. C. Guerra, A. Redondas and J. J. Bustos, Stratosphere-troposphere exchange processes driven by the subtropical jet, 7th *EMS Annual Meeting / 8th ECAM Abstracts*, Vol. 4, EMS2007-A-00452, 2007.

DeCaria, A. J., Pickering, K. E., Stenchikov, G. L. and L. E. Ott, Lightning-generated NOx and its impact on tropo- spheric ozone production: A three-dimensional modelling study of a Stratosphere-troposphere experiment, radiation, aerosols and ozone (STERAO-A) thurderstorm, *J. Geophys. Res.,* 110, 2005.

Dee, D.P., S. M., Uppala, A.J. Simmons, P. Berrisford, P. Poli, S. Kobayashi, U. Andrae, M. A. Balmaseda, G. Balsamo, P. Bauer, P. Bechtold, A. C. M. Beljaars, L. van de Berg, J. Bidlot, N. Bormann, C. Delsol, R. Dragani, M. Fuentes, A. J. Geer, L. Haimberger, S. B. Healy, H. Hersbach, E. V. Hólm, L. Isaksen, P. Kållberg, M. Köhler, M. Matricardi, A. P. McNally, B. M. Monge-Sanz, J. J. Morcrette, B. K. Park, C. Peubey, P. de Rosnay, C. Tavolato, J.N. Thépaut, F. Vitart. The ERA-Interim reanalysis: configuration and performance of the data assimilation system. *Q. J. R. Meteorol. Soc.* **137**: 553–597. DOI:10.1002/qj.828, 2011.

Dix. B, U.Friei, T. Wagner and U Platt, MAX-DOAS measurements of ozone in the tropics. *Proceedings Quadrennial Ozone Symposium, 1-8 June 2004*, Kos, Greece Pg-1175.

Dobson, G. M. B., Measurements of the amount of ozone in the earth's atmosphere and its relations to other geophysical conditions, Part IV, *Proc. Roy. Soc.*, 1930.

Dobson, G. M.,Origin and distribution of the polyatomic molecules in the atmosphere, *Proc. R. Soc. Lon. Ser.-A*, 236, 187–193, 1956.

Dubrovsky, M., Analysis of UV-B irradiances measured simultaneously at two stations in the Czech Republic. *J. Geophys. Res.*, 105, 4907–4913, 2000.

Echer, E., Multi-resolution analysis of global total ozone column during 1979–1992 Nimbus-7 TOMS period, *Ann. Geophys.* 22: 1487–1493, 2004.

Eerme. K., U. Veismann, and R. Koppel, Estonian total ozone climatology, *Annales Geophysicae* , 20: 247–255, 2002.

Eyring V, N. Butchart, D.W. Waugh, H. Akiyoshi, J. Austin, S. Bekki, G. E Bodeker, B.A. Boville, C. Brühl, M. P. Chipperfield, E. Cordero, M. Dameris, M. Deushi, V.E. Fioletov, S.M. Frith, R. R.Garcia, A. Gettelman, M. A. Giorgetta, V. Grewe, L. Jourdain, D. E. Kinnison, E. Mancini, E. Manzini, M. Marchand, D. R. Marsh, T. Nagashima, P.A. Newman, J. E. Nielsen, S. Pawson, G. Pitari, D. A. Plummer, E. Rozanov, M. Schraner, T.G. Shepherd, K. Shibata, R. S. Stolarski, H. Struthers, W. Tian, M. Yoshiki , Assessment of temper- ature, trace species, and ozone in chemistry climate model simulations of the recent past. *J Geophys Res* 111:D22308, 2006.

Dütch. H. U., Uniform evaluation of Umkehr observations from the world ozone network, *Part III. NCAR Rept.,* 34 pp.165, 1964.

Fadnavis, S., G. Beig, Spatiotemporal variation of the ozone QBO in MLS data by wavelet analysis. *Annales Geophysicae*, 26 . pp. 3719-3730. ISSN 0755-0685, 2008.

Fadnavis, S., G. Beig, and S.D. Polade. Features of ozone quasi-biennial oscillation in the vertical structure of tropics and subtropics. *Meteor. and. Atmos. Phys.* 99, pp 221-231. 2008.

Fadnavis, S., G. Beig, Features of SAO in ozone and temperature over tropical stratosphere by wavelet analysis. *Int. J. Rem. Sens.*, 31 (2). pp. 299-311. ISSN 0143-1161, 2010.

Farman, J., B. Gardiner and J. Shanklin, Large losses of total ozone in Antarctica reveal seasonal ClOx/NOx interaction. *Nature*, 315: 207–210, 1985.

Folkins, I. And C. Appenzeller , Ozone and potential vorticity at the subtropical tropopause break. *J. Geophys. Res*. 101, 18,787-18,792, 1996.

Folkins, I., C. Braun, A. M. Thompson and J. Witte, Tropical ozone as an indicator of deep convection. *J. Geophys. Res.*, 107, NO. D13, 4184, 10.1029/2001JD001178, 2002.

Forster, P. M. D. And K. P. Shine, Radiative forcing and temperature trends from stratospheric ozone changes, *J. Geophys. Res.-Atmos.*, 102, 10 841-10 855, 1997.

Forster P. M. D F and K. Tourpali., Effect of tropopause height changes on the calculation of ozone trend and their radiative forcing. *J.Geophys.Res.*, 106, 12241-12252, 2001.

Fortuin, J. P. F., and H. Kelder, An ozone climatology based on ozonesonde and satellite measurements, *J. Geophys. Res.*, 103(24), 31,709–31,734, 1998.

Funk, J. P. and G. L. Garnham,  Australian ozone observations and a suggested 24-month cycle, *Tellus*, 14, 378–382, 1962.

Fusco, A. C. and M. L. Salby, Interannual Variations of Total Ozone and Their Relationship to Variations of Planetary Wave Activity. *J. Climate*, 12, 1619–1629, 1999.

Garcia, R. R. and W. J Randel, Acceleration of the Brewer-Dobson circulation due to increases in greenhouse gases, *J. Atmos. Sci.,* 65, 2731–2739, doi:10.1175/2008JAS2712.1, 2008.

Gray. L. J. And T. J. Dunkerton, The Role of seasonal cycle in the Quasi-biennial Oscillation of ozone*. J. Atmos. Sci*., 47, 2429–2451, 1990.

Gray L.J, J.A.Pyle, A two dimensional model of the quasi- biennial oscillation of ozone. *J Atmos Sci* 46:203–220, 1989.

Grewe, V., The origin of ozone, *Atmos. Chem. Phys.,* 6, 1495–1511, 2006

Gupta. S., S. Lal, S. Venkataramani, T.A. Rajesh and Y.B. Acharya ,  Variability in the vertical distribution of ozone over a subtropical site in India during a winter month. *J. Atmos. Sol.-Terres Phys.* 69. 1502–1512 , 2007.

Hansen, J., M.Sato, and R. Ruedy, Radiative forcing and climate response, *J. Geophys. Res.-Atmos*., 102, 6831–6864, 1997.

Hamilton, K., Interhemispheric asymmetry and annual synchronization of the ozone quasi-biennial oscillation, *J. Atmos. Sci*., 46, 1019–1025, 1989.

Hasebe, F., Dynamical response of the tropical total ozone to sea surface temperature changes. *J. Atmos. Sci.,* 50, 345-356, 1993.

Hegglin, M.I., and T.G. Shepherd, Large climate-induced changes in ultraviolet index and stratosphere-to- troposphere ozone flux, *Nature Geosci*., 2, 687-691, doi: 10.1038/ngeo604, 2009.

Herman, J. R., R. McPeters, R. Stolarski, D. Larko, R. Hudson, Global Average Ozone Change From November 1978 to May 1990. *J. Geophys. Res.*, Vol.96. D9.  17, 297-17, 305, 1991.

Hollandsworth, S. M., K. P. Bowman, and R. D. McPeters , 1995, Observational study of the quasi-biennial oscillation in ozone, *J. Geophys. Res.*, 100(D4), 7347–7361, doi:10.1029/95JD00193, 1989.

Holton, J. R. and R. S. Lindzen, An updated theory for the quasi-biennial cycle of the tropical stratosphere, *J. Atmos. Sci.*, 29, 1076–1080, 1972.

Holton, J. R., Influence of the annual cycle in meridional transport on the quasi-biennial oscillation in total ozone. *J. Atmos. Sci.,* **46**, 1434-1439, 1989.

Holton, J. R.: An Introduction to Dynamic Meteorology, Academic Press, San Diego, USA, 511 , 1992.

Holton, J. R., P. H. Haynes, M. E. McIntyre, A. R. Douglass, R. B. Rood, and L. Pfister, Stratosphere-troposphere exchange, Rev. Geophys., 33, 403–439, 1995.

Hood, L.L., The solar cycle variation of total ozone: Dynamical forcing in the lower stratosphere. *J. Geophys. Res.*, 102, 1570, 1997.

Hoskins B.J., M. E McIntyre and A.W Robertson, On the use and significance of isentropic potential vorticity maps. *Q. J. R. Meteorol. Soc.,* 111, 877–946, 1985.

Hu, X. M., J. D. Fuentes and F. Zhang, Downward transport and modification of tropospheric ozone through moist convection. *J . Atmos Chem .* 65, 13–35, 2010.

Intergovernmental Panel on Climate Change (IPCC), Climate Change 2001, The Scientific Basis, Contribution of Working Group 1 to the Third Assessment Report, Houghton, J.T., Y. Ding, D.J. Griggs, M. Noguer, P.J. van der Linden, X. Dai, K. Maskell, and C.A. Johnson (Eds.). Cambridge University Press, Cambridge, United Kingdom and New York, NY, USA, 881pp, 2001.

Jiang, X., B. A. J. Dylan, R. Shia, D. E. Waliser, and Y. L. Yung, Spatial patterns and mechanisms of the quasi-biennial oscillation–annual beat of ozone. *J.Geophys.Res*. 110, D23308, 2005.

Isaksen, I.S.A. and N.R.P. Harris, Ozone-climate interactions, European Commission, Air Pollution Research Report No-81, 2003.

Isaksen I. S. A., C. S. Zerefos, K. Kourtidis, C. Meleti, S. B. Dalsoren, J. K. Sundet, A. Grini, P. Zanis, D.Balis, Tropospheric ozone changes at unpolluted and semipolluted regions induced by stratospheric ozone changes, *J. Geophys. Res.*, 110, D02302, doi:10.1029/2004JD004618, 2005.

Kalapureddy, M. C. R., P. Et Raj, and P. C. S. Devara, Total column ozone variations over oceanic region around Indian sub-continent during pre monsoon of 2006. *Atmos. Chem. Phys. Discuss*., 8, 3143–3162, 2008.

Kalnay et al.,The NCEP/NCAR 40-year reanalysis project, *Bull. Amer. Meteor. Soc.*, 77, 437-470, 1996.

Kane, R. P., Y.Sahai, and C. Casiccia, Latitude dependence of the quasi-biennial oscillation and quasitriennial oscillation charac teristics of total ozone measured by TOMS*, J. Geophys. Res.*, 103, 8477–8490, 1998.

Kar. J., C. R. Trepte, L. W. Thomason and J. M. Zawodny, Observations of layers in ozone vertical profiles from SAGE II (v 6.0) measurements, *Geophys. Res. Lett*, Vol. 29, 1433, 4. doi:10.1029/2001GL014230 , 2002.

Karandikar, R. V. And K. R. Ramanathan, Vertical distribution of atmospheric ozone in low latitudes. *Proceedings of the Indian Academy of Sciences - Section A*, Volume 29, pp 330-348. 1949.

Kayano, M., Principal modes of the total ozone on the Southern Oscillation timescale and related temperature variations. *J. Geophys. Res.*, 102, 25797-25806, 1997.

Kiehl, J. T., T. L. Schneider, R. W. Portmann and S. Solomon, Climate forcing due to tropospheric and stratospheric ozone, *J. Geophys. Res.*, 104, 31 239–31254, 1999.

Klenk, K. F., Bhartia, P. K., Hilsenrath, E., and Fleig, A. J., Standard ozone profiles from balloon and satellite data sets. *J. Climate Appl. Meteor.*, 22, 2012–2022, 1983.

Krizan, P. and J. Lastovicka, Trends in positive and negative ozone laminae in the Northern Hemisphere , *J. Geophys. Res*. 110, doi:10.1029/2004JD005477, 2005.

Lacis, A. A., D. J. Wuebbles and J. A. Logan, Radiative forcing by changes in the vertical distribution of ozone, *J.Geophys. Res.*, 95, 9971–9981, 1990.

Lait, L.R., M. R. Schoeberl and P.A. Newman, Quasi-biennial modulation of the Antarctic ozone depletion, *J.Geophys. Res*., 94, 11559-11571, 1989.

Langematz, U., M. Kunze, K. Kruger, K. Labitzke, and G. L. Roff, Thermal and dynamical changes of the stratosphere since 1979 and their link to ozone and $CO_2$ changes, *J. Geophys. Res.,* 108, 4027, 2003.

Lelieveld, J. And F. J. Dentener, What controls tropospheric ozone? *J. Geophys. Res.*, 105, 3531–3551, 2000.

Lemoine, R., Secondary maxima in ozone profiles, *Atmos. Chem. Phys*., 4, 1085–1096, 2004.

Levelt P. F., G. H. J. van den Oord, M. R. Dobber, A. Mälkki, H. Visser, J de Vries, P. Stammes, J. O. V. Lundell, and H. Saari, The Ozone Monitoring Instrument, *Geosci. Remote Sens.*, 44(5), 1093–1101, 2006.

Li, F., Austin, J., and J. Wilson, The strength of the Brewer-Dobson circulation in a changing climate: coupled chemistry-climate model simulations, *J. Climate*, 21, 40–57, 2007.

Liang, Q., A. R. Douglas, B. N. Duncan, R. S. Stolaski, and J. C. Witte, The governing processes and time scales of stratosphere to troposphere transport and its contribution to ozone in the Arctic troposphere. *Atmos. Chem. Phys. Discuss.*, 8, 19377– 19414, 2008.

Lindfors, A., A. Tanskanen, A. Arola, A, R. van der, A. Bais, U. Feister, M. Janouch, W. Josefsson, T. Koskela, K. Lakkala, P. N.den Outer, A. R. D. Smedley, H. Slaper, and A. R.Webb, The PROMOTE UV Record: Toward a Global Satellite-Based Climatology of Surface Ultraviolet Irradiance, *J.Sel. Top. Appl. Ear. Obs. Rem. Sens., 2(3)*, 207–212, 2009.

Lindzen , R. S. and J. R. Holton, A theory of the quasi-biennial oscillation, *J. Atmos. Sci.*, 25, 1095–1107, 1968.

Liu, Y., W. L. Li, X. J. Zhou, et al., Mechanism of formation of the ozone valley over the Tibetan plateau in summer-transport and chemical process of ozone, *Adv. Atmos. Sci.,* 20(1), 103− 109, 2003.

Logan, J. A., D. B. A. Jones, I. A. Megretskaia, S. J. Oltmans, B. J. Johnson, H. Vömel, W. J. Randel, W. Kimani and F. J. Schmidlin, Quasibiennial oscillation in tropical ozone as revealed by ozonesonde and satellite data, *J. Geophys.Res.* 108, 4244, 2003.

Mäder, J. A., J. Staehelin, D. Brunner, W. A. Stahel, I. Wohltmann and T. Peter, Statistical modeling of total ozone: Selection of appropriate explanatory variables, *J. Geophys. Res*., 112, D11108, doi:10.1029/2006JD007694, 2007.

Madronich S., The atmosphere and UV-B radiation at ground level. *Environmental UV Photobiology*: 1–39, Bjorn LO, Young AR (eds). Plenum Press: New York. 1993.

Madronich, S., R. McKenzie, R. Bjorn and M.Caldwell, Changes in biologically active ultraviolet radiation reaching the Earth's surface, *J. Photoch. Photobio.*, 46, 5–19, 1998.

Mani, A., and C. R. Sreedharan, Studies of variations in the vertical ozone profiles over India, *Pure and Appl. Geophys*., Volume 106-108, Issue 1, pp 1180-1191, 1973.

Marécal, V., E. D. Rivi`ere, G. Held, S. Cautenet, and S. Freitas, Modelling study of the impact of deep convection on the UTLS air composition – Part I: Analysis of ozone precursors *Atmos. Chem. Phys.,* 6, 1567–1584, 2006.

Mari, C., D. J. Jacob, and P. Bechtold, Transport and scavenging of soluble gases in a deep convective cloud, *J. Geophys. Res*., 105(D17), 22, 255–22, 268, 2000.

Mariotti. A., M.Moustaoui, B.Legras and H.Teitelbaum, Comparison between vertical ozone soundings and reconstructed potential vorticity maps by contour advection with surgery. *J. Geophys. Res.*, 102, 6131-6142, 2007.

McKenzie, R. L., W. A. Matthews, and P. V. Johnston, The relationship between erythemal UV and ozone, derived from spectral irradiance measurements, *Geophys.Res. Lett.*, 18, 2269-2272, 1991.

McLinden. C.A., S. Tegtmeier, and V. Fioletov, A SAGE-corrected SBUV zonal-mean ozone data set., *Atmos. Chem. Phys*., 9, 7963–7972, 2009.

McPeters, R. D., G. J. Labow, and B. J. Johnson, A satellite-derived ozone climatology for balloonsonde estimation of total column ozone, *J. Geophys. Res.*, 102(D7), 8875–8885, doi:10.1029/96JD02977, 1997.

Mohanakumar K. 2008. Stratosphere Troposphere Interactions. An Introduction. Springer, New York.

Molina, M. J., and F. S. Rowland, Stratospheric sink for chlorofluoromethanes: chlorine atom catalysed destruction of ozone, Nature, 249, 810–812, 1974.

Murphy, D. M. and Fahey, D.W.: An estimate of the flux of stratospheric reactive nitrogen and ozone into the troposphere, J. *Geophys. Res.*, 99, D3, 5325–5332, 1994.

Myhre, G., S. Karlsdòttir, I. S. A. Isaksen and F. Stordal, Radiative forcing due to changes in tropospheric ozone in the period 1980 to 1996, *J. Geophys. Res.,* 105, 28 935–28 942, 2000.

Myhre, G., A.Myhre and F. Stordal, Historical evolution of radiative forcing of climate, *Atmos. Environ*., 35, 2361–2373, 2001.

Naujokat, B., An update of the observed Quasi-Biennial Oscillation of stratospheric winds over the tropics. *J. Atmos. Sci.*, 43, 1873-1877, 1986.

Newman. P. Stratospheric Ozone: An Electronic Textbook.NASA,GSFC.

Newman, P. A., E. Nash, and J. Rosenfield, What controls the temperature of the Arctic stratosphere during the spring? *J. Geophys. Res.,* 106, 19999–20010, 2001.

Oltmans, S. J., et al., Trends of ozone in the troposphere, *Geophys. Res. Lett*., 25, 139-142, 1998.

OMI-ATBD: OMI Algorithm Theoretical Basis Document Volume II OMI Ozone Products, Tech. rep., NASA-GSFC, edited by: Barthia, P. K., ATB-OMI-02, Version 2.0, available at: http: //eospso.gsfc.nasa.gov/eos homepage/for scientists/atbd/docs/OMI/ATBD-OMI-02.pdf (last access: May, 2012)

Orsolini, Y. J., H. Eskes, G.Hansen, U. P. Hoppe, A. Kylling, E. Kyrö, J. Notholt, R. A.Van der, and P. von der Gathen, P. Summertime low ozone episodes at northern high latitudes. *Q. J. R. Meteorol. Soc*. 129: 3265–3275. 2003.

Pal, C, Variability of total ozone over India and its adjoining regions during 1997-2008, *Atmospheric Environment.,* 44, 2010.

Pan, L. L., W. J. Randel, B. L.Gary, M. J. Mahoney, and E. J.Hintsa, Definitions and sharpness of the extratropical tropopause: A trace gas perspective, *J. Geophys. Res*., 109, D23103, doi:10.1029/2004jd004982, 2004.

Patil .S. D and J. V. Revadekar, Extremes in total ozone content over northern India, *International Journal of Remote Sensing,* 2008.

Peter, T., Microphysics and heterogeneous chemistry of polar stratos pheric clouds. *Ann. Rev. Phys. Chem.,* 48, 785–822, 1997.

Pierce, R. B. and W. B. Grant, Seasonal evolution of Rossby and gravity wave induced laminae in ozonesonde data obtained from Wallops Island, Virginia, *Geophys. Res. Lett.*, 43, 1859-1862, 1998.

Plumb, R. A.: Stratospheric transport, *J. Meteorol. Soc. Jpn.,* 80, 793–809, 2002.

Pommereau, J.P., A. G. F. Borchi and M. N. Pinharanda: Ozone and $NO_2$ zonal distribution in the tropical UT/LS fromSAOZ circumnavigating MIR ballon flights: relation to horizontal transport, convection and lightning, *Proceedings Quadrennial Ozone Symposium, 1-8 June 2004, Kos, Greece* Pg-1184.

Prabhakara, C, and E. B, Rodgers,  Study of the lower stratospheric thermal structure and total ozone from Nimbus-4 Iris, NASA TN D-8134., 1976.

Paulik, L.C and T. Birner, Quantifying the deep convective temperature signal within the tropical tropopause layer. *Atmos.Chem.phys.,*12, 12183-12195, 2012.

Pyle, J. A., and R. G. Derwent, Possible ozone reductions and UV changes at the Earth's surface, *Nature*, 286, 373-375, 1980.

Ramanathan, K.R., Bi-annual variation of atmospheric ozone over the tropics,  *Q. J. R. Meteorol. Soc.,*, 89, 540-542, 1963.

Ramanathan, K. R. , R. N. Kulkarni, Height distribution of atmospheric ozone, *Proceedings of the Indian Academy of Sciences*, Section A, 37 (2). pp. 321-331. ISSN 0370-0089, 1953.

Ramanathan, K. R., and J.V. Dave, The calculation of vertical distribution of ozone by Gotz-Umkehr effect, method B. *Ann.I.G.Y.,*5,23-45, 1957.

Ramaswamy, V., M. D. Schwarzkopf and K.P. Shine, Radiative forcing of climate from halocarbon induced global stratospheric ozone loss, *Nature*, 355, 810-812, 1992.

Ramaswamy, V.; O. Boucher, J. Haigh, D. Hauglustaine, J. Haywood, G. Myhre, T. Nakajima, G.Y. Shi and S. Solomon (Lead Authors), Radiative Forcing of Climate Change. In: Climate Change 2001: The Scientific Basis, Contribution of Working Group 1 to the Third Assessment Report of the Intergovernmental Panel on Climate Change, J.T. Houghton, Y. Ding, D.J. Griggs, M. Noguer, P.J. van der Linden, X. Dai, K. Maskell and C.A. Johnson (Eds), Cambridge University Press, Cambridge, U.K., 881 pp, 2001.

Ramaswamy V, M. D. Schwarzkopf, W. J. Randel, B. D. Santer, B.J. Soden, G.L. Stenchikov, Anthropogenic and natural influences in the evolution of lower stratospheric cooling. *Science* 311:1138–1141. doi:10.1126/ science. 1122587, 2006.

Randel, W. J., and J. B. Cobb, Coherent variations of monthly mean total ozone and lower stratospheric temperature. *J. Geophys. Res.*, 99, 5433-5447, 1994.

Randel. W. J. and F. Wu, Isoolation of the Ozone QBO in SAGE II Data By Singular- Value Decomposition, *J. Atmos.Sci.* 53, 2546–2559, 1996.

Randel. W. J, F. Wu, A stratospheric ozone profile data set for 1979– 2005: variability, trends, and comparisons with column ozone data. *J. Geophys. Res.,* 112:D06313. doi:10.1029/2006JD007339, 2007.

Rao, Y. J., P. C. S Devara, P.E. Raj, D.N. Rao and C. Schiller , Vertical velocity and heating rates associated with tropical cirrus: Combined lidar and MST radar observations, , *Geophy. Res. Abs.*, 8, 2006.

Reed, R.J., Zonal wind behaviour in the equatorial stratosphere and lower mesosphere. *J.Geophys. Res.,* 71(18), 4223-4233, 1966.

Reid, G. C., Seasonal and interannual temperature variations in the tropical stratosphere. *J. Geophys. Res.*, 99, 18923-18932, 1994.

Sahoo, A., Sarkar, S, Singh, R. P., Kafatos, M. And M. E. Summers, Declining trend of total ozone column over the northern parts of India, *International Journal of Remote Sensing*,26:16,3433 — 3440, 2005.

Sathyamoorthy,V., Stratosphere Troposphere Interactions Associated with the dynamical processes in the atmosphere. *Ph.D thesis , Cochin University of Science and Technology, India,* 2001.

Schoeberl, M. R., A. R., Douglass, E. Hilsenrath, P. K. Bhartia, J.Barnett, R. Beer, J. Waters, M. Gunson, L. Froidevaux, J. Gille, P. F. Levelt and P. DeCola, Overview of the EOS Aura Mission, /IEEE Trans. *Geosci. Remote Sens.*, 44/(5), 1066–1074, May 2006.

Scwarzkopf , M.D. and V.Ramaswamy, Radiative forcing due to ozone in the 1980s. Dependence on altitude of ozone change. *Geophy. Res.Lett*. 20, 205-208, 1993.

Sembhi .H. Remedios J. J: Ozone in the upper troposphere/lower stratosphere (UT/LS) as measured by the MIPAS instrument, *Proceedings Quadrennial Ozone Symposium,1-8 June 2004, Kos, Greece Pg-1191*.

Serrano A., M. Antón, M. L. Cancillo, and J. A. García, Proposal of a new erythemal UV radiation amplification factor, *Atmos. Chem. Phys. Discuss.*, 8, 1089–1111, 2008.

Shindell, D., D. Rind, N. Balachandran, J. Lean, and P. Lonergan, Solar cycle variability, ozone and climate, *Science*, 284, 305-308, doi:10.1126/science.284.5412.305, 1999.

Shiotani, M., Annual, quasi-biennnial, and El Nino-Southern Oscillation (ENSO) time-scale variations in equatorial total ozone. *J. Geophys. Res.*, 97, 7625-7633, 1992.

Shiotani, M. and F. Hasebe, Stratospheric ozone variations in the equatorial region as seen in Stratospheric Aerosol and Gas Experiment data, *J. Geophys. Res.*, 99(D7), 14,575–14,584, doi:10.1029/94JD00741, 1994.

Singh, M. S., Westerly upper air troughs and development of western disturbance over India, *Mausam,* 30, 405-414, 1979.

Sola, Y. and J. Lorente, Impact of two low ozone events on surface solar UV radiation over the northeast of Spain. *Int. J. Climatol*., 31: 1724–1734. doi: 10.1002/joc.2194, 2011.

Solomon, S., K. H. Rosenlof, R. W. Portmann,  J. S. Daniel, S. M.Davis, T. J. Sanford,  and G. K. Plattner, Contributions of Stratospheric Water Vapor to Decadal Changes in the Rate of Global Warming, *Science,* 327, 1219–1223, doi:10.1126/science.1182488, 2010.

Staehelin, J., N. R. P. Harris, C. Appenzeller, et al., Ozone trends: A review, *Rev. Geophys.*, 39, 231−290, 2001.

Thompson, A. M., and R. D. Hudson, Tropical Tropospheric Ozone (TTO) maps from Nimbus-7 and Earth-Probe TOMS by the modified-residual method: Evaluation with sondes, ENSO signals and trends from Atlantic regional time series. *J. Geophys.Res.*, 104, 26,961-26,975, 1999.

Thompson, A. M., A. M. MacFarlane, G. A. Morris, J. E. Yorks, S. K. Miller, B. F. Taubman, G.Verver, H. Vömel, M. A. Avery, J. W. Hair, G. S. Diskin, E. V. Browell, J. V Canossa, T. L. Kucsera, C. A. Klich, and D. L. Hlavka , Convective and wave signatures in ozone profiles over the equatorial Americas: Views from TC4 2007 and SHADOZ. *J. Geophys. Res*. 115, 2010.

Tian, W.,M. Chipperfield and Q. Huangi, Effects of the Tibetan Plateau on  total column ozone distribution, *Tellus,* 60B, 622–635, 2008.

Tilmes, S., J.F. Lamarque, L. K. Emmons, A. Conley, M. G. Schultz, M. Saunois, V. Thouret, A. M. Thompson, S. J. Oltmans, B. Johnson, and D. Tarasick ., Technical Note: Ozonesonde climatology between 1995 and 2011: description, evaluation and applications. *Atmos. Chem. Phys.*, 12, 7475-7497, 2012.

Tobo, Y., Y. Iwasaka, D. Zhang, G. Shi, Y.S. Kim, K. Tamura, and T. Ohashi, Summertime "ozone valley" over the Tibetan Plateau derived from ozonesondes and EP/TOMS data, *Geophys. Res. Lett.*, 35, 2008.

Tulet, P., K .Suhre, C. Mari, F. Solmon, and R. Rosset, Mixing of boundary layer and upper troposphere ozone during a deep convective event over Western Europe, *Atmos. Env*., 36, 4491– 4501, 2002.

Tung, K. K., and H. Yang, Global QBO in circulation and ozone.Part 1. Reexamination of observational evidence, *J. Atmos. Sci*., 51(19), 2699–2707, 1994.

Van der, A, R. J., M.A.F. Allaart, H.J. Eskes, Multi Sensor Reanalysis of Total Ozone, *Atmos. Chem. Phys.*, 2010.

Varotsos, C., Comment on connection between the 11-year solar cycle, the QBO and the total ozone. *J. Atmos. Sol.Terres Phys.*, 51, pp. 367–370, 1989.

Wang, W.C. and Sze, N. D., Coupled effects of atmospheric $N_2O$ and $O_3$ on the Earth's atmosphere, *Nature*, 286, 589–590, 1980.

Wang.W.C., Y.C.Zhuang, R.D.Bojkov, Climate implications of observed changes in ozone vertical distributions at middle and high latitudes of the northern hemisphere. *Geophy. Res.Lett.* 20,1567-1570, 1993.

Wang, C. and R. G. Prinn, On the roles of deep convective clouds in tropospheric chemistry, *J. Geophys. Res.*, 105, 22, 269-22, 297, 2000.

Wang, J., and  H. J. Wang, The relationship between total ozone and local climate at Kunming using Dobson and TOMS data, *Atmos. Oceanic Sci. Lett*., 3, 207–212, 2010.

Wang, J., S. Pawson, B. Tian, M.C. Liang, R.L. Shia, Y. L. Yung, X. Jiang, El Niño–Southern Oscillation in Tropical and Midlatitude Column Ozone. *J. Atmos. Sci.*, 68, 1911–1921, 2011.

Waugh, D. W. and Hall, T. M., Age of stratospheric air: theory, observations, and models, *Geophys. Rev.*, 40, 1010, doi:10.1029/2000RG000101, 2002.

World Meteorological Organization (WMO) Scientific Assessment of Ozone Depletion, Global Ozone Research and Monitoring Project --Report 50, *World Meteorological Organization, Geneva, Switzerland*, 2007

World Meteorological Organization (WMO) Scientific Assessment of Ozone Depletion: 2010, Global Ozone Research and Monitoring Project— *Report No. 52, World Meteorological Organization, Geneva, Switzerland*, 2011.

Witte J. C., M. R. Schoeberl, A. R. Douglass, and A. M. Thompson, The Quasi-biennial Oscillation and annual variations in tropical ozone from SHADOZ and HALOE. *Atmos. Chem. Phys.*, 8, 3929–3936, 2008.

Wong S., W. C. Wang, I. S. A. Isaksen, T. K. Berntsen, and J. K. Sundet, A global climate chemistry model study of present- day tropospheric chemistry and radiative forcing from changes in tropospheric $O_3$ since the preindustrial period, *J. Geophys. Res.*, 109(D11), D11309, doi:10.1029/2003JD003998, 2004.

Yang H., Three-dimensional Transport of the Ertel Potential Vorticity and N2O in the GFDL SKYHI Model. *J. Atmos. Sci.* 52: 1513–1528, 1995.

Ye, Z. J., and Y. F. Xu, Climate characteristics of ozone over Tibetan Plateau, *J. Geophys. Res.*, 108(D20), 2003.

Zerefos, C. S., A. F. Bais, J. C. Ziomas, and R. D. Bojkov, On the relative importance of Quasi-Biennial Oscillation and El Niño/Southern Oscillation in the Revised Dobson Total Ozone Records, *J. Geophys. Res.,* 97, 10 135–10 144, 1992.

Zerefos, C., Long-term ozone and UV variations at Thessaloniki, Greece, *Phys. Chem. Earth*, 27, 455–460, 2002.

Zerefos, C. S., Tourpali, K. and Balis, D., Solar activity-ozone relationships in the vertical distribution of ozone, *Int. J. Rem. Sens.*,26:16,3449 — 3454, 2005.

Zhou, X. and C. Luo, Ozone valley over Tibetan Plateau, *Acta Meteorologica Sinica.*, 8(4): 505- 506, 1994.

Zhou, X., C. Luo, W. Li, et al., Ozone change over China and ozone valley over Tibetan Plateau, *Chinese Sci. Bull.*, 40(15), 1396−1398, 1995.

Ziemke, J.R., S.Chandra, G.J.Labow, P.K.Bhartia, I.Froidevaux and J.C.Witte, A Global Climatology of tropospheric and stratospheric ozone derived from Aura OMI and MLS measurements. *Atmos.Chem.Phys.*, 11,9237-9251, .doi:10.5194, 2011.

Zossi, M., D. Artigas, P. Fernandez and D. Campra, Total ozone and equatorial zonal wind., *Journal of Atmospheric and Solar-Terrestrial Physics*, *72*(16), 1180–1183. doi:10.1016/j.jastp.2010.07.014, 2010.

Zou, Han, Seasonal variation and trends of TOMS ozone over Tibet, *Geophys. Res. Lett.,* 23(9), 1029-1032, 1996.